

University of Alberta

Functional Characterization of PKD2, TRPP3 and Fibrocystin

by

Xiao-Qing Dai



A thesis submitted to the Faculty of Graduate Studies and Research
in partial fulfillment of the requirements for the degree of

Doctor of Philosophy

Physiology

Edmonton, Alberta
Fall 2007



Library and
Archives Canada

Bibliothèque et
Archives Canada

Published Heritage
Branch

Direction du
Patrimoine de l'édition

395 Wellington Street
Ottawa ON K1A 0N4
Canada

395, rue Wellington
Ottawa ON K1A 0N4
Canada

Your file *Votre référence*
ISBN: 978-0-494-32948-1
Our file *Notre référence*
ISBN: 978-0-494-32948-1

NOTICE:

The author has granted a non-exclusive license allowing Library and Archives Canada to reproduce, publish, archive, preserve, conserve, communicate to the public by telecommunication or on the Internet, loan, distribute and sell theses worldwide, for commercial or non-commercial purposes, in microform, paper, electronic and/or any other formats.

The author retains copyright ownership and moral rights in this thesis. Neither the thesis nor substantial extracts from it may be printed or otherwise reproduced without the author's permission.

AVIS:

L'auteur a accordé une licence non exclusive permettant à la Bibliothèque et Archives Canada de reproduire, publier, archiver, sauvegarder, conserver, transmettre au public par télécommunication ou par l'Internet, prêter, distribuer et vendre des thèses partout dans le monde, à des fins commerciales ou autres, sur support microforme, papier, électronique et/ou autres formats.

L'auteur conserve la propriété du droit d'auteur et des droits moraux qui protègent cette thèse. Ni la thèse ni des extraits substantiels de celle-ci ne doivent être imprimés ou autrement reproduits sans son autorisation.

In compliance with the Canadian Privacy Act some supporting forms may have been removed from this thesis.

Conformément à la loi canadienne sur la protection de la vie privée, quelques formulaires secondaires ont été enlevés de cette thèse.

While these forms may be included in the document page count, their removal does not represent any loss of content from the thesis.

Bien que ces formulaires aient inclus dans la pagination, il n'y aura aucun contenu manquant.


Canada

ABSTRACT

Autosomal dominant polycystic kidney disease (ADPKD) is an inherited nephropathy, primarily characterized by the formation of fluid-filled cysts in the kidneys. It is mainly caused by mutations in the *PKD1* or *PKD2* gene. Autosomal recessive PKD (ARPKD) is caused by mutations in *PKHD1* (polycystic kidney and hepatic disease gene 1), encoding fibrocystin. *PKD2* and its homologue *TRPP3* are Ca-regulated, Ca-permeable non-selective cation channels, while *PKD1* and fibrocystin are receptor-like proteins. The two genetic PKDs are also associated with abnormalities at the cellular level, such as increased cell proliferation, de-differentiation and altered epithelial solute transport. *TRPP3*, not directly related to PKD, is present in both neuron and non-neuron cells and is reported to be implicated in acid sensing.

The channel function of *TRPP3* and the interactions of *PKD2*, *TRPP3* and fibrocystin with partner proteins have been studied. Electrophysiology, molecular biology and protein-protein interaction were used in combination with different expression systems. *PKD2* and fibrocystin are in the same complex though they do not appear to bind each other. *KIF3B*, a motor subunit of microtubule-associated kinesin-2, mediates the complexing by forming triplex *PKD2*-*KIF3B*-fibrocystin; this cross talk may be part of a common pathway between ADPKD and ARPKD. Fibrocystin and filamin, an actin-binding protein, regulate the expression and function of epithelial Na channel (ENaC), via direct binding, presumably by forming triplex fibrocystin-filamin-ENaC. This may account for the reported abnormal expression and function of ENaC in ARPKD cells.

TRPP3 is permeable to organic monovalent cations of sizes less than 7 Å but is impermeable to large tetra-alkylammonium cations which act as inhibitors. This allowed

an estimate of its pore size of ~ 7 Å. In addition, amiloride and its analogs, phenamil, benzamil and EIPA, are inhibitors of TRPP3 (phenamil > benzamil > EIPA > amiloride), suggesting that TRPP3 may account in part for amiloride-sensitive Na reabsorption in various tissues. α -actinin, an actin-bundling protein, not only attaches TRPP3 to the cytoskeleton but also increases TRPP3 channel function. Taken together, our discoveries are important contributions to elucidating the function and regulation of PKD2, TRPP3 and fibrocystin, and to understanding the molecular mechanisms underlying cystogenesis and acid sensing.

ACKNOWLEDGEMENTS

There are a number of people whose assistance made this thesis possible. First and foremost my gratitude goes to my supervisor Dr. Xing-Zhen Chen. Thank you for your encouragement and direction throughout all the projects. I am grateful for the many opportunities you presented me with, and I consider it a privilege to have worked with you. Due to your supervision I now have a stronger desire than ever to pursue research. I wish to express my deepest gratitude to Dr. Edward Karpinski for his expertise in teaching me electrophysiological methods to conduct research, for spending time on discussing results and manuscripts. I also wish to thank Dr. Marek Duszyk for his many valuable suggestions and to Dr. Horacio Cantiello (Harvard University) for his warm help on electrophysiology and discussing results.

I wish to thank the previous (Patrick YP Shen, Yan Liu, Shiva Shefiei, Alkarim Ramji, Shayla Li and Dr. Yuliang Wu) and present (Drs. Qiang Li and Genqing Liang, JungWoo Yang and Carlos Lara) members of the laboratory for their company, and creating an atmosphere that I enjoyed working in. More specially, I thank Qiang for training me in, and sharing his extensive knowledge of, molecular biology. I am grateful for his collaboration over the years.

I was fortunate to have been able to obtain support from Dr. Christopher Cheeseman's laboratory, for using the scintillation counter many times.

My family and their love and support meant a lot to me during my studies. Most importantly, my parents, whom I love deeply and who made my life so rich in so many ways throughout all the years.

TEBLE OF CONTENTS

<u>CHAPTER 1</u>	1
INTRODUCTION	1
1.1. Autosomal dominant polycystic kidney disease (ADPKD)	2
1.1.1. Clinical features	2
1.1.2. Molecular basis	5
1.1.3. Polycystin-1 (PKD1)	9
1.1.4. Polycystin-2 (PKD2)	10
1.1.4.1. Domain structure	10
1.1.4.2. Subcellular localization	11
1.1.4.3. Ion channel properties and pharmacology of PKD2	12
PKD2 as an ER channel	14
PKD2 as a PM channel	16
Regulated trafficking between ER and PM	17
Modes of activation of PKD2	18
1.1.4.4. Physiological roles	19
Biological relevance, emerging and established roles of PKD2	19
PKD1–PKD2 complex	21
PKD2-interacting proteins	23
1.2. Autosomal recessive polycystic kidney disease (ARPKD)	23
1.2.1. Clinical features	23
1.2.2. Genetics	24
1.2.3. The ARPKD protein, fibrocystin	25
1.2.4. Cellular pathophysiology of ARPKD	26
1.3. Epithelial Na channel (ENaC)	28
1.3.1. Structure and localization	28
1.3.2. Biophysical characterization	29
1.3.3. Interact with cytoskeletal protein	31
1.3.4. Cross-link between ENaC and ARPKD	32
1.4. TRPP3	35
1.4.1. Structure	36
1.4.2. Tissue and cellular localization	37
1.4.3. Nonselective cation channel properties and function	40

1.4.4. Physiological roles	41
1.5. Thesis Objectives	44
Aim 1. To determine the cross talk between ADPKD and ARPKD	44
Aim 2. To study the cross talk between ARPKD and ENaC	44
Aim 3. To estimate the pore size of TRPP3 channel	45
Aim 4. To determine physiological roles and pharmacological inhibitors for TRPP3	45
Aim 5. To examine the physical interaction and functional modulation of TRPP3 by α -actinin	46
1.6. REFERENCES	47
<u>CHAPTER 2</u>	63
KIF3B MEDIATES PHYSICAL AND FUNCTIONAL INTERACTIONS BETWEEN POLYCYSTIN-2 AND FIBROCYSTIN (FPC)	
2.1. INTRODUCTION	64
2.2. MATERIALS AND METHODS	66
2.3. RESULTS	71
2.4. DISCUSSION	78
2.5. FIGURES	83
2.6. REFERENCES	98
<u>CHAPTER 3</u>	103
CROSS TALK BETWEEN FIBROCYSTIN (FPC) AND EPITHELIAL Na CHANNEL (ENaC): ROLES OF FILAMIN A	
3.1. INTRODUCTION	104
3.2. MATERIALS AND METHODS	107
3.3. RESULTS	111
3.4. DISCUSSION	114
3.5. FIGURES	119
3.6. REFERENCES	128

<u>CHAPTER 4</u>	132
PERMEATION AND INHIBITION OF PCL CHANNEL BY MONOVALENT ORGANIC CATIONS	
4.1. INTRODUCTION	133
4.2. MATERIALS AND METHODS	135
4.3. RESULTS	137
4.4. DISCUSSION	140
4.5. FIGURES	143
4.6. REFERENCES	150
<u>CHAPTER 5</u>	153
INHIBITION OF TRPP3 BY AMILORIDE ANALOGS	
5.1. INTRODUCTION	154
5.2. MATERIALS AND METHODS	156
5.3. RESULTS	159
5.4. DISCUSSION	163
5.5. FIGURES	168
5.6. REFERENCES	178
<u>CHAPTER 6</u>	182
DIRECT BINDING OF α-ACTININ ENHANCES TRPP3 CHANNEL ACTIVITY	
6.1. INTRODUCTION	183
6.2. MATERIALS AND METHODS	185
6.3. RESULTS	188
6.4. DISCUSSION	193
6.5. FIGURES	198
6.6. REFERENCES	215

<u>CHAPTER 7</u>	218
GENERAL DISCUSSION	
7.1. Cross talk between ADPKD and ARPKD	219
7.2. Regulation of ENaC by filamin and fibrocystin	221
7.3. TRPP3 channel function, pharmacology and modulation by the cytoskeleton	225
7.3.1. Permeation and inhibition of TRPP3 by monovalent by organic cations	225
7.3.2. Inhibition of TRPP3 by amiloride and its analogs	226
7.3.3. Modulation of TRPP3 by α -actinin	227
7.3.4. Physiological roles of TRPP3 and complexing between a TRPP channel and a PKD1 homologue	228
7.4. Conclusion	230
7.5. REFERENCES	232

LIST OF FIGURES

CHAPTER 1

Fig. 1-1.	Diagram of the PKD proteins, PKD1, PKD2 and FPC	9
Fig. 1-2.	Model for the activation of polycystin complex	22
Fig. 1-3.	PKD proteins in multimeric complexes	27
Fig. 1-4.	Schematic representation of the TRPP3	36

CHAPTER 2

Fig. 2-1.	Interactions between PC2, FPC and kinesin-2 identified by yeast two-hybrid experiments	83
Fig. 2-2.	Validation of antibody specificity	84
Fig. 2-3.	Association of KIF3B with PC2 and FPC revealed by GST pull-down, dot blot and co-IP.	86
Fig. 2-4.	Interaction between PC2 and FPC revealed by co-IP and pull-down	88
Fig. 2-5.	Roles of KIF3B in the PC2 x FPC interaction revealed by <i>in vitro</i> binding and co-IP	91
Fig. 2-6.	Roles of KIF3B in the PC2 x FPC interaction revealed by Far WB	93
Fig. 2-7.	Immunofluorescence staining for PC2, FPC and KIF3B in IMCD cells	94
Fig. 2-8.	Multiple conductance states of PC2 channel and effects of FPCC and KIF3BC	95
Fig. 2-9.	Effects of FPCC and KIF3BC on PC2 channel represented by NPo, current density and mean current	97

CHAPTER 3

Fig. 3-1.	Physical binding between ENaC and filamins	119
Fig. 3-2.	Modulation of ENaC channel function by FLNA in <i>Xenopus</i> oocytes	120
Fig. 3-3.	Effects of filamins on α -ENaC expression	121
Fig. 3-4.	Tandem affinity purification of human α -, β -, and γ -ENaC from MDCK stable cell lines and channel function of α ENaC reconstituted in lipid bilayer	122
Fig. 3-5.	Modulation of α -ENaC channel function by FLNAC in lipid bilayer and effects of FLNAC on α -ENaC single-channel parameters	123
Fig. 3-6.	Physical interactions among ENaC, FPC and filamins	125
Fig. 3-7.	Effects of FPCC on whole-cell transport mediated by $\alpha\beta\gamma$ -ENaC channel overexpressed in <i>Xenopus</i> oocytes	126
Fig. 3-8.	Physical interactions between FPC and filamins	127

CHAPTER 4

Fig. 4-1.	Permeation of organic amines and TMA	143
Fig. 4-2.	Permeation of and inhibition by TAA cations TEA, TPA, TBA and TPeA	144
Fig. 4-3.	Effects of TEA on PCL	145
Fig. 4-4.	Effects of TPA on PCL	146
Fig. 4-5.	Inhibition of PCL by TBA	147

Fig. 4-6.	Effects of TPeA on PCL single-channel currents	148
Fig. 4-7.	Inhibition of PCL whole-cell currents by TPeA	149

CHAPTER 5

Fig. 5-1.	Effects of amiloride analogs on the uptake mediated by TRPP3 expressed in <i>Xenopus</i> oocytes	168
Fig. 5-2.	Effects of amiloride analogs on the Ca-activated whole-cell currents mediated by TRPP3 channel	170
Fig. 5-3.	Effects of amiloride analogs on the TRPP3-mediated basal Na currents	171
Fig. 5-4.	Effects of amiloride on TRPP3 single-channel properties	173
Fig. 5-5.	Effects of EIPA	174
Fig. 5-6.	Effects of benzamil	175
Fig. 5-7.	Effects of phenamil	176
Fig. 5-8.	Effects of amiloride analogs on TRPP3 single-channel parameters	177

CHAPTER 6

Fig. 6-1.	Characterization of the TRPP3 antibody PR71	198
Fig. 6-2.	Tandem affinity purification procedure for human TRPP3 channel protein in MDCK cells	200
Fig. 6-3.	Channel activity of TRPP3 reconstituted in planar lipid bilayer	202
Fig. 6-4.	Effect of α -actinin on TRPP3 channel activities	204
Fig. 6-5.	Effect of α -actinin on the single-channel conductance, open probability and mean current of TRPP3	206
Fig. 6-6.	Interaction between endogenous TRPP3 and α -actinins in MDCK and HEK 293 cells, and mouse brain, human kidney and heart tissues by co-IP	208
Fig. 6-7.	Interaction between endogenous TRPP3 and α -actinin-2 in mouse brain	210
Fig. 6-8.	Schematic representation of interaction between various TRPP3 and α -actinin fragments by yeast two-hybrid system	212
Fig. 6-9.	<i>In vitro</i> interaction between TRPP3 fragments and α -actinin by GST pull-down and dot blot overlay	214

CHAPTER 7

Fig. 7-1.	PKD proteins-initiated signaling pathways and targeted cellular functions	231
-----------	---	-----

ABBREVIATIONS

aa	amino acids
ADPKD	autosomal dominant PKD
ARPKD	autosomal recessive PKD
[Ca] _i	intracellular free Ca ion concentration
cAMP	cyclic adenosine monophosphate
CD	collecting duct
CFTR	cystic fibrosis transmembrane conductance regulator
Co-IP	co-immunoprecipitation
EGF	epidermal growth factor
EGFR	epidermal growth factor receptor
ENaC	epithelial Na channel
α-ENaC	α subunit of ENaC
β-ENaC	β subunit of ENaC
γ-ENaC	γ subunit of ENaC
ER	endothelial reticulum
FPC	fibrocystin-polyductin
FPCC	C-terminus of fibrocystin-polyductin
GPCR	G-protein coupled receptor
GSK3	glycogen synthase kinase 3
I _{sc}	short-circuit current
IC ₅₀	half maximal inhibitory concentration
IMCD	inner medullary collecting duct
IP ₃ R	inositol 1,4,5-trisphosphate receptor
K _i	inhibition affinity constant or dissociation constant
MDCK	Madin–Derby canine-kidney
P _o	open probability
PACS1	phosphofurin acidic cluster protein 1
PIGEA14	PKD2 interactor, Golgi- and ER-associated protein
PKD	polycystic kidney disease
PKD1 (PC1)	polycystin-1
PKD1L1	PKD1 like 1 homologue
PKD1L3	PKD1 like-3 homologue
PKD2 (PC2)	polycystin-2
PKDREJ	PKD receptor for egg jelly
PKHD1	polycystic kidney and hepatic disease gene 1
PM	plasma membrane
TM	transmembrane
TRP	transient receptor potential
TRPP	TRP polycystin

CHAPTER 1

INTRODUCTION

Polycystic kidney disease (PKD) has been recognized for about one and half centuries and is a group of genetic and non-genetic disorders of which a major phenotypic feature is the development of fluid-filled cysts in the kidney. Genetic PKD includes autosomal dominant PKD (ADPKD), which is the predominant form of PKD and typically affects adults, and autosomal recessive PKD (ARPKD), mainly an infantile disease. Although cyst development is classically considered different in nature in the two diseases – it is focal in ADPKD, compared with fusiform dilatation in ARPKD – the cellular events associated with both disorders appear to be similar. These include dedifferentiation of the epithelial phenotype (including re-expression of proteins usually found during development), increased proliferation and apoptosis, aberrant targeting and trafficking of proteins and fluid-transport abnormalities (Harris & Torres, 2006). Thus, it raises the possibility that there exists a common pathway or molecular mechanism underlying the pathogenesis of the two genetic PKDs. This thesis covers two parts. The first part includes my studies on the cross talk between ADPKD and ARPKD, and between ARPKD and epithelial Na channel (ENaC), and on roles of the cytoskeleton in this cross talk. The second part includes my studies on TRPP3 channel that is homologous to ADPKD proteins but not directly related to ADPKD.

1.1. Autosomal dominant polycystic kidney disease (ADPKD)

1.1.1. Clinical features

ADPKD is one of the most common inherited disorders in humans, with an estimated prevalence of 0.1 ~ 0.2% in the general population. The disease is 15 times more common than cystic fibrosis. The clinical presentation of this disease is usually related to renal manifestations, which may encompass structural, functional, and endocrine abnormalities as well as complications. However, ADPKD is a systemic disease with extrarenal manifestations involving several organs (Gabow, 1990; Gabow, 1993; Milutinovic *et al.*, 1984; Wilson & Falkenstein, 1995).

The most important structural change is enlargement of both kidneys due to development of a large number of cysts of tubular derivation. The renal cysts vary considerably in size and appearance, from a few millimeters to many centimeters. The appearance may vary from slightly cloudy to chocolate colored, suggesting hemorrhage.

Secondary infection may also be encountered. These cysts may develop in utero or appear after birth and enlarge slowly over many decades (Fick *et al.*, 1993; Pretorius *et al.*, 1987). As a result of the relentless enlargement of the cysts, functioning renal parenchyma is progressively destroyed, leading to renal insufficiency and ultimately resulting in end-stage renal disease (ESRD) (Al-Bhalal & Akhtar, 2005).

Noncystic manifestations of ADPKD are also common. Renal complications of this disease arise largely as a consequence of structural abnormalities. Of these complications, hypertension is the most frequent, affecting 30% of children and up to 60% of adults. The frequency is even higher in patients with ESRD. Pain is also one of the most frequent complications of polycystic disease. Renal failure is the most serious renal complication of this disease. About 45% of patients with ADPKD develop ESRD by the age of 60. The age at onset of renal failure, however, varies from 2 to 80 years. The range in age at onset of renal failure may be related to the type of genetic mutation and other factors such as severity of hypertension and presence of infection.

Extrarenal manifestations of ADPKD may be cystic and noncystic. Epithelial cysts are encountered in the liver, ovary, pancreas, spleen, and central nervous system. The frequency of hepatic cyst occurrence varies considerably but generally increases with age, so that by the age of 60, approximately 73% of patients have hepatic cysts. The frequency of cysts in the pancreas and ovary is not known. These cysts are usually asymptomatic (Gabow, 1990; Gabow, 1993; Milutinovic *et al.*, 1984; Wilson & Falkenstein, 1995). The most important noncystic extrarenal manifestations of the disease are cardiovascular abnormalities. A large, prospective study reported a 26% frequency of mitral valve prolapse in PKD. The most serious extrarenal manifestation is intracerebral vascular aneurysm, but the exact frequency of this complication is not known. Spontaneous rupture of these aneurysms may contribute to sudden death in these patients. The principal noncystic gastrointestinal complication of polycystic disease is colonic diverticuli, which may perforate (Boucher & Sandford, 2004).

Diagnosis

ADPKD is typically diagnosed in adults by the detection of bilaterally enlarged polycystic kidneys using trans-abdominal ultrasound scanning. However, ADPKD in

children, if detectable, may be unilateral or markedly asymmetrical leading to diagnostic difficulty and necessitating a different approach than in adults. Computed tomography and magnetic resonance imaging (MRI) are also used where additional information on renal structure and function are required or where ultrasound resolution is poor such as in the obese individual. In addition to screening asymptomatic adult family members at-risk of inheriting ADPKD, individuals with renal tract symptoms or signs (children and adults) including macroscopic haematuria, loin pain, urinary infection or renal colic; early-onset hypertension; a sibling with early onset disease or a personal or family history of cerebral aneurysm, should also be offered screening. The presence of at least two renal cysts (unilateral or bilateral) in individuals younger than 30 years may be regarded as sufficient to establish a diagnosis; among those aged 30–59 years, the presence of at least two cysts in each kidney and among those aged 60 years and above, at least four cysts in each kidney should be required (Al-Bhalal & Akhtar, 2005)⁹.

Clinical management and potential therapies

There are no disease-specific therapies for any form of PKD. No evidence-based guidelines on the management of ADPKD have been reported, perhaps due to the very slow rate of disease progression. In ADPKD, only blood pressure control has been shown to have a favorable impact on disease progression and cardiovascular complication rate. No trials have identified which anti-hypertensive agent is the agent of choice in ADPKD but angiotensin-converting enzyme inhibitors are the usual first-line agents and may be safer than diuretics. Patients with ADPKD are suitable for all forms of renal replacement therapy. Pre-dialysis or -transplant nephrectomy may be required for nephromegaly or recurrent sepsis. Surgical intervention in ADPKD may also be indicated for the management of pain, haemorrhage and recurrent infection. All individuals with or at-risk of inheriting ADPKD should be offered genetic counseling to discuss genetic risk, screening, prenatal and predictive testing (Harris & Torres, 2006).

Recent studies using different rodent models of renal cystic diseases have suggested that various pharmacological interventions may modify disease progression. A novel tyrosine kinase inhibitor EKI-785, pioglitazone, a thiazolidinedione compound and a vasopressin V2 receptor antagonist have all been shown to beneficially modify the course

of murine cystic disease. This clearly demonstrates that a better understanding of the molecular and cellular defects underlying cystogenesis may lead to the design of novel, or the use of existing, therapeutic agents. It is therefore likely that trials in human ADPKD will be carried out in the near future, especially as methods for assessing disease progression in the short term are now available.

1.1.2. Molecular basis

Cytogenesis

The origin of renal cysts in ADPKD has been subject of numerous studies encompassing a variety of techniques, including micro-dissection, ultrastructural studies, and analysis of fluid within the cysts. It appears that the cysts arise as an outpouching from the renal tubule, resulting from excessive proliferation of tubular cells. All segments of the nephron, including glomeruli, may give rise to cysts. Initially, the cyst lumen is in continuity with the parental nephron. However, as the cysts enlarge, the connection with the nephron is lost. Studies have shown that most cysts larger than 1 mm are disconnected from the tubule and continue to enlarge as independent structures. Contrary to earlier belief, accumulation of glomerular filtrate cannot explain the enlargement and growth of the cyst beyond the earliest stage of cyst formation. This would imply that the clue to the independent enlargement of the cyst must lie in the cyst itself.

The cells lining the cysts are relatively flattened and lack the distinctive apical microvilli brush border normally present in mature renal tubular epithelium, suggesting that they might be dedifferentiated. The lack of an apical microvilli configuration is not due simply to flattening and stretching of the lining epithelium since the enlargement of the cyst is associated with an increase in the number of the lining cells due to cellular proliferation. This view is supported by the fact that proliferation-associated genes (c-myc, Ki-67, and PCNA) are significantly overexpressed in cystic epithelia from ADPKD subjects. Furthermore, in transgenic mice, overexpression of c-myc is associated with development of polycystic kidneys. The epithelial proliferation in the cysts is not haphazard and disorganized but tends to follow the general architectural arrangement present in the parental tubule. The presence of cyst fluid appears to play an important role

in maintaining the cystic configuration and preventing the cellular proliferation to continue uninhibited, which would result in a solid mass rather than a cystic structure.

The cyst fluid in the early stages of cystogenesis is derived from the glomerular filtrate. However, as the cyst connection with the tubule is severed, active fluid secretion by the cyst epithelium is the only mechanism for accumulation of fluid within the cystic cavity. Thus, it seems that in addition to structural dedifferentiation, the cystic epithelial cells also undergo a functional dedifferentiation whereby the epithelium acquires a secretory function as opposed to the normal absorptive function of the tubule.

The cellular mechanism involved in this important deviation from the normal function of parental tubular epithelium is not fully understood. *In vitro* studies on cyst formation in Madin–Derby canine-kidney (MDCK) cell cultures suggest that stimulation of cyclic AMP results in fluid secretion and enlargement of the cyst. Another potential mechanism underlying fluid secretion may be the abnormal location of Na/K-ATPase in cystic epithelium. Human cystic epithelium has the Na/K-ATPase dislocated from its usual basolateral location to an apical location. This results in active secretion of fluid and Na into the cystic cavity. Interestingly, apical location of Na/K-ATPase has been noted early during the embryonic development of collecting tubule (CT), suggesting a dedifferentiation of the cystic epithelium to an early embryonic developmental stage and a primitive evolutionary stage of renal tubules.

Alteration in the extracellular matrix is also suspected to play a role in the growth of cysts. In primary culture, the cystic epithelium elaborates extracellular proteins that are not produced by normal renal cells. Furthermore, immunocytochemical studies and measurement of mRNA levels of matrix constituents identify matrix abnormalities in ADPKD. Similar abnormalities of the extracellular matrix have been demonstrated in a variety of experimental models of renal cystic disease, suggesting a central role for matrix alterations in cystogenesis. Alterations in the cell–matrix interactions may also cause marked functional disturbances and contribute to cyst formation. For example, ADPKD epithelia are more adherent to the matrix than normal epithelia and have decreased motility against growth factor gradients. Such defects may impair the cell movements required for normal morphogenesis of the kidney.

Molecular genetics

ADPKD is a genetically heterogeneous disease with at least two genes involved: The *PKD1* gene located on chromosome 16 (16p.13.3) accounts for approximately 80 ~ 85% of cases, while the *PKD2* gene mapped to chromosome 4 (4q13-q23) accounts for ~10% of ADPKD patients. Rare cases of ADPKD might have both *PKD1* and *PKD2* mutated, with a resulting complex disease pattern. The features of ADPKD caused by mutations in either *PKD1* or *PKD2* are indistinguishable, suggesting that these two genes function in the same biochemical pathway or complex. However, patients with a mutation in *PKD2* reach ESRD on average 15 ~ 20 years later than those with a mutation in *PKD1* (69 years versus 53 years, respectively) (Hateboer et al., 1999).

The *PKD1* gene contains 46 exons and produces a transcript of over 14 kb (Hughes et al., 1995). The first 34 exons are duplicated several times elsewhere on chromosome 16, which has made routine mutation analysis technically demanding. Using a combination of novel polymerase chain reaction strategies, mutations have been identified in all parts of the gene (Rossetti et al., 2001; Thomas et al., 1999). Most mutations are nonsense or frameshifting and predict a truncated protein product. Small deletions and splicing defects are also common. A mutation detection rate in the *PKD1* gene of over 75% has been achieved in some recent reports. Some genotype - phenotype correlations have been documented, with mutations in the 5' end of *PKD1* predicting an earlier age of ESRD and an increased risk of vascular complications. Large deletions of *PKD1* are rare but can include the adjacent *TSC2* gene, thereby causing a contiguous gene deletion syndrome of ADPKD with tuberous sclerosis (TSC) (Brook-Carter et al., 1994). The *PKD2* gene contains 15 exons and is single copy. Mutation analysis has identified mostly loss-of-function changes in families with ADPKD linked to this gene. A milder phenotype is seen with splice-site mutations in *PKD2* compared with truncating mutations (Magistrini et al., 2003).

Several studies have confirmed earlier findings indicating that many different mutations in *PKD1* cause PKD and that most families have unique changes, indicating a significant level of new mutations. It has been estimated that 85% of mutations will be found in the duplicated region of the gene. Most mutations in *PKD2* are unique and are dispersed over the entire gene, without evidence of clustering. The *PKD1* and *PKD2* gene

products are called polycystin-1 (PC1 or PKD1) and polycystin-2 (PC2, PKD2 or TRPP2), respectively. The two proteins will be reviewed in more detail in Sections 1.1.3 and 1.1.4.

Polycystins form an expanding family of proteins composed of members and orthologues in fish, invertebrates, mammals and humans that are widely expressed in various cell types and whose cellular functions are still not well understood. The polycystins can be divided structurally in two main subgroups, the PKD1-like and PKD2-like proteins. They have markedly different molecular architectures and represent the prototypical members of the two general classes of polycystins. PKD2-like proteins include PKD2, PKD2L1 and PKD2L2, and are members of a subfamily of the transient receptor potential (TRP) superfamily of cation channels. The TRP superfamily currently includes 56 related 6-transmembrane domain cation channels classified in 7 superfamilies. Some have weak homology but have potentially similar topological features. The TRP polycystin (TRPP) subfamily, which exists through the animal kingdom but is absent from unicellular organisms, is a newcomer in the TRP channel family (Delmas, 2005). PKD2, PKD2L1 and PKD2L2 are also named TRPP2, TRPP3 and TRPP5, respectively. Sequence analysis of these PKD2 homologues revealed them to be distant relatives of TRP channels (Delmas, 2005).

PKD1 homologues include PKD1, PKD1L1, PKD1L2, PKD1L3 and PKDREJ (PKD receptor for egg jelly), and are large multidomain proteins. Of note, although the C-terminal part of PKD1 homologues has moderate sequence similarity to PKD2 homologues they are not classified as TRPP members. PKDREJ shows homology to the sea urchin receptor for egg jelly and appears to be restrictedly present in the testis. It is hypothesized that it may be involved in human fertilization. Although PKD1 and PKD1L1 lack a structurally defined surface channel pore domain, recent data suggest that PKD1L2, PKD1L3 and PKDREJ contain strong ion-channel signature motifs, suggesting their potential function as pore-forming channel subunits (Li *et al.*, 2003a). Recent advances in research on ADPKD have opened up new opportunities for a better understanding of polycystin functions. An introduction to polycystin members PKD1, PKD2 and TRPP3 will be given in the next Sections.

1.1.3. PKD1

PKD1 is a protein of 4302 amino acids (aa) with an expected molecular mass of 462 kDa. Experimental studies have shown that PKD1 is a highly glycosylated 520 kDa polypeptide present in the plasma membrane (PM). It is predicted to have an extracellular N-terminal segment of 3000 aa, 11 transmembrane (TM) domains and an short intracellular C-terminus (C-terminus) of ~ 200 aa (Fig. 1-1, left). The extracellular portion includes motifs commonly involved in protein–protein and protein–carbohydrate interactions, and a proteolytic G-protein-coupled-receptor proteolytic site. The last 6 TM domains share a moderate degree of sequence similarity to PKD2 homologues. The intracellular C-terminus includes a coiled-coil domain that mediates binding to PKD2, several predicted phosphorylation sites and a putative binding sequence for heterotrimeric G proteins (Boletta & Germino, 2003). PKD1 has been localized to the PM of renal epithelial cells in a basal distribution in relation to cell-cell contacts such as adherent junctions, areas of cell-matrix contact and also in the central apical cilia (Kottgen & Walz, 2005). PKD1 is thought to be a cell–cell and cell-matrix adhesion receptor,

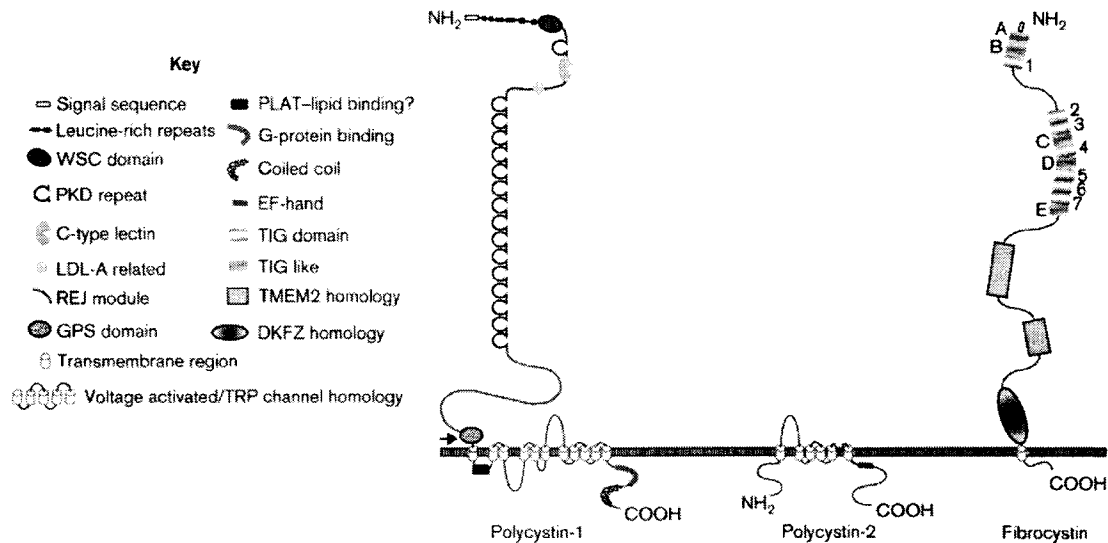


Fig. 1-1. Diagram of the PKD proteins, PKD1, PKD2 and Fibrocystin. Conserved domains and regions of homology with other proteins are shown. The cleavage site in the GP5 domain of PKD1 is arrowed (Harris, 2002).

possibly a member of the immunoglobulin superfamily of cell adhesion molecules, and might function as an atypical G-protein coupled receptor (Boletta & Germino, 2003).

Expression of both PKD1 and PKD2 can alter the Ca permeability of cells. PKD1 is homologous to a receptor in sea urchin sperm, which plays a role in Ca influx during the acrosome reaction (Moy et al., 1996). Expression of the C-terminus of PKD1 increases Ca permeability in *Xenopus* oocytes (Vandorpe et al., 2001). The increase in Ca permeability is associated with the up-regulation of Ca permeable cation channels, suggesting that PKD1 modifies the activity of endogenous cation channels in oocytes. In order to elucidate the mechanism of fluid secretion by ADPKD cysts, Ikeda et al. examined the effect of PKD1 on the PM expression of cystic fibrosis transmembrane conductance regulator (CFTR), a key Cl secretory protein. PKD1 selectively maintains low cell surface expression of CFTR. Moreover, these findings suggest that the malfunction of PKD1 enhances plasma membrane expression of CFTR, thus causing abnormal Cl secretion into the cyst lumen (Ikeda *et al.*, 2006).

1.1.4. PKD2

1.1.4.1. Domain structure

PKD2 is a 110 ~ kDa protein of 968 aa. Hydropathy analysis of PKD2 predicts 6 membrane-spanning domains with both its N- and C-terminus extending into the cytoplasm (Mochizuki et al., 1996) (Fig. 1-1, middle), but so far no experimental data have been presented to support this assumption except for the fact that an antibody directed against the N-terminus of PKD2 failed to stain non-permeabilized transfected cells (Cai *et al.*, 1999), which suggests that at least the N-terminus of PKD2 is located in the cytoplasm and does not protrude into the extracellular space. Between the fifth and sixth membrane-spanning domain a pore-forming region has been postulated. The C-terminus of PKD2 supposedly contains a coiled-coil domain and a Ca-binding EF-hand, but again experimental evidence for the presence of these motifs is lacking. Stretches of the protein share similarities with voltage activated Ca channels and TRP channels, leading investigators to conclude that PKD2 probably has similar functional properties (Boletta & Germino, 2003).

1.1.4.2. Subcellular localization

The cellular location of PKD2 is controversial. Expression studies in *Xenopus* oocytes show that PKD2 is mainly present intracellularly (Vassilev *et al.*, 2001). An intracellular localization of PKD2 was supported by expression studies in LLC-PK1 cells, where PKD2 was found exclusively in the endoplasmic reticulum (ER) (Koulen *et al.*, 2002). PKD2 encompasses an ER-retention signal within its carboxyl terminus, which seems to prevent transport to the cell surface and to keep the protein in the ER membrane when expressed alone (Cai *et al.*, 1999). Deletion mutants for this ER-retention signal translocation to the cell surface and can be detected by immunological and electrophysiological methods (Chen *et al.*, 2001). PKD2 synthesized in CHO cells in the absence of PKD1 remained in the ER, whereas in its presence it reached the PM, which correlated with the fact that novel currents were only seen when PKD2 was synthesized together with PKD1. A truncation mutant of PKD2 which lacked a large portion of the C-terminus including the putative EF-hand and PKD1-interacting domain (R742X mutant) generated no currents (Hanaoka *et al.*, 2000).

Opposing these findings are reports that PKD2 is present at the PM of MDCK cells (Scheffers *et al.*, 2000;Gonzalez-Perret *et al.*, 2001;Luo *et al.*, 2003;Vassilev *et al.*, 2001). PKD2 has been localized to the membrane of renal primary cilium where it forms a channel complex with PKD1 (Nauli *et al.*, 2003). PKD2 has been also localized to basolateral PM, lamellipodia, primary cilia and mitotic spindles (Cai *et al.*, 1999;Foggensteiner *et al.*, 2000;Nauli *et al.*, 2003;Newby *et al.*, 2002;Rundle *et al.*, 2004;Yoder *et al.*, 2002). Interestingly, the PM expression of PKD2 is increased by the use of chemical chaperones.

Recent data have begun to clarify the localization of PKD2. First, Köttgen *et al* reported that PKD2 transport between the ER, Golgi and PM compartments might be directed by the phosphofurin acidic cluster proteins PACS1 and PACS2—two sorting proteins that bind to an acidic cluster in the C-terminal domain of PKD2 (Kottgen & Walz, 2005). Binding of these adaptor proteins to PKD2 is promoted by casein kinase 2 dependent phosphorylation of Ser812. Mutation of Ser812 to Ala or destruction of the acidic cluster abrogates the interaction between PKD2 and the PACS proteins, and increases whole-cell PKD2 currents. Thus, mechanisms that regulate the interaction of

PACS proteins with PKD2 are likely to have a key role in PKD2 transport. Importantly, TRPP3 and TRPP5 lack the PACS-binding acidic cluster, suggesting that their transport is regulated in a different way to that of PKD2. This might explain why TRPP3 is targeted at the cell surface of oocytes, whereas PKD2 is retained in the ER. However, TRPP3 in mammalian culture cells also targets to intracellular compartments. Second, a recently discovered protein called PIGEA14 (PKD2 interactor, Golgi- and ER-associated protein) has been shown to interact with the C-terminus of PKD2. Co-expression of both proteins in HeLa cells and in pig kidney LLC-PK1 cells causes a redistribution of PKD2 and PIGEA14 from the ER to a putative trans-Golgi compartment (Hidaka *et al.*, 2004), indicating that transport of PKD2 is regulated at the ER and the trans-Golgi network. Finally, the PKD2 amino-terminus contains signal domains that are required for PM and cilia localizations. PM, but not cilia, localization of PKD2 is regulated by glycogen synthase kinase 3 phosphorylation of Ser76 (Streets *et al.*, 2006), whereas another N-terminal motif (R6V7xP8) is necessary for localization in cilia (Geng *et al.*, 2006). The study by Geng *et al.* (Geng *et al.*, 2006) also provides evidence that PKD2 transport to cilia is independent of PKD1 because PKD2 mutants lacking the PKD1 interaction region still transport to cilia.

Therefore, it is clear, there is a significant controversy over the PM versus intracellular (eg ER membrane) localization of PKD2. It is not sure whether cell type difference is sufficient to account for the discrepancy.

1.1.4.3. Ion channel properties and pharmacology of PKD2

The first report on the channel properties of PKD2 was based on the expression of the human PKD2 complementary DNA in transiently transfected CHO cells (Hanaoka *et al.*, 2000). Measurements of whole-cell currents showed novel cation currents with slightly outwardly rectifying characteristics. La ions, which inhibit nonselective cation channels, and niflumic acid, which inhibits nonselective cation and Cl channels, blocked the current in a dose-dependent manner. Consistent with these observations was the finding that PKD2 is permeable to Ca, Na and Cs (with permeability ratios of 1.12: 1: 0.57, $P_{Ca} : P_{Na} : P_{Cs}$), but not Cl ions.

The main observation of the first report was confirmed by another group, which expressed the murine PKD2 cDNA in *Xenopus* oocytes, although there were some differences (Chen *et al.*, 2001). Whole-cell conductance of *Xenopus* oocytes did not change after injection of the murine PKD2 cDNA, consistent with the predominant intracellular localization of full-length PKD2, although the uptake of radioactive Ca ions increased 4-fold. Using cell-attached or excised membrane patches, again a novel nonselective cation channel activity was detected which conducted both monovalent (Na, K, Li, Rb and NH₄) and divalent (Ca, Sr and Ba) ions and was inhibited by La but not nifedipine, a blocker of voltage-dependent Ca channels, ryanodine and inositol 1,4,5-trisphosphate (IP₃) receptors (Vassilev *et al.*, 2001). This time, however, the channel was slightly inwardly rectifying and no single channels recordings were observed in the presence of Cs (permeability ratios were 0.14: 1: 0.73, P_{Na}: P_K: P_{NH₄}, and 0.21:1, P_{Ca}:P_K). The addition of 1 μM Ca to the bath solution transiently increased the open probability (P_o) of PKD2, but millimolar concentrations of Ca inhibited currents. The findings in *Xenopus oocytes* were extended to non-transfected and transfected inner medullary collecting duct (IMCD) cells in which very similar conductance and permeability ratios for different cations were obtained as in oocytes (Luo *et al.*, 2003).

Koulen *et al.* stably expressed PKD2 in LLC-PK1 cells, isolated ER-enriched membrane vesicles, and reconstituted onto planar lipid bilayer to study PKD2 channel function (Koulen *et al.*, 2002). They demonstrated that PKD2 exhibited a large conductance, nonselective, voltage-dependent cation channel activity. Using various organic cations of different sizes, it was estimated that the pore diameter of PKD2 was at least 11 Å (Anyatonwu & Ehrlich, 2005). A truncated PKD2 protein, mutant L703X, showed a lower conductance (28 pS vs 114 pS for full-length PKD2 in the presence of Ba) and required a larger negative membrane potential for activation. Confirming previous results, intracellular free Ca concentration ([Ca]_i) up to 1260 μM increased the P_o of PKD2, whereas higher concentrations were inhibitory; no such modulatory activity of Ca was observed for L703X. Phosphorylation of the serine residue at position 812, possibly by casein kinase 2, appears to increase the calcium sensitivity of PKD2 (Cai *et al.*, 2004).

Another area of controversy in PKD2 arises from the reported discrepancy in its channel properties. Endogenous PKD2 in mouse IMCD cells is Ca permeable, cation selective and has a greater selectivity for K over Na ($P_{Na}: P_K = 0.19$) (Luo *et al.*, 2003). Over the physiological potential range -100 to -50 mV this channel does not demonstrate any voltage dependence. The PKD2 cation channel in human placenta cells, on the other hand, does not discriminate between Na and K (Gonzalez-Perret *et al.*, 2001). In placenta cells, PKD2 is slightly more selective for Ca than monovalent cations, inhibited by Gd, and shows voltage-dependent P_o at positive potentials, with a reduction in P_o at +40 and +60 mV. Overexpression of PKD2 in LLC-PK1 cells produces ER located cation channels that are also Ca permeable and, like in the human placenta, shows reduced P_o at positive potentials. Intracellular Ca also regulates the channels, with concentrations up to 1260 μ M activating the channels; further increases in Ca concentration produced inhibition. Expression in oocytes (Vassilev *et al.*, 2001) produced channels that are similar to those observed in mouse CD, with a lower selectivity to Na compared to K. These channels are also activated by 1 μ M Ca, although activation is transient. They also have a lower Ca selectivity, with $P_{Ca}: P_K = 0.21$. Finally, studies using transfected CHO cells have produced Ca permeable, cation selective channels that are inhibited by niflumic acid. These channels were recorded in the whole cell configuration, and currents detected over the potential range of +100 to -100 mV, suggesting that, in contrast to other studies, the PKD2 channels in this system are active at positive potentials.

PKD2 as an ER channel

PKD2 might act as a Ca-release channel in ER membranes, which amplifies Ca transients initiated by IP₃-generating PM receptors (Koulen *et al.*, 2002). This led to the suggestion that PKD2 is a novel type of intracellular receptor that might be involved in mediating Ca-induced Ca release. PKD2 seems to be directly activated by Ca and displays a bell-shaped dependence on cytoplasmic Ca. Although it is not yet clear whether the Ca-binding EF-hand of PKD2 is involved in Ca-dependent modulation of PKD2, it is worth noting that pathogenic PKD2 mutants with a premature termination of the peptide chain in their C-tail lost their ability to detect Ca. However, TRPP3 artificial truncation mutants lacking the EF-hand show Ca-activated channel activities, suggesting

that, at least for TRPP3, the EF-hand and other parts of the C-tail are not key determinants of the Ca-dependent activation (Li *et al.*, 2002).

Phosphorylation of Ser812 by a putative casein kinase 2 results in a significant increase in the sensitivity of the PKD2 channel to Ca stimulation (Cai *et al.*, 2004). The S812A substitution shifts the Ca dependence such that PKD2-S812A has a maximum P_o at 10-fold higher Ca concentrations ($\sim 3 \mu\text{M} [\text{Ca}]_i$) than phosphorylated PKD2. Reticular PKD2 is therefore likely to have enhanced Ca sensitivity, as casein kinase 2 is opportunistically associated with the ER and most PKD2 channels are phosphorylated *in vivo* (Cai *et al.*, 2004).

In line with a role for ER-localized PKD2 in regulating intracellular Ca, PKD2 \pm vascular smooth muscle cells have altered intracellular Ca homeostasis (Qian *et al.*, 2003). Moreover, PKD2 has been recently shown to interact functionally and physically with IP₃ receptor in a *Xenopus* oocyte Ca imaging system (Li *et al.*, 2005b). Overexpression of PKD2 in oocytes, as well as type I IP₃ receptor, significantly prolonged the half-decay time of IP₃-induced Ca transients. However, overexpressing the disease-associated PC2 mutants, the point mutation D511V, and the C-terminally truncated mutation R742X did not alter the half-decay time. Co-immunoprecipitation assays indicated that PC2 physically interacts with IP₃ receptor through its C terminus. Therefore, mutations in PC2 could result in the misregulation of intracellular Ca signaling, which in turn could contribute to the pathology of ADPKD.

Cai *et al.* first reported that native or transfected PKD2 was accumulated in the ER (Cai *et al.*, 1999). While it was expected that a channel protein destined to be forwarded to the PM would show considerable expression in the ER while en route to the PM, Cai *et al.* could not detect a significant amount of PKD2 in the PM (Cai *et al.*, 1999). In fact, careful EndoH/PNGaseF experiments revealed that PKD2 could not get past the ER. Deletion studies identified a cluster of acidic residues in the C-terminal cytosolic tail of PKD2 that was responsible for the retention of the protein in the ER. Interestingly, the pathogenic mutant PKD2 (R742X) which lacked the ER retention signal was forwarded to the PM and displayed constitutive channel activity (Chen *et al.*, 2001). It is possible that PM expression of PKD2 is not sufficient for function, but perhaps interactions with other subunits are needed for channel activity. It was subsequently shown that PKD2

functioned as a novel intracellular Ca channel, which was activated in response to increases in intracellular Ca concentration. Moreover, PKD2 activity was solely dependent on intracellular rather than extracellular Ca. Therefore these data indicated that PKD2 functioned exclusively as an intracellular Ca induced Ca release channel in kidney epithelial cells. The implication of these findings was that it could enhance local intracellular Ca concentration in response to an initial rise in Ca and therefore, PKD2 could regulate intracellular Ca concentration in a localized fashion.

Subsequent reports confirmed the role of PKD2 in intracellular Ca release and further showed that it interacted with the isoform 1 of the IP₃ receptor (Li *et al.*, 2005a). However, PKD2 overexpression augmented mostly the duration rather than the amplitude of the Ca release transient. Moreover, overexpression of the naturally occurring mutant PKD2-D511V had a dominant negative effect on Ca release transients (Li *et al.*, 2005b) lending support to the idea that endogenous PKD2 was likely to function as an intracellular Ca-induced Ca release channel. Experiments in vascular smooth muscle cells (Mene, 2006) and immortalized lymphoblasts (Reynolds *et al.*, 1999) from PKD2 knock out mice and ADPKD patients, respectively, showed that PKD2 played a role in G protein coupled receptor-induced Ca signaling, but the possibility that PKD2 could have also contributed to Ca signaling through Ca influx was not clearly addressed in these studies. Overall, despite the differences, there is significant gain- and loss-of-function evidence to suggest that in addition to residing in the ER, PKD2 also has a functional role in regulating intracellular Ca release in response to localized changes in intracellular Ca.

PKD2 as a PM channel

Functional expression of PKD2 as an ion channel was first reported by Hanaoka *et al.* (Hanaoka *et al.*, 2000). In this study, it was demonstrated that PKD2 alone was unable to form a functional channel in CHO-K1 cells, but in association with PKD1, PKD2 displayed channel activity. It was also shown that PKD1 facilitated targeting of PKD2 to the PM, which was necessary for channel activity. In further support of the relevance of the interaction to ADPKD, naturally occurring mutations in PKD1 or PKD2 that would eliminate their interaction resulted in loss of channel activity. Therefore, it set the stage for functional expression of PKD2 and indicated that the role of PKD1 was simply to

chaperone PKD2 to the PM, where PKD2 formed a constitutively active channel. Subsequently, single channel studies in placental preparations, expressed PKD2 in *Xenopus* oocytes and HEK 293 cells, and in vitro translated purified PKD2 in cell-free systems further characterized PKD activity. Despite subtle disparities among these studies, it was concluded that PKD2 could form a functional channel in the PM with constitutive activity upon overexpression. It allowed nonselective passing of cations, with slightly higher selectivity for Ca over Na and K, but higher conductance in K (Cantiello, 2004). However, the high single channel conductance (100 ~ 200 pS) in combination with the relatively high P_o (~20-40%) (Hanaoka *et al.*, 2000; Luo *et al.*, 2003) did not correlate well with the moderate amplitude of whole cell currents (several hundreds pA at -100 mV) in cells over-expressing PKD2. This, along with the observation that the vast amount of PKD2 was in the ER raised the question of whether PKD2 alone or even in combination with PKD1 could actually form a functional channel in the PM. It is now accepted that PKD2 can function at the PM, but its activity there is under complex regulation involving shuttling between ER and PM, protein-protein interactions, and modes of activation. Specifically, it has been shown that the amount of PKD2 in the PM is dynamically regulated by interacting proteins, including PKD1, PIGEA-14, casein kinase 2, glycogen synthase kinase 3 (GSK3), and epidermal growth factor receptor (EGFR) (Luo *et al.*, 2003; Tsiokas *et al.*, 2006).

Regulated trafficking between ER and PM

Köttgen *et al.* reasoned that the ER and PM pools of PKD2 must be dynamically regulated so that PKD2 activity can be tightly controlled (Kottgen, 2007). They showed that serine phosphorylation within the ER retention sequence by casein kinase 2 reconstituted a binding site for a group of PACS 1 and 2. Binding of PACS2 to PKD2 prevented its movement to the PM. Conversion of S812 to A within the acidic cluster in human PKD2 resulted in increased expression in the PM in cultured kidney epithelial cells (Kottgen, 2007). Support for this model was obtained by the heterologous expression of wild type and S812A mutant form of PKD2 in *Xenopus* oocytes. Injection of wild type PKD2 cRNA had no significant effect on channel activity, whereas injection of the S812A mutant resulted in large Na currents mediated by PKD2. In support of the

idea that protein phosphorylation may regulate the amount of PKD2 in the PM, Streets *et al.* (Streets *et al.*, 2006) showed that constitutive phosphorylation of S76 of human PKD2 by GSK3 was necessary for its targeting to the PM. Mutation of S76 (or S80 in zebrafish) to A resulted in PKD2 accumulation in intracellular compartments and failed to rescue the cystic phenotype in zebrafish injected with a PKD2-specific antisense morpholino oligonucleotide (Streets *et al.*, 2006). Interestingly, the S76/S80 mutation did not affect the ciliary expression of PKD2, questioning the functional role of PKD2 in the primary cilium in zebrafish. It would be interesting to know whether the S76/S80 mutation affected PKD2 channel function in the ER. In a separate study, Hidaka *et al.* (Hidaka *et al.*, 2004) identified PIGEA-14 as an interacting protein with PKD2 and proposed that binding to PIGEA-14 facilitated the movement of PKD2 from the ER to the Golgi. In conclusion, all these studies illustrate the fact that the amount of PKD2 in the PM can be regulated. Further, this regulation has functional consequences as it may represent a surrogate mode of activation, if PKD2 forms a constitutively active channel in physiological conditions.

Modes of activation of PKD2

So far, only a very limited data are available on how PKD2 is activated. In particular it is not known whether there is a natural ligand for PKD2. Consistent with the biochemical interaction between PKD2 and PKD1 (Qian *et al.*, 1997; Tsiokas *et al.*, 1997), PKD1 was able to reactivate the channel activity of PKD2 in lipid bilayer membranes (Xu *et al.*, 2003). The interaction of PKD2 with cytoskeletal components such as Hax-1 (Gallagher *et al.*, 2000), troponin I (Li *et al.*, 2003b), tropomyosin-1 (Li *et al.*, 2003c) and α -actinin (Li *et al.*, 2005a) could also be very important in such a scenario, and indeed it was shown for α -actinin that it significantly increases the channel activity of PKD2. Employing membrane preparations from human syncytiotrophoblast cells, it was demonstrated that the activity of a cation channel, possibly PKD2, was modulated by gelsolin and the polymerization status of the actin cytoskeleton (Montalbetti *et al.*, 2005).

Other factors directly or indirectly modulating the activity of PKD2 are pH, hydro-osmotic pressure, vasopressin, epidermal growth factor (EGF) and ATP. The channel

activity of full-length PKD2 (Gonzalez-Perrett *et al.*, 2002;Montalbetti *et al.*, 2005) and its R742X truncation mutant was inhibited by a decreased extracellular pH (Chen *et al.*, 2001). Using again apical membrane preparations from human syncytiophoblast cells, it was also shown that PKD2 channel activity can be modulated by hydro-osmotic pressure (Montalbetti *et al.*, 2005). LLC-PK1 cells stably transfected with the human PKD2 cDNA were used to demonstrated that PKD2 can be activated by vasopressin (Koulen *et al.*, 2002), EGF (apparently through releasing the inhibition by phosphatidylinositol-4,5-bisphosphate) (Ma *et al.*, 2005) and ATP (Gallagher *et al.*, 2006). In addition to acting as a nonselective cation channel itself, PKD2 also interacts with the IP₃ receptor and may thereby influence [Ca]_i (Li *et al.*, 2005b).

1.1.4.4. Physiological roles

Biological relevance, emerging and established roles of PKD2

The most exciting data indicate that PKD2 (together with PKD1) plays an essential role for mechanosensation of kidney epithelial cells by primary cilia (Nauli *et al.*, 2003). PKD2 is believed to be responsible for the flow-mediated rise in [Ca]_i and thereby possibly for determining the correct width of renal tubules. At this point it is not clear how the mechanical stimulus is transmitted through PKD2: whether it is a direct action on PKD2 or PKD1, or whether other proteins sense the mechanical stimulation and subsequently act on PKD2. Experiments performed with *C. elegans* have provided evidence for a chemosensory role of cilia (Barr & Sternberg, 1999;Barr *et al.*, 2001) and it therefore can not be ruled out that the orthologue of PKD2 is activated by chemical stimuli in the worm. The activation of PKD2, possibly by phosphorylation, in turn can inhibit the cell cycle through its interaction with the helix-loop-helix protein Id2 (Li *et al.*, 2005a). Such a scenario is consistent with the finding that cyst wall epithelial cells proliferate at a higher rate than regular tubular epithelial cells (Lanoix *et al.*, 1996;Ramasubbu *et al.*, 1998).

Another surprising finding in PKD2 knockout mice was the development of *situs inversus* (Pennekamp *et al.*, 2002), thus indicating that PKD2 also plays an important role in axis differentiation. A phenotypic connection between PKD and *situs inversus*, for which primary cilia may be the key, had already been made earlier for other proteins

(Mochizuki *et al.*, 1998; Murcia *et al.*, 2000). The correct placement of the internal organs, eg of the heart on the left and the liver on the right, may already be determined very early on (Levin *et al.*, 2002), although the best investigated stage of development represents that of the primitive node. The primitive node is a temporary structure during embryonic development, which serves as an essential signaling center for left-right axis development. Cells in the primitive node elaborate primary cilia, but surprisingly some of these cilia are motile - they are able to rotate, and this rotational movement has been proposed to break the symmetry of the left-right axis (Cartwright *et al.*, 2004). There is another population of cells in the primitive node, which have immotile cilia that contain PKD2. According to the current model, the motile cilia are responsible for generating a gradient for an extracellular signaling molecule which in turn is transduced into an intracellular Ca signal by PKD2 (McGrath *et al.*, 2003). It is noteworthy that *Pkd1* knockout mice do not exhibit *situs inversus*, which is consistent with the absence of PKD1 in primary cilia of the embryo node (Karcher *et al.*, 2005).

There are some other functions associated with PKD2. A recent study using *C. elegans* has shown that KLP-6, a member of the kinesin-3 family, is required for PKD2 localization and function within cilia, and proposed that KLP-6 and the polycystins function as an evolutionarily conserved ciliary unit (Peden & Barr, 2005). In the sea urchin, the PKD2 orthologue (suPKD2) localizes exclusively to the PM of sperm acrosomal vesicles, where it associates with suREJ3, a PKD1 homologue (Neill *et al.*, 2004). Neill *et al.* have proposed that suPKD2 and suREJ3 act as a nonselective cation channel mediating the acrosome reaction, a step crucial in the fertilization of sea urchin and human, and involved Na and Ca influx that drive the exocytosis of acrosomal vesicles when a sperm contacts the egg jelly. Interestingly, suREJ3 most resembles PKDREJ, which is expressed exclusively in mammalian testis (Galindo *et al.*, 2004). It is tempting to speculate that PKDREJ also interacts with a PKD2 homologue in mammalian testis and that the putative complex may play a role in mammalian fertilization. It should be noted that male sterility has been observed in ADPKD patients (Manno *et al.*, 2005). Studies in *Drosophila* have also provided clues to the role of polycystin homologues in fertilization. Heterologous expression of *Drosophila* PKD2 in *Drosophila* S2 cells

produces a novel channel activity in the PM that is activated transiently by micromolar concentrations of Ca (Venglarik et al., 2004).

PKD1–PKD2 complex

Although progress in understanding the function of PKD2 has been relatively rapid, one major obstacle hampering investigation of PKD1 and PKD1/PKD2 functions has been the lack of an efficient expression system for the large, full-length recombinant PKD1. Using sympathetic neurons as a novel expression system in which it was possible to deliver stoichiometric concentrations of cDNAs and to use overexpressed ion channels as real-time signaling biosensor (Delmas *et al.*, 2002), people could study the functions of recombinant PKD1-PKD2 complexes and their dynamic regulations in living cells. Using this approach, it was demonstrated that PKD1 and PKD2 form functionally-associated 'subunits' of a heteromultimeric receptor-ion channel signaling complex and that structural rearrangement of this complex dynamically regulates PKD2 channel activity and triggers G-protein activation (Fig. 1-2). This coupling mechanism represents a new type of transduction device that may account for the multifunctional roles of polycystins in the regulation of cell differentiation, proliferation and ion transport.

PKD1-PKD2 complex functionally reconstitutes a novel surface Ca-permeant nonselective cation channel, in line with recent electrophysiological and biochemical findings (Hanaoka *et al.*, 2000;Newby *et al.*, 2002). Pharmacological and permeation properties of PKD1-PKD2 complex resemble those of recombinant homomeric PKD2 or native PKD2 channels in human syncytiotrophoblasts reconstituted in lipid bilayer (Gonzalez-Perret *et al.*, 2001;Gonzalez-Perrett *et al.*, 2002). Channel activity is not observed when the C-terminal interaction between PKD1 and PKD2 is inhibited, indicating that co-assembly of PKD1 and PKD2 is required for the proper targeting of PKD2 to the PM. Together with the observation that an anti-mPKD2 antibody blocks PKD1-PKD2 channel activity, it strongly suggests that PKD2 is the pore-forming subunit of the PKD1-PKD2 complex (Delmas *et al.*, 2002;Hanaoka *et al.*, 2000). Several investigators have demonstrated that PKD1 and PKD2 interact physically with each

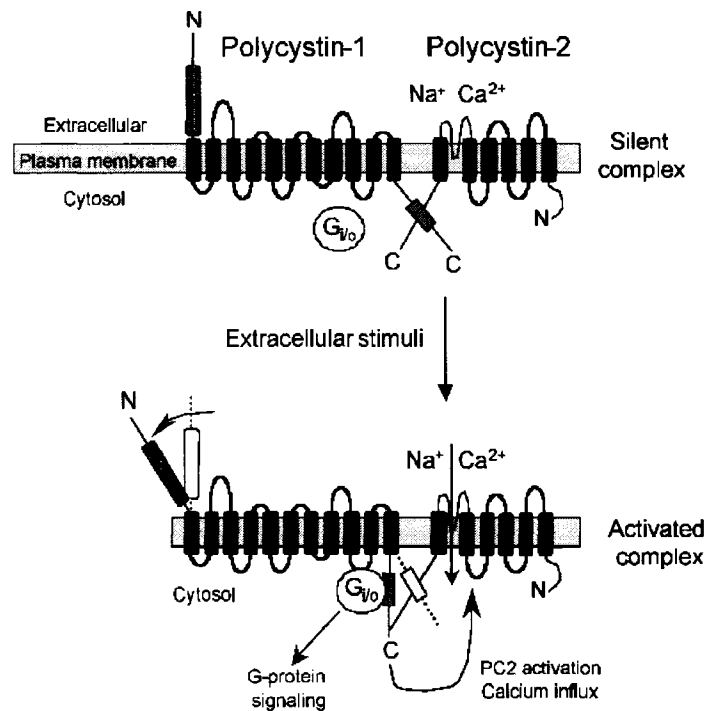


Fig. 1-2. Model for the activation of polycystin complex. *Upper:* PKD1 and PKD2 co-assemble in the plasma membrane via their C-termini to form a stable polycystin complex. *Bottom:* extracellular stimuli (antibody binding or flow) acting on the N-terminal extracellular domain of PKD1 causes a structural rearrangement of the polycystin complex that unmasks the G-protein binding site located on the C-terminus of PKD1 (gray boxes) and opens PKD2. This leads to bi-directional signaling events via $G_{i/o}$ G-proteins and intracellular calcium (Delmas, 2004).

other. The coiled structure in the cytoplasmic C-terminus of PKD1 is essential for binding PKD2 while the domain of PKD2 responsible for binding PKD1 is within the last 97 amino acids of this protein. This interaction suggests that PKD1 and PKD2 may function through a common signaling pathway. It has also been suggested that the binding of PKD2 is required to provide stability to PKD1 and prevent its rapid degradation, which is mediated by the PEST (Pro-Glu-Ser-Thr) sequence present in its C-terminus.

In the complex, PKD1 seems to regulate PKD2 channel activity (Delmas, 2004; Xu *et al.*, 2003). Conversely, PKD2 binding to PKD1 reduces the ability of PKD1 to constitutively activate G-proteins, possibly by competitive interaction (Delmas *et al.*, 2002; Delmas, 2004). These data support the view that, in addition to its ion channel function, PKD2 also regulates the downstream effects of PKD1 on its target effectors.

Therefore the balance between PKD2 and PKD1 expression and their normal interaction, which may be disrupted in ADPKD, might have a crucial role in normal PKD1–PKD2 signaling.

PKD2-interacting proteins

In addition to PKD1, PACS1 and PACS2, PKD2 interacts with a diverse range of other proteins (Qamar *et al.*, 2007). Interactions with Hax1, α -actinin and CD2-AP (CD2-associated protein), tropomyosin-1 and troponin I all suggest that PKD2 regulates or is regulated by the actin cytoskeleton (Lehtonen *et al.*, 2000; Li *et al.*, 2005a; Gallagher *et al.*, 2000). This is supported by loss of physical-stress-induced PKD2 activity in the presence of the actin cytoskeleton disrupter cytochalasin D (Montalbetti *et al.*, 2005). The functional implications of a PKD2 interaction with another TRP channel, TRPC1, remain unknown, but the recent identification of TRPC1 as a stretch-activated cation channel further supports the hypothesis that PKD2 forms part of a mechanosensitive channel complex (Tsiokas *et al.*, 1999). The recently described interaction of PKD2 with IP₃R suggests a central role of PKD2 in regulating intracellular Ca concentrations (Li *et al.*, 2005b). Thus, PKD2 may interact with different partners in different tissues for executing various physiological roles.

1.2. Autosomal recessive polycystic kidney disease (ARPKD)

1.2.1. Clinical features

ARPKD was first recognized as a distinct morphologic form of cystic disease in 1902 (Osathanondh V & Potter EL, 1964). ARPKD is a pediatric disease that primarily affects the CD of the kidney and is associated with biliary duct ectasia and portal fibrosis in the liver. ARPKD belongs to a group of congenital hepatorenal fibrocystic syndromes characterized by dual renal and hepatic involvement of variable severity. Renal manifestations are characterized by both ectasia and cystic dilation of renal CT (Sweeney, Jr. & Avner, 2006). ARPKD has a high mortality rate (40 ~ 60%) in the newborn period and accounts for ~35% of all ESRD in children.

Detailed studies of salt and water transport in renal cysts detached from the nephron of origin and primary cultures of renal epithelial cells isolated from ADPKD

patients suggest that fluid accumulation in the cysts is the result of NaCl secretion. Grantham and co-workers demonstrated that cAMP-stimulated, cystic fibrosis transmembrane conductance regulator (CFTR)-dependent Cl secretion contributes to fluid accumulation in renal cysts. Because the cysts are detached from the segment of origin, it is difficult to identify the precise alterations in tubule transport that accompany development of a renal cyst in ADPKD. In contrast, the predominant site of renal disease in ARPKD is the CD, and late in the disease most of the kidney is composed of dilated, fluid-filled CD rather than isolated, detached cysts.

There also exists a contrary report that the Cl secretory responses due to elevation of cAMP or Ca are the same in normal and cystic cells, whereas amiloride-sensitive Na absorption is significantly reduced in cystic cells (Veizis *et al.*, 2003). It may be due to different types of human and animal ARPKD. Although human ARPKD has only one type, i.e., one due to mutations in FPC, animals have several models of ARPKDs, eg, *orpk*, *pck*, etc. These results suggest that dys-regulation of principal cell Na reabsorption may contribute to the CD dilatation and fluid retention in the kidney characteristic of ARPKD. Aberrant ion transport in the kidney is not linked directly to the genetic defects that cause PKD but may play an important role in the rate of disease progression. In ADPKD, fluid accumulation driven by NaCl secretion increases cyst size, leading to kidney parenchymal destruction and, ultimately, renal failure. Little is known about ion transport in ARPKD, mostly due to the lack of relevant experimental systems (Blyth & Ockenden, 1971;Guay-Woodford, 2003;Harris & Rossetti, 2004).

1.2.2. Genetics

Despite the variable clinical spectrum of ARPKD, genetic linkage studies indicate that mutations at a single locus, *PKHD1* (polycystic kidney and hepatic disease 1), mapped to human chromosome region 6p21.1 - p12 are responsible for all phenotypes of ARPKD (Guay-Woodford *et al.*, 1995;Zerres *et al.*, 1998). *PKHD1* is amongst the largest disease genes identified to date in the human genome, with a complicated transcription profile that probably generates multiple variants of the fibrocystin protein. Both *PKHD1* and its mouse orthologue encode a complex and extensive array of splice variants, with most abundant transcriptional expression in fetal and adult kidney and weaker expression

in other tissues including liver and pancreas (Harris & Rossetti, 2004; Nagasawa *et al.*, 2002; Ward *et al.*, 2002; Onuchic *et al.*, 2002). The mouse and human protein sequences are 73% identical overall and 55% identical in the C-terminus (Harris & Rossetti, 2004; Nagasawa *et al.*, 2002).

1.2.3. The ARPKD protein, fibrocystin (FPC)

FPC (also known as polyductin and tigmin) is a novel integral membrane protein of 4074 aa (4059 aa in mouse) with a signal peptide, an extensive (3860 aa) highly glycosylated, N-terminal extracellular region, a single TM domain, and a short (192 aa) cytoplasmic tail containing four putative cAMP/cGMP phosphorylation sites (Fig. 1-1, right) (Nagasawa *et al.*, 2002; Onuchic *et al.*, 2002; Ward *et al.*, 2002). FPC has areas of similarity to several known proteins; this provides some clues to the function of the protein. The function of this protein remains to be determined, but the structure and homology suggest a role as a receptor protein involved in the regulation of cellular adhesion, repulsion, proliferation, and/or the regulation and maintenance of renal CD and hepatic bile ducts (Onuchic *et al.*, 2002; Ward *et al.*, 2002). Delineation of the normal role of FPC in the development, differentiation, and maintenance of renal CD and hepatic bile ducts will provide important insights into the way that mutations in a single gene cause cyst formation with a wide variation in cellular and clinical phenotype. When FPC was initially identified, there were no known homologues until the identification of FPC-L (Hogan *et al.*, 2003). This protein is encoded by the *PKHDLL1* gene at chromosome region 8q23. FPC-L (4243 aa; 466 kDa) has homology (overall identity of 25% and similarity of 42%) within the extracellular region to FPC. Despite its similarity to FPC, mutation analysis indicates that it is not associated with ARPKD or any renal or biliary phenotype. Indeed, expression studies suggest a possible role in cellular immunity with up-regulation in activated T-cells (Hogan *et al.*, 2003).

During embryogenesis, FPC is expressed in epithelial derivatives, including ureteric bud branches, intra- and extra-hepatic bile ducts, and pancreatic ducts (Ward *et al.*, 2002). This temporal and spatial expression pattern of FPC parallels the CD and biliary epithelial pathology of ARPKD. Immunohistochemical analysis demonstrates that FPC is expressed along the apical and upper lateral cell surface and within the cytoplasm

in cortical and medullary CD epithelia (Nagao *et al.*, 1995; Menezes *et al.*, 2004), biliary and pancreatic duct epithelia, and thick ascending limbs of Henle (Menezes *et al.*, 2004). Immunofluorescence studies have revealed that, like other cystoproteins, including PKD1 and PKD2, FPC localizes in centrosomes, basal bodies or primary apical cilia of renal epithelial cells (Menezes *et al.*, 2004; Ward *et al.*, 2002; Ward *et al.*, 2002) and in the cilia of cholangiocytes of isolated intrahepatic bile ducts (Masyuk *et al.*, 2003).

1.2.4. Cellular pathophysiology of ARPKD

In ADPKD, evidence indicates that Cl is secreted via a cAMP-mediated co-transport mechanism in the basolateral membrane and CFTR in the apical membrane, leading to expansion of cysts, especially after they have detached from the nephron of origin (Belibi *et al.*, 2004; Sullivan *et al.*, 1998). This does not appear to be the case in ARPKD. By using a genetic complementation approach, the BPK mouse (deficient in B-cell progenitor kinase) has been crossed with a CFTR knockout mouse. The results demonstrate that the absence of CFTR does not alter the course of renal or biliary cyst development or growth (Nakanishi *et al.*, 2001).

Cross-link between ADPKD and ARPKD

Common features of ADPKD and ARPKD include renal CD as the predominant site of cystogenesis, abnormal epithelial solute transport, increased cell proliferation and de-differentiation, mis-targeted Na/K ATPase to the apical membrane, thickening and disorganization of the basement membrane, increased cAMP levels, altered localization of polycystins and FPC in renal primary cilia. Although ADPKD and ARPKD exhibit similarities in cystic phenotypes, whether there exist common pathogenic pathways or molecular links between PKD1/PKD2 and FPC remains obscure. Recently, some people have speculated that FPC may interact with the PKD1 and PKD2, and also regulate $[Ca]_i$ (Torres & Harris, 2007). PKD1, PKD2 and FPC co-localize on cilia and in other apical, lateral, and basal locations. Cilia may be one of the sites that link ADPKD and ARPKD. The expression of these PKD proteins in cilia, basal bodies, and intercellular junctions and at focal adhesions suggests that there may be common signaling pathways for cyst

formation through the abnormal integration of signal transduction pathways, as shown in Fig. 1-3. The pathogenic link between PKD proteins expression in cilia, basal bodies, and centrosomes, on the one hand, and the renal cystic phenotype, on the other hand, remains unknown. However, it was demonstrated that physical manipulation of the primary cilium, including bending or removal, elicits changes in Ca flux demonstrating that cilia

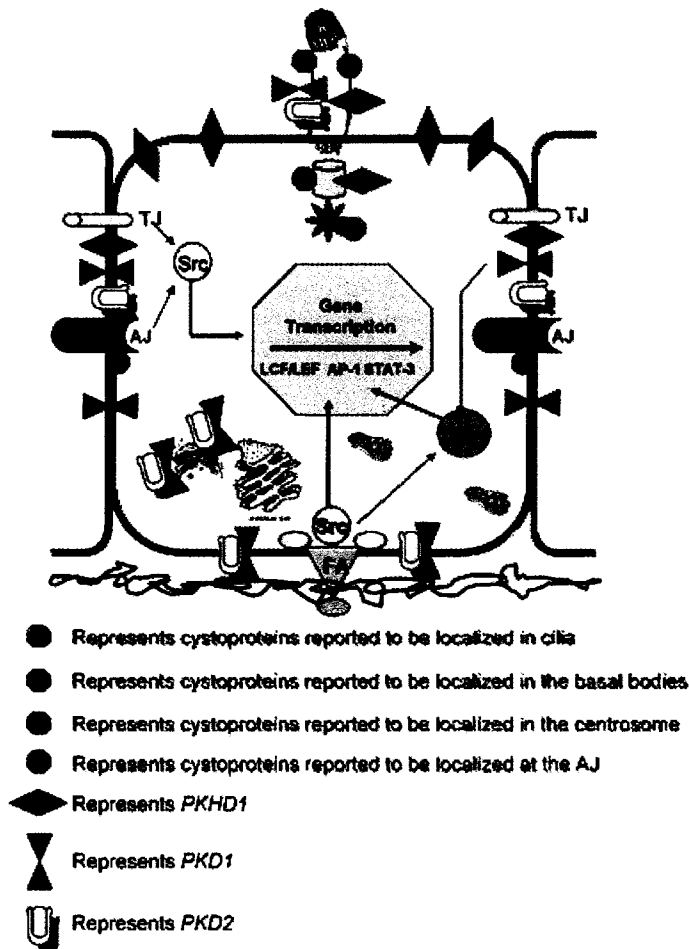


Fig. 1-3. PKD proteins in multimeric complexes. Summary of recent advances suggesting that PKD proteins exist in multimeric protein complexes and function at distinct sites within epithelial cells that include: basal cell-matrix focal adhesion sites to regulate epithelial cell adhesion and migration; apical-lateral cell-cell adherens sites to regulate differentiated cell shape; within Golgi; apical-central ciliary sites to sense flow and regulate tubule diameter. Expression and signaling from multiple sites establishes signaling platforms and feedback loops that regulate cell growth, proliferation, and dedifferentiation. (AJ: adherens junction, TJ: tight junction) (Sweeney, Jr. & Avner, 2006).

can function as mechanosensors or chemosensors to sense fluid movement or ionic composition in the kidney. The physiological consequence of alterations of calcium concentrations in the renal CT epithelium remains to be clearly defined, particularly in ARPKD (Sweeney, Jr. & Avner, 2006). Of note, the only binding partner for FPC identified to date is Ca-modulating cyclophilin ligand, a protein involved in Ca signaling (Nagano *et al.*, 2005). In addition, PKD1 has been shown to form multi-subunit complexes with many adhesion proteins and it may activate a number of intracellular signaling pathways regulating fluid secretion, proliferation, cell polarity, differentiation and cell cycle (Igarashi & Somlo, 2002). The exact functions of FPC are not known, but

it may be receptors of growth signals and also participate in mediating cell adhesion. This fact may create an obvious link between these diseases.

1.3. Epithelial Na channel (ENaC)

1.3.1. Structure and localization

The amiloride-sensitive ENaC is a member of the degenerin/epithelial sodium channel superfamily. ENaC is composed of three homologous subunits (α , β , and γ) that contain two transmembrane domains, a large extracellular loop, and short intracellular amino and carboxyl termini. The full-length forms are 90 ~ 95 kDa in size (Bhalla et al., 2006). ENaC expressed in oocytes has a presumed 2 α : β : γ stoichiometry (Firsov et al., 1998), although alternate subunit stoichiometries have also been proposed (Garty & Palmer, 1997). ENaC is expressed at the apical surface of polarized epithelia and plays a critical role in fluid and electrolyte homeostasis and widely expressed in absorptive epithelia such as the aldosterone-sensitive distal nephron, the distal colon, respiratory epithelia, sweat and salivary ducts. It is localized in amphibian skin, kidney (distal convoluted tubule, connecting tubule, cortical CT, outer and inner medullary CT), unitary bladder, intestine, lung, sweat, salivary ducts, salt-taste cells, excitable cells, mechanosensory cells, and other cells (Cultured endothelial cells from brain microvessels and cells from the thyroid gland) (Garty & Palmer, 1997). In kidney, ENaC is mainly localized in connecting tubule and the cortical CD and initial medullary CD. Patch-clamp studies performed on isolated renal principal cells suggest that ENaC is functionally expressed in the ciliary membrane itself, which thus establishes a direct link between ENaC and the principle cells (Raychowdhury et al., 2005). Improper functioning of ENaC is associated with two known diseases. One is Liddle's syndrome in which the channel activity is upregulated and there is a gain in ENaC function where the β or γ subunit is altered by missense mutations in the cytosolic carboxyl termini in the PPPnY domain. The second is pseudohypoaldosteronism (PHA) where there is a loss of ENaC function and downregulation of channel activity caused by a decrease in the number of channels at the cell surface (Garty & Palmer, 1997).

1.3.2. Biophysical characterization

ENaC was first examined in flat epithelia such as frog skin and toad urinary bladder mounted in Ussing-type chambers. It is characterized by a very high selectivity for Na over K. Measurements of macroscopic short-circuit current (I_{sc}) and isotope fluxes suggest permeability ratios for Na over K are at least 100:1 and perhaps as high as 1000:1. The channel is selective for Li over Na by a factor of $\sim 1.3 \sim 1.5:1$. Similar results were obtained from rENaC channels. The only other ion for which an appreciable permeability has been proposed is H^+ . These observations are consistent with the idea that the pore of the Na channel selects for Na in part on the basis of the size of the completely dehydrated ion. Such a physical narrowing of the pore could explain why ions smaller than Na (Li, H) pass through but larger ones (K, Rb, Cs) are impermeant (Garty & Palmer, 1997). With > 100 mM Na in the outer solution, the single-channel conductance for inward currents for this channel type is $4 \sim 5$ pS. The conductance when Li is the primary permeant ion is ~ 8 pS, reflecting the selectivity for Li over Na, as discussed above.

Although ENaC is comprised of three subunits, coexpression of all three subunits reconstitutes a channel with ion selective permeability, gating properties, and a pharmacological profile is similar to the native channel (Canessa *et al.*, 1994; Firsov *et al.*, 1996). Whereas expression of the α -subunit alone produces a small macroscopic amiloride-sensitive current, β , and γ subunits alone or together do not induce a Na current (Canessa *et al.*, 1994). The temporal relationship between ENaC α -subunit expression and both short-circuit current in aldosterone-treated A6 kidney cells (May *et al.*, 1997), and appearance of conducting apical ENaC in the maturing rodent principal cells (Satlin & Palmer, 1996; Huber *et al.*, 1999) provides additional evidence that the α -subunit is essential for assembly, targeting, and activation of apical ENaC.

Amiloride, a substituted pyrazine with a carbonyl guanidinium side chain, is one of the widely defining characteristics of the family of ENaC channels. Amiloride blockade of Na channels is usually quite rapid in onset when it is added to the apical side of the epithelium, suggesting a site of action on the extracellular surface. Indeed, blocking of channels in the cortical CD could be observed only when the outside surface was exposed to the drug (Palmer & Frindt, 1986). The K_i value for amiloride is in the range of $0.1 \sim 1$

μM , depending on the epithelium and on the experimental conditions used (Kleyman & Cragoe, Jr., 1988; Benos, 1982).

The affinity of the channels for amiloride depends on transmembrane voltage, the extracellular pH, and the extracellular Na concentration. Hyperpolarization of the membrane increases the affinity for amiloride (Palmer, 1985). Amiloride is a weak base, and studies of the pH dependence of block have indicated that it is the positively charged form of the drug that is effective in blocking the channel (Benos *et al.*, 1976; Cuthbert, 1976). The voltage dependence of block can therefore be explained if the transmembrane potential pulls the cationic form of amiloride onto its binding site. This suggests that the binding site is within the transmembrane electric field, and possibly within the pore itself. Both the on rate and the off rate for amiloride block are affected (in opposite directions) by voltage. It was hypothesized that amiloride might block the channel by a simple physical occlusion of the pore, i.e., by acting as a molecular plug (Palmer & Andersen, 1989). Another interpretation is that block by the drug involves a voltage-dependent conformation change of the protein.

If amiloride binds within the pore, it would be expected that permeating ions in the channel should repel the amiloride electrostatically and that Na should therefore reduce the affinity for the drug through a competitive mechanism. Here the data are more controversial. Evidence for a competitive interaction between Na and amiloride was found for a number of epithelia including toad bladder and frog skin (Palmer, 1984; Sudou & Hoshi, 1977). In the toad bladder, for example, increases in mucosal Na concentration decreased the on rate for amiloride block with little or no effect on the off rate, consistent with a competitive effect (Palmer, 1985). However, detailed measurements in a variety of epithelia indicated that in some cases the interaction was best described as noncompetitive or mixed (Benos *et al.*, 1979). These differences have not been resolved. Intracellular Na can also apparently decrease the amiloride affinity. Treatment of frog skin with ouabain decreased the on rate and increased the off rate of the blocker (Van & Erlij, 1983), consistent with interactions between the increased intracellular Na and the extracellular blocker.

Both the guanidinium group and the pyrazine ring of amiloride are necessary for high-affinity binding. Addition of a benzyl or a phenyl group to the guanidinium side

chain (eg, in benzamil or phenamil) increases the affinity of block by a factor of 10 (Kleyman & Cragoe, Jr., 1988). This suggests that hydrophobic interactions with a part of the channel or the membrane very close to the amiloride binding site can stabilize the bound state of the drug. A number of modifications of the structure, particularly involving additions to the side chain, alter the on rate (as well as the off rate) for block (Li *et al.*, 1987). This implies that the formation of the blocked state is not simply diffusion limited but involves specific interactions with the channel.

1.3.3. Interaction with cytoskeletal proteins

A great deal of information is known about the biophysical properties of ENaC. However, less is known about the proteins that interact with ENaC. Cytoskeletal elements participate in many cellular events, including regulation of a variety of ion transport events (Cantiello, 1997;Cantiello, 2001). Such a role for the cytoskeleton has been also proposed regarding regulation of ENaC (Cantiello *et al.*, 1991). A partially purified ENaC complex from bovine renal epithelia copurifies with ankyrin (Rotin *et al.*, 1994), spectrin (Zuckerman *et al.*, 1999), and actin (Copeland *et al.*, 2001), suggesting that these cytoskeletal proteins may be associated with ENaC. Actin, a major component of the cytoskeleton, reduces the single-channel conductance, and it was completely abolished by buffering free intracellular Ca in the solution bathing the ENaC-containing bilayer to < 10 nM (Berdiev *et al.*, 2001). Rotin and coworkers have demonstrated a direct interaction between the α subunit of the ENaC and α - spectrin (Rotin *et al.*, 1994). Spectrin is an α/β heterodimer that also interacts with ENaC and Na,K-ATPase (Zuckerman *et al.*, 1999). The activity of the ENaC is modulated by F-actin, and there is a direct interaction between α -ENaC and actin (Mazzochi *et al.*, 2006).

Electrophysiological data provide further support for an interaction between ENaC and the actin-based cytoskeleton. In cell-attached patches of A6 renal epithelial cells treated with the actin filament disrupter cytochalasin D, an induction of ENaC activity was observed, thereby suggesting that changes in the actin cytoskeleton affect the activity of ENaC. ENaC activation was also observed when short F-actin filaments were added to excised patches, and this effect was increased with the addition of cytochalasin D and/or ATP. The application of gelsolin, a Ca-activated protein that severs actin filaments and

caps the plus end of the actin filament, preventing the repolymerization of actin and keeping it in a soluble state, was found to cause a sustained activation of rENaC. In addition, actin was required for the transient activation of rENaC by protein kinase A and ATP when ENaC was reconstituted into planar lipid bilayer. These data indicate that a direct interaction between actin and ENaC may underlie the regulation of ENaC by short actin filaments. Identification of regions involved in a direct protein interaction between actin and α -ENaC have only been deduced using biophysical methods. Current evidence suggests that actin interacts with the C-terminal domain of α -ENaC.

1.3.4. Cross talk between ENaC and ARPKD

Detailed studies of salt and water transport in renal cysts detached from the nephron of origin and primary cultures of renal epithelial cells isolated from ADPKD patients suggest that fluid accumulation in the cysts is the result of NaCl secretion. In contrast, the predominant site of renal disease in ARPKD is the CD, and late in the disease most of the kidney is composed of dilated, fluid-filled CDs rather than isolated, detached cysts. Principal cells in CD play a vital role in salt and water homeostasis via regulated alterations in Na absorption and water permeability. The expression and activity of ENaC, located in the apical PM of CD principal cells, are rate-limiting for CD Na absorption. ARPKD is generally considered to be a disorder with developmental arrest or cellular dedifferentiation to a less mature phenotype. Therefore, ENaC-mediated Na absorption capacity, which is considered an indication of CD maturation, represents an important ion transport pathway that may not fully develop or might be lost from less mature cystic CD cells. ARPKD cystic CDs are composed almost exclusively of principal cells; however, almost little is known about the ion transport properties of cystic CD principal cells.

Aberrant ion transport in the kidney is not linked directly to the genetic defects that cause PKD but may play an important role in the rate of disease progression. In ADPKD, fluid accumulation driven by NaCl secretion increases cyst size, leading to kidney parenchyma destruction and, ultimately, renal failure. Little is known about ion transport in ARPKD mostly due to the lack of relevant experimental systems.

ARPKD is a rapidly progressive pediatric disease that leads to renal failure due to the formation of extremely dilated CDs and destruction of kidney parenchyma. The dilated CDs (referred as CD cysts due to the analogy with ADPKD) are lined with a single layer of highly proliferative CD principal cells. Anatomically, the dilated nephron segments retain up- and downstream connections, but they appear to result in “functional cysts.” Hypertension frequently accompanies ARPKD, but the precise mechanisms responsible for high blood pressure in this disease remain unknown. Because ARPKD is a complex disease, hypertension might develop as a result of renin-angiotensin-aldosterone axis over-activity, local and systemic effects of substances released in response to kidney hypoxia, or aberrant renal tubule ion transport (Veizis *et al.*, 2003). CDs are the site of the kidney lesions in ARPKD, and ion transport phenotype changes in the disease might provide clues about fluid retention in dilated tubules and/or the etiology of hypertension.

Renal CD principal cells isolated from ARPKD mice form high-resistance, polarized monolayers in primary culture. Veizis *et al.* found that amiloride-sensitive Na absorption is significantly reduced in cystic CD cells (Veizis *et al.*, 2003). This result suggests that dysregulation of principal cell Na absorption may contribute to the CD dilatation and fluid retention in the kidney characteristic of ARPKD. The amiloride-sensitive I_{sc} are also lower in the CD principal cells. Therefore, taken together, electrogenic Na absorption is significantly reduced in cystic CD cells. It is also likely that reduced apical Na permeability (ENaC activity) in cystic cells is responsible for the decrease in Na transport. Postnatal maturation of CDs is associated with an increase in Na absorptive capacity which parallels ENaC expression. It is possible that in cystic disease the highly proliferative principal cells do not fully differentiate (Calvet, 1993), and as such they do not develop a mature Na absorptive capacity. The reduced ENaC activity might be due to lower expression or aberrant signaling processes that regulate ENaC activity. Up to now, little is known about the mechanisms responsible for reduced Na absorption in principal cells of ARPKD. Veizis and Cotton also reported that abnormal EGF-dependent regulation of ENaC function and expression may contribute to PKD pathophysiology. Cystic cell proliferation is further increased by activation of the EGFR axis (Veizis & Cotton, 2005).

Rohatgi et al. revealed that the rate of Na absorption in fetal ARPKD cyst-lining principal cells is approximately 50% greater and α -ENaC expression is increased 100% than those measured across age-matched control cells, (Rohatgi *et al.*, 2003). A pathway that is modestly sensitive to apical amiloride and basolateral ouabain mediates the unidirectional lumen-to-bath Na flux in ARPKD cells, at least in part. The presence of relatively abundant α -ENaC message and protein in ARPKD kidneys and cell lines, suggests that it is possible that ENaC mediates Na absorption in ARPKD, at least in part. However, the α , β , γ -ENaC complex is exquisitely sensitive to amiloride ($K_i = 150$ nM) (Canessa *et al.*, 1994; Satlin & Palmer, 1996), yet inhibition of Na absorption across the ARPKD monolayers required significantly higher amiloride concentrations than those necessary to inhibit single-channel activity of the typical heterotrimeric channel (Canessa *et al.*, 1994; Satlin & Palmer, 1996).

The amiloride sensitivity of ENaC depends on subunit composition. McNicholas and Canessa showed that the K_i of amiloride for the ENaC channel composed of $\alpha + \gamma$ subunits was 0.13 ± 0.05 μ M, whereas the K_i for amiloride for ENaC channel composed of α alone or $\alpha + \beta$ subunits was approximately 30-fold greater (4 ± 0.4 μ M) (McNicholas & Canessa, 1997). Thus the relative insensitivity of Na absorption to apical amiloride in the present analysis of fetal principal cells may simply reflect the presence of a developmental stage and/or disease-specific ENaC channel of non-classical composition (*eg*, α alone or $\alpha + \beta$ subunits) (Kizer *et al.*, 1997; Weisz *et al.*, 2000), with ion selectivity, inhibitor sensitivity, and regulatory properties that differ from ENaC expressed in the fully differentiated cell. Alternatively it was suggested that the molecular entity for the apical Na entry in ARPKD cells may be a nonselective cation channel unrelated to ENaC (Huber & Horster, 1996; Korbmacher *et al.*, 1995; Light *et al.*, 1988).

In summary, little is known about the transport characteristics of ARPKD cystic epithelium, although emerging evidence suggests that some significant differences exist between ARPKD and ADPKD cell phenotypes. Recently, in *orpk* (Oak Ridge polycystic kidney) mouse model of ARPKD (a ARPKD mouse carries a hypomorphic mutation in the *Tg737* gene, and ductal epithelia from multiple tissues lack a well-formed central monocilium in the apical membrane), ENaC expression and/or function are unregulated in the luminal membrane of mutant, cilium-deficient *orpk* CCD principal cell

monolayers. These results reflect a heightened activity and/or expression of luminal amiloride-sensitive Na channels in the *orpk* CD (Olteanu *et al.*, 2006). As related to the clinical observation, infants and children with ARPKD frequently present with hypertension, which appears well in advance of renal insufficiency (Kaplan *et al.*, 1989). The parallels between the avid Na absorption in immortalized cells and low cyst fluid Na concentrations in freshly harvested ARPKD nephrectomy specimens (Rohatgi *et al.*, 2003) suggest that ARPKD CD cysts *in vivo* may be Na-reabsorptive epithelia. When the genetic lesion causes loss or malformation of the monocilium, ENaC-driven Na hyperabsorption may explain the rapid emergence of severe hypertension in a majority of patients with ARPKD.

1.4. TRPP3

The third gene member of PKD gene family, TRPP3 (also called PKD2L1, polycystin-L or PCL), initially cloned from human retina EST (Nomura *et al.*, 1998; Wu *et al.*, 1998), is a novel member of the transient receptor potential (TRP) superfamily of cation channels. TRPP3 has two isoforms, PKD2 and TRPP5 (also refer to PKD2L2 or popolycystin-2L2). TRPP3 functions as a Ca-regulated, Ca-permeable nonselective cation channel when overexpressed in *Xenopus* oocytes (Chen *et al.*, 1999), but its physiological function, as well as that of other polycystins, remains unknown. Unlike the PKD1 and PKD2, TRPP3 is not yet known to be mutated in ADPKD or other human genetic disorders, but its murine orthologue is deleted in *Krd* (kidney and retinal defects) mice with renal and retinal defects. TRPP3 has been assigned to 10q24 by radiation hybrid mapping and fluorescent *in situ* hybridization (Nomura *et al.*, 1998). Several inherited disease loci, including partial epilepsy (Ottman *et al.*, 1995), infantile-onset spinocerebellar ataxia (Nikali *et al.*, 1997), and urofacial syndrome (Wang & Strandgaard, 1997) have been mapped to this region (Guo *et al.*, 2000). It is unlikely that TRPP3 plays a role in ARPKD, as mutations in most ARPKD families have been mapped to chromosome 6. The TRPP3 locus can, however, be considered as a candidate for unmapped human genetic cystic disorders such as dominantly transmitted glomerulocystic kidney disease of post-infantile onset, isolated polycystic liver disease, and Hajdu-Cheney syndrome/serpentine fibula syndrome.

1.4.1. Structure

TRPP3, an 805-aa protein, has 50% sequence identity and 74% similarity to PKD2. TRPP3 and PKD2 also share similarity in sequence, domain organization and/or membrane topology with other TRP channels and the α subunits of voltage-gated Ca, Na and K channels (Kiselyov *et al.*, 1998; Mochizuki *et al.*, 1996; Nomura *et al.*, 1998; Perez-Reyes *et al.*, 1998). Sequence analysis and comparison to other channels support a six membrane-spanning plus one pore-region for TRPP3 (Fig. 1-4). One common feature of

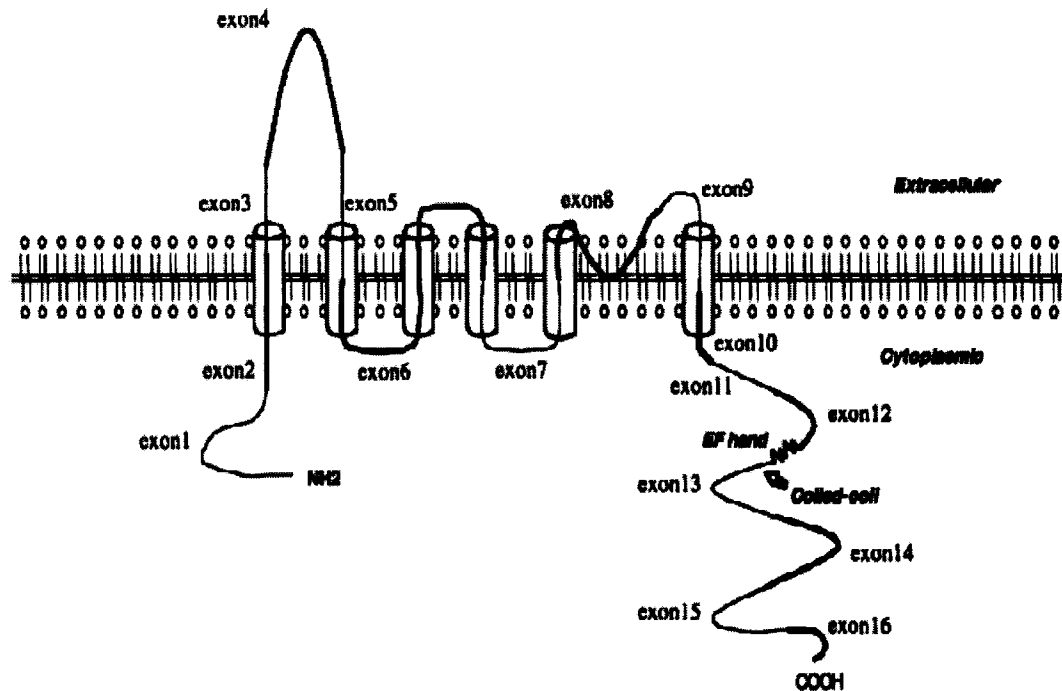


Fig. 1-4 Schematic representation of the TRPP3. Exons are represented by alternating thick and thin lines. The six predicted transmembrane spans are shown. The wavy line in exon 12 denotes the EF-hand. The coiled-coil domain is indicated by an arrow (Guo *et al.*, 2000).

the TRPP3/PKD2 structure that is rarely observed in known ion channels is that they both have relatively long extracellular loops between the first and second putative transmembrane segments. Although this loop region does not show high similarity to any known ion channels, PKD2 and TRPP3 maintain a high level of homology with each other in this region.

Moreover, this region contains a 13-aa stretch with 3 to 4 basic residues that are conserved not only between PKD2 and TRPP3 but also in PKD1. The function of this polycystin-shared motif is not clear. Two algorithms predict that TRPP3 has a coiled-coil

domain in its cytoplasmic C-terminal tail. TRPP3 also has a putative Ca binding EF-hand domain that generally consists of two helices and a loop between them (Fig. 1-4). The C-terminal helix in the EF-hand of TRPP3 overlaps with the predicted coiled-coil region, which has the potential to tightly interact with molecules with a similar structure like PKD1, and there is a putative cAMP phosphorylation site in the C terminus. Putative PKC phosphorylation sites are all in regions predicted to be cytoplasmic. Four of five putative casein kinase II phosphorylation sites with strong motif sequences (positions 249, 563, 674, 703, 719) are also found in the C-terminal cytoplasmic domain. TRPP3 differs from PKD2 most significantly in the N-terminal cytoplasmic domain where it lacks a 100-amino acid segment. TRPP3 and PKD2 have three positively charged residues in S4 as opposed to five to eight in voltage-gated channels. Whereas the S4 region in voltage-gated Ca channels is considered to be a voltage sensor, it is not clear whether a membrane-spanning region with only three basic residues could act as a voltage sensor. Maybe this is why TRPP3 shows weak voltage-dependence. TRPP3 also has several putative phosphorylation sites: one cyclic nucleotide, two PKC, and four casein kinase II phosphorylation sites with strong motif sequences in the C-terminal cytoplasmic domain. Two other putative PKC phosphorylation sites are also found in the N-terminal cytoplasmic domain. Phosphorylation of these motif sequences may be involved in the gating process of the channel.

1.4.2. Tissue and cellular localization

Immunostaining of the developing mouse kidney showed that expression of TRPP3 was first detectable at E16 in the inner medulla, which coincides with the maturation of inner medullary CDs. Higher levels of TRPP3 were found in the adult kidney, where its expression in the inner medulla was further supported by detection of *Pkd* mRNA from this region. Unlike PKD1 and PKD2, TRPP3 was detected in only one type of nephron segment, as demonstrated by colocalization experiments with AQP3. The restricted localization of TRPP3 to IMCD is not compatible with the wide distribution of cystic lesions in ADPKD, which involves all nephron segments. Therefore, studies about distribution suggest that TRPP3's direct involvement in ADPKD is unlikely. However, a secondary role for TRPP3 in cystogenesis should not be excluded, because the functional

relationships between TRPP3 and PKD1 and/or PKD2 have not yet been determined. PKD1 and TRPP3 appear to co-localize in some of the same structures of the adult mouse kidney, including the apical region of the CDs.

Endogenous TRPP3 subcellular distribution is different in proliferative and nonproliferative cultures. TRPP3 is found mostly in the ER in subconfluent cell cultures, while in confluent cells it is redistributed to sites of cell-cell contact and to the primary cilium as PKD1. Subcellular fractionation confirmed a common distribution of TRPP3 and PKD1 in the fractions corresponding to those containing the PM of post-confluent cells. Reciprocal co-IP experiments showed that TRPP3 was associated with PKD1 in a common complex in both sub-confluent and confluent cell cultures. Interestingly, they also identified a novel site for TRPP3 in non-ciliated cells, the centrosome, which allowed us to reveal an involvement of TRPP3 in cell proliferation (Bui-Xuan *et al.*, 2006). TRPP3 distribution largely overlapped with, and was associated to PKD1. It was showed that both PKD1 and TRPP3 were identified in the primary cilia, confirming previous studies on PKD1 and suggesting that residence in cilia is a characteristic of polycystin family members. Distribution of PKD1 was more extensive with the desmosomes than with E-cadherin. In fact, close inspection of PKD1 staining in the cell lines studied here revealed a "beads on a string" pattern, characteristic of desmosomal components and has been shown by others. TRPP3 also displayed a highly similar punctuate pattern, like the desmosomal structures. A significant fraction of TRPP3 was also found in the ER. Whether TRPP3 is functional in each of these compartments, as has been suggested for PKD2, remains to be determined.

Proper function of TRPP3, like PKD2, may require distinct contexts, possibly in different subcellular compartments. The cytoskeleton is most likely important for polycystin function as experiments aimed at identifying interacting proteins have found a number of actin-binding proteins, which bind to PKD1 (Geng *et al.*, 2000), PKD2 (Lehtonen *et al.*, 2000;Li *et al.*, 2003c), and TRPP3 (Li *et al.*, 2003d) and intermediate filament proteins, which bind to PKD1 (Xu *et al.*, 2001). This hypothesis is strongly supported by a number of recent papers which report the modulation of polycystin-2 or TRPP3 channel function by actin cytoskeletal components (Li *et al.*, 2003c;Li *et al.*, 2005a;Montalbetti *et al.*, 2005). Association of TRPP3 with PKD1 in a common complex

was confirmed by reciprocal co-immunoprecipitation (co-IP), in both sub-confluent and confluent cell cultures. Combined analyses from indirect immunofluorescence and subcellular fractionation experiments suggest that a PKD1/TRPP3 complex would reside in the PM and/or in the cilia. However, the nature of this interaction, whether direct or indirect, remains to be confirmed. *In vitro* yeast two-hybrid analyses found no direct binding between the C-terminus of PKD1 and TRPP3 (Q. Li and X.Z. Chen, unpublished observations). It is possible, however, that other domains in PKD1 and TRPP3 mediate their binding.

The PKD1-PKD2 complex has been shown to modulate intracellular calcium levels in response to fluid flow due to its location in the primary cilia. The impact of the coexistence of a PKD1/TRPP3 channel in the same structure is not known. One hypothesis could be that these different channels are activated in response to different rates of flow. This would be analogous to structurally related TRPV (vanilloid) receptors. TRPV1 and TRPV2 channels are both activated by heat, but at different threshold temperatures; TRPV1 (VR-1) is activated at temperatures greater than 43°C while TRPV2 (VRL-1), which is 50% identical to TRPV1, is activated at temperatures greater than 53°C (Benham *et al.*, 2002).

Bui-Xuan's results also showed the resident site of TRPP3 to the centrosome in dividing (sub-confluent) and non-dividing (confluent) cells. It is believed that there are ~200 centrosomal or centrosomal-associated proteins, not all of which have been identified. Centrosomes have long been known to act as microtubule organizing structures, involved in various cell processes such as active participation in the coordination of cell cycle initiation/progression, regulation of gene transcription, and protein recycling (Badano *et al.*, 2005). A recent study showed that polycystin-2 was associated with mitotic spindles, but did not appear to be in centrosomes in dividing cells (Rundle *et al.*, 2004). The exact opposite appears to be the case for TRPP3, which was undetectable in microtubule structures. The localization of channel proteins to non-membrane regions of the cell is perplexing but may provide an unsuspected link between polycystins, cell cycle, and epithelial polarity. A possible role for TRPP3 in cell proliferation is underscored by the BrdU incorporation assays. Their results showed that

overexpression of an N-terminal tagged TRPP3 construct inhibited cell growth, reflected by the significantly reduced number of cells in S-phase.

1.4.3. Nonselective cation channel properties and function

Chen's study (1999) showed that TRPP3 functions as a Ca-regulated nonselective cation channel that is permeable to Ca, Ba, Na, and K ions when expressed in *Xenopus* oocytes. Its ion selectivity, large single-channel conductance and relatively long open time distinguish it from structurally related channels of the TRP family, voltage-gated Ca, K and Na channels and known endogenous cation channels in *Xenopus* oocytes, including the stretch-activated cation channel and hyperpolarization-activated cation channel (Chen *et al.*, 1999).

TRPP3 has a 4:1 divalent-monovalent permselectivity ratio, and the channel displays slight outward rectification in the presence of asymmetrical Na/K (Chen *et al.*, 1999). Channel activity by TRPP3 is regulated by Ca, whose channel activity can be substantially increased when either extracellular or intracellular Ca is raised (Chen *et al.*, 1999). TRPP3-expressing oocytes pre-incubated in a Ca-free solution evoke large transient (<30 s) currents after addition of external Ca (5 mM) (Chen *et al.*, 1999). A second addition of Ca, however, inhibits the currents. Thus external Ca induces both activation and subsequent inhibition of TRPP3. This suggests a Ca-induced inactivation process somewhat reminiscent of that observed in voltage-gated cation channels and some members of the TRP family. This may be in contrast with TRP, TRPL, and TRPV6, which are blocked by varying concentrations of Mg, but whose function has little dependence on extracellular Ca. Extracellular Ca, however, modulates the Mg block in some TRP channels. The putative Ca binding EF-hand region in the C-terminal tail of TRPP3 may be implicated in its Ca regulation. Spliced versions of TRPP3 from liver and testis, containing and lacking this region, respectively, showed the same extent of channel inactivation by external Ca, indicating functional differences for Ca regulation between TRPP3 and voltage-gated cation channels. The two TRPP3 splice variants have different activating currents, however, suggesting that the role of this region will require further study (Cantiello, 2004).

1.4.4. Physiological roles

More recently, there has been very important progress about the physiological roles of TRPP3, TRPP3 was identified a candidate mammalian sour taste sensor (Huang *et al.*, 2006). It was shown to localize to a subset of taste receptor cells in the tongue where it may play a crucial role in sour tasting and acid sensing (Huang *et al.*, 2006; Ishimaru *et al.*, 2006; LopezJimenez *et al.*, 2006), and to neurons surrounding the central canal of spinal cord where it may account for the long-sought mechanism of a proton-dependent regulation of action potential.

In the tongue, it is localized to all four taste areas while its partner protein PKD1L3 is present in circumvallate and foliate, but not fungiform or palate (Huang *et al.*, 2006). In fact, TRPP3 is concentrated in the apical membrane (facing taste pores) of bipolar cells in taste buds (Huang *et al.*, 2006; Ishimaru *et al.*, 2006), suggesting that it allows an initial cation influx triggered by low pH at the taste pore, which activates local voltage-gated cation channels via membrane depolarization and then leads to the firing of an action potential. In the tongue, TRPP3 is expressed in a subset of taste receptor cells distinct from those responsible for sweet and bitter and umami taste. To examine the role of TRPP3-expressing taste cells *in vivo*, in Huang's paper (2006), they engineered mice with targeted genetic ablations of selected populations of taste receptor cells. Animals lacking TRPP3-expressing cells are completely devoid of taste responses to sour stimuli. Notably, responses to all other tastants remained unaffected, proving that the segregation of taste qualities even extends to ionic stimuli. In 2006, another group reported that PKD1L3 and TRPP3 are coexpressed in a subset of taste receptor cells in specific taste areas (Ishimaru *et al.*, 2006). Cells expressing these molecules are also distinct from taste cells having receptors for bitter, sweet, or umami tastants. The TRPP3 proteins are accumulated at the taste pore region, where taste chemicals are detected. PKD1L3 and TRPP3 proteins can interact with each other, and coexpression of the PKD1L3 and TRPP3 is necessary for their functional cell surface expression. Finally, various acids when coexpressed in heterologous cells but not by other classes of tastants activate PKD1L3 and TRPP3. These results suggest that PKD1L3 and TRPP3 heteromers may function as sour taste receptor.

PKD1L3 and TRPP3 are co-expressed raises the possibility that within taste receptor cells they function as heteromultimers. Although there is no direct evidence that PKD1L3 functions as an ion channel, the channel activity of TRPP3 is firmly established. Therefore, within taste receptor cells, TRPP3 is likely to function as an ion channel, with its activity possibly modulated by PKD1L3. Furthermore, studies indicate that Pkd113 and TRPP3 are selectively expressed in a subpopulation of taste receptor cells, suggesting that they are not components of the bitter, sweet or umami taste transduction pathways (LopezJimenez *et al.*, 2006). In the whole length of the spinal cord, TRPP3 is present in neurons that project into the central canal, suggesting that it may also trigger an initial cation entry following a decrease in the canal pH (Huang *et al.*, 2006). However, it remains unclear as to why TRPP3 responds to two very different pH ranges in the tongue and spinal cord. In particular, it is unknown whether PKD1L3 plays a role in acid sensing.

Murine orthologue of human TRPP3 (murine TRPP3) was also reported to interact or co-localize with PKD1. Human TRPP3 forms cation channels when expressed in *Xenopus* oocytes, but it has not been examined in a eukaryotic expression system to date (Chen *et al.*, 1999). Murakami *et al.* find coexpression of murine TRPP3 together with PKD1 resulted in the expression of murine TRPP3 channels on the cell surface, whereas murine TRPP3 expressed alone was retained within the ER in cultured human embryonic kidney 293 (HEK 293) cells (Murakami *et al.*, 2005). Interaction between PKD1 and murine TRPP3 is essential for murine TRPP3 trafficking and channel formation. Deletion analysis at the C-terminus of murine TRPP3 revealed that the coiled-coil domain was important for both interaction between PKD1 and murine TRPP3, and murine TRPP3 trafficking by PKD1. This indicated that the coiled-coil domain was responsible for retaining murine TRPP3 within the ER. Subcellular localization of murine TRPP3 and the interaction between murine TRPP3 and PKD1 are determined by the ER retention signal-like sequences (Murakami *et al.*, 2005). Bui-Xuan *et al.* (2006) reported that reciprocal coimmunoprecipitation experiments showed that TRPP3 was associated with PKD1 in a common complex in both subconfluent and confluent IMCD cell cultures (Bui-Xuan *et al.*, 2006). The heterodimeric interaction between PKD1 and PKD2 at their C-terminal cytoplasmic tails led us to speculate that TRPP3, which has the highest

homology to PKD2 among the members of the PKD family, might have similar features. Because the cytoplasmic C-terminal fragment of PKD1 regulates Ca-permeable cation channels, it is likely that the interaction between PKD1 and TRPP3 (or PKD2), and the trafficking of murine TRPP3 by PKD1, might be essential to the formation of functional cation channels. The pathophysiological implication of this interaction remains unclear; it might modulate PKD1-related pathogenesis.

Coexpression of PKD1 and murine TRPP3 resulted in the formation of functional cation channels that were opened by hypo-osmotic stimulation. Based their functional study of murine TRPP3 channels on studies of the mechanosensing properties of PKD1 and PKD2 channels (Hanaoka *et al.*, 2000), which raises the possibility that murine TRPP3 channels might also be mechanosensitive; this idea has yet to be tested. Up to now, as far as we know, PKD1-PKD2 complex is flow sensor in primary cilia; PKD1L3-TRPP3 is an acid sensor, at least in the tongue and spinal cord. These also provide new support to the notion that TRP members are molecular sensors (Clapham, 2003).

PKD2-deficient mice have cardiac defects (Wu *et al.*, 2000), and PKD2 channels might be involved in cardiac development. However, TRPP3 is thought to be expressed in the epicardium and ventricular blood vessels to a greater degree than in heart muscle (Basora *et al.*, 2002), and no phenotype in the cardiovascular system has been observed in *Krd* mice. Therefore, further studies are required to clarify the physiological importance of TRPP3, and to determine the role of TRPP3 in cardiac development.

It is interesting to note that TRPP3 was found in a variety of cell types, including epithelial, neuronal, and endothelial cells. The subcellular distribution of TRPP3 expression appeared to be different in these cell types. In polarized epithelial cells, such as in the kidney and the epicardium, staining was clearly predominant in or near the PM. In retinal neurons, however, the staining pattern of TRPP3 was distinctly intracellular. The reasons for these differences in distribution are currently unknown, but they could suggest diverse functions of TRPP3 in specific cell types or diverse targeting of TRPP3 as a result of alternative splicing (Guo *et al.*, 2000). Mainly because the physiological role of TRPP3 has remained unclear, research on the protein has not been as dynamic as that on PKD2. However, we believe that, as a member of TRP superfamily, which is known to be sensory channels, TRPP3 should have important roles.

1.5. Thesis objectives

It is now known that mutations in three cystoproteins, PKD1, PKD2, and FPC, lead to human renal ADPKD cystogenesis and extrarenal phenotypes, but the molecular mechanisms underlying these manifestations remain largely obscure. The objectives of this thesis are to describe 1) characterization of the channel function of PKD2 and its homologue TRPP3 (or PKDL), 2) cross talks between PKD2 and FPC, and between ENaC and FPC, and 3) roles of cytoskeleton components in regulating these proteins and mediating the cross talks. Despite of similarity in protein sequence (74%), membrane topology and channel function to PKD2, TRPP3 is not directly related to ADPKD. Recently, TRPP3 was found to be implicated in acid sensing and sour tasting in neuron cells. My studies include functional characterization of TRPP3 and its modulation by α -actinin, an important actin bundling protein. ENaC expression and amiloride-sensitive Na transport were abnormally regulated in ARPKD cystic cells. My studies include physical and functional interaction between ENaC and FPC, which may constitute an important molecular basis to account for the anomalies. This thesis includes the following specific aims:

Aim 1. To determine the cross talk between ADPKD and ARPKD

Although there is significant similarity in phenotypes associated with ADPKD and ARPKD, whether there exists a common molecular pathway underlying the two genetic PKDs remains unclear. On the other hand, the cytoskeleton apparatus is important for cell morphology, cytokinesis and physiology, and numerous intra-/intercellular processes, and is suggested to be implicated in cyst formation and progression. In this aim we describe the role of KIF3B, a motor subunit of microtubule-associated shuttle protein kinesin-2, in mediating physical and functional interaction between PKD2 and FPC. For this a variety of experimental techniques were utilized, including molecular biology, protein-protein interaction, protein expression and purification, and electrophysiology.

Aim 2. To study the cross talk between ARPKD and ENaC

Amiloride-sensitive renal Na reabsorption substantially increases in ARPKD cystic CD cells, suggesting a possible cross talk between FPC and ENaC, or an involvement of ENaC in cystogenesis. In this aim we describe the association of filamin, an actin-binding protein, FPC and ENaC. We also describe the role of filamin in the complexing between FPC and ENaC. Further, we describe roles of filamin and FPC in the modulation of the channel function of ENaC. Various expression systems are used in this study, including *Xenopus* oocytes, mammalian culture cells and planer lipid bilayer. Both single-channel and whole-cell electrophysiology is employed to characterize modulation of ENaC channel by filamin and FPC. This corresponds to a manuscript in preparation for submission so we still have few going projects to be completed soon, including data from using filamin-deficient M2 and -revert A7 melanoma cells, and MDCK cells stably expressing ENaC channels.

Aim 3. To estimate the pore size of TRPP3 channel

This corresponds to a published paper (Dai *et al.*, 2006). In this aim, we employed biophysical approaches, including *Xenopus* oocyte expression, radiotracer uptake measurements and whole-cell and single-channel voltage clamping to examine the permeability of organic cations to TRPP3 channels. In this study, we discovered several new permeant organic cations (organic amines and small tetra-alkylammonium compounds) and inhibitors (larger tetra-alkylammonium compounds) of the channel, and estimated its pore size. We found that, although TRPP3 has much larger single-channel conductance than its homologue PKD2, it has smaller pore diameter (~ 7 Å) than that of PKD2 (at least 11 Å), indicating that the pore dimension is not the major determinant of the channel conductance for these two homologous channels.

Aim 4. To determine physiological roles and pharmacological inhibitors for TRPP3

Up to now, there is no known specific inhibitor for TRPP3 channel. In this aim we describe the effect of amiloride and three of its analogues, EIPA, benzamil and phenamil, on TRPP3 channels. We found that they all are inhibitors of the channel but at distinct inhibitor affinities. We also found amiloride and tetra-alkylammonium compounds are not competitive inhibitors, suggesting that they bind different sites in TRPP3. For this

study, we used *Xenopus* oocytes as the expression system, the two-microelectrode voltage-clamp technique and cell-attached patch clamping, in combination with radiolabelled ^{45}Ca transport. This manuscript has now been submitted for review.

Aim 5. To examine the physical interaction and functional modulation of TRPP3 by α -actinin

Little is known about how this channel is modulated by its binding partners. This aim describes physical and functional interaction between TRPP3 and α -actinin, in collaboration with Dr. Qiang Li. We first discovered that the two proteins directly associate with each other by in vitro and in vivo protein-protein interaction methods, including yeast two-hybrid, in vitro biochemical binding assays, and in vivo co-immunoprecipitation. We then utilized planer lipid bilayer to reconstitute TRPP3 channels purified from our modified tandem affinity purification protocol, and studied its modulation by α -actinin purified from *E. coli*. We found that α -actinin substantially augmented TRPP3 channel activity. Thus, the cytoskeleton not only anchors TRPP3 to the plasma membrane but also functionally regulates TRPP3. This interaction may be important for executing the physiological functions of TRPP3, such as acid sensing in various types of cells.

1.6. References

Al-Bhalal L & Akhtar M (2005). Molecular basis of autosomal dominant polycystic kidney disease. *Adv Anat Pathol* **12**, 126-133.

Anyatonwu GI & Ehrlich BE (2005). Organic cation permeation through the channel formed by polycystin-2. *J Biol Chem* **In press**.

Badano JL, Teslovich TM, & Katsanis N (2005). The centrosome in human genetic disease. *Nat Rev Genet* **6**, 194-205.

Barr MM, DeModena J, Braun D, Nguyen CQ, Hall DH, & Sternberg PW (2001). The *Caenorhabditis elegans* autosomal dominant polycystic kidney disease gene homologs *lov-1* and *pkd-2* act in the same pathway. *Curr Biol* **11**, 1341-1346.

Barr MM & Sternberg PW (1999). A polycystic kidney-disease gene homologue required for male mating behaviour in *C. elegans*. *Nature* **401**, 386-389.

Basora N, Nomura H, Berger UV, Stayner C, Guo L, Shen X, & Zhou J (2002). Tissue and cellular localization of a novel polycystic kidney disease-like gene product, polycystin-L. *J Am Soc Nephrol* **13**, 293-301.

Belibi FA, Reif G, Wallace DP, Yamaguchi T, Olsen L, Li H, Helmkamp GM, Jr., & Grantham JJ (2004). Cyclic AMP promotes growth and secretion in human polycystic kidney epithelial cells. *Kidney Int* **66**, 964-973.

Benham CD, Davis JB, & Randall AD (2002). Vanilloid and TRP channels: a family of lipid-gated cation channels. *Neuropharmacology* **42**, 873-888.

Benos DJ (1982). Amiloride: a molecular probe of sodium transport in tissues and cells. *Am J Physiol* **242**, C131-C145.

Benos DJ, Mandel LJ, & Balaban RS (1979). On the mechanism of the amiloride-sodium entry site interaction in anuran skin epithelia. *J Gen Physiol* **73**, 307-326.

Benos DJ, Simon SA, Mandel LJ, & Cala PM (1976). Effect of amiloride and some of its analogues of cation transport in isolated frog skin and thin lipid membranes. *J Gen Physiol* **68**, 43-63.

- Berdiev BK, Latorre R, Benos DJ, & Ismailov II (2001). Actin modifies Ca²⁺ block of epithelial Na⁺ channels in planar lipid bilayers. *Biophys J* **80**, 2176-2186.
- Bhalla V, Oyster NM, Fitch AC, Wijngaarden MA, Neumann D, Schlattner U, Pearce D, & Hallows KR (2006). AMP-activated kinase inhibits the epithelial Na⁺ channel through functional regulation of the ubiquitin ligase Nedd4-2. *J Biol Chem* **281**, 26159-26169.
- Blyth H & Ockenden BG (1971). Polycystic disease of kidney and liver presenting in childhood. *J Med Genet* **8**, 257-284.
- Boletta A & Germino GG (2003). Role of polycystins in renal tubulogenesis. *Trends Cell Biol* **13**, 484-492.
- Boucher C & Sandford R (2004). Autosomal dominant polycystic kidney disease (ADPKD, MIM 173900, PKD1 and PKD2 genes, protein products known as polycystin-1 and polycystin-2). *Eur J Hum Genet* **12**, 347-354.
- Brook-Carter PT, Peral B, Ward CJ, Thompson P, Hughes J, Maheshwar MM, Nellist M, Gamble V, Harris PC, & Sampson JR (1994). Deletion of the TSC2 and PKD1 genes associated with severe infantile polycystic kidney disease--a contiguous gene syndrome. *Nat Genet* **8**, 328-332.
- Bui-Xuan EF, Li Q, Chen XZ, Boucher CA, Sandford R, Zhou J, & Basora N (2006). More than colocalizing with polycystin-1, polycystin-L is in the centrosome. *Am J Physiol Renal Physiol* **291**, F395-F406.
- Cai Y, Anyatonwu G, Okuhara D, Lee KB, Yu Z, Onoe T, Mei CL, Qian Q, Geng L, Witzgall R, Ehrlich BE, & Somlo S (2004). Calcium dependence of polycystin-2 channel activity is modulated by phosphorylation at Ser812. *J Biol Chem* **279**, 19987-19995.
- Cai Y, Maeda Y, Cedzich A, Torres VE, Wu G, Hayashi T, Mochizuki T, Park JH, Witzgall R, & Somlo S (1999). Identification and Characterization of Polycystin-2, the PKD2 Gene Product. *J Biol Chem* **274**, 28557-28565.
- Calvet JP (1993). Polycystic kidney disease: primary extracellular matrix abnormality or defective cellular differentiation? *Kidney Int* **43**, 101-108.

- Canessa CM, Schild L, Buell G, Thorens B, Gautschi I, Horisberger JD, & Rossier BC (1994). Amiloride-sensitive epithelial Na⁺ channel is made of three homologous subunits. *Nature* **367**, 463-467.
- Cantiello HF (1997). Role of actin filament organization in cell volume and ion channel regulation. *J Exp Zool* **279**, 425-435.
- Cantiello HF (2001). Role of actin filament organization in CFTR activation. *Pflugers Arch* **443 Suppl 1:S75-80.**, S75-S80.
- Cantiello HF (2004). Regulation of calcium signaling by polycystin-2. *Am J Physiol Renal Physiol* **286**, F1012-F1029.
- Cantiello HF, Stow JL, Prat AG, & Ausiello DA (1991). Actin filaments regulate epithelial Na⁺ channel activity. *Am J Physiol* **261**, C882-C888.
- Cartwright JH, Piro O, & Tuval I (2004). Fluid-dynamical basis of the embryonic development of left-right asymmetry in vertebrates. *Proc Natl Acad Sci U S A* **101**, 7234-7239.
- Chen XZ, Segal Y, Basora N, Guo L, Peng JB, Babakhanlou H, Vassilev PM, Brown EM, Hediger MA, & Zhou J (2001). Transport function of the naturally occurring pathogenic polycystin-2 mutant, R742X. *Biochem Biophys Res Commun* **282**, 1251-1256.
- Chen XZ, Vassilev PM, Basora N, Peng JB, Nomura H, Segal Y, Brown EM, Reeders ST, Hediger MA, & Zhou J (1999). Polycystin-L is a calcium-regulated cation channel permeable to calcium ions. *Nature* **401**, 383-386.
- Clapham DE (2003). TRP channels as cellular sensors. *Nature* **426**, 517-524.
- Copeland SJ, Berdiev BK, Ji HL, Lockhart J, Parker S, Fuller CM, & Benos DJ (2001). Regions in the carboxy terminus of alpha-bENaC involved in gating and functional effects of actin. *Am J Physiol Cell Physiol* **281**, C231-C240.
- Cuthbert AW (1976). Importance of guanidinium groups of blocking sodium channels in epithelia. *Mol Pharmacol* **12**, 945-957.

Dai XQ, Karpinski E, & Chen XZ (2006). Permeation and inhibition of polycystin-L channel by monovalent organic cations. *Biochim Biophys Acta* **1758**, 197-205.

Delmas P (2004). The gating of polycystin signaling complex. *Biol Res* **37**, 681-691.

Delmas P (2005). Polycystins: polymodal receptor/ion-channel cellular sensors. *Pflugers Arch* **451**, 264-276.

Delmas P, Nomura H, Li X, Lakkis M, Luo Y, Segal Y, Fernandez-Fernandez JM, Harris P, Frischauf AM, Brown DA, & Zhou J (2002). Constitutive activation of G-proteins by polycystin-1 is antagonized by polycystin-2
2. *J Biol Chem* **277**, 11276-11283.

Fick GM, Johnson AM, Strain JD, Kimberling WJ, Kumar S, Manco-Johnson ML, Duley IT, & Gabow PA (1993). Characteristics of very early onset autosomal dominant polycystic kidney disease. *J Am Soc Nephrol* **3**, 1863-1870.

Firsov D, Gautschi I, Merillat AM, Rossier BC, & Schild L (1998). The heterotetrameric architecture of the epithelial sodium channel (ENaC). *EMBO J* **17**, 344-352.

Firsov D, Schild L, Gautschi I, Merillat AM, Schneeberger E, & Rossier BC (1996). Cell surface expression of the epithelial Na channel and a mutant causing Liddle syndrome: a quantitative approach. *Proc Natl Acad Sci U S A* **93**, 15370-15375.

Foggensteiner L, Bevan AP, Thomas R, Coleman N, Boulter C, Bradley J, Ibraghimov-Beskrovnya O, Klinger K, & Sandford R (2000). Cellular and subcellular distribution of polycystin-2, the protein product of the PKD2 gene. *J Am Soc Nephrol* **11**, 814-827.

Gabow PA (1990). Autosomal dominant polycystic kidney disease--more than a renal disease. *Am J Kidney Dis* **16**, 403-413.

Gabow PA (1993). Autosomal dominant polycystic kidney disease. *N Engl J Med* **329**, 332-342.

Galindo BE, Moy GW, & Vacquier VD (2004). A third sea urchin sperm receptor for egg jelly module protein, suREJ2, concentrates in the plasma membrane over the sperm mitochondrion. *Dev Growth Differ* **46**, 53-60.

Gallagher AR, Cedzich A, Gretz N, Somlo S, & Witzgall R (2000). The polycystic kidney disease protein PKD2 interacts with Hax-1, a protein associated with the actin cytoskeleton. *Proc Natl Acad Sci U S A* **97**, 4017-4022.

Gallagher AR, Hoffmann S, Brown N, Cedzich A, Meruvu S, Podlich D, Feng Y, Konecke V, de VU, Hammes HP, Gretz N, & Witzgall R (2006). A truncated polycystin-2 protein causes polycystic kidney disease and retinal degeneration in transgenic rats. *J Am Soc Nephrol* **17**, 2719-2730.

Garty H & Palmer LG (1997). Epithelial sodium channels: function, structure, and regulation. *Physiol Rev* **77**, 359-396.

Geng L, Burrow CR, Li HP, & Wilson PD (2000). Modification of the composition of polycystin-1 multiprotein complexes by calcium and tyrosine phosphorylation. *Biochim Biophys Acta* **1535**, 21-35.

Geng L, Okuhara D, Yu Z, Tian X, Cai Y, Shibasaki S, & Somlo S (2006). Polycystin-2 traffics to cilia independently of polycystin-1 by using an N-terminal RVxP motif. *J Cell Sci* **119**, 1383-1395.

Gonzalez-Perret S, Kim K, Ibarra C, Damiano AE, Zotta E, Batelli M, Harris PC, Reisin IL, Arnaout MA, & Cantiello HF (2001). Polycystin-2, the protein mutated in autosomal dominant polycystic kidney disease (ADPKD), is a Ca²⁺-permeable nonselective cation channel. *Proc Natl Acad Sci U S A* **98**, 1182-1187.

Gonzalez-Perrett S, Batelli M, Kim K, Essafi M, Timpanaro G, Moltabetti N, Reisin IL, Arnaout MA, & Cantiello HF (2002). Voltage dependence and pH regulation of human polycystin-2-mediated cation channel activity
2. *J Biol Chem* **277**, 24959-24966.

Guay-Woodford LM (2003). Murine models of polycystic kidney disease: molecular and therapeutic insights. *Am J Physiol Renal Physiol* **285**, F1034-F1049.

Guay-Woodford LM, Muecher G, Hopkins SD, Avner ED, Germino GG, Guillot AP, Herrin J, Holleman R, Irons DA, & Primack W (1995). The severe perinatal form of autosomal recessive polycystic kidney disease maps to chromosome 6p21.1-p12: implications for genetic counseling. *Am J Hum Genet* **56**, 1101-1107.

Guo L, Chen M, Basora N, & Zhou J (2000). The human polycystic kidney disease 2-like (PKDL) gene: exon/intron structure and evidence for a novel splicing mechanism. *Mamm Genome* **11**, 46-50.

Hanaoka K, Qian F, Boletta A, Bhunia AK, Piontek K, Tsiokas L, Sukhatme VP, Guggino WB, & Germino GG (2000). Co-assembly of polycystin-1 and -2 produces unique cation-permeable currents. *Nature* **408**, 990-994.

Harris PC (2002). Molecular basis of polycystic kidney disease: PKD1, PKD2 and PKHD1. *Curr Opin Nephrol Hypertens* **11**, 309-314.

Harris PC & Rossetti S (2004). Molecular genetics of autosomal recessive polycystic kidney disease. *Mol Genet Metab* **81**, 75-85.

Harris PC & Torres VE (2006). Understanding pathogenic mechanisms in polycystic kidney disease provides clues for therapy. *Curr Opin Nephrol Hypertens* **15**, 456-463.

Hateboer N, Dijk MA, Bogdanova N, Coto E, Saggar-Malik AK, San Millan JL, Torra R, Breuning M, & Ravine D (1999). Comparison of phenotypes of polycystic kidney disease types 1 and 2. European PKD1-PKD2 Study Group. *Lancet* **353**, 103-107.

Hidaka S, Konecke V, Osten L, & Witzgall R (2004). PIGEA-14, a novel coiled-coil protein affecting the intracellular distribution of polycystin-2. *J Biol Chem* **279**, 35009-35016.

Hogan MC, Griffin MD, Rossetti S, Torres VE, Ward CJ, & Harris PC (2003). PKHD1, a homolog of the autosomal recessive polycystic kidney disease gene, encodes a receptor with inducible T lymphocyte expression. *Hum Mol Genet* **12**, 685-698.

Huang AL, Chen X, Hoon MA, Chandrashekar J, Guo W, Trankner D, Ryba NJ, & Zuker CS (2006). The cells and logic for mammalian sour taste detection. *Nature* **442**, 934-938.

Huber SM, Braun GS, & Horster MF (1999). Expression of the epithelial sodium channel (ENaC) during ontogenic differentiation of the renal cortical collecting duct epithelium. *Pflugers Arch* **437**, 491-497.

Huber SM & Horster MF (1996). Ontogeny of apical membrane ion conductances and channel expression in cortical collecting duct cells. *Am J Physiol* **271**, F698-F708.

Hughes J, Ward CJ, Peral B, Aspinwall R, Clark K, San Millan JL, Gamble V, & Harris PC (1995). The polycystic kidney disease 1 (PKD1) gene encodes a novel protein with multiple cell recognition domains. *Nat Genet* **10**, 151-160.

Igarashi P & Somlo S (2002). Genetics and pathogenesis of polycystic kidney disease. *J Am Soc Nephrol* **13**, 2384-2398.

Ikeda M, Fong P, Cheng J, Boletta A, Qian F, Zhang XM, Cai H, Germino GG, & Guggino WB (2006). A regulatory role of polycystin-1 on cystic fibrosis transmembrane conductance regulator plasma membrane expression. *Cell Physiol Biochem* **18**, 9-20.

Ishimaru Y, Inada H, Kubota M, Zhuang H, Tominaga M, & Matsunami H (2006). Transient receptor potential family members PKD1L3 and PKD2L1 form a candidate sour taste receptor. *Proc Natl Acad Sci U S A* **103**, 12569-12574.

Kaplan BS, Fay J, Shah V, Dillon MJ, & Barratt TM (1989). Autosomal recessive polycystic kidney disease. *Pediatr Nephrol* **3**, 43-49.

Karcher C, Fischer A, Schweickert A, Bitzer E, Horie S, Witzgall R, & Blum M (2005). Lack of a laterality phenotype in Pkd1 knock-out embryos correlates with absence of polycystin-1 in nodal cilia. *Differentiation* **73**, 425-432.

Kiselyov K, Xu X, Mozhayeva G, Kuo T, Pessah I, Mignery G, Zhu X, Birnbaumer L, & Muallem S (1998). Functional interaction between InsP3 receptors and store-operated Htrp3 channels. *Nature* **396**, 478-482.

Kizer N, Guo XL, & Hruska K (1997). Reconstitution of stretch-activated cation channels by expression of the alpha-subunit of the epithelial sodium channel cloned from osteoblasts. *Proc Natl Acad Sci U S A* **94**, 1013-1018.

Kleyman TR & Cragoe EJ, Jr. (1988). Amiloride and its analogs as tools in the study of ion transport. *J Membr Biol* **105**, 1-21.

Korbmacher C, Volk T, Segal AS, Boulpaep EL, & Fromter E (1995). A calcium-activated and nucleotide-sensitive nonselective cation channel in M-1 mouse cortical collecting duct cells. *J Membr Biol* **146**, 29-45.

Kottgen M (2007). TRPP2 and autosomal dominant polycystic kidney disease. *Biochim Biophys Acta* ..

- Kottgen M & Walz G (2005). Subcellular localization and trafficking of polycystins. *Pflugers Arch* **451**, 286-293.
- Koulen P, Cai Y, Geng L, Maeda Y, Nishimura S, Witzgall R, Ehrlich BE, & Somlo S (2002). Polycystin-2 is an intracellular calcium release channel. *Nat Cell Biol* **4**, 191-197.
- Lanoix J, D'Agati V, Szabolcs M, & Trudel M (1996). Dysregulation of cellular proliferation and apoptosis mediates human autosomal dominant polycystic kidney disease (ADPKD). *Oncogene* **13**, 1153-1160.
- Lehtonen S, Ora A, Olkkonen VM, Geng L, Zerial M, Somlo S, & Lehtonen E (2000). In vivo interaction of the adapter protein CD2-associated protein with the type 2 polycystic kidney disease protein, polycystin-2. *J Biol Chem* **275**, 32888-32893.
- Levin M, Thorlin T, Robinson KR, Nogi T, & Mercola M (2002). Asymmetries in H⁺/K⁺-ATPase and cell membrane potentials comprise a very early step in left-right patterning. *Cell* **111**, 77-89.
- Li A, Tian X, Sung SW, & Somlo S (2003a). Identification of two novel polycystic kidney disease-1-like genes in human and mouse genomes. *Genomics* **81**, 596-608.
- Li JH, Cragoe EJ, Jr., & Lindemann B (1987). Structure-activity relationship of amiloride analogs as blockers of epithelial Na channels: II. Side-chain modifications. *J Membr Biol* **95**, 171-185.
- Li Q, Shen Y, Wu G, & Chen X-Z (2003b). Polycystin-2 interacts with troponin I, an angiogenesis inhibitor. *Biochemistry* **42**, 450-457.
- Li Q, Dai Y, Guo L, Liu Y, Hao C, Wu G, Basora N, Michalak M, & Chen X-Z (2003c). Polycystin-2 associates with tropomyosin-1, an actin microfilament component. *J Mol Biol* **325**, 949-962.
- Li Q, Liu Y, Shen PY, Dai XQ, Wang S, Smillie LB, Sandford R, & Chen XZ (2003d). Troponin I binds polycystin-L and inhibits its calcium-induced channel activation. *Biochemistry* **42**, 7618-7625.
- Li Q, Liu Y, Zhao W, & Chen X-Z (2002). The calcium binding EF-hand in polycystin-L is not a domain for channel activation and ensuing inactivation. *FEBS Lett* **516**, 270-278.

- Li Q, Montalbetti N, Shen PY, Dai XQ, Cheeseman CI, Karpinski E, Wu G, Cantiello HF, & Chen XZ (2005a). Alpha-actinin associates with polycystin-2 and regulates its channel activity. *Hum Mol Genet* **14**, 1587-1603.
- Li Y, Wright JM, Qian F, Germino GG, & Guggino WB (2005b). Polycystin 2 interacts with type I inositol 1,4,5-trisphosphate receptor to modulate intracellular Ca²⁺ signaling. *J Biol Chem* **280**, 41298-41306.
- Light DB, McCann FV, Keller TM, & Stanton BA (1988). Amiloride-sensitive cation channel in apical membrane of inner medullary collecting duct. *Am J Physiol* **255**, F278-F286.
- LopezJimenez ND, Cavenagh MM, Sainz E, Cruz-Ithier MA, Battey JF, & Sullivan SL (2006). Two members of the TRPP family of ion channels, Pkd113 and Pkd211, are co-expressed in a subset of taste receptor cells. *J Neurochem* **98**, 68-77.
- Luo Y, Vassilev PM, Li X, Kawanabe Y, & Zhou J (2003). Native polycystin 2 functions as a plasma membrane Ca²⁺-permeable cation channel in renal epithelia. *Mol Cell Biol* **23**, 2600-2607.
- Ma R, Li WP, Rundle D, Kong J, Akbarali HI, & Tsiokas L (2005). PKD2 functions as an epidermal growth factor-activated plasma membrane channel. *Mol Cell Biol* **25**, 8285-8298.
- Magistroni R, He N, Wang K, Andrew R, Johnson A, Gabow P, Dicks E, Parfrey P, Torra R, San-Millan JL, Coto E, Van DM, Breuning M, Peters D, Bogdanova N, Ligabue G, Albertazzi A, Hateboer N, Demetriou K, Pierides A, Deltas C, St G, Ravine D, & Pei Y (2003). Genotype-renal function correlation in type 2 autosomal dominant polycystic kidney disease. *J Am Soc Nephrol* **14**, 1164-1174.
- Manno M, Marchesan E, Tomei F, Cicutto D, Maruzzi D, Maieron A, & Turco A (2005). Polycystic kidney disease and infertility: case report and literature review. *Arch Ital Urol Androl* **77**, 25-28.
- Masyuk TV, Huang BQ, Ward CJ, Masyuk AI, Yuan D, Splinter PL, Punyashthiti R, Ritman EL, Torres VE, Harris PC, & LaRusso NF (2003). Defects in cholangiocyte fibrocystin expression and ciliary structure in the PCK rat. *Gastroenterology* **125**, 1303-1310.

May A, Puoti A, Gaeggeler HP, Horisberger JD, & Rossier BC (1997). Early effect of aldosterone on the rate of synthesis of the epithelial sodium channel alpha subunit in A6 renal cells. *J Am Soc Nephrol* **8**, 1813-1822.

Mazzochi C, Bubien JK, Smith PR, & Benos DJ (2006). The carboxyl terminus of the alpha-subunit of the amiloride-sensitive epithelial sodium channel binds to F-actin. *J Biol Chem* **281**, 6528-6538.

McGrath J, Somlo S, Makova S, Tian X, & Brueckner M (2003). Two populations of node monocilia initiate left-right asymmetry in the mouse. *Cell* **114**, 61-73.

McNicholas CM & Canessa CM (1997). Diversity of channels generated by different combinations of epithelial sodium channel subunits. *J Gen Physiol* **109**, 681-692.

Mene P (2006). Transient receptor potential channels in the kidney: calcium signaling, transport and beyond. *J Nephrol* **19**, 21-29.

Menezes LF, Cai Y, Nagasawa Y, Silva AM, Watkins ML, Da Silva AM, Somlo S, Guay-Woodford LM, Germino GG, & Onuchic LF (2004). Polyductin, the PKHD1 gene product, comprises isoforms expressed in plasma membrane, primary cilium, and cytoplasm. *Kidney Int* **66**, 1345-1355.

Milutinovic J, Fialkow PJ, Agodoa LY, Phillips LA, Rudd TG, & Bryant JI (1984). Autosomal dominant polycystic kidney disease: symptoms and clinical findings. *Q J Med* **53**, 511-522.

Mochizuki T, Saijoh Y, Tsuchiya K, Shirayoshi Y, Takai S, Taya C, Yonekawa H, Yamada K, Nihei H, Nakatsuji N, Overbeek PA, Hamada H, & Yokoyama T (1998). Cloning of *inv*, a gene that controls left/right asymmetry and kidney development. *Nature* **395**, 177-181.

Mochizuki T, Wu G, Hayashi T, Xenophontos SL, Veldhuisen B, Saris JJ, Reynolds DM, Cai Y, Gabow PA, Pierides A, Kimberling WJ, Breuning MH, Deltas CC, Peters DJ, & Somlo S (1996). PKD2, a gene for polycystic kidney disease that encodes an integral membrane protein. *Science* **272**, 1339-1342.

Montalbetti N, Li Q, Timpanaro GA, Gonzalez-Perrett S, Dai XQ, Chen XZ, & Cantiello HF (2005). Cytoskeletal regulation of calcium-permeable cation channels in the human syncytiotrophoblast: role of gelsolin. *J Physiol* **566**, 309-325.

Moy GW, Mendoza LM, Schulz JR, Swanson WJ, Glabe CG, & Vacquier VD (1996). The sea urchin sperm receptor for egg jelly is a modular protein with extensive homology to the human polycystic kidney disease protein, PKD1. *J Cell Biol* **133**, 809-817.

Murakami M, Ohba T, Xu F, Shida S, Satoh E, Ono K, Miyoshi I, Watanabe H, Ito H, & Iijima T (2005). Genomic organization and functional analysis of murine PKD2L1. *J Biol Chem* **280**, 5626-5635.

Murcia NS, Richards WG, Yoder BK, Mucenski ML, Dunlap JR, & Woychik RP (2000). The Oak Ridge Polycystic Kidney (orpk) disease gene is required for left-right axis determination
1. *Development* **127**, 2347-2355.

Nagano J, Kitamura K, Hujer KM, Ward CJ, Bram RJ, Hopfer U, Tomita K, Huang C, & Miller RT (2005). Fibrocystin interacts with CAML, a protein involved in Ca²⁺ signaling. *Biochem Biophys Res Commun* **338**, 880-889.

Nagao S, Watanabe T, Ogiso N, Marunouchi T, & Takahashi H (1995). Genetic mapping of the polycystic kidney gene, pcy, on mouse chromosome 9. *Biochem Genet* **33**, 401-412.

Nagasawa Y, Matthiesen S, Onuchic LF, Hou X, Bergmann C, Esquivel E, Senderek J, Ren Z, Zeltner R, Furu L, Avner E, Moser M, Somlo S, Guay-Woodford L, Buttner R, Zerres K, & Germino GG (2002). Identification and characterization of Pkhd1, the mouse orthologue of the human ARPKD gene. *J Am Soc Nephrol* **13**, 2246-2258.

Nakanishi K, Sweeney WE, Jr., MacRae DK, Cotton CU, & Avner ED (2001). Role of CFTR in autosomal recessive polycystic kidney disease. *J Am Soc Nephrol* **12**, 719-725.

Nauli SM, Alenghat FJ, Luo Y, Williams E, Vassilev P, Li X, Elia AE, Lu W, Brown EM, Quinn SJ, Ingber DE, & Zhou J (2003). Polycystins 1 and 2 mediate mechanosensation in the primary cilium of kidney cells. *Nat Genet*.

Neill AT, Moy GW, & Vacquier VD (2004). Polycystin-2 associates with the polycystin-1 homolog, suREJ3, and localizes to the acrosomal region of sea urchin spermatozoa. *Mol Reprod Dev* **67**, 472-477.

Newby LJ, Streets AJ, Zhao Y, Harris PC, Ward CJ, & Ong AC (2002). Identification, characterisation and localisation of a novel kidney polycystin-1/polycystin-2 complex. *J Biol Chem* **277**, 20763-20773.

Nikali K, Isosomppi J, Lonnqvist T, Mao JI, Suomalainen A, & Peltonen L (1997). Toward cloning of a novel ataxia gene: refined assignment and physical map of the IOSCA locus (SCA8) on 10q24. *Genomics* **39**, 185-191.

Nomura H, Turco AE, Pei Y, Kalaydjieva L, Schiavello T, Weremowicz S, Ji W, Morton CC, Meisler M, Reeders ST, & Zhou J (1998). Identification of PKDL, a novel polycystic kidney disease 2-like gene whose murine homologue is deleted in mice with kidney and retinal defects. *J Biol Chem* **273**, 25967-25973.

Olteanu D, Yoder BK, Liu W, Croyle MJ, Welty EA, Rosborough K, Wyss JM, Bell PD, Guay-Woodford LM, Bevenssee MO, Satlin LM, & Schwiebert EM (2006). Heightened epithelial Na⁺ channel-mediated Na⁺ absorption in a murine polycystic kidney disease model epithelium lacking apical monocilia. *Am J Physiol Cell Physiol* **290**, C952-C963.

Onuchic LF, Furu L, Nagasawa Y, Hou X, Eggermann T, Ren Z, Bergmann C, Senderek J, Esquivel E, Zeltner R, Rudnik-Schoneborn S, Mrug M, Sweeney W, Avner ED, Zerres K, Guay-Woodford LM, Somlo S, & Germino GG (2002). PKHD1, the polycystic kidney and hepatic disease 1 gene, encodes a novel large protein containing multiple immunoglobulin-like plexin-transcription-factor domains and parallel beta-helix 1 repeats. *Am J Hum Genet* **70**, 1305-1317.

Osathanondh V & Potter EL (1964). PATHOGENESIS OF POLYCYSTIC KIDNEYS. SURVEY OF RESULTS OF MICRODISSECTION. *Arch Pathol* **77:510-2.**, 510-512.

Ottman R, Risch N, Hauser WA, Pedley TA, Lee JH, Barker-Cummings C, Lustenberger A, Nagle KJ, Lee KS, Scheuer ML, & . (1995). Localization of a gene for partial epilepsy to chromosome 10q. *Nat Genet* **10**, 56-60.

Palmer LG (1984). Voltage-dependent block by amiloride and other monovalent cations of apical Na channels in the toad urinary bladder. *J Membr Biol* **80**, 153-165.

Palmer LG (1985). Interactions of amiloride and other blocking cations with the apical Na channel in the toad urinary bladder. *J Membr Biol* **87**, 191-199.

Palmer LG & Andersen OS (1989). Interactions of amiloride and small monovalent cations with the epithelial sodium channel. Inferences about the nature of the channel pore. *Biophys J* **55**, 779-787.

Palmer LG & Frindt G (1986). Epithelial sodium channels: characterization by using the patch-clamp technique. *Fed Proc* **45**, 2708-2712.

Peden EM & Barr MM (2005). The KLP-6 kinesin is required for male mating behaviors and polycystin localization in *Caenorhabditis elegans*. *Curr Biol* **15**, 394-404.

Pennekamp P, Karcher C, Fischer A, Schweickert A, Skryabin B, Horst J, Blum M, & Dworniczak B (2002). The ion channel polycystin-2 is required for left-right axis determination in mice
1. *Curr Biol* **12**, 938-943.

Perez-Reyes E, Cribbs LL, Daud A, Lacerda AE, Barclay J, Williamson MP, Fox M, Rees M, & Lee JH (1998). Molecular characterization of a neuronal low-voltage-activated T-type calcium channel. *Nature* **391**, 896-900.

Pretorius DH, Lee ME, Manco-Johnson ML, Weingast GR, Sedman AB, & Gabow PA (1987). Diagnosis of autosomal dominant polycystic kidney disease in utero and in the young infant. *J Ultrasound Med* **6**, 249-255.

Qamar S, Vadivelu M, & Sandford R (2007). TRP channels and kidney disease: lessons from polycystic kidney disease. *Biochem Soc Trans* **35**, 124-128.

Qian F, Germino FJ, Cai Y, Zhang X, Somlo S, & Germino GG (1997). PKD1 interacts with PKD2 through a probable coiled-coil domain. *Nat Genet* **16**, 179-183.

Ramasubbu K, Gretz N, & Bachmann S (1998). Increased epithelial cell proliferation and abnormal extracellular matrix in rat polycystic kidney disease. *J Am Soc Nephrol* **9**, 937-945.

Raychowdhury MK, McLaughlin M, Ramos AJ, Montalbetti N, Bouley R, Ausiello DA, & Cantiello HF (2005). Characterization of single channel currents from primary cilia of renal epithelial cells. *J Biol Chem* **280**, 34718-34722.

Reynolds DM, Hayashi T, Cai Y, Veldhuisen B, Watnick TJ, Lens XM, Mochizuki T, Qian F, Maeda Y, Li L, Fossdal R, Coto E, Wu G, Breuning MH, Germino GG, Peters DJ, & Somlo S (1999). Aberrant splicing in the PKD2 gene as a cause of polycystic kidney disease. *J Am Soc Nephrol* **10**, 2342-2351.

Rohatgi R, Greenberg A, Burrow CR, Wilson PD, & Satlin LM (2003). Na transport in autosomal recessive polycystic kidney disease (ARPKD) cyst lining epithelial cells. *J Am Soc Nephrol* **14**, 827-836.

Rossetti S, Strmecki L, Gamble V, Burton S, Sneddon V, Peral B, Roy S, Bakkaloglu A, Komel R, Winearls CG, & Harris PC (2001). Mutation analysis of the entire PKD1 gene: genetic and diagnostic implications. *Am J Hum Genet* **68**, 46-63.

Rotin D, Bar-Sagi D, O'Brodovich H, Merilainen J, Lehto VP, Canessa CM, Rossier BC, & Downey GP (1994). An SH3 binding region in the epithelial Na⁺ channel (alpha rENaC) mediates its localization at the apical membrane. *EMBO J* **13**, 4440-4450.

Rundle DR, Gorbsky G, & Tsiokas L (2004). PKD2 interacts and co-localizes with mDia1 to mitotic spindles of dividing cells: role of mDia1 IN PKD2 localization to mitotic spindles. *J Biol Chem* **279**, 29728-29739.

Satlin LM & Palmer LG (1996). Apical Na⁺ conductance in maturing rabbit principal cell. *Am J Physiol* **270**, F391-F397.

Scheffers MS, van Der BP, Prins F, Spruit L, Breuning MH, Litvinov SV, de HE, & Peters DJ (2000). Polycystin-1, the product of the polycystic kidney disease 1 gene, co-localizes with desmosomes in MDCK cells. *Hum Mol Genet* **9**, 2743-2750.

Streets AJ, Moon DJ, Kane ME, Obara T, & Ong AC (2006). Identification of an N-terminal glycogen synthase kinase 3 phosphorylation site which regulates the functional localization of polycystin-2 in vivo and in vitro. *Hum Mol Genet* **15**, 1465-1473.

Sudou K & Hoshi T (1977). Mode of action of amiloride in toad urinary bladder. An electrophysiological study of the drug action on sodium permeability of the mucosal border. *J Membr Biol* **32**, 115-132.

Sullivan LP, Wallace DP, & Grantham JJ (1998). Chloride and fluid secretion in polycystic kidney disease. *J Am Soc Nephrol* **9**, 903-916.

Sweeney WE, Jr. & Avner ED (2006). Molecular and cellular pathophysiology of autosomal recessive polycystic kidney disease (ARPKD). *Cell Tissue Res* **326**, 671-685.

Thomas R, McConnell R, Whittacker J, Kirkpatrick P, Bradley J, & Sandford R (1999). Identification of mutations in the repeated part of the autosomal dominant polycystic kidney disease type 1 gene, PKD1, by long-range PCR. *Am J Hum Genet* **65**, 39-49.

Torres VE & Harris PC (2007). Polycystic kidney disease: genes, proteins, animal models, disease mechanisms and therapeutic opportunities. *J Intern Med* **261**, 17-31.

Tsiokas L, Arnould T, Zhu C, Kim E, Walz G, & Sukhatme VP (1999). Specific association of the gene product of PKD2 with the TRPC1 channel. *Proc Natl Acad Sci U S A* **96**, 3934-3939.

Tsiokas L, Kim E, Arnould T, Sukhatme VP, & Walz G (1997). Homo- and heterodimeric interactions between the gene products of PKD1 and PKD2. *Proc Natl Acad Sci U S A* **94**, 6965-6970.

Tsiokas L, Kim S, & Ong EC (2006). Cell biology of polycystin-2. *Cell Signal* ..

Van DW & Erlj D (1983). Noise analysis of inward and outward Na⁺ currents across the apical border of ouabain-treated frog skin. *Pflugers Arch* **398**, 179-188.

Vandorpe DH, Chernova MN, Jiang L, Sellin LK, Wilhelm S, Stuart-Tilley AK, Walz G, & Alper SL (2001). The cytoplasmic C-terminal fragment of polycystin-1 regulates a Ca²⁺-permeable cation channel. *J Biol Chem* **276**, 4093-4101.

Vassilev PM, Guo L, Chen XZ, Segal Y, Peng JB, Basora N, Babakhanlou H, Cruger G, Kanazirska M, Ye C, Brown EM, Hediger MA, & Zhou J (2001). Polycystin-2 is a novel cation channel implicated in defective intracellular Ca²⁺ homeostasis in polycystic kidney disease. *Biochem Biophys Res Commun* **282**, 341-350.

Veizis EI, Carlin CR, & Cotton CU (2003). Decreased amiloride-sensitive Na⁺ absorption in collecting duct principal cells isolated from bpk ARPKD mice. *Am J Physiol Renal Physiol* ..

Veizis IE & Cotton CU (2005). Abnormal EGF-dependent regulation of sodium absorption in ARPKD collecting duct cells. *Am J Physiol Renal Physiol* **288**, F474-F482.

Venglarik CJ, Gao Z, & Lu X (2004). Evolutionary conservation of *Drosophila* polycystin-2 as a calcium-activated cation channel. *J Am Soc Nephrol* **15**, 1168-1177.

Wang D & Strandgaard S (1997). The pathogenesis of hypertension in autosomal dominant polycystic kidney disease. *J Hypertens* **15**, 925-933.

Ward CJ, Hogan MC, Rossetti S, Walker D, Sneddon T, Wang X, Kubly V, Cunningham JM, Bacallao R, Ishibashi M, Milliner DS, Torres VE, & Harris PC (2002). The gene mutated in autosomal recessive polycystic kidney disease encodes a large, receptor-like protein. *Nat Genet* **30**, 259-269.

Weisz OA, Wang JM, Edinger RS, & Johnson JP (2000). Non-coordinate regulation of endogenous epithelial sodium channel (ENaC) subunit expression at the apical membrane of A6 cells in response to various transporting conditions. *J Biol Chem* **275**, 39886-39893.

Wilson PD & Falkenstein D (1995). The pathology of human renal cystic disease. *Curr Top Pathol* **88:1-50.**, 1-50.

Wu G, Hayashi T, Park JH, Dixit M, Reynolds DM, Li L, Maeda Y, Cai Y, Coca-Prados M, & Somlo S (1998). Identification of PKD2L, a human PKD2-related gene: tissue-specific expression and mapping to chromosome 10q25. *Genomics* **54**, 564-568.

Wu G, Markowitz GS, Li L, D'Agati VD, Factor SM, Geng L, Tibara S, Tuchman J, Cai Y, Park JH, van Adelsberg J, Hou H, Jr., Kucherlapati R, Edelmann W, & Somlo S (2000). Cardiac defects and renal failure in mice with targeted mutations in Pkd2. *Nat Genet* **24**, 75-78.

Xu GM, Gonzalez-Perrett S, Essafi M, Timpanaro GA, Montalbetti N, Arnaout MA, & Cantiello HF (2003). Polycystin-1 activates and stabilizes the polycystin-2 channel 1. *J Biol Chem* **278**, 1457-1462.

Xu GM, Sikaneta T, Sullivan BM, Zhang Q, Andreucci M, Stehle T, Drummond I, & Arnaout MA (2001). Polycystin-1 interacts with intermediate filaments. *J Biol Chem* **276**, 46544-46552.

Yoder BK, Hou X, & Guay-Woodford LM (2002). The polycystic kidney disease proteins, polycystin-1, polycystin-2, polaris, and cystin, are co-localized in renal cilia. *J Am Soc Nephrol* **13**, 2508-2516.

Zerres K, Rudnik-Schoneborn S, Steinkamm C, Becker J, & Mucher G (1998). Autosomal recessive polycystic kidney disease. *J Mol Med* **76**, 303-309.

Zuckerman JB, Chen X, Jacobs JD, Hu B, Kleyman TR, & Smith PR (1999). Association of the epithelial sodium channel with Apx and alpha-spectrin in A6 renal epithelial cells. *J Biol Chem* **274**, 23286-23295.

CHAPTER 2

KINESIN-2 MEDIATES PHYSICAL AND FUNCTIONAL INTERACTIONS BETWEEN POLYCYSTIN-2 AND FIBROCYSTIN

This chapter was published in 2006:

Wu, Y.#, Dai, X.-Q.#, Li, Q., Chen, C.X., Mai, W., Hussain, Z., Long, W., Montalbetti, N., Li, G., Glynne, R., Wang, S., Cantiello, H.F., Wu, G., and Chen, X.-Z. (2006) Kinesin-2 mediates physical and functional interactions between polycystin-2 and fibrocystin. *Hum. Mol. Genet.* **15**, 3280-3292. #equal contribution

2.1. INTRODUCTION

The formation of kidney cysts is a pathological entity common to a number of inherited and acquired human diseases. Of these disorders, autosomal dominant polycystic kidney disease (ADPKD) is the most prominent, affects up to one in 500 individuals, and is caused by mutations in the *PKD1* or *PKD2* gene, encoding, respectively, the transmembrane proteins polycystin-1 (PC1) or polycystin-2 (PC2) (1-3). Autosomal recessive PKD (ARPKD) is less common than ADPKD, occurring in 1/20,000 infants and children (4), which is caused by mutations in the *PKHD1* (polycystic kidney and hepatic disease 1) gene, encoding fibrocystin (also named polyductin and tigmin, abbreviated as FPC) (5-7).

PC2 is a 968 amino-acid protein with a molecular mass of 110 kDa, and has six putative transmembrane domains and intracellular N- and C-termini. PC2 is a member of the transient receptor potential (TRP) superfamily of channels and is indeed a non-selective cation channel permeable to Ca, K and Na (8,9). PC2 is known to co-assemble with the following proteins: PC1 (10), PC2 (11), TRPC1 (12), Golgi- and endoplasmic reticulum-associated protein PIGEA-14 (13), actin filament-associated proteins Hax-1 and CD2AP (14,15), actin filament proteins tropomyosin-1, troponin I, α -actinin (16-18), and RhoA GTPase-binding protein mDial (19). PC2 is present in a variety of tissues, including kidney, testis, cardiac, skeletal and smooth muscles (2), but not all organs display known phenotypes associated with *PKD2* mutation.

FPC is a 4074 amino-acid protein with a single transmembrane domain near its intracellular carboxyl tail and contains IPT/TIG (immunoglobulin-like fold shared by plexins and transcription factors) and Parallel Beta-Helix 1 (PbH1) repeats in its large extracellular amino terminus (5). This suggests that FPC may be a cell surface receptor implicated in protein-protein interactions. FPC shares a modest sequence similarity (23% identity) with two proteins of unknown function D86, a putative lymphocyte-secreted protein and TMEM2 (type II transmembrane protein) (5,6). FPC also shares structural similarity with hepatocyte growth factor receptor and plexins, which are involved in regulation of cell adhesion and proliferation. FPC is highly expressed in kidney, but is also found in liver, pancreas, lung and testis (5-7,20). In kidney, FPC is expressed in various segments of a nephron, including collecting ducts, proximal convoluted tubules,

and thick ascending limbs of the loop of Henle (20-23). Interestingly, like other cystoproteins, such as polycystins (PC1 and PC2), polaris (which is homologous to *Chlamydomonas* intraflagellar transport protein 88 or IFT88) and inversin, FPC is also present in renal primary cilia (21-24).

Kinesins represent a diverse group of microtubule-associated motor proteins that drive a number of cellular transport events (25). Kinesin-2, first identified from sea urchin eggs (26), transports cargo to the plus end of a cilium (or flagellum) while dynein transports materials from tip to the cell body (27). Unlike the conventional heterotetrameric kinesin (kinesin-1), kinesin-2 is a heterotrimeric complex formed by a pair of homologous motor subunits, KIF3A and KIF3B, and a non-motor subunit KAP3 (kinesin associated polypeptide 3). KIF3A and KIF3B are composed of three domains, an N-terminal motor domain, which contains ATP hydrolysis and microtubule binding sites, a central stalk domain, where two motor subunits form a α -helical coiled-coil structure, and a globular C-terminus (28,29) (Fig. 2-1A). In neurons, kinesin-2 is also responsible for sorting and transporting materials that are synthesized within the cell body into and along extensive dendritic and axonal processes (30).

In the present study, we demonstrated that both PC2 and FPC associate with the motor subunit, KIF3B. We then utilized various *in vitro* and *in vivo* approaches to show that PC2, KIF3B and FPC form a complex. Using a planar lipid bilayer electrophysiology system we investigated the functional modulation of PC2 channel by FPC and the mediator role of KIF3B.

2.2. MATERIALS AND METHODS

Yeast two-hybrid analysis

A yeast two-hybrid screen was performed in the yeast strain AH109 containing *Ade2*, *His3* and *LacZ* reporter genes under the control of the GAL4 upstream activating sequences as described recently (18) and the whole kit was purchased from Clontech (Palo Alto, CA). Briefly, the cDNA fragments encoding human PC2C or FPCC were subcloned in frame into the GAL4 DNA binding domain of the vector pGBKT7 by a PCR-based approach. PC2C was used as bait to screen a human heart cDNA library constructed in the vector pACT2 containing the GAL4 activation domain. Transformants were grown on the minimal synthetic dropout medium lacking leucine, tryptophan, adenine and histidine. Colonies survived were further screened for activation of a *LacZ* reporter gene by a filter lift assay. Plasmid cDNAs were isolated from the positive colonies and individually tested against the bait pGBKT7-PC2C and empty vector pGBKT7. Constructs of FPC, PC2, kinesin-2 (Fig. 2-1A) in the pGBKT7 or pGADT7 vector, were transformed into yeast strain Y187 containing *LacZ* reporter gene for pairwise interaction assay. Furthermore, a liquid culture assay was used to quantify β -galactosidase activity using ONPG as substrate according to the manufacturer's instructions.

Cell culture and transfection

MDCK, IMCD and human embryonic kidney (HEK293) cells were cultured in Dulbecco's modified Eagle's medium (DMEM) supplemented with 10% fetal bovine serum (FBS). Cells of less than 25 cycles were cultured to full confluence before collection. Transient transfection of PC2, FPC and KIF3B were performed on MDCK cells cultured to 90-95% confluence using lipofectamine 2000 (Invitrogen, Carlsbad, CA) according to the manufacturer's recommendation. Stable cell line was selected by applying G418 (0.5 mg/ml) and FACS Aria cell sorting (BD Biosciences, San Jose, CA).

Plasmids and antibodies

The cDNAs of KIF3A and KIF3B were generous gifts of Dr. Tetsu Akiyama (University of Tokyo, Tokyo, Japan). The KAP3 and IFT20 cDNAs were obtained by

RT-PCR from HEK293 cells. pEGFPC2 (Clontech) was used to construct individual genes with an EGFP tag. These constructs were then used as templates to make cDNA constructs with a HA or FLAG tag. All plasmids were verified by sequencing. Mouse monoclonal (Cat #: 611535) and goat polyclonal (C-18) antibodies against KIF3B were purchased from BD Biosciences (Mississauga, ON Canada) and Santa Cruz (Santa Cruz, CA), respectively. Rabbit polyclonal antibody against KIF3A (Cat#: K3513) and actin (Cat#: A2066) were from Sigma-Aldrich Canada (Oakville, ON). Mouse monoclonal anti-PC2 antibody 1A11 was raised against human GST-PC2C fusion protein (aa 682-968), and goat polyclonal anti-PC2 antibody G-20 was purchased from Santa Cruz and characterized previously (18). Mouse monoclonal anti-FPC antibody hAR-C2m3C10 and rabbit polyclonal anti-FPC antibody hAR-C2p were raised against its cytoplasmic domain (aa 3872-4074), and mouse monoclonal anti-FPC antibody hAR-Nm3G12 was raised against its N-terminal domain (aa 481-700), as described previously (23). Rabbit polyclonal anti-GFP was from BD Biosciences. The secondary antibodies, both fluorescein-labeled and peroxidase-conjugated IgGs, were from Chemicon International (Temecula, CA).

GST pull-down

Precleared bacterial protein extracts (250 μ l) containing GST-PC2C, GST-FPCC, or GST alone was incubated with 2 μ g of purified His-KIF3AC, His-KIF3BC or His-KIF3BN protein in the binding buffer (50 mM Tris, pH 7.5, 150 mM NaCl, 1 mM CaCl_2). The mixture was incubated at room temperature (RT) for 1 hr with gentle shaking, followed by another hour of incubation after addition of 100 μ l glutathione-agarose beads (Sigma-Aldrich Canada). The beads were then washed several times with 140 mM NaCl, 10 mM Na_2HPO_4 , 1.8 mM KH_2PO_4 , pH 7.5, and the remaining proteins were eluted using 10 mM glutathione, 50 mM Tris, pH 8.0. The protein samples were resolved by SDS-PAGE (10%) and transferred onto nitrocellulose membranes (Bio-Rad, Hercules, CA). The filters were then blocked with 3% skim milk powder, immunoblotted with KIF3A or KIF3B antibodies respectively, and visualized with enhanced chemiluminescence (Amersham, Baie d'Urfe, Canada). Similar procedure was used for

GST-pull down analysis between PC2 and FPC, except that all proteins were purified and that extensive washing was applied.

Dot blot overlay

Proteins of GST-PC2N, GST-PC2C and GST were prepared and described previously (18), GST-FPCC and GST-KIF3BC were prepared similarly. All these proteins were spotted on dry nitrocellulose membrane strips that were then allowed to air dry for 10 min and saturated with phosphates-buffered saline (PBS) containing 3% BSA for 1 hr at RT. The strips were subsequently incubated at 4°C overnight with native IMCD or MDCK cell lysates in 50 mM Tris, pH 7.5, 150 mM NaCl, 1 mM CaCl₂ or 1 mM EGTA, 1% BSA, washed with PBS twice (10 min each) and immunoblotted with KIF3B antibody. Purified GST-KIF3BC fusion protein was used as positive control.

Far Western blot

Equal amounts of BSA and cell lysates were run on SDS-PAGE and transferred to nitrocellulose membrane. Proteins were denatured and renatured in AC buffer (100mM NaCl, 20 mM Tris, pH 7.6, 0.5mM EDTA, 10% glycerol, 0.1% Tween-20, 2% milk powder, 1 mM DTT) by reducing guanidine-HCl. Briefly, it was denatured with 6 M Guanidine-HCl in AC buffer for 30 min at RT. Then it was washed in 3M Guanidine-HCl for 30 min at RT, then 1M Guanidine-HCl in AC buffer for 30 min at 4°C, and then in 0.1M for 30 min at 4°C. Finally, it was further renatured in AC buffer (without guanidine-HCl) overnight at 4°C. Then membranes were incubated with bacterially purified protein in 4°C for 3 hr in AC buffer, followed by regular WB.

Co-immunoprecipitation

Reciprocal co-IP was performed using lysates of native IMCD, MDCK cells (2 X 10⁷ cells), human kidney and heart tissues (10 mg total proteins). Cell monolayers in 100 mm dishes were washed twice with PBS and solubilized in ice-cold CellLytic-M lysis buffer and proteinase inhibitor cocktail (Sigma-Aldrich Canada). Fresh kidney and heart tissues were flash-frozen in liquid nitrogen, macerated to fine powder and solubilized in the lysis buffer. Supernatant was collected following centrifugation at 16,000 g for 20

min. Equal amounts of total protein from postnuclear supernatants were precleared for 1 hr with protein G-/or A-sepharose (Sigma-Aldrich Canada) and then incubated for another hour on ice with antibody against PC2, FPC or KIF3B. After the addition of 150 μ l of 50% protein G-/or A-sepharose, the mixtures were incubated for another hour with gentle shaking. The immune complexes absorbed to protein G-/or A-sepharose were washed three times with the lysis buffer. The precipitated proteins were analyzed by WB using antibodies against kinesin-2, FPC or PC2. Co-IP experiments were conducted reciprocally.

Immunofluorescence

Cells were grown on coverslips, fixed with 4% freshly prepared paraformaldehyde for 10 min at RT, washed twice with PBS, and permeabilized in 0.2% Triton X-100 at RT for 10 min. Cells were blocked by 5% nonfat milk in PBST (PBS plus 0.05% Tween 20) at RT for 1hr, then incubated at RT for 1 hr with the PC2, FPC or KIF3B primary antibodies, followed by another hour of incubation with secondary antibodies. Cells were finally washed with PBS. Vectashield mounting medium (Vector Laboratories, Burlingame, CA) was used to protect immunofluorescence signals from fading. Fluorescent images were captured on a motorized Olympus IX81 microscopy installed with a CCD cooling RT SE6 monochrome camera (Diagnostic Instruments, Sterling Heights, MI). Final composite images were Image-Pro Plus 5.0 (Media Cybernetics Inc., Silver Spring, MD).

Small Interfering RNA

Three double-stranded RNA were synthesized for each of the mouse *pkd2* and *kif3b* genes by Invitrogen (Supplementary data Table). For mouse FPC, the reported sequence (5'-AAAGTCAGGAGCTCCACCTAC-3') (47) was chosen. The altered expression of the target proteins was evaluated by immunoblot, and mixed siRNAs were utilized to maximize the knock down effect. A double stranded RNA against human mitogen-activated protein kinase p38 α isoform was used as a control. IMCD cells at 50-60% confluency were transiently transfected using lipofectamine 2000 according to the

manufacturer's instructions. Cell lysates were collected 48 hr after transfection for WB and Co-IP assays.

Protein preparation and planar lipid bilayer electrophysiology

His-KIF3BC, His-KIF3BN and His-FPCC proteins were purified from *E. coli* in pET28a(+) vector (Novagen, La Jolla, CA). TAP-PC2 was prepared and reconstituted in a lipid bilayer system as previously described (32) to assess the channel activity. Briefly, a lipid bilayer was formed with a mixture of 1-palmitoyl-2-oleoyl phosphatidyl-choline and phosphatidyl-ethanolamine (Avanti Polar Lipids, Birmingham, AL) at a 3:7 ratio in a Delrin cup inserted in an acrylic chamber (Harvard Apparatus, Montreal, QC). The *cis* (or *trans*) compartment contained 150 (or 15) mM KCl, 15 μ M Ca (by 1 mM EGTA and 1.01 mM CaCl₂), pH 7.4 (adjusted by MOPS-KOH). TAP-PC2 protein was added to the *cis* chamber in proximity of the membrane or used to directly 'paint' the membrane. Alternatively, TAP-PC2-containing proteoliposome was directly painted to form the membrane with PC2 channel proteins expectedly inserted. KIF3BC/KIF3BN and/or FPCC proteins were added to the *cis* chamber when studying their effects on PC2 channel. The *cis* compartment was clamped to a range of voltages using a Gapfree protocol generated by Clampex 8 (Axon Instruments, Union City, CA) and the *trans* compartment was held at ground (0 mV). Currents and voltages were recorded at 200 μ s per sample, Bessel filtered at 1K or 3K Hz with the amplifier PC-ONE (Dagan Corporation, Minneapolis, MN), the AD/DA converter Digidata 1320A and the software Clampex 8 (Axon Instruments).

Data analysis

Data obtained from lipid bilayer experiments were analyzed using Clampfit 9. The all-point histogram was used to calculate single-channel amplitudes and obtain data for current density plotting. The open probability times the number of channels in the bilayer membrane (NP_o, designated 'open probability') was obtained from currents generated by gap-free recordings of 20 s long. Analyzed data were plotted using Sigmaplot 9 (Jandel Scientific Software, San Rafael, CA) and expressed in the form of mean \pm SE (N), where SE is the standard error and N the number of independent measurements.

2.3. RESULTS

Interaction of PC2 and FPC with KIF3B revealed by yeast two-hybrid

A yeast two-hybrid system was used to screen proteins that associate with the C-terminus of PC2 (PC2C, aa 682-968, Fig. 2-1A). A bait construct, pGBKT7-PC2C, was used to screen a human heart cDNA library (Clontech, Palo Alto, CA). One plasmid isolated from the library represented a C-terminal fragment of human KIF3B protein (called thereafter KIF3BC, aa 407-747, Fig. 2-1A), containing part of the coiled-coil region and the whole globular tail. Interestingly, the FPC intracellular C-terminus (FPCC, aa 3882-4074) and the PC2 intracellular N-terminus (PC2N, aa 1-215, Fig. 2-1A) also strongly associated with KIF3BC. We further found that a smaller fragment within KIF3BC (KIF3BC1, aa 592-670) associates with FPCC. On the other hand, our liquid β -galactosidase quantitative and colony lift assays revealed no binding between FPCC and the following fragments: PC2C, PC2N and the C-terminus of PC1 (PC1C, aa 4088-4302), between KIF3BC and PC1C, and between the KIF3B N-terminus (KIF3BN, aa 1-406) and PC2C (or FPCC) (Fig. 2-1B and C). No β -galactosidase activity was detected between empty vectors pGBKT7 and pGADT7 (Fig. 2-1B), which served as a negative control.

We also tested the KIF3A and KAP3 subunits utilizing the yeast colony lift assay. PC2C associated with KIF3A (full-length and the C-terminus, KIF3AC, aa 403-702, but not the N-terminus, KIF3AN, aa 1-402) while FPCC exhibited no association with these KIF3A fragments (Fig. 2-1C). Neither PC2C nor FPCC interacted with KAP3 (full length and truncated fragments KAP3N, aa 1-448, and KAP3C, aa 449-792). We also found no association between KIF3B and three extracellular fragments of FPC: FPCN1 (aa 30-396), FPCN2 (aa 1313-1852) and FPCN3 (aa 3465-3849) (Fig. 2-1A and C). Of note, we confirmed the previously reported association between KIF3B and IFT20 (31), but found no binding between IFT20 and PC2 (or FPC) (Fig. 2-1C). Thus, KIF3B is the only identified intermediate protein in these assays that directly binds both PC2 and FPC.

***In vitro* and *in vivo* association of PC2 or FPC with KIF3B**

We first employed immunoprecipitation (IP) and peptide blocking to validate the specificity of antibodies against FPC (hAR-C2m3C10, or C10), PC2 (1A11), both being

previously reported (18,23), and KIF3B (Cat #: 611535). The specificity of C10 was verified in combination with the use of a FLAG antibody in Madin-Darby canine kidney (MDCK) cells expressing FLAG-FPCC (Fig. 2-2A), and with the use of the antibody hAR-Nm3G12 (G12) against the FPC N-terminus in native mouse inner medulla collecting duct (IMCD) cells (Fig. 2-2B). The presence of a small band of ~135 kDa, recognized by C10 but not G12, was previously reported and presumably corresponds to a N-terminal truncated variant of FPC (23). The specificity of 1A11 (Fig. 2-2C), #611535 (Fig. 2-2D), G-20 (PC2, not shown), and C-18 (KIF3B, not shown) was verified in native IMCD cells as well. We then utilized *in vitro* biochemical methods to further characterize the interaction between PC2/FPC and KIF3B. We first employed a glutathione S-transferase (GST) fusion protein affinity binding method. For this purpose poly-histidine-tagged (His-) KIF3AC and KIF3BC and GST-tagged (GST-) PC2C and FPCC were expressed in bacteria BL21 (DE3) in the presence of 1 mM IPTG (Fig. 2-3A, panels 1 and 2). Cell extracts containing PC2C or FPCC were incubated with purified KIF3AC or KIF3BC, and detected with a specific antibody against KIF3A or KIF3B. GST-PC2C co-precipitated with KIF3BC and KIF3AC, while GST-FPCC co-precipitated with KIF3BC, but not with KIF3AC (Fig. 2-3A, panels 3 and 4). GST alone exhibited no binding with KIF3AC or KIF3BC.

Because KIF3A was able to bind PC2 but not FPC, in next experiments we focused on using KIF3B. We also performed dot blot overlay experiments to examine the PC2-KIF3B and FPC-KIF3B interactions. GST-PC2N, GST-PC2C, GST-FPCC and GST proteins purified from *E. coli* were spotted onto a nitrocellulose membrane followed by incubation with lysates of IMCD or MDCK cells (not shown). The membrane was then washed and probed with a mouse monoclonal antibody against KIF3B. Immunoreactive spots were observed with GST-PC2N, GST-PC2C and GST-FPCC, but not with GST, bovine serum albumin (BSA) or binding buffer alone (Fig. 2-3B), further demonstrating that PC2 and FPC associate with KIF3B.

To determine whether PC2 and FPC interact with kinesin-2 *in vivo* we performed co-IP experiments using native IMCD cells, MDCK cells and human kidney tissues. Using antibodies against KIF3B, PC2 or FPC for precipitation, we detected associated proteins via immunoblotting. PC2 and FPC were detected in the immunoprecipitates

using a KIF3B antibody, but not in the control immunoprecipitates using non-immune serum (Fig. 2-3C). Reciprocal co-IP using an antibody against PC2 or FPC also precipitated KIF3B from these cells or tissue lysates. These results demonstrate that the protein complexes in the forms of PC2-KIF3B and FPC-KIF3B are present *in vivo* in these cells and tissues. Note that the fact that KIF3B associates with both PC2 and FPC does not guarantee that these three proteins are in a common complex. In fact, even without the existence of the triplex PC2-KIF3B-FPC, the simultaneous presence of the duplexes KIF3B-PC2 and KIF3B-FPC *in vivo* is sufficient to account for all our observed data. Therefore, whether PC2 and FPC are in a same protein complex requires further verification.

Interaction between PC2 and FPC

We performed reciprocal co-IP experiments using native cells and tissues and revealed that the two proteins are in the same complex (Fig. 2-4A). Furthermore, we used siRNA to decrease the expression of FPC or PC2 in IMCD cells, and found that FPC was more efficiently diminished than PC2. Thus we chose native IMCD cells and those with either *pkhd1* siRNA or FPCC over-expression for further co-IP assays. As expected, we found that the amount of immunoprecipitated PC2 in siRNA cells was smaller than the one in native cells, which itself is smaller than the one in over-expressed cells (right panel, Fig. 2-4B). Note that, compared to native IMCD cells, there was no appreciable change in the PC2 level in cells over-expressing FPCC (106% \pm 10%, from three WB data after normalization by the actin expression) or in those with *pkhd1* siRNA (114% \pm 6%, N = 3) (left panels, Fig. 2-4B).

To further substantiate a physical interaction between PC2 and FPC we transfected MDCK cells with the FLAG-tagged FPC transmembrane domain plus FPCC (FPCTMC, aa 3850-4074) or TAP-PC2, a PC2 construct containing two protein A and one calmodulin binding domains used in a modified tandem affinity purification (TAP) (32). Analysis of derived cell lysates by FLAG-M2 beads chromatography and immunoblotting revealed retention of PC2, KIF3A and KIF3B along with FLAG-FPCTMC. Reciprocally, using protein A pull-down and immunoblotting we observed retention of FPC, KIF3A and KIF3B along with TAP-PC2 (Fig. 2-4C). Similar results

were found when FPCC was used in place of FPCTMC (data not shown). These results provide further support that PC2 and FPC are in a common complex, either via direct binding or via intermediate proteins that could include KIF3B. Note that no direct binding was revealed by yeast two-hybrid assays performed by J. Zhou's group (personal communication) and the present study (Fig. 2-1), which is in favor of the involvement of a mediator protein for the PC2-FPC interaction. However, due to limitations associated with the yeast two-hybrid method, we can't exclude the possibility that PC2 and FPC direct bind, eg, via transmembrane domains or other soluble fragments not tested. Because no direct binding between FPC and KIF3A was found so far (Fig. 2-1 and 2-3), the positive interaction between FPCTMC and KIF3A revealed here is presumably indirect and because KIF3A binds KIF3B (abundantly present in native cells, see Fig. 2-5B) which binds FPC. We consider KIF3B a candidate for the mediator protein as it binds both PC2 and FPC. However, for KIF3B to act as an intermediate protein, a single KIF3B molecule must be able to simultaneously bind PC2 and FPC, which has so far not been proved.

Complexing between PC2 and FPC, and roles of KIF3B

We first examined the direct binding between PC2 and FPC by *in vitro* binding experiments. We found that GST-PC2C associated with His-FPCC and that His-PC2C associated with GST-FPCC in the presence of KIF3BC, but not in its absence or in the presence of KIF3BN (Fig. 2-5A). This result is in agreement with the finding by yeast two-hybrid, indicating that there is no direct association between PC2 and FPC, and demonstrates that KIF3B acts as a mediator of the interaction between PC2 and FPC. Thus, this *in vitro* binding assay indicates the existence of a PC2-KIF3B-FPC complex.

To verify the mediator role of KIF3B in the complexing between FPC and PC2, we used siRNA to decrease the KIF3B expression in IMCD cells and found that KIF3B was effectively diminished. We then compared the PC2-FPC complexing between native IMCD cells and those with diminished KIF3B or with over-expression of KIF3BC, by use of co-IP. Indeed we found that the complexing strength between PC2 and FPC was significantly decreased in *kif3b* siRNA cells and increased in over-expressed cells (Fig. 2-5B), which confirms a bridging role of KIF3B. Of note, compared to native IMCD cells,

there was no appreciable change in the PC2 and FPC expression levels in cells over-expressing KIF3BC (PC2, 109% \pm 12%; FPC, 96% \pm 12%; N = 3), or in those with *kif3b* siRNA (PC2, 108% \pm 3%; FPC, 103% \pm 2%; N = 3) (Fig. 2-5B).

We next created conditions under which native mediator proteins in MDCK cells, eg, KIF3B, are separated from PC2 and FPC. For this we performed Far Western blot (WB) experiments using transfected MDCK cell lines stably expressing GFP-tagged PC2, PC2C or FPCC (see Fig. 2-6A), and purified GST-PC2C, GST-FPCC, His-KIF3AC and His-KIF3BC proteins from *E. coli*. To separate individual proteins, including mediator proteins, from any complexes present in the cell lysates, we ran SDS-PAGE of cell lysates. The samples were transferred to nitrocellulose membrane where proteins were denatured, then renatured, and followed by incubation with purified partner proteins for 3 hr to allow potential associations. This was followed by wash and regular WB to detect binding of incubated proteins. Incubation of FPCC alone (Fig. 2-6B, left panel) or of FPCC plus KIF3AC (Fig. 2-6C, left panel) did not result in the detection of FPCC on the sites where over-expressed GFP-PC2C (~60 kDa) or GFP-PC2 (~140 kDa) is found indicating that FPCC is not bound directly to PC2C or full-length PC2 and that KIF3AC did not promote their binding. In contrast, Incubation of FPCC plus KIF3BC resulted in the detection of FPCC on the sites where over-expressed GFP-PC2C or GFP-PC2 is found (Fig. 2-6D, left panel, lanes 3 and 4, indicated by arrows), demonstrating that KIF3BC mediates the complexing between PC2 and FPCC. Reciprocally, purified PC2C bound to the over-expressed GFP-FPCC (~50 kDa) in MDCK cells in the presence of KIF3BC (Fig. 2-6D, right panel, lane 3, indicated by arrow), but not in its absence or in the presence of KIF3AC (Fig. 2-6B and C, right panels). Thus, because in these assays any native mediator proteins were separated from PC2 and FPC, KIF3BC acted as a necessary and sufficient linker for complexing between PC2 and FPC, presumably by forming a PC2-KIF3B-FPC triplex.

To lend further support to the existence of a complex containing PC2, KIF3B and FPC, we conducted an iodixanol gradient fractionation experiment using native IMCD cells. KIF3B, FPC and KIF3A were found in light and medium fractions while PC2 was distributed in middle and dense fractions. All four proteins co-existed in some fractions,

especially in fraction #8, indicative of the presence of a large protein complex containing these four proteins in IMCD cells.

Subcellular co-localization of PC2 and FPC with KIF3B

To examine where these three proteins are colocalized in cells we performed indirect immunofluorescence assays in cultured over-confluent (ciliated) and sub-confluent IMCD cells. Consistent with reported ciliary localization of these proteins (22,23,33,34), we found that PC2, FPC and KIF3B were indeed present and partially colocalized in primary cilia of IMCD cells (Fig. 2-7A). When cells were sub-confluent, we found that PC2 and FPC were mostly intracellularly localized, and the three proteins seemed to co-localize to a perinuclear region (Fig. 2-7B).

Functional modulation of PC2 channel by FPC through KIF3B

We next wanted to determine whether functional interaction occurs among the three members of the complex PC2-KIF3B-FPC. Because PC2 is a cation channel we examined whether/how FPC and/or KIF3B modulate PC2 channel activity. For this we employed the lipid bilayer electrophysiology assay (see Materials and Methods). We prepared full-length PC2 from MDCK stable cell line by a modified TAP method and purified His-KIF3BC and His-FPCC from *E. coli*. In the presence of PC2 alone, PC2 opened at three different conductance states (Fig. 2-8A and B). The main state opened only occasionally with an averaged open probability (NPo) value of 0.018 ± 0.003 and an averaged single-channel conductance (G) value of 141 ± 13 pS (N = 5) (-20 to +160 mV) (Fig. 2-8B). The intermediate state opened with an NPo value of 0.07 ± 0.01 and a G value of 68.6 ± 7.5 pS (N = 14) (0 to +160 mV). The small (conductance) state opened most often, with an NPo value of 0.18 ± 0.02 and a G value of 50.6 ± 5.4 pS (N = 25) (+80 to +160 mV). Addition of KIF3BC and FPCC to the *cis* chamber substantially augmented the likelihood of PC2 channel opening at the main state, with a G value of 150 ± 7 pS (N = 14) (Fig. 2-8C and D), not significantly different from the value obtained in the absence of KIF3BC and FPCC (P = 0.51). The corresponding NPo value increased to 0.48 ± 0.04 pS (N = 14) (P = 0.0001) (0 to +140 mV) (Fig. 2-9A). Under this condition, the intermediate and small conductance states of PC2 were also observed, with G values

of 80.3 ± 11.6 pS (N = 9) and 32.0 ± 5.5 pS (N = 19), respectively (Fig. 2-8C and D). The increased activity of PC2 at the main state by KIF3BC plus FPCC was also demonstrated by current density plotting of recordings at +20 mV (Fig. 2-9B). The small (conductance) state was observed less often than in the absence of both KIF3BC and FPCC. When FPCC or KIF3BC alone was added, multiple conductance states of PC2 were also present (Fig. 2-9C). However, addition of FPCC or KIF3BC alone was unable to increase the likelihood of PC2 opening at the main state (Fig. 2-9A). With only FPCC added, the G values were 157 ± 26 pS (N = 5) (main state, -40 to +60 mV), 76.3 ± 10.8 pS (N = 16) (intermediate state, 0 to +160 mV), and 53.6 ± 7.9 pS (N = 27) (small state, +80 to +160 mV). With only KIF3BC added, the G values were correspondingly 144 ± 27 pS (N = 3) (-40 to +60 mV), 62.7 ± 10.2 pS (N = 8) (0 to +160 mV), and 45.6 ± 8.0 pS (N = 20) (+80 to +160 mV). We also employed mean currents (without discerning various conductance states) to assess PC2 channel activity. No significant difference in the mean currents was observed among the three conditions where PC2 alone, PC2 + FPCC or PC2 + KIF3BC was present. In average, the presence of KIF3BC and FPCC together increased the mean single-channel currents of PC2 by about 5 fold (Fig. 2-9D), consistent with the results presented by NPo and histogram plotting. We utilized the KIF3B truncation mutant, KIF3BN, as a negative control of KIF3B as it does not bind PC2 or FPC (Fig. 2-1) nor mediate the link between PC2 and FPC (Fig. 2-5A). From five paired experiments we found that neither of FPCC+KIF3BN and KIF3BN exhibited significant modulation effect on PC2 channel. Further, when we added FPCC or KIF3BC protein alone to the *trans* side we did not observe significant functional effects on PC2 channel activity (N = 10). Of note, KIF3A is not suitable candidate as a negative control in this regard because it exhibits functional modulation of PC2 channel (35). Thus, although KIF3B directly associates with PC2, it did not exert a significant effect on PC2; the stimulatory effect on PC2 was by the indirect partner, FPC, when KIF3B was present. In summary, together with the presence of the PC2-KIF3B-FPC triplex supported by our physical interaction data (Fig. 2-1 ~ 2-6), our functional data demonstrated that KIF3B mediates the stimulation of PC2 channel activity by FPC.

2.4. DISCUSSION

Human ADPKD and ARPKD share similar clinical manifestations despite of different genetic backgrounds. Moreover, mutations in a diverse number of proteins, including kinesin-2, polaris, cystin and inversin, which have no sequence similarity with either polycystins or fibrocystin, also result in renal cyst development (36-39). This raises the possibility that common molecular mechanisms of cystogenesis exist, namely, the possibility that these cystoproteins are present in same complexes. Indeed, our present studies demonstrate that PC2 and FPC are part of the same protein complex. Using co-IP, two other groups recently found that FPC and PC2 are present in the same complex (personal communications). However, co-IP assays do not tell whether two proteins directly bind to each other. Data from our current study using several approaches and those by Zhou's group using yeast two-hybrid method (personal communication) show that FPC and PC2 do not bind directly to each other. Thus, the protein(s) mediating the PC2-FPC complexing remained to be identified. Using a combination of *in vitro* and *in vivo* approaches, including yeast two-hybrid, GST pull-down and Far WB, we have demonstrated that the kinesin-2 motor subunit KIF3B acts as a linker protein, which enables the formation of a triplex, presumably in the form of PC2-KIF3B-FPC. Thus KIF3B represents the first molecular linker between ADPKD and ARPKD proteins, suggesting that the protein complex PC2-KIF3B-FPC is part of a common molecular pathway generally implicated in renal cystic diseases.

Kinesin-2, as a heterotrimer formed by KIF3A, KIF3B and KAP3, is important for numerous cell functions, in particular, cilium growth and cell cycle (25,28,33,40), and has profound pathological implications. Disruption of KIF3B in nodal cilia damages ciliary growth, which alters leftward nodal flow and consequently results in abnormal embryonic left-right asymmetry development (41). Similarly, mice with KIF3A knockout fail to synthesize cilia in the embryonic node and exhibits randomization of the left-right asymmetry and structural abnormalities of the neural tube, pericardium, brachial arches and somites (42,43). Kidney-specific inactivation of KIF3A resulted in cyst formation in renal tubular epithelial cells at postnatal day 5 and caused renal failure by postnatal day 21 (36). KAP3 is associated with adenomatous polyposis coli and responsible for its

transportation along microtubules (44) and is required for axoneme growth and maintenance of the cilia in *Drosophila* type 1 sensory neurons (45).

Given the existence of a triplex PC2-KIF3B-FPC, it is important to determine where the three proteins colocalize as this would provide hints as to their possible physiological roles. In ciliated IMCD cells, PC2 partially colocalized with KIF3B and FPC in primary cilia. Together with a recent report that PC2 and PC1 in renal primary cilia constitute part of a shear stress sensor responsive to tubular flow (34), our data suggest the possibility that the flow sensor is composed of a larger complex, containing not only PC1 and PC2, but also KIF3B, FPC and possibly other proteins. Under this scenario, PC2 as a Ca-permeable channel in the primary cilium would be regulated by several proteins, including PC1, FPC and others. Interestingly, single-channel activity of PC2 on the membrane of isolated primary cilia was recently detected (46).

Using the lipid bilayer electrophysiology assay we demonstrated that FPC is capable of increasing PC2 channel function in the presence, but not in the absence of KIF3B. Thus KIF3B likely links PC2 and FPC together not only in a structural complex but also for the regulation of PC2 channel function, which establishes both physical and functional links between key proteins responsible for the pathogenesis of ADPKD and ARPKD. PC2 was previously reported to be functionally regulated by partner proteins, including PC1 (34) and α -actinin (18). Our study shows that fibrocystin is another partner of PC2, which functionally up-regulates its channel function through KIF3B. Interestingly, although KIF3B directly binds PC2, it has no significant effect on PC2 channel function, indicating that it primarily serves as a linker protein.

Our lipid bilayer system to investigate the modulation of PC2 in the membrane by KIF3B and FPC introduced from *cis* (intracellular) side of the membrane is a highly simplified model in which microtubule and kinesin-2 motor are not present. However, the beauty and novelty here are that functional modulation occurs in such a simple setting. In a more physiological setting such as primary cilium membrane that envelops a microtubule plus motor machineries, modulation should be more fine tuned and may simply be different, eg, where the associations of KIF3B with the two cystoproteins may be dynamic and under cellular regulations. It is also possible that the roles that KIF3B plays in the PC2-FPC complexing and in the modulation of PC2 by FPC are different

from its roles as a kinesin-2 motor subunit. Studies on their interaction using more physiological models will further help understanding cross talk between ADPKD and ARPKD.

The pathways involved in renal and hepatic cyst formation and non-cystic manifestations in other organs for ADPKD and ARPKD remain illusive. In both *C. elegans* and *Chlamydomonas*, the kinesin-2 complex appears to interact with a large proteinaceous "raft" complex that is composed of 15 different proteins (33). Our current study found that the ADPKD-related protein PC2, the ARPKD-related protein FPC and the kinesin-2 motor subunit KIF3B are in part together in primary cilia and the perinuclear cytoplasm of renal epithelial cells. Among the previously reported binding partners of PC2, FPC and KIF3B, such as PC1, α -actinin, TRPC1, KIF3A (which has a direct association with PC2, see Fig. 2-1 and 2-3), and KAP3 etc, some partners, eg PC1, may also be in the same complex with PC2-KIF3B-FPC. Thus PC2-KIF3B-FPC may potentially be part of a large protein complex which itself is part of a common pathway for dominant and recessive PKDs. Thus one possible scenario would be that a triggering to the complex, eg a ligand binding to FPC or PC1, induces conformational changes to partners in the complex, which leads to modulated PC2 channel activity, which will then affect downstream processes.

ACKNOWLEDGEMENTS

This work was supported by the Canadian Institutes of Health Research, the Canada Foundation for Innovation, the Kidney Foundation of Canada (X.Z.C.), and the Heart and Stroke Foundation of Canada (X.Z.C. and S.W.). X.Z.C. is a recipient of the Alberta Heritage Foundation for Medical Research Scholarship. X.Q.D. is a recipient of AHFMR studentship. Q.L. is a recipient of the Kidney Foundation of Canada Biomedical fellowship

Fig. 2-1. Interactions between PC2, FPC and kinesin-2 identified by yeast two-hybrid experiments. (A) Illustration of FPC, PC2, KIF3B and KIF3A proteins, and their fragments. Numbers refer to amino acid positions; TM, transmembrane. (B) Quantification of interactions between PC1, PC2, FPC and KIF3B in a yeast liquid β -galactosidase assay. Constructs were co-expressed in yeast strain Y187 as fusion proteins with either the GAL4 activation or DNA-binding domain. P53+T-antigen serves as a positive control while empty vectors (pGBKT7+pGADT7) as a negative control. Quantitative data are plotted with error bars corresponding to the S.E. based on three or more independent experiments. (C) Summary of interactions between PC2, FPC and kinesin-2 by a yeast colony lift assay. '+' and '-' indicate the presence and absence of interaction, respectively.

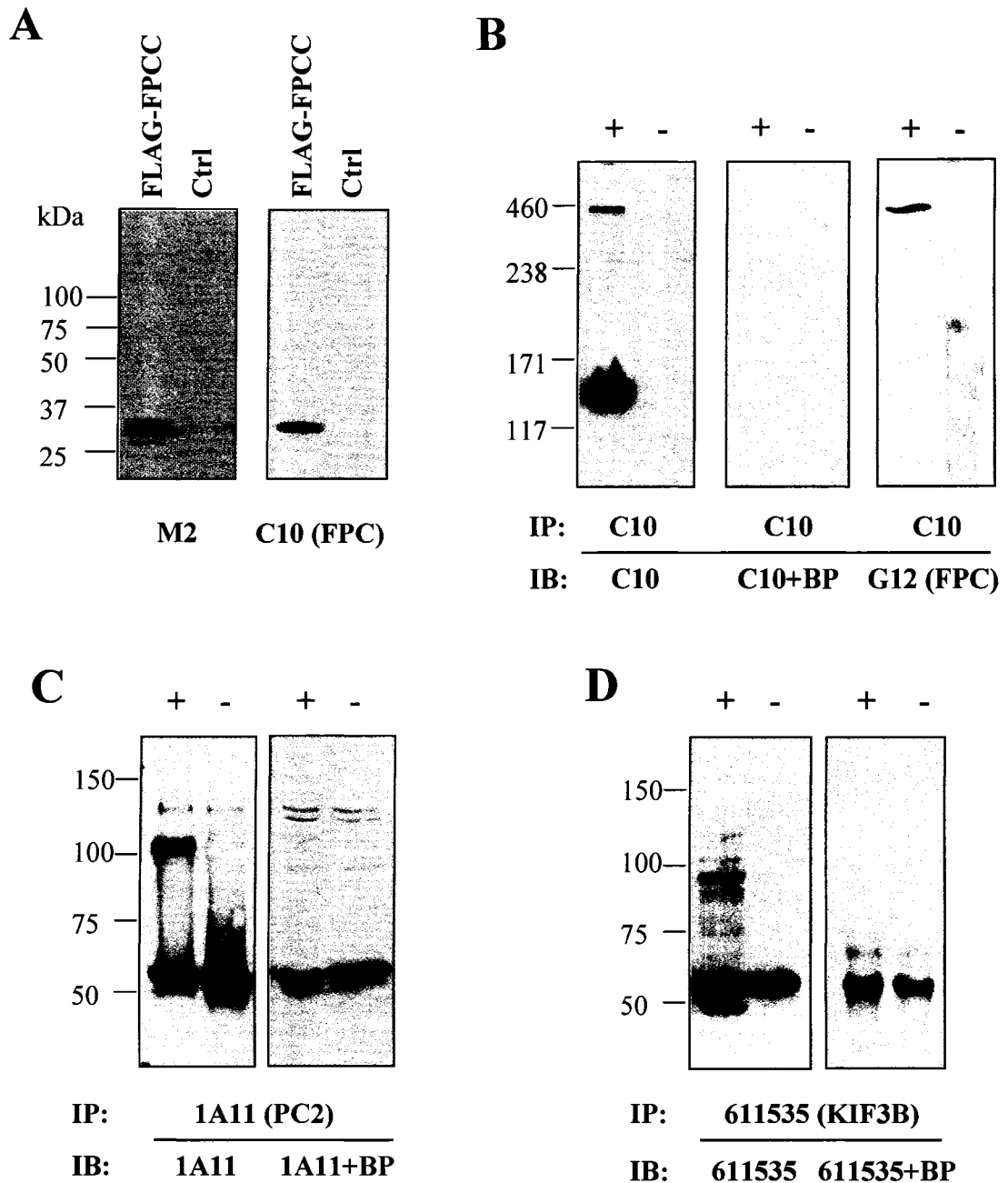


Fig. 2-2. Validation of antibody specificity. (A) MDCK cells were transfected with FLAG-tagged FPCC and cells lysates were detected with anti-FLAG antibody (M2, left panel) or anti-FPC antibody hAR-C2m3C10 (C10, right panel). (B) IMCD cells lysates were immunoprecipitated (IP) with C10, immunoblotted (IB) with the same antibody (left panel) in the presence of FPCC protein as blocking peptide (BP, center panel), and IB with FPC antibody hAR-Nm3G12 (G12, right panel). +, with antibody; -, with non-immune mouse IgG. (C) IMCD cells lysates were IP with PC2 antibody 1A11, IB with the same antibody (left panel) in the presence of blocking peptides PC2C (right panel). (D) IMCD cells lysates were IP with KIF3B antibody (no. 611535), IB with the same antibody (left panel), and blocked with blocking peptides KIF3BC (right panel).

Fig. 2-3. Association of KIF3B with PC2 and FPC revealed by GST pull-down, dot blot and co-IP. (A) Purified His-tagged KIF3BC and KIF3AC proteins were stained by Coomassie Brilliant Blue (CBB). *E. Coli* extract expressing GST alone, GST-PC2C or GST-FPCC were incubated with purified His-KIF3BC or His-KIF3AC. GST-agarose was used to precipitate GST epitope-binding proteins. The resultant protein samples were IB with an antibody against GST, KIF3B (#611535) or KIF3A, as indicated. (B) Purified GST-KIF3BC, -PC2N, -PC2C, -FPCC and GST protein alone were spotted on nitrocellulose membranes, incubated with IMCD cell lysates in a blocking buffer, and then detected by the KIF3B antibody (#611535). GST-KIF3BC acts as a positive control while BSA and PBS binding buffer are negative controls. (C) MDCK and IMCD cell lysates and total proteins from human kidney tissues were IP with an antibody against KIF3B (C-18), PC2 (G-20) or FPC (C2p). The precipitates were immunoblotted with an antibody against PC2 (1A11), FPC (C10) or KIF3B (#611535), as indicated. +, with antibody; -, with non-immune goat or rabbit IgG.

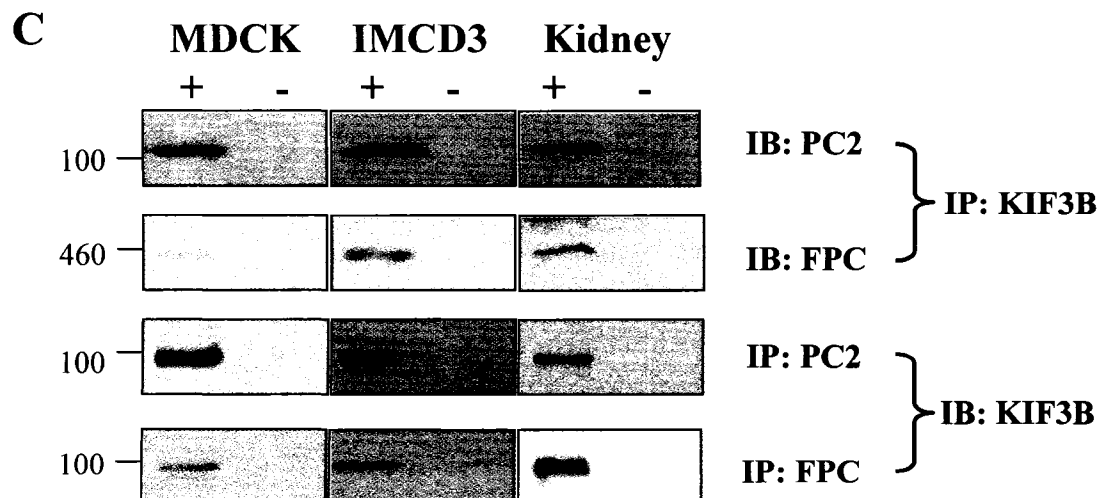
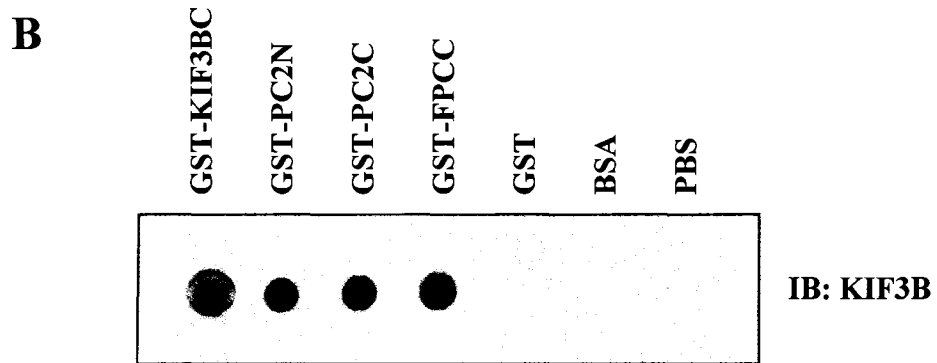
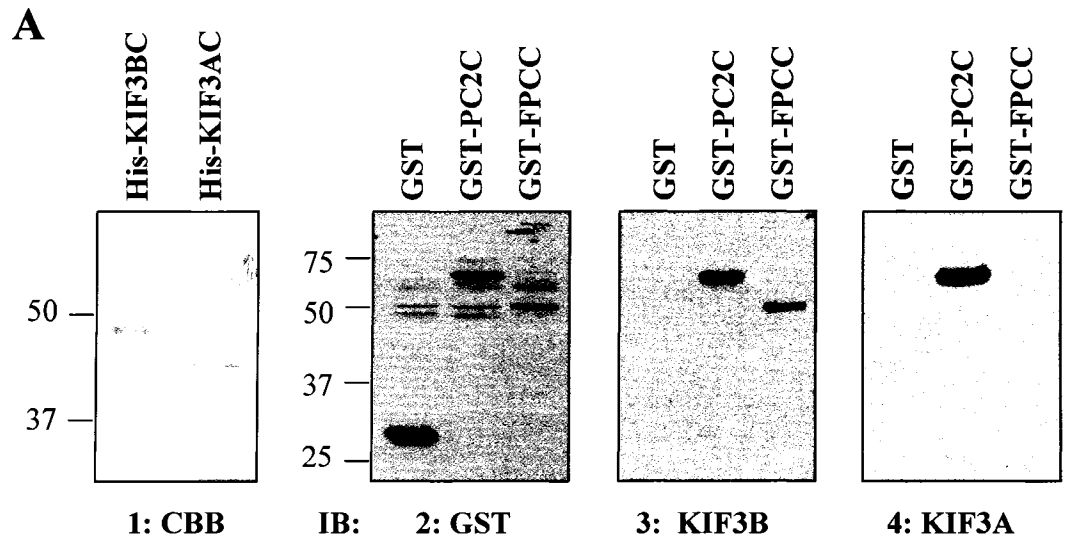
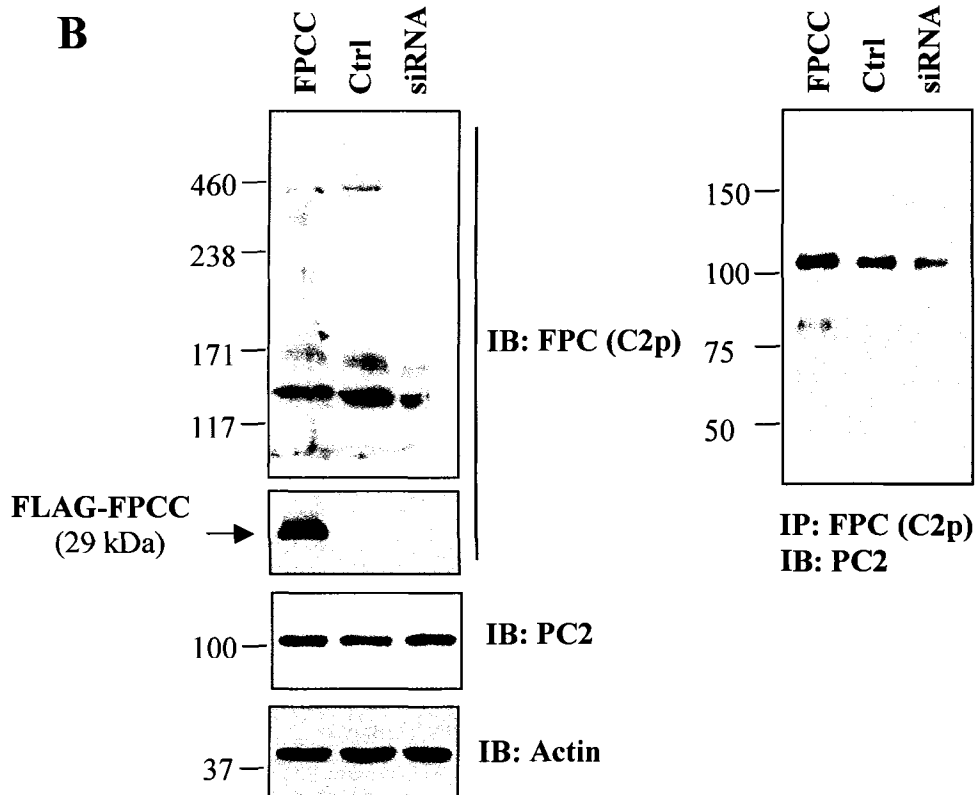
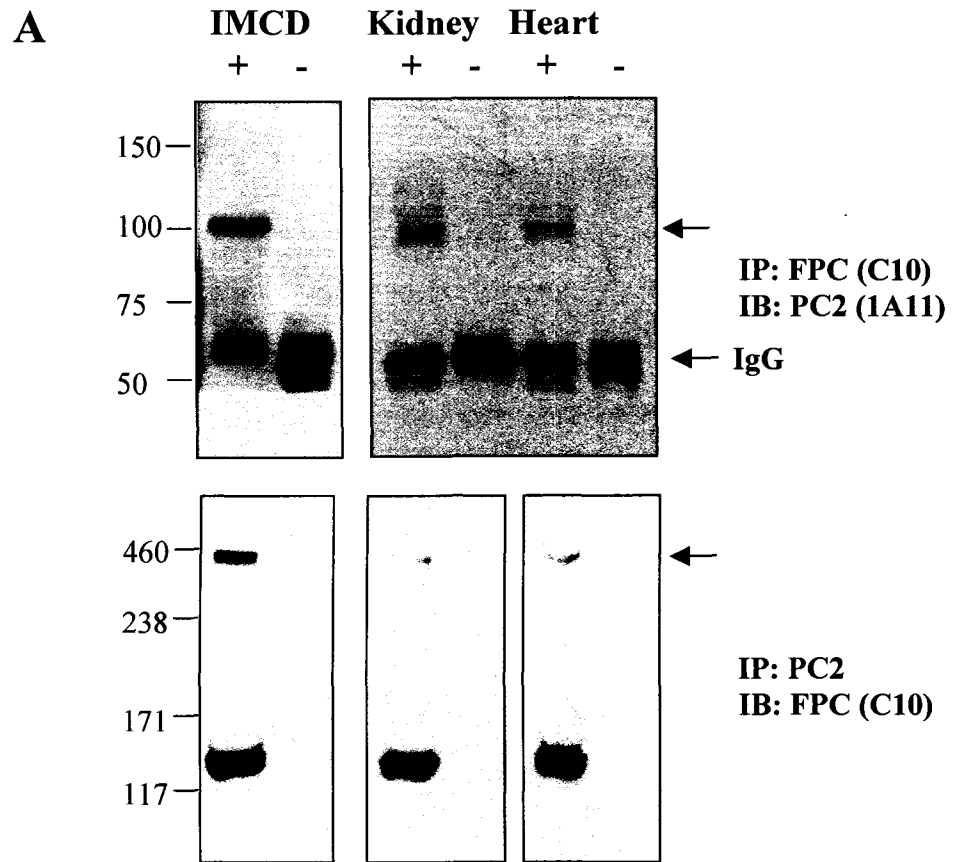


Fig. 2-4. Interaction between PC2 and FPC revealed by co-IP and pull-down. (A) IMCD cell lysates and total proteins from human kidney and heart tissues were IP with FPC (C10, upper panels) or PC2 (1A11, lower panels) antibody and detected by 1A11 or C10. +, with antibody; -, with non-immune mouse IgG. (B) IMCD cells were IP with an FPC antibody (C2p) and IB with PC2 antibody (1A11, right panel). The expression of FPC and PC2 were detected with C2p and 1A11, respectively, in cells over-expressing FLAG-FPCC, native cells (Ctrl), and *pkhd1* siRNA cells. Actin was used as a loading control (left panels). (C) Pull-down experiments using MDCK cells over-expressing FLAG-FPCTMC (upper panels) or TAP-PC2 (lower panels). Proteins eluted from FLAG-M2 beads or protein A agarose were detected with indicated antibodies.



Continued

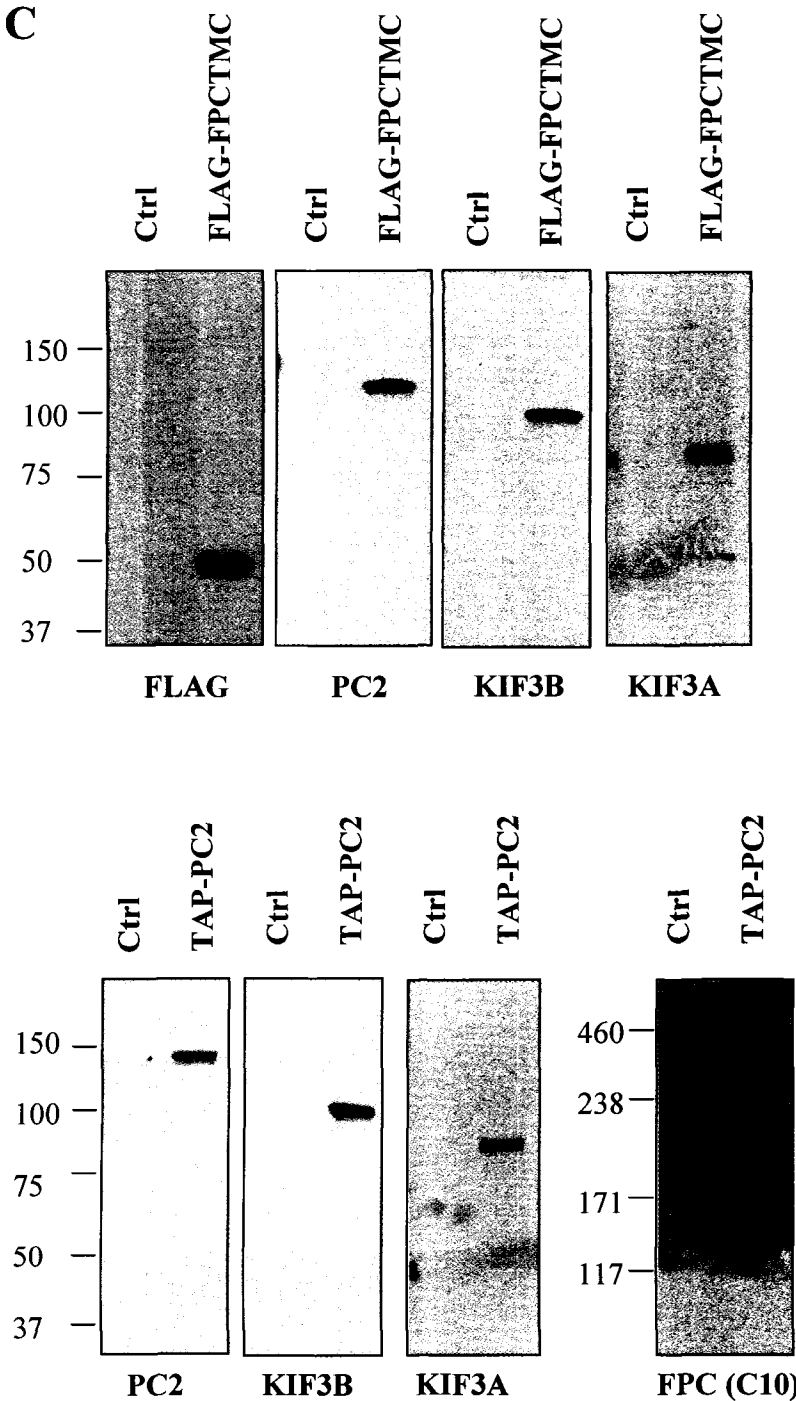


Fig. 2-5. Roles of KIF3B in the PC2 x FPC interaction revealed by *in vitro* binding and co-IP. (A) GST pull-down assay. Purified GST-PC2C (left panel), GST-FPCC (right panel) or GST alone (both panels) was incubated with purified His-FPCC (left panel) or His-PC2C (right panel) with or without His-KIF3BC, His-KIF3BN proteins, as indicated. After extensive wash, the resultant protein samples were immunoblotted with an antibody against FPC (C10) or PC2 (1A11). (B) IMCD cells were precipitated with FPC antibody (C2p) and detected by PC2 antibody (1A11, right panel). The expression of KIF3B, FPC and PC2 were detected with KIF3B antibody (C-18), FPC (C2p) and PC2 (1A11), respectively, in cells over-expressing HA-KIF3BC, native cells (Ctrl), and *kif3b* siRNA cells.

A

GST	+	-	-	-
GST-PC2C	-	+	+	+
His-KIF3BC	-	-	+	-
His-KIF3BN	-	-	-	+
His-FPCC	+	+	+	+

GST	+	-	-	-
GST-FPCC	-	+	+	+
His-KIF3BC	-	-	+	-
His-KIF3BN	-	-	-	+
His-PC2C	+	+	+	+



B

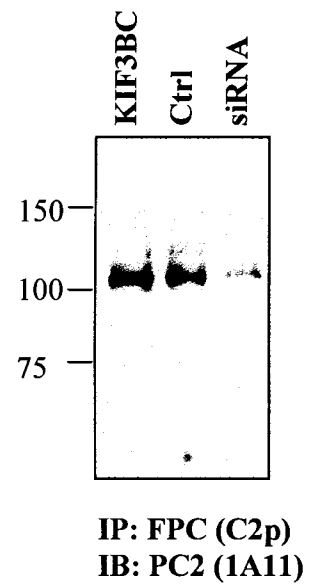
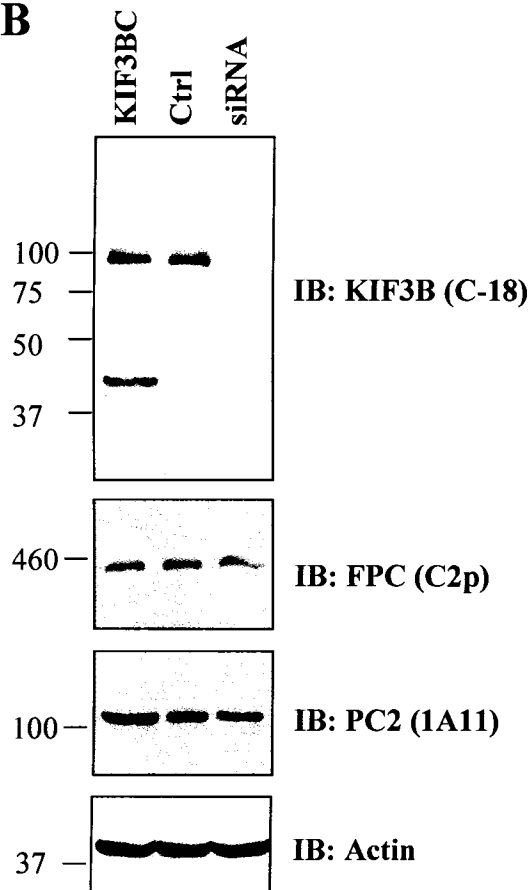


Fig. 2-6. Roles of KIF3B in the PC2 x FPC interaction revealed by Far WB. (A) GFP, GFP-PC2C, GFP-PC2 or GFP-FPCC was stably expressed in MDCK cells. Shown are WB data for GFP-PC2C, GFP-PC2 (left panel), GFP-FPCC (right panel) and GFP (both panels). (B-D) Cell lysates were separated by SDS-PAGE and transferred onto nitrocellulose membranes. Proteins were denatured, renatured, and then incubated with purified FPCC (left panels) or PC2C (right panels) proteins together with none (B, control), KIF3AC (C) or KIF3BC (D). Bound proteins were detected by FPC (C10, left panels) or PC2 antibody (1A11, right panels). BSA and GFP vector (lanes 1 and 2) serve as negative controls. In D panels, arrows point to three novel bands (compared with panels B and C) corresponding to the binding of FPCC to the sites of PC2C (left panel, lane 3) and PC2 (left panel, lane 4), and to the binding of PC2C to the site of FPCC (right panel, lane 3), respectively.

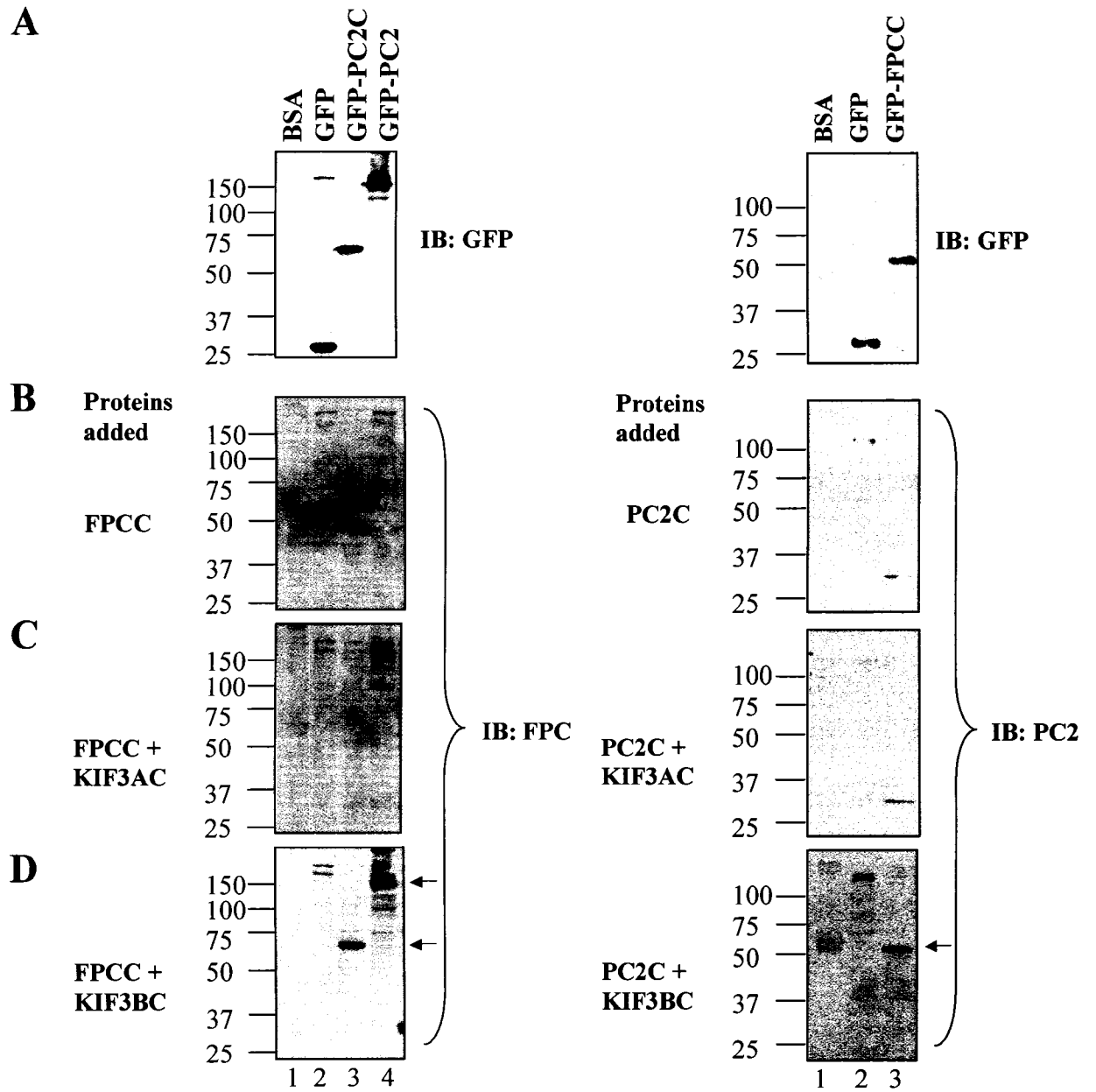




Fig. 2-7. Immunofluorescence staining for PC2, FPC and KIF3B in IMCD cells. (A) Ciliated IMCD cells were co-stained for PC2 (G-20), KIF3B (#611535) and FPC (C2p). **(B)** Sub-confluent cells were co-stained for PC2, KIF3B and FPC. Horizontal bars = 20 μ m.

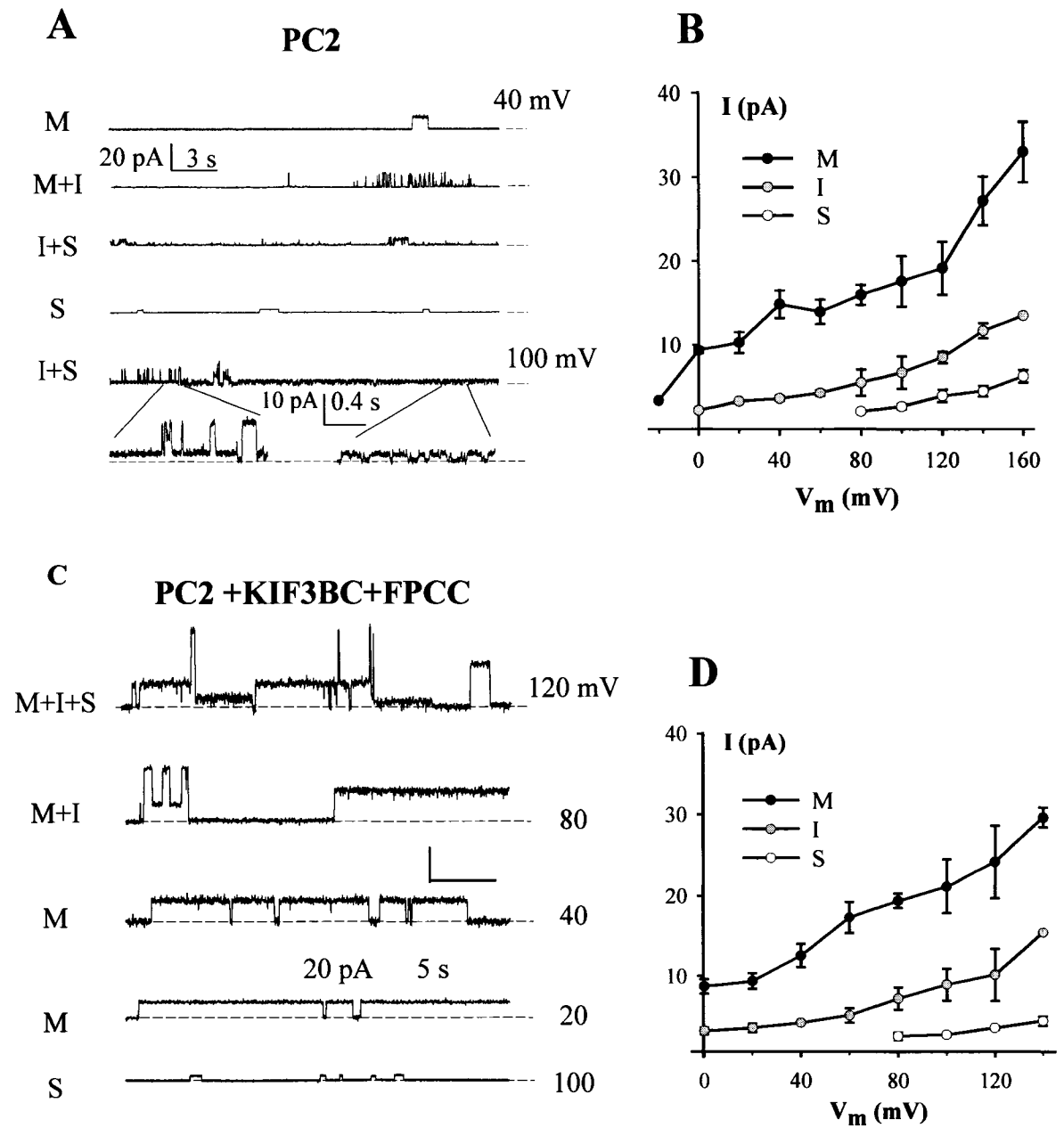
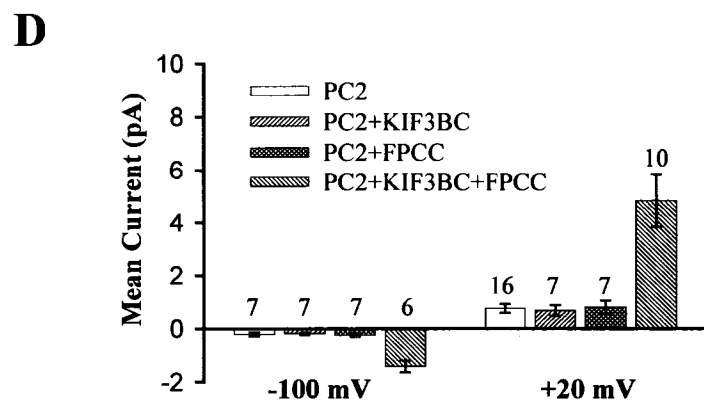
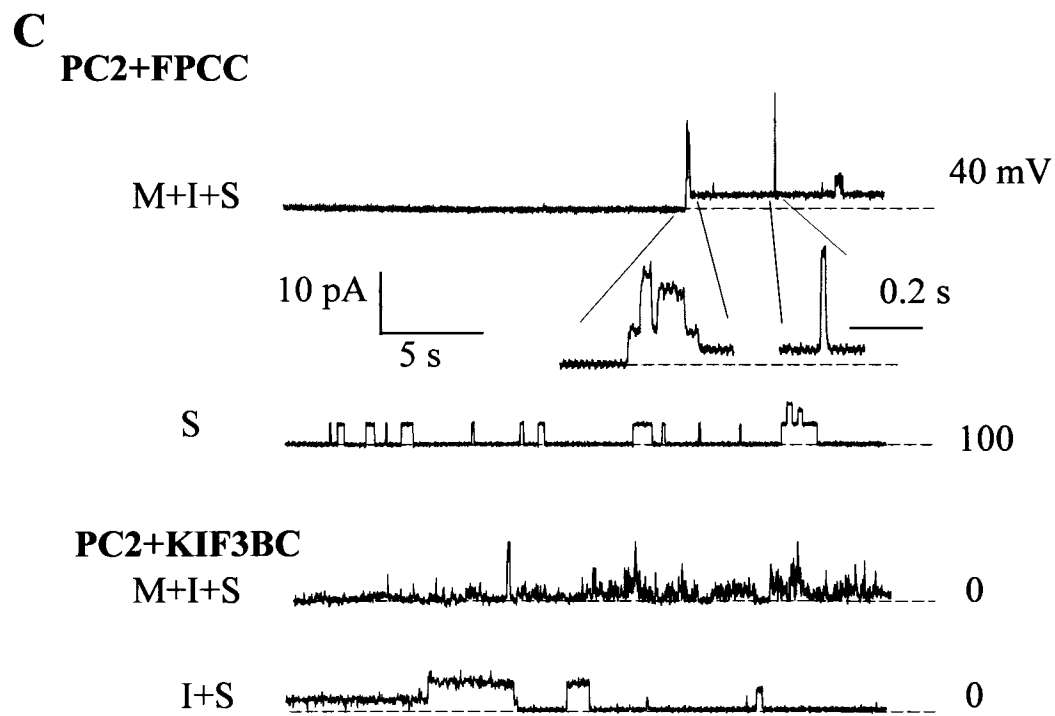
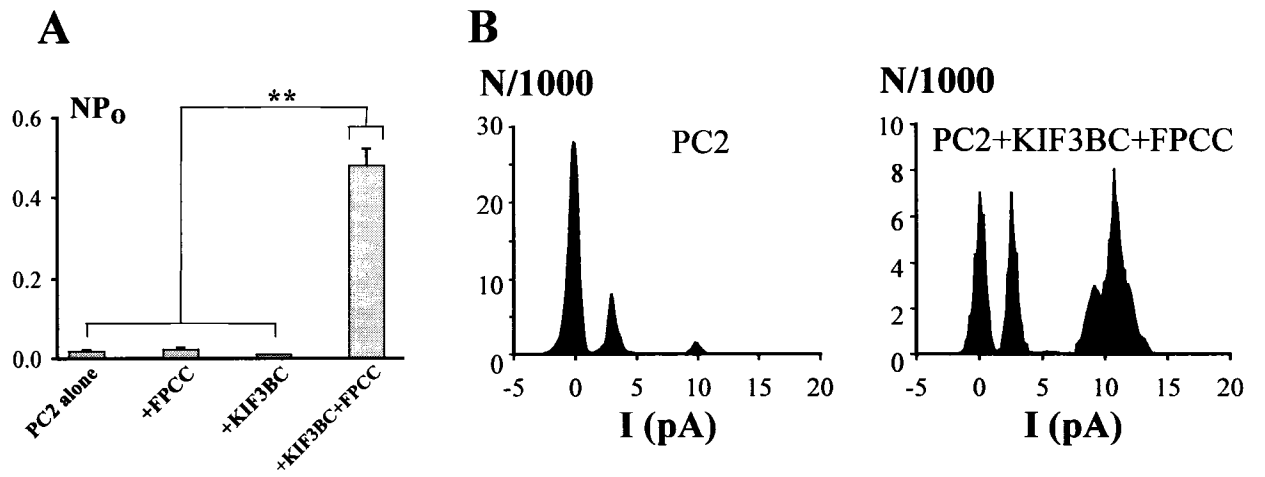


Fig. 2-8. Multiple conductance states of PC2 channel and effects of FPCC and KIF3BC. TAP-PC2 together with purified KIF3BC and FPCC proteins were used in lipid bilayer experiments under asymmetrical solution condition (150 mM *cis* KCl and 15 mM *trans* KCl). Shown trace recordings are not intended to reflect the actual open probability (NPo) values. (A) Representative tracings of PC2 channel activity in the absence of FPCC and KIF3BC, illustrating multiple conductance states at indicated voltages. 'M' = main state, 'I' = intermediate state and 'S' = small state. Closed levels are indicated by horizontal dashed lines. Inserts are shown with a different time and current scale. Traces were Gaussian filtered at 200 Hz in Clampfit 9. (B) Averaged I-V relationships, corresponding to the three conductance states, in the absence of FPCC and KIF3BC. (C) Representative tracings of PC2 channel activity in the presence of both FPCC and KIF3BC, illustrating multiple conductance states. (D) Averaged I-V curves, corresponding to the three states, in the presence of both FPCC and KIF3BC.

Fig. 2-9. Effects of FPCC and KIF3BC on PC2 channel represented by NPo, current density and mean current. Experiment conditions are the same as in Fig. 2-8. (A) Averaged open probability for PC2 channel opening at the main state in the presence or absence of FPCC and/or KIF3BC, as indicated. '**' means $P < 0.01$. Data were obtained for voltages between 0 and +140 mV. (B) Current density plots obtained from the all-point histogram analysis of 11 independent recordings in the presence of PC2 alone (left panel) and of 7 independent recordings in the presence of PC2+KIF3BC+FPCC (right panel). Each recording is of 10 s long and was obtained at +20 mV. The three peaks in each panel (from left to right) correspond to the close, intermediate and main states, respectively. (C) Representative tracings of PC2 channel activity in the presence of FPCC or KIF3BC only, illustrating multiple conductance states at indicated voltages. (D) Mean PC2 single-channel current was calculated using the Clampfit 9 program from each tracing of 60 s long obtained at -100 mV or +20 mV, in the presence of PC2, PC2+KIF3BC, PC2+FPCC or PC2+KIF3BC+FPCC, as indicated. Several (numbers are indicated in the figure) mean current values calculated by this way were averaged to produce an averaged value, as presented.



2.6. REFERENCES

1. Igarashi, P. and Somlo, S. (2002) Genetics and pathogenesis of polycystic kidney disease. *J. Am. Soc. Nephrol.*, **13**, 2384-2398.
2. Mochizuki, T., Wu, G., Hayashi, T., Xenophontos, S.L., Veldhuisen, B., Saris, J.J., Reynolds, D.M., Cai, Y., Gabow, P.A., Pierides, A. et al. (1996) PKD2, a gene for polycystic kidney disease that encodes an integral membrane protein. *Science*, **272**, 1339-1342.
3. The European Polycystic Kidney Disease Consortium (1994) The polycystic kidney disease 1 gene encodes a 14 kb transcript and lies within a duplicated region on chromosome 16. *Cell*, **77**, 881-894.
4. Zerres, K., Rudnik-Schoneborn, S., Steinkamm, C., Becker, J. and Mucher, G. (1998) Autosomal recessive polycystic kidney disease. *J. Mol. Med.*, **76**, 303-309.
5. Ward, C.J., Hogan, M.C., Rossetti, S., Walker, D., Sneddon, T., Wang, X., Kubly, V., Cunningham, J.M., Bacallao, R., Ishibashi, M. et al. (2002) The gene mutated in autosomal recessive polycystic kidney disease encodes a large, receptor-like protein. *Nat. Genet.*, **30**, 259-269.
6. Onuchic, L.F., Furu, L., Nagasawa, Y., Hou, X., Eggermann, T., Ren, Z., Bergmann, C., Senderek, J., Esquivel, E., Zeltner, R. et al. (2002) PKHD1, the Polycystic Kidney and Hepatic Disease 1 Gene, Encodes a Novel Large Protein Containing Multiple Immunoglobulin-Like Plexin-Transcription-Factor Domains and Parallel Beta-Helix 1 Repeats. *Am. J. Hum. Genet.*, **70**, 1305-1317.
7. Xiong, H., Chen, Y., Yi, Y., Tsuchiya, K., Moeckel, G., Cheung, J., Liang, D., Tham, K., Xu, X., Chen, X.Z. et al. (2002) A novel gene encoding a TIG multiple domain protein is a positional candidate for autosomal recessive polycystic kidney disease. *Genomics*, **80**, 96-104.
8. Hanaoka, K., Qian, F., Boletta, A., Bhunia, A.K., Piontek, K., Tsiokas, L., Sukhatme, V.P., Guggino, W.B. and Germino, G.G. (2000) Co-assembly of polycystin-1 and -2 produces unique cation-permeable currents. *Nature*, **408**, 990-994.
9. Gonzalez-Perrett, S., Kim, K., Ibarra, C., Damiano, A.E., Zotta, E., Batelli, M., Harris, P.C., Reisin, I.L., Arnaout, M.A. and Cantiello, H.F. (2001) Polycystin-2, the protein mutated in autosomal dominant polycystic kidney disease (ADPKD), is a Ca²⁺-permeable nonselective cation channel. *Proc. Natl. Acad. Sci. U. S. A.*, **98**, 1182-1187.
10. Qian, F., Germino, F.J., Cai, Y., Zhang, X., Somlo, S. and Germino, G.G. (1997) PKD1 interacts with PKD2 through a probable coiled-coil domain. *Nat. Genet.*, **16**, 179-183.

11. Tsiokas, L., Kim, E., Arnould, T., Sukhatme, V.P. and Walz, G. (1997) Homo- and heterodimeric interactions between the gene products of PKD1 and PKD2. *Proc. Natl. Acad. Sci. U. S. A.*, **94**, 6965-6970.
12. Tsiokas, L., Arnould, T., Zhu, C., Kim, E., Walz, G. and Sukhatme, V.P. (1999) Specific association of the gene product of PKD2 with the TRPC1 channel. *Proc. Natl. Acad. Sci. U. S. A.*, **96**, 3934-3939.
13. Hidaka, S., Konecke, V., Osten, L. and Witzgall, R. (2004) PIGEA-14, a novel coiled-coil protein affecting the intracellular distribution of polycystin-2. *J. Biol. Chem.*, **279**, 35009-35016.
14. Gallagher, A.R., Cedzich, A., Gretz, N., Somlo, S. and Witzgall, R. (2000) The polycystic kidney disease protein PKD2 interacts with Hax-1, a protein associated with the actin cytoskeleton. *Proc. Natl. Acad. Sci. U. S. A.*, **97**, 4017-4022.
15. Lehtonen, S., Ora, A., Olkkonen, V.M., Geng, L., Zerial, M., Somlo, S. and Lehtonen, E. (2000) In vivo interaction of the adapter protein CD2-associated protein with the type 2 polycystic kidney disease protein, polycystin-2. *J. Biol. Chem.*, **275**, 32888-32893.
16. Li, Q., Dai, Y., Guo, L., Liu, Y., Hao, C., Wu, G., Basora, N., Michalak, M. and Chen, X.Z. (2003) Polycystin-2 associates with tropomyosin-1, an actin microfilament component. *J. Mol. Biol.*, **325**, 949-962.
17. Li, Q., Shen, P.Y., Wu, G. and Chen, X.Z. (2003) Polycystin-2 interacts with troponin I, an angiogenesis inhibitor. *Biochemistry*, **42**, 450-457.
18. Li, Q., Montalbetti, N., Shen, P.Y., Dai, X.Q., Cheeseman, C.I., Karpinski, E., Wu, G., Cantiello, H.F. and Chen, X.Z. (2005) Alpha-actinin associates with polycystin-2 and regulates its channel activity. *Hum. Mol. Genet.*, **14**, 1587-1603.
19. Rundle, D.R., Gorbsky, G. and Tsiokas, L. (2004) PKD2 interacts and co-localizes with mDia1 to mitotic spindles of dividing cells: role of mDia1 in PKD2 localization to mitotic spindles. *J. Biol. Chem.*, **279**, 29728-29739.
20. Nagasawa, Y., Matthiesen, S., Onuchic, L.F., Hou, X., Bergmann, C., Esquivel, E., Senderek, J., Ren, Z., Zeltner, R., Furu, L. et al. (2002) Identification and characterization of Pkhd1, the mouse orthologue of the human ARPKD gene. *J. Am. Soc. Nephrol.*, **13**, 2246-2258.
21. Menezes, L.F., Cai, Y., Nagasawa, Y., Silva, A.M., Watkins, M.L., Da Silva, A.M., Somlo, S., Guay-Woodford, L.M., Germino, G.G. and Onuchic, L.F. (2004) Polyductin, the PKHD1 gene product, comprises isoforms expressed in plasma membrane, primary cilium, and cytoplasm. *Kidney Int.*, **66**, 1345-1355.
22. Ward, C.J., Yuan, D., Masyuk, T.V., Wang, X., Punyashthiti, R., Whelan, S., Bacallao, R., Torra, R., LaRusso, N.F., Torres, V.E. et al. (2003) Cellular and subcellular

localization of the ARPKD protein; fibrocystin is expressed on primary cilia. *Hum. Mol. Genet.*, **12**, 2703-2710.

23. Zhang, M.Z., Mai, W., Li, C., Cho, S.Y., Hao, C., Moeckel, G., Zhao, R., Kim, I., Wang, J., Xiong, H. et al. (2004) PKHD1 protein encoded by the gene for autosomal recessive polycystic kidney disease associates with basal bodies and primary cilia in renal epithelial cells. *Proc. Natl. Acad. Sci. U. S. A.*, **101**, 2311-2316.

24. Wang, S., Luo, Y., Wilson, P.D., Witman, G.B. and Zhou, J. (2004) The autosomal recessive polycystic kidney disease protein is localized to primary cilia, with concentration in the basal body area. *J. Am. Soc. Nephrol.*, **15**, 592-602.

25. Miki, H., Setou, M., Kaneshiro, K. and Hirokawa, N. (2001) All kinesin superfamily protein, KIF, genes in mouse and human. *Proc. Natl. Acad. Sci. U. S. A.*, **98**, 7004-7011.

26. Cole, D.G., Chinn, S.W., Wedaman, K.P., Hall, K., Vuong, T. and Scholey, J.M. (1993) Novel heterotrimeric kinesin-related protein purified from sea urchin eggs. *Nature*, **366**, 268-270.

27. Vale, R.D. (2003) The molecular motor toolbox for intracellular transport. *Cell*, **112**, 467-480.

28. Cole, D.G. (1999) Kinesin-II, the heteromeric kinesin. *Cell Mol. Life Sci.*, **56**, 217-226.

29. Scholey, J.M. (2003) Intraflagellar transport. *Annu. Rev. Cell Dev. Biol.*, **19**, 423-443.

30. Goldstein, L.S. and Yang, Z. (2000) Microtubule-based transport systems in neurons: the roles of kinesins and dyneins. *Annu. Rev. Neurosci.*, **23**, 39-71.

31. Baker, S.A., Freeman, K., Luby-Phelps, K., Pazour, G.J. and Besharse, J.C. (2003) IFT20 links kinesin II with a mammalian intraflagellar transport complex that is conserved in motile flagella and sensory cilia. *J. Biol. Chem.*, **278**, 34211-34218.

32. Li, Q., Dai, X.Q., Shen, P.Y., Cantiello, H.F., Karpinski, E. and Chen, X.Z. (2004) A modified mammalian tandem affinity purification procedure to prepare functional polycystin-2 channel. *FEBS Lett.*, **576**, 231-236.

33. Cole, D.G., Diener, D.R., Himelblau, A.L., Beech, P.L., Fuster, J.C. and Rosenbaum, J.L. (1998) Chlamydomonas kinesin-II-dependent intraflagellar transport (IFT): IFT particles contain proteins required for ciliary assembly in *Caenorhabditis elegans* sensory neurons. *J. Cell Biol.*, **141**, 993-1008.

34. Nauli, S.M., Alenghat, F.J., Luo, Y., Williams, E., Vassilev, P., Li, X., Elia, A.E., Lu, W., Brown, E.M., Quinn, S.J. et al. (2003) Polycystins 1 and 2 mediate mechanosensation in the primary cilium of kidney cells. *Nat. Genet.*, **33**, 129-137.

35. Li, Q., Montalbetti, N., Wu, Y., Ramos, A.J., Raychowdhury, M.K., Chen, X.Z. and Cantiello, H.F. (2006) Polycystin-2 cation channel function is under the control of microtubular structures in primary cilia of renal epithelial cells. *J. Biol. Chem.*, in press.
36. Lin, F., Hiesberger, T., Cordes, K., Sinclair, A.M., Goldstein, L.S., Somlo, S. and Igarashi, P. (2003) Kidney-specific inactivation of the KIF3A subunit of kinesin-II inhibits renal ciliogenesis and produces polycystic kidney disease. *Proc. Natl. Acad. Sci. U. S. A.*, **100**, 5286-5291.
37. Otto, E.A., Schermer, B., Obara, T., O'Toole, J.F., Hiller, K.S., Mueller, A.M., Ruf, R.G., Hoefele, J., Beekmann, F., Landau, D. et al. (2003) Mutations in INVS encoding inversin cause nephronophthisis type 2, linking renal cystic disease to the function of primary cilia and left-right axis determination. *Nat. Genet.*, **34**, 413-420.
38. Pazour, G.J., Dickert, B.L., Vucica, Y., Seeley, E.S., Rosenbaum, J.L., Witman, G.B. and Cole, D.G. (2000) Chlamydomonas IFT88 and its mouse homologue, polycystic kidney disease gene tg737, are required for assembly of cilia and flagella. *J. Cell Biol.*, **151**, 709-718.
39. Avner, E.D., Studnicki, F.E., Young, M.C., Sweeney, W.E., Jr., Piesco, N.P., Ellis, D. and Fettermann, G.H. (1987) Congenital murine polycystic kidney disease. I. The ontogeny of tubular cyst formation. *Pediatr. Nephrol.*, **1**, 587-596.
40. Haraguchi, K., Hayashi, T., Jimbo, T., Yamamoto, T. and Akiyama, T. (2005) Role of the kinesin-2 family protein, KIF3, during mitosis. *J. Biol. Chem.*, **281**, 4094-4099.
41. Nonaka, S., Tanaka, Y., Okada, Y., Takeda, S., Harada, A., Kanai, Y., Kido, M. and Hirokawa, N. (1998) Randomization of left-right asymmetry due to loss of nodal cilia generating leftward flow of extraembryonic fluid in mice lacking KIF3B motor protein. *Cell*, **95**, 829-837.
42. Marszalek, J.R., Ruiz-Lozano, P., Roberts, E., Chien, K.R. and Goldstein, L.S. (1999) Situs inversus and embryonic ciliary morphogenesis defects in mouse mutants lacking the KIF3A subunit of kinesin-II. *Proc. Natl. Acad. Sci. U. S. A.*, **96**, 5043-5048.
43. Takeda, S., Yonekawa, Y., Tanaka, Y., Okada, Y., Nonaka, S. and Hirokawa, N. (1999) Left-right asymmetry and kinesin superfamily protein KIF3A: new insights in determination of laterality and mesoderm induction by kif3A^{-/-} mice analysis. *J. Cell Biol.*, **145**, 825-836.
44. Jimbo, T., Kawasaki, Y., Koyama, R., Sato, R., Takada, S., Haraguchi, K. and Akiyama, T. (2002) Identification of a link between the tumour suppressor APC and the kinesin superfamily. *Nat. Cell Biol.*, **4**, 323-327.
45. Sarpal, R., Todi, S.V., Sivan-Loukianova, E., Shirolkar, S., Subramanian, N., Raff, E.C., Erickson, J.W., Ray, K. and Eberl, D.F. (2003) Drosophila KAP interacts with the kinesin II motor subunit KLP64D to assemble chordotonal sensory cilia, but not sperm tails. *Curr. Biol.*, **13**, 1687-1696.

46. Raychowdhury, M.K., McLaughlin, M., Ramos, A.J., Montalbetti, N., Bouley, R., Ausiello, D.A. and Cantiello, H.F. (2005) Characterization of single channel currents from primary cilia of renal epithelial cells. *J. Biol. Chem.*, **280**, 34718-34722.

47. Mai, W., Chen, D., Ding, T., Kim, I., Park, S., Cho, S.Y., Chu, J.S., Liang, D., Wang, N., Wu, D. et al. (2005) Inhibition of Pkhd1 Impairs Tubulomorphogenesis of Cultured IMCD Cells. *Mol Biol. Cell*, **16**, 4398-4409.

CHAPTER 3

CROSS TALK BETWEEN FIBROCYSTIN (FPC) AND EPITHELIAL Na CHANNEL (ENaC): ROLES OF FILAMIN A

This chapter is a manuscript in preparation for submission:

Xiao-Qing Dai, Qiang Li, Genqing Liang, Shayla S. Li, Horacio F. Cantiello, Xing-Zhen Chen*

*Corresponding author: Xing-Zhen Chen

3.1. INTRODUCTION

Autosomal recessive polycystic kidney disease (ARPKD) is a genetic disorder with an occurrence of 1/20,000, mostly in infants and children (Zerres *et al.*, 2003). ARPKD phenotypes include dilation of renal collecting and hepatic biliary ducts, and portal tract fibrosis, with more frequent lesions in kidney than in liver. The first human gene for ARPKD, *PKHD1* (polycystic kidney and hepatic disease gene 1), was identified in 2002 and encodes fibrocystin/polyductin (FPC) (Onuchic *et al.*, 2002;Ward *et al.*, 2002). ARPKD has a high mortality rate (40–60%) in the newborn period and accounts for ~35% of all end-stage renal disease in children (Onuchic *et al.*, 2002;Ward *et al.*, 2002). The precise molecular mechanisms underlying these phenotypes remain largely obscure. But, it seems likely that pathogenic mutations involve in multiple cellular signalling pathways, which together eventually produce ARPKD phenotypes. Cystic cells are associated with abnormal renal trans-epithelial fluid and solute transport. Interestingly, Na reabsorption was reported to increase by 50% and epithelial sodium channel (ENaC) expression by 100% in ARPKD cyst lining epithelial collecting duct cells conditionally immortalized from human ARPKD fetal kidneys (Rohatgi *et al.*, 2003). Veizis and Cotton reported that abnormal EGF-dependent regulation of ENaC function and expression may contribute to PKD pathophysiology (Veizis & Cotton, 2005). Thus there may exist a molecular pathway linking ENaC to ARPKD, which is important to understanding ARPKD pathogenesis.

The epithelial sodium channel (ENaC)/degenerin (DEG) family represents a class of ion channels discovered in early 90's (Canessa *et al.*, 1993). Members of this family of proteins are involved in Na and H₂O reabsorption, taste, touch, acidic pH, and can be classified into four main subfamilies: ENaC proteins, expressed in epithelia of the vertebrate kidney, colon, lung, tongue and brain; FMRF (Phe-Met-Arg-Phe)-amide-gated channels; acid-sensing ion channels; and mechanosensory channel proteins of nematode degenerins. This family comprises more than 20 members, all possessing two transmembrane domains plus intracellular N- and C-termini, selective for Na and blocked by amiloride (Barbry & Hofman, 1997;Kellenberger & Schild, 2002;Mano & Driscoll, 1999). ENaC is a highly Na-selective channel with a small conductance (~5 pS), putatively composed of two α subunits (α -ENaC, 669 aa), one regulatory β subunit

(β -ENaC, 640 aa) and one regulatory γ subunit (γ -ENaC, 649 aa) ($2\alpha1\beta1\gamma$) arranged pseudosymmetrically around the channel pore. It is known that the actin filament is an important regulator of ENaC channel function and that ENaC directly bind α -spectrin, ankyrin and F-actin (Mazzochi *et al.*, 2006; Zuckerman *et al.*, 1999). ENaC is sensitive to membrane stretch, hydrostatic pressure and shear stress flow, as showed in *Xenopus* oocytes, mammalian cultured cells, artificial lipid bilayer system, and native tissue systems (Awayda & Subramanyam, 1998; Satlin *et al.*, 2001). In the kidney, ENaC plays a critical role in Na balance, extracellular volume and blood pressure. In the lung, ENaC has a distinct role in controlling the ionic content of the air-liquid interface and thereby determining the rate of mucociliary transport. In human and animal models, imbalance of ENaC activity leads to a number of pathologies, eg hypertension, altered mucociliary transport, respiratory distress, and high-altitude pulmonary edema. Loss-of-function mutations in ENaC cause salt-wasting syndrome in pseudohypoaldosteronism type 1, while gain-of-function mutations in β - and γ -ENaC cause Liddle's syndrome, a form of salt-sensitive hypertension (Gormley *et al.*, 2003; Kellenberger & Schild, 2002; Rossier *et al.*, 2002; Schild, 2004; Barbry & Hofman, 1997).

Filamins are large cytoplasmic proteins that cross-link cortical actin into a dynamic three-dimensional structure and were discovered as the first family of non-muscle actin-binding proteins. Mammalian filamins consist of three actin-binding homologs (A, B, and C), each of ~280 kDa and containing an N-terminal actin-binding domain (~300 aa), followed by a long rod-like domain made of 24 repeats of anti-parallel β -sheets (~96 aa each) and two "hinge" regions (Fig. 3-1B). Two filamin molecules self-associate to form a homodimer through the last carboxyl-terminal repeat, which allows the formation of a V-shaped flexible structure that is essential for function (Feng & Walsh, 2004; van der & Sonnenberg, 2001). Current data suggest that filamins are involved in the organization of the cytoskeleton, which is important for cell adhesion and motility, interacts with and regulate several membrane proteins (ion channels, receptors, β -integrins and glycoprotein Iba) and cytoplasmic signaling proteins (Rho GTPases, TRAF2, Smads and SEK-1) (Cantiello *et al.*, 1991; Feng & Walsh, 2004; Thelin *et al.*, 2007; van der & Sonnenberg, 2001; Stossel *et al.*, 2001; Takafuta *et al.*, 2003). Nevertheless, a clear mechanistic explanation for their importance is still lacking. Recent genetic evidence indicates that

filamins are essential for human development, and mutations in either filamin A (FLNA) or -B (FLNB) have been associated with abnormal development of brain, bone, cardiovascular system and many other organs. Although different filamin isoforms seem to have distinct roles in development, they may also functional similarity and confer genetic redundancies that lead, upon mutations, to a wide degree of variances in the genetic syndromes.

The COOH terminus of α -ENaC has been shown to contribute to the modulation of the channel by the actin cytoskeleton (Jovov et al., 1999). However, whether and how the actin-binding protein influences the function of ENaC by either indirect or direct binding to the integral membrane protein is poorly understood. Previous reports support the concept that ENaC and actin-binding protein filamin are in a novel pathway linked to solute transport. Therefore, in order to elucidate the molecular pathway linking ENaC to ARPKD, we propose to study the interaction of ENaC with and its regulation by filamin and FPC. In the present studies we employed various approaches of molecular biology and electrophysiology to investigate physical and functional interactions between ENaC, filamins and FPC, with an emphasis on using the pore-forming α -ENaC and the predominant FLNA isoform.

3.2. METHODS AND MATERIALS

Antibodies and reagents

Three rabbit polyclonal antibodies, anti- α -ENaC (324870, Calbiochem, San Diego, CA), anti- α -ENaC (ENACA11-A, Alpha Diagnostic Inc., San Antonio, TX), anti- α -ENaC H-95 (sc-21012, Santa Cruz Biotechnology, Inc., Santa Cruz, CA) were used in this study. Mouse monoclonal anti-filamin FIL2 and goat polyclonal antibody (Sigma-Aldrich Canada, Oakville, Canada) were raised using the filamin antigen purified from chicken gizzard and mouse monoclonal anti-filamin 1 E-3 (Santa Cruz Biotechnology, Inc.).

Plasmid construction

The C-terminus of human filamin A (NM_001456, aa 2150-2647) and filamin B (NM_001457, 2105-2602) were isolated from either human kidney cDNA library or HEK293 cells. The C-terminus of filamin C was cut from pACT2 vector. cDNAs were subcloned into pGBKT7 or pGADT7 for yeast two-hybrid, PGEX5X1 (GST-tagged GE Healthcare, Baie d'Urf, Qu) pET28a (poly-His-tagged, Novagen, San Diego, CA) for bacterial expression, a modified vector (Hygromycin resistance) based on pEGFPC2 (Clontech, Palo Alto, CA) for mammalian cell expression. All plasmid construction has been done and confirmed by sequencing.

Yeast two-hybrid analysis

A yeast two-hybrid screen was performed in the yeast strain Y187 containing *LacZ* reporter genes under the control of the GAL4 upstream activating sequences as described recently (Li et al., 2005). Briefly, the cDNA fragments encoding ENaC were subcloned in frame into the GAL4 DNA binding domain of the vector pGBKT7 (Clontech) by a PCR-based approach. The COOH terminus of α -ENaC was used as bait to search for other partners constructed in the vector pGADT7 containing the GAL4 activation domain (Clontech). Survived colonies were examined for activation of a *LacZ* reporter gene by a filter lift assay.

Oocyte preparation

Capped synthetic rabbit α , β , and γ subunits of ENaC mRNAs were synthesized by *in vitro* transcription from a linearized template inserted in a home-made vector called pMST, using the mMESSAGE mMACHINE1 Kit (Ambion, Austin, TX). The oocytes were prepared as same as before. Oocytes were injected with 50 nl of water containing 20 or 40 ng of each subunit mRNA 5 hr following defolliculation. An equal volume of RNAase-free water was injected into each control oocyte. Injected oocytes were incubated at 16-18°C in the Barth's solution supplemented with sodium penicillinand/streptomycin sulfate for 2 ~ 3 days prior to experiments.

Two-electrode voltage clamp

Two-electrode voltage clamp was performed as described previously (Liu *et al.*, 2002). Briefly, the two electrodes (Capillary pipettes, Warner Instruments, Hamden, CT) impaling *Xenopus* oocytes were filled with 3 M KCl to form a tip resistance of 0.3 - 2 M Ω . Oocyte whole-cell currents were recorded using a Geneclamp 500B amplifier and a Digidata1320A AD/DA converter (Axon Instruments, Union City, CA). In experiments using a ramp protocol, currents and voltages were sampled at internals of 200 μ s and filtered at 2 kHz using an 8 pole Bessel filter. In experiments using a gap-free protocol, current/voltage signals were sampled at intervals of 200 ms. The standard sodium solution contained (in mM): 100 Na-Cl, 2 KCl, 1 CaCl₂, 1 MgCl₂, 10 HEPES, pH 7.5.

Protein preparation and lipid bilayer electrophysiology

The His-tagged FPC C-terminus (His-FPCC, aa 3882-4074) (Check HMG paper, the same construct) was purified from *E. coli*. TAP- α -ENaC was prepared and reconstituted in a lipid bilayer system as previously described (Li *et al.*, 2004) to assess the channel activity. The *cis* (or *trans*) compartment contained 150 (or 15) mM NaCl, 15 μ M Ca (by 1 mM EGTA and 1.01 mM CaCl₂), pH 7.4 (adjusted by MOPS-KOH). TAP- α -ENaC protein was added to the *cis* chamber in proximity of the membrane or used to directly 'paint' the membrane. The COOH terminus of FLNA proteins (FLNAC) was added to the *cis* chamber when studying their effects on α -ENaC channel.

Cell culture and transfection

IMCD, LLC-PK1, M2 and A7 cells were cultured in Dulbecco's modified Eagle's medium (DMEM) supplemented with L-glutamine, penicillin-streptomycin, and 10% fetal bovine serum (FBS). Transfection was performed on M2/A7 cells cultured to 90% confluency using Lipofectamine 2000 (Invitrogen, Toronto, Canada) according to the manufacturer's protocol. For generation of stable cell lines, 100 µg/µl hygromycin (Invitrogen) was added to DMEM to select viable clones one recovery day following transfection.

Western blotting

Membrane blocking was carried out using 3% skimmed milk in PBST-buffered saline. Primary antibodies were incubated for 18 h at 4 °C followed by 3 washes for 10 min each, after which biotinylated secondary antibodies were used for 1.5 h at room temperature (RT). Proteins were peroxidase-labelled using the Standard ABC Reagent (Vector Laboratories Inc., Burlington, Ontario, Canada) for 1.5 h at RT, followed by ECL development. A minimum of three runs was carried out, and a representative example is shown.

Co-immunoprecipitation (co-IP)

Co-IP was performed using lysates of IMCD and LLC-PK1 cells (2×10^7 cells). Cell monolayers in 100 mm dishes were washed twice with PBS and solubilized in ice-cold CellLytic-M lysis buffer and proteinase inhibitor cocktail (Sigma-Aldrich Canada). Supernatant was collected following centrifugation at 16,000 g for 20 min. Equal amounts of total protein from postnuclear supernatants were precleared for 1 hr with protein G-/or A-sepharose (Sigma-Aldrich Canada) and then incubated for another hour on ice with antibody against α -ENaC or FLNA. After the addition of 150 µl of 50% protein G-/or A-sepharose, the mixtures were incubated for another hour with gentle shaking. The immune complexes absorbed to protein G-/or A-sepharose were washed three times with the lysis buffer. The precipitated proteins were analyzed by Western blotting using antibodies against FLNA or α -ENaC.

Statistics and data analysis

Data obtained from the two-microelectrode voltage-clamp and lipid bilayer experiments were analyzed using Clampfit 9. Single-channel conductance values were obtained from Gaussian fits to All-Point Histograms. The open probability (NP_o) was obtained from currents generated by gap-free recordings of 30 s long. The all-point histogram was used to calculate single-channel amplitudes and obtain data for current density plotting. Analyzed data were plotted using Sigmaplot 9 (Jandel Scientific Software, San Rafael, CA) and expressed in the form of mean \pm SE (N), where SE represents the standard error of the mean and N indicates the number of oocytes or bilayers. Curve fitting and data filtering were performed using Clampfit 9 or Sigmaplot 9. A probability value (P) of less than 0.05 and 0.01 was considered significant and very significant, respectively.

3.3. RESULTS

Physical interaction between ENaC and filamins

ENaC was known to interact with some components of the cytoskeleton (Mazzochi *et al.*, 2006). In particular, in 1991 it was found that filamin inhibited ENaC currents in A6 cells but whether filamin associates with ENaC subunits has remained unclear. We employed one-to-one yeast two-hybrid assay and indeed found that the C-terminal fragments of all three human filamins (FLNAC, aa 2150-2647; FLNBC, aa 2105-2602; FLNCC, aa 2144-2725) bind the C-terminus of human α -ENaC (α -ENaCC, aa 588-669) and β -ENaC (β -ENaCC, aa 559-640) (Fig. 3-1A). FLNAC, FLNBC and FLNCC show 70-75% sequence similarity.

To determine whether α -ENaC binds FLNA *in vivo*, we performed co-IP experiments using native IMCD and LLC-PK1 cell lines. FLNA protein was detected in the precipitates of IMCD and LLC-PK1 cells using an anti- α -ENaC antibody, but not in precipitates using non-immune IgG (Fig. 3-2). Reciprocally, α -ENaC signal was observed in the precipitates using an antibody against FLNA. These data demonstrated that α -ENaC and FLNA are in the same complex *in vivo*.

Modulation of ENaC by FLNA channel function and expression in *Xenopus* oocytes

We co-injected α -, β - and γ -ENaC mRNAs into oocytes with a concentration ratio of 2:1:1. The average Na current, equal to the total current in the presence of 100 mM Na minus the one when Na was replaced by the equimolar N-methyl-D-glucamine (NMDG), was $2.7 \pm 0.3 \mu\text{A}$ ($N = 70$) at -50 mV in oocytes expressing ENaC. This Na current was reversibly inhibited by 10 μM amiloride present in the extracellular solution, with the amiloride-sensitive currents averaging $2.0 \pm 0.3 \mu\text{A}$ ($N = 30$) (see eg Fig. 3-2A, *top*), accounting for $92 \pm 7\%$ ($N = 30$) of the Na currents. Co-expression of FLNAC or FLNBC substantially reduced the Na current as well as the amiloride-sensitive current (Fig. 3-2A, *bottom, left and right*). In the presence of FLNAC, the Na current averaged $0.580 \pm 0.09 \mu\text{A}$ ($N = 25$) and the amiloride-sensitive current was $0.360 \pm 0.1 \mu\text{A}$ ($N = 23$), which represent $21 \pm 6\%$ and $18 \pm 8\%$ of the corresponding currents in the absence of FLNAC. Inhibition effect of FLNBC was similar to that of FLNAC (Fig. 3-2B). With 10 μM amiloride, the amiloride inhibition affinity was not changed by the co-expression

of FLNAC and FLNBC. The IC_{50} value for ENaC alone was $0.18 \pm 0.01 \mu\text{M}$ ($N = 6$), which is not significantly different from the value obtained in the presence of ENaC and FLNAC and FLNBC.

To determine whether filamins reduced ENaC expression to account for the reduced channel activity we performed WB and quantify their expression by densitometry. We found that the α -ENaC expression significantly decreased in the presence of FLNAC or FLNBC (Fig. 3-3A). We also detected endogenous FLNA in oocytes by WB (Fig. 3-3B). However, this decrease is not sufficient to fully account for the substantially decreased channel function, suggesting that α -ENaC single-channel activity is also inhibited by FLNAC.

Modulation of α -ENaC by FLNAC in planar lipid bilayer

Our data obtained from *Xenopus* oocytes suggested that FLNAC and FLNBC inhibit ENaC single-channel activity, in addition to reducing its expression. To test this we utilized a planer lipid bilayer electrophysiology in combination with tandem affinity purification to purify full-length α -ENaC proteins from MDCK stable cell line and with *E. coli* purification of FLNAC. We have recently modified and improved the vector construct and affinity purification protocol for use with PKD2 and TRPP3 channels (Li *et al.*, 2004). Indeed, purified α , β and γ subunits were detectable in Coomassie blue stain and WB (Fig. 3-4A). After α -ENaC was reconstituted into lipid membrane single channel openings were observed and showed single-channel conductance value compatible with the activities of α -ENaC channels (Fig. 3-4B). In fact, in the presence of 150 mM *cis* NaCl and 15 mM *trans* NaCl (asymmetrical condition), single-channel conductance was in the 18~21 pS range, larger than when all α , β and γ subunits are co-expressed, which is consistent with previous reports (Kizer *et al.*, 1997; Ismailov *et al.*, 1996).

To examine whether/how FLNAC reduces ENaC single-channel activity we introduced purified FLNAC proteins into the *cis* chamber of the lipid bilayer system. We found that FLNAC substantially inhibited the open probability (NP_o) and mean current, but not mean open time, of α -ENaC channels (Fig. 3-5). The corresponding NP_o and

mean current values at 0 mV decreased from 2.0 ± 0.4 to 0.5 ± 0.2 (N = 4, P < 0.01) and from 4.1 ± 1.2 to 1.1 ± 0.4 pA (N = 4, P < 0.01), respectively.

Roles of filamin in the cross talk between ENaC and fibrocystin

YTH assays revealed no binding between FPCC and the C-terminus of α , β and γ -ENaC (Fig. 3-6A). However, our co-IP assays showed that ENaC and FPC are in the same protein complex, suggesting either that they bind each other via domains other than their C-termini or that there exists an intermediate protein bridging their complexing. Our data showed that siRNA of FPC in IMCD cells results in a substantial increase in ENaC (Fig. 3-6C). Further, over-expression of FPCC in oocytes leads to decreased α -ENaC expression (Fig. 3-6D) and function (Fig. 3-7). Thus, these exist physical and functional cross talk between FPC and ENaC. Because filamin binds ENaC, next we will test possible binding between filamin and FPC. Indeed, FPCC was able to bind the C-terminus of α , β and γ -ENaC in YTH assays (Fig. 3-8A). Further, the FPCC- α -ENaC interaction was confirmed by co-IP (Fig. 3-8B). These data together indicate that filamin plays an intermediate role in forming triplex ENaC-filamin-FPC.

3.4. DISCUSSION

In the present study we have examined physical, functional and regulation interactions between ENaC, filamin and fibrocystin. We found the physical interaction between ENaC and filamin by various *in vitro* and *in vivo* protein-protein binding approaches. Yeast two-hybrid experiments showed that the C-terminal fragment of FLNA binds the C-terminus of human α and β -ENaC. Co-IP experiments confirmed that the FLNA- α -ENaC association in native IMCD and LLC-PK1 cell lines. Western blotting showed that FLNA decreased the α -ENaC expression in oocytes. We further studied how filamin modulates ENaC channel function in *Xenopus* oocytes and lipid bilayer. FLNAC reduces both the channel activity and protein expression of ENaC over-expressed in oocytes. In lipid bilayer experiments, we also found that FLNAC inhibits the NPo and mean currents but not the amplitude of current of α -ENaC channels. Thus FLNA regulates ENaC expression and channel function through direct binding. We also demonstrated that ENaC and FPC are in the same protein complex but seem do not bind directly with each other. Our recent data showed that siRNA of FPC in IMCD cells results in a substantial increase in ENaC. Further, over-expression of FPC in oocytes leads to decreased α -ENaC expression and function.

We propose that FPC regulates ENaC expression and channel function in a filamin-dependent manner. Cystic cells are associated with abnormal renal trans-epithelial fluid and solute transport. Interestingly, Na reabsorption was reported to increase by 50% and ENaC expression by 100% in ARPKD cyst lining epithelial collecting duct cells conditionally immortalized from human ARPKD fetal kidneys (Rohatgi *et al.*, 2003). Thus our data are in agreement with the reported data and all this indicates a cross talk between FPC and ENaC, which may account for abnormal renal trans-epithelial transport mediated in part by ENaC once the cross talk is altered by mutations in FPC.

ARPKD phenotypes include renal collecting duct as the predominant site of cystogenesis, abnormal epithelial solute transport, increased cell proliferation and de-differentiation, increased cAMP levels, altered localization of FPC in renal primary cilia. Up to now, the precise molecular mechanisms underlying the phenotypes for ARPKD

remain largely obscure. The predominant site of renal disease in ARPKD is the collecting duct (CD), and late in the disease most of the kidney is composed of dilated, fluid-filled CDs rather than isolated, detached cysts. The CD of the mammalian kidney is a cytologically diverse segment comprised of principal cells and intercalated cells. Intercalated cells account for 10 ~ 30% of the cells in the CD and are responsible for H/HCO₃ excretion in the distal nephron (Kim *et al.*, 1999). Principal cells are more numerous (70 ~ 90%) and are characterized by hormonally regulated (eg, aldosterone and vasopressin) Na, K, and water transport (Nielsen *et al.*, 1995; Pacha *et al.*, 1993). Principal cells play a vital role in salt and water homeostasis via regulated alterations in Na absorption and water permeability. The expression and activity of ENaC are the rate-limiting steps for CD Na absorption. ENaC expression, although established early in nephrogenesis (Huber *et al.*, 1999), is developmentally regulated and is important for postnatal Na homeostasis (Satlin & Palmer, 1996). ARPKD is generally considered to be a disorder with developmental arrest or cellular dedifferentiation to a less mature phenotype. Therefore, ENaC-mediated Na absorption capacity, which is considered an indication of CD maturation, represents an important ion transport pathway that may not fully develop or might be lost from less mature cystic CD cells. ARPKD cystic CD is composed almost exclusively of principal cells. Cystic cells in ARPKD are associated with abnormal renal trans-epithelial fluid and solute transport. However, almost nothing is known about the ion transport properties of cystic CD principal cells.

Our data suggest a cross talk between ARPKD and ENaC or an involvement of ENaC in cystogenesis. ENaC may be one of many branch pathways linking to FPC. Mutations in one pathway may not be sufficient for cyst formation, but may contribute to or modulate cyst formation. Thus elucidating the molecular pathway(s) linking ENaC to ARPKD is important to understanding the PKD pathogenesis. Besides the contribution to the physiological implications of ENaC in ARPKD, the results also support the important roles of cytoskeletal proteins in channel regulation. The actin-based cytoskeleton, consisting of actin filament and associated proteins, is assembled in a dynamic intracellular network, which is essential in the regulation of a variety of cellular events, including the stability of cell shape and the onset of cell motility, intracellular trafficking

of ion channels and transporter proteins, and hormone action (Cantiello, 1997). The actin cytoskeleton has also been shown to interact both directly and indirectly with ion channels and transporters (Noda *et al.*, 2004; Chasan *et al.*, 2002). The hypothesis that the actin cytoskeleton was directly involved in the regulation of ENaC was first supported by immuno-colocalization studies showing that Na channels always appeared on the cell surface in close proximity to actin filaments (Cantiello *et al.*, 1991). This finding raised the possibility that a potential Na channel-actin filament interaction might be an early feature of epithelial cell development. Filamins are a family of high molecular mass cytoskeletal proteins that organize filamentous actin in networks and stress fibers. Filamins play important roles in actin organization and membrane stabilization. In the last decade, it has been found that several repeat domains of filamins bind to a wide variety of proteins, including transmembrane receptors and signaling molecules (van der & Sonnenberg, 2001). Our study showed that filamins anchor ENaC to the actin cytoskeleton not only for structural purposes but also functionally modulate ENaC function. It indicated that filamins play an essential role in determining the activity of ENaC. Because FPC complexes with ENaC via filamin we think that its modulation of ENaC channel function and expression is also mediated by filamin.

In summary, our current results together with previous reports support the concept that actin-binding protein filamin and ENaC are in a novel pathway linking the solute transport by ENaC to ARPKD. We speculate that FPC regulates ENaC expression and channel function in an FLNA-dependent manner, presumably via the triplex FPC-filamin-ENaC in which filamin acts as a bridging protein. Of note, that filamin is able to bind FPC and ENaC does not automatically infer that a given filamin molecule can simultaneously bind the two partner proteins. Eg, if ENaC and FPC compete for binding the same site in filamin, bind two overlapped sites, they can not bind the same molecule at the same time, which would mean that triplex FPC-filamin-ENaC is unlikely to exist. Receptor-like FPC acts here more like a modulator of ENaC, which may be similar to its role in the PKD2-KIF3B-FPC triplex (Wu *et al.*, 2006). Our study thus provides a novel evidence for the involvement of ENaC in the abnormal Na transport in ARPKD. Future

studies may include functional interaction and regulation in more physiological models such as mammalian cells and animals.

ACKNOWLEDGEMENTS

This work was supported by the Canadian Institutes of Health Research, the Kidney Foundation of Canada, and the Heart and Stroke Foundation of Canada (X.Z.C.). X.Q.D. is a recipient of the AHFMR studentship. Q.L. is a recipient of the Polycystic Kidney Disease Foundation Fellowship. X.Z.C. is a Senior Scholar of the Alberta Heritage Foundation for Medical Research.

3.5. FIGURES

A

prey (PGADT7) bait (PGBKT7)	FLNAC (2150-2647)	FLNBC (2105-2602)	FLNCC (2144-2725)	Vector (Control)
α -ENaC-N (1-82)	-	-	-	-
α -ENaC-C (588-669)	++	++	++	-
β -ENaC-N (1-47)	-	-	-	-
β -ENaC-C (559-640)	++	++	++	-
γ -ENaC-N (1-76)	-	-	-	-
γ -ENaC-C (568-649)	Self-activation, not tested for binding			
Vector (Control)	-	-	-	-

B

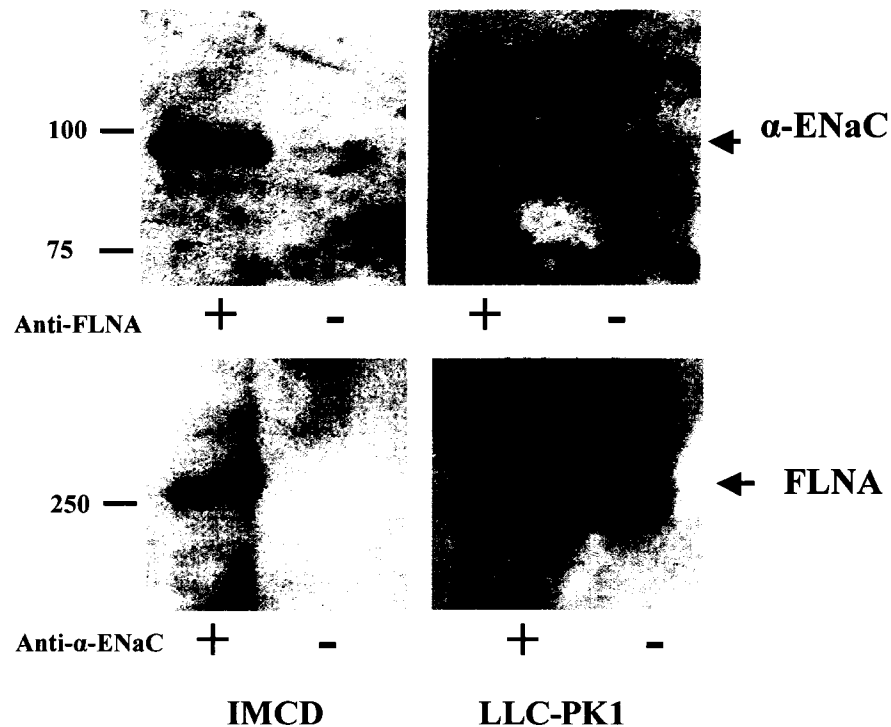


Fig. 3-1. Physical binding between ENaC and filamins. **A.** Direct interactions of three ENaC subunits and three filamin isoforms revealed by yeast two-hybrid assays. Various bait fragments from ENaC and prey fragments from filamins were co-transformed in Y187 strain and β -GAL activity were determined from the time that was taken for the colonies to turn blue in X-gal filter lift assays performed at 30°C. “++”, “+” and “-” indicated for development of blue color within 1, 3 and 24 hr and no development of blue color within 24 hr, respectively. **B.** *In vivo* interaction between α -ENaC and FLNA. Total proteins from IMCD and LLC-PK1 cells, were precipitated with either anti-FLNA antibody FIL2 (+) or non-immune mouse IgG (-) and detected with anti- α -ENaC antibody.

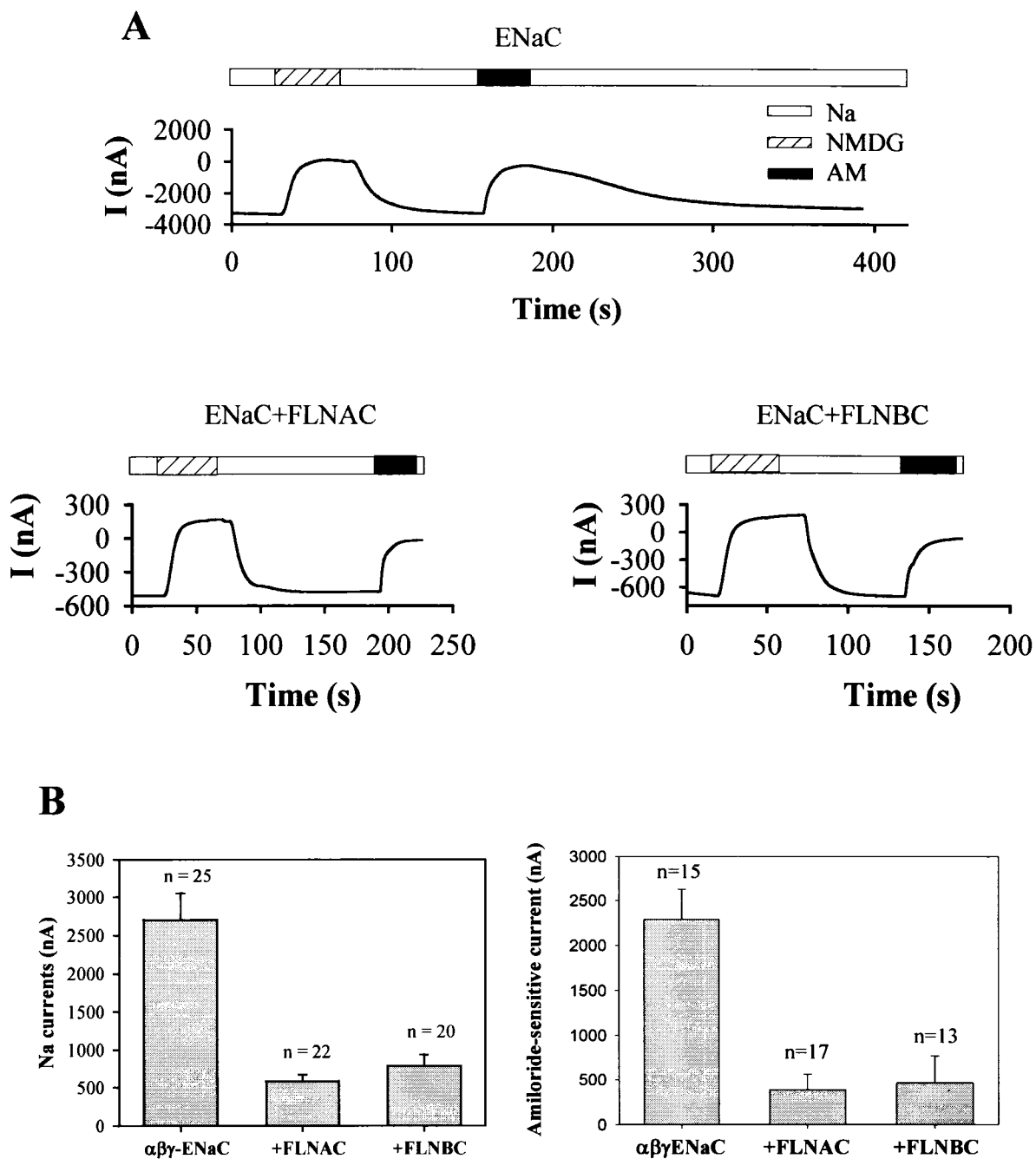


Fig. 3-2. Modulation of ENaC channel function by FLNA in *Xenopus* oocytes. **A.** Representative recordings of Na currents and amiloride (10 μ M)-sensitive Na currents in *Xenopus* oocytes expressing $\alpha\beta\gamma$ -ENaC (top), $\alpha\beta\gamma$ -ENaC + FLNAC (bottom, left), and $\alpha\beta\gamma$ -ENaC + FLNBC (bottom, right). Data were obtained using the two-microelectrode voltage-clamp technique at -50 mV. Extracellular solution contained 100 mM Na. 'Na' = 100 mM NaCl-containing solution. 'NMDG' = 100mM NMDG-containing solution. 'Amiloride' = 10 μ M amiloride. **B.** Shown are averaged Na currents and amiloride (10 μ M)-sensitive currents. For both FLNAC and FLNBC, the P values are < 0.001.

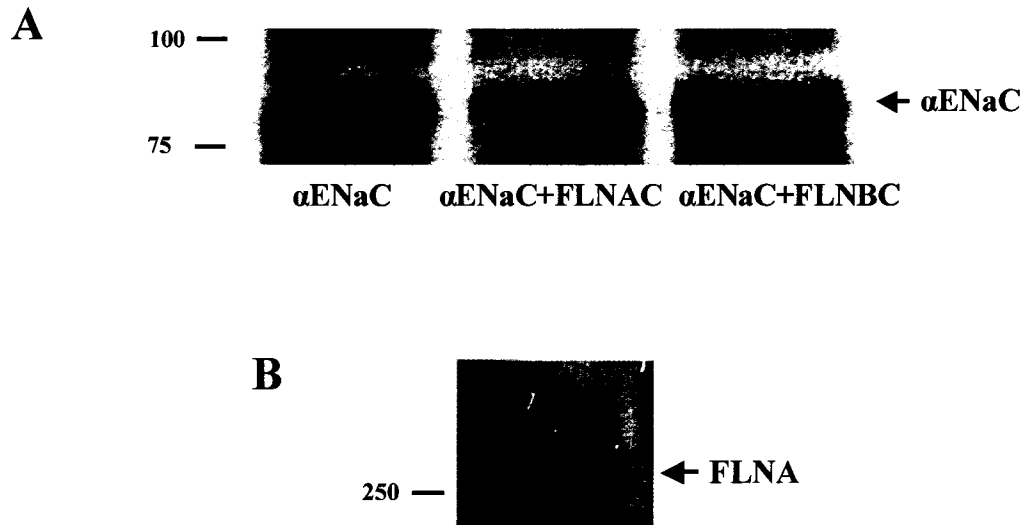


Fig. 3-3. Effects of filamins on α -ENaC expression. **A.** In *Xenopus* oocytes, expression of α -ENaC in the presence or absence of the FLNAC/FLNBC expression. **B.** Endogenous FLNA in oocytes detected by an antibody against human FLNA, in the presence or absence of FLNAC or FLNBC.

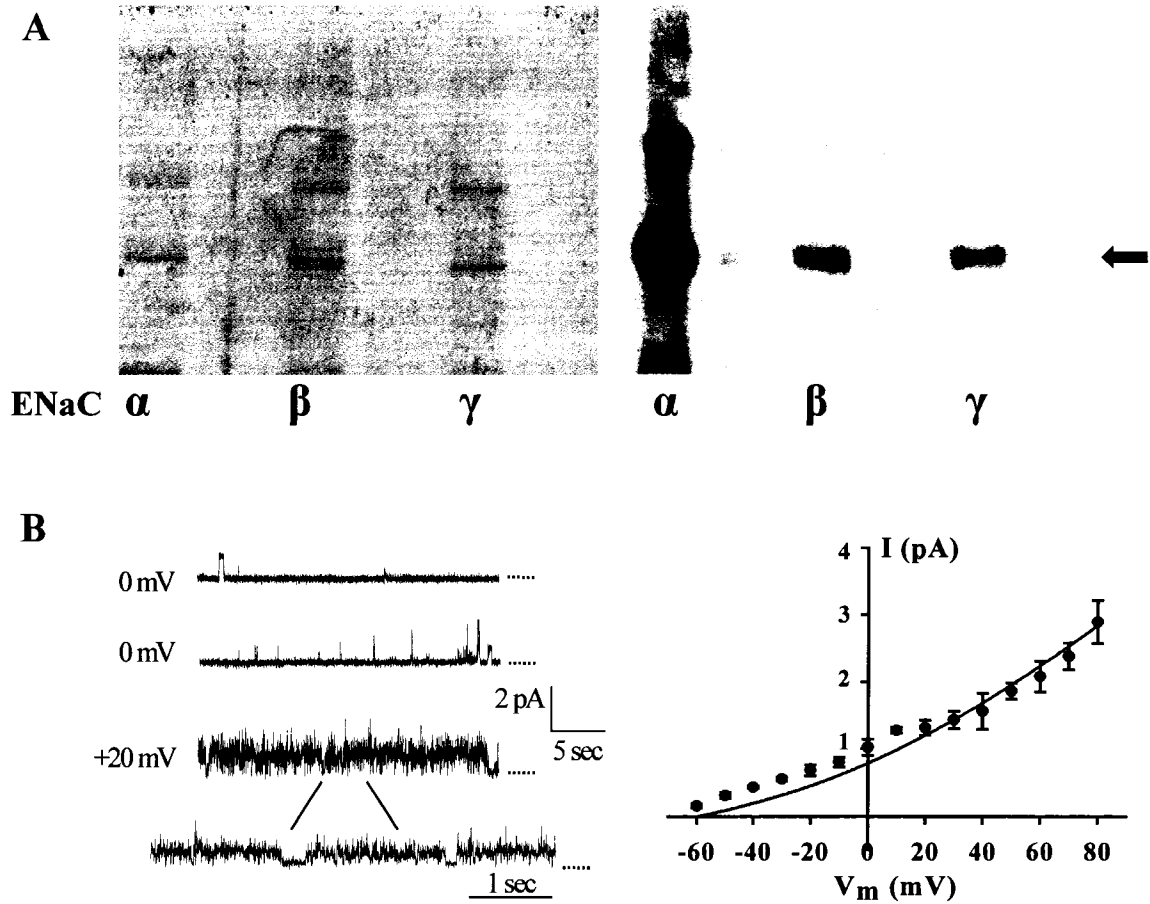
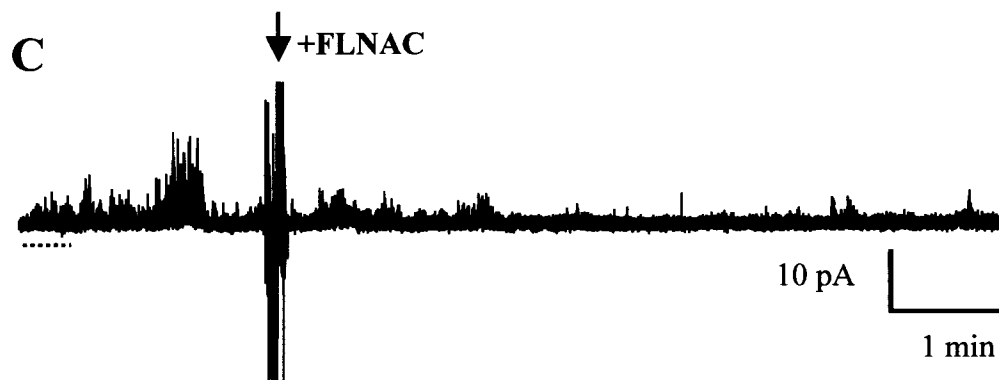
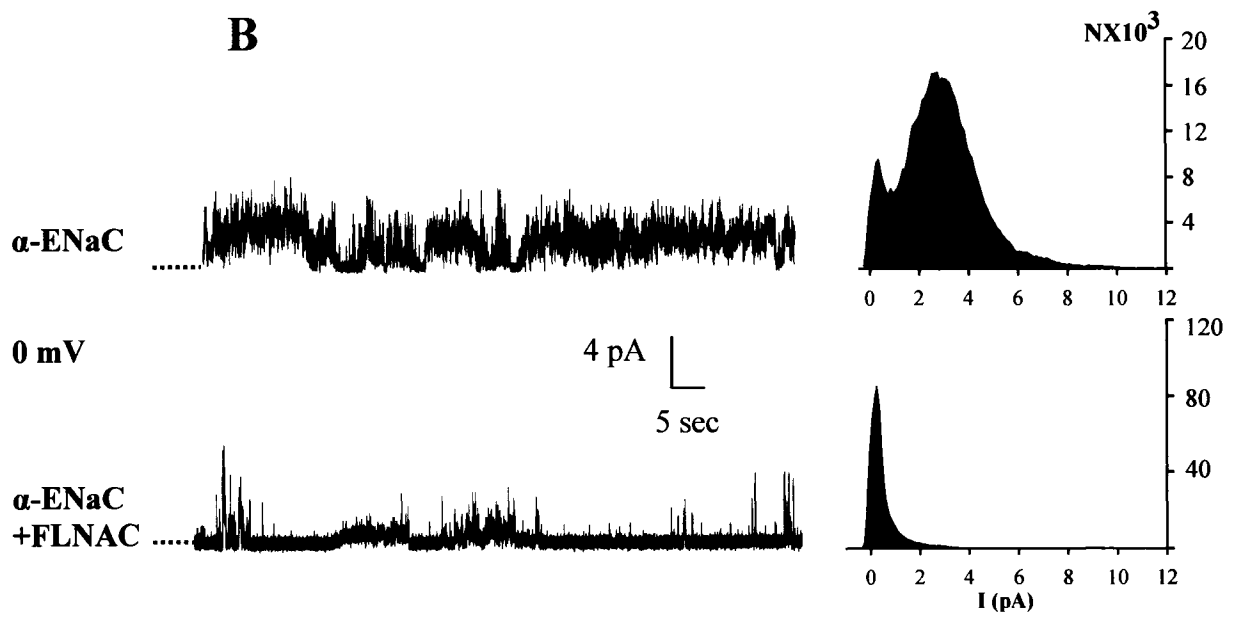


Fig. 3-4. Tandem affinity purification of human α -, β -, and γ -ENaC from MDCK stable cell lines and channel function of α -ENaC reconstituted in lipid bilayer. A, purified human α -, β -, and γ -ENaC channel proteins visualized by Coomassie blue staining (left panel) and WB (right panel). All proteins were purified from MDCK cell lines stably transfected with pGTAP3F-ENaC $\alpha/\beta/\gamma$. B, representative tracings of the GTAP3F-purified α -ENaC channels reconstituted in the lipid bilayer system (left panel) and current-voltage relationships (right panel). Single-channel activities were recorded under asymmetrical condition (150/15 mM NaCl on *cis/trans* compartments).



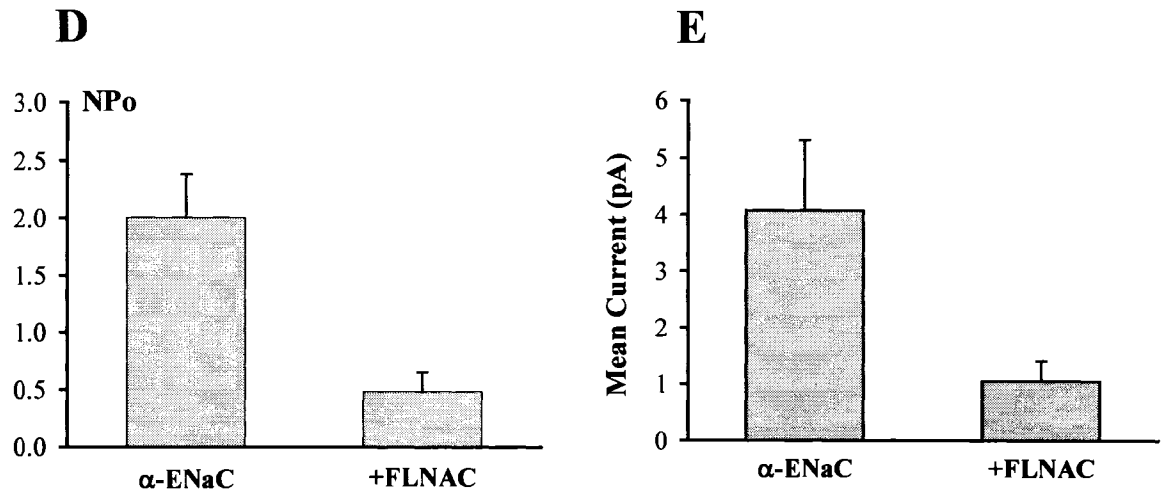


Fig. 3-5. Modulation of α -ENaC channel function by FLNAC in lipid bilayer and effects of FLNAC on α -ENaC single-channel parameters. A. Representative tracings of unitary conductance states at +40 mV and effects of FLNAC on α -ENaC channel function. α -ENaC together with purified FLNAC proteins were used in lipid bilayer experiments under asymmetrical solution condition (150 mM *cis* NaCl and 15 mM *trans* NaCl). Traces were Gaussian filtered at 200 Hz in Clampfit 9. Horizontal dashed lines indicate closed levels. B. *Left*, representative tracings of α -ENaC channel activity in the absence and presence of FLNAC, illustrating multiple conductance states at 0 mV. *Right*, current density plots obtained from the all-point histogram analysis of data shown on the left. C. Representative recording showing real-time inhibition of α -ENaC activity by FLNAC. D-E. Averaged NPo and mean current in the presence and absence of FLNAC (N=4, P<0.01). Data were obtained at 0 mV under asymmetrical condition.

A

Prey (PGADT7) Bait (PGBKT7)	FPCC (3882-4074)	Vector (Control)
α -ENaC-N (1-82)	-	-
α -ENaC-C (588-669)	-	-
β -ENaC-N (1-47)	-	-
β -ENaC-C (559-640)	-	-
γ -ENaC-N (1-76)	-	-
γ -ENaC-C (568-649)	Self-activation, not for testing	
Vector (Control)	-	-

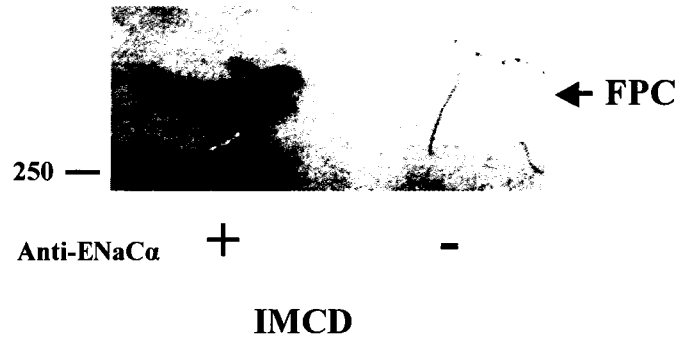
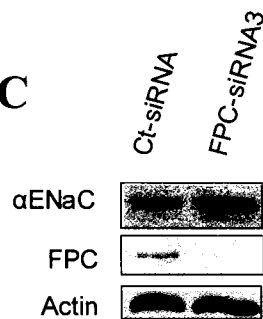
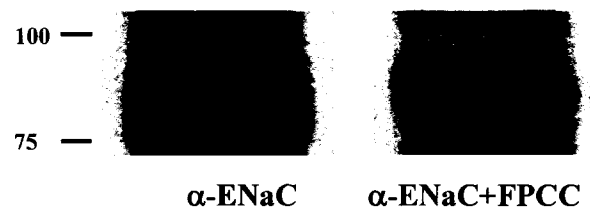
B**C****D**

Fig. 3-6. Physical interactions among ENaC, FPC and filamins. **A.** YTH assays for ENaC-FPC interactions. **B.** Association between endogenous FPC and α -ENaC in IMCD cells by co-immunoprecipitation. **C.** Effect of FPC knockdown on ENaC expression by WB. **D.** Effects of FPC on α -ENaC expression in oocytes.

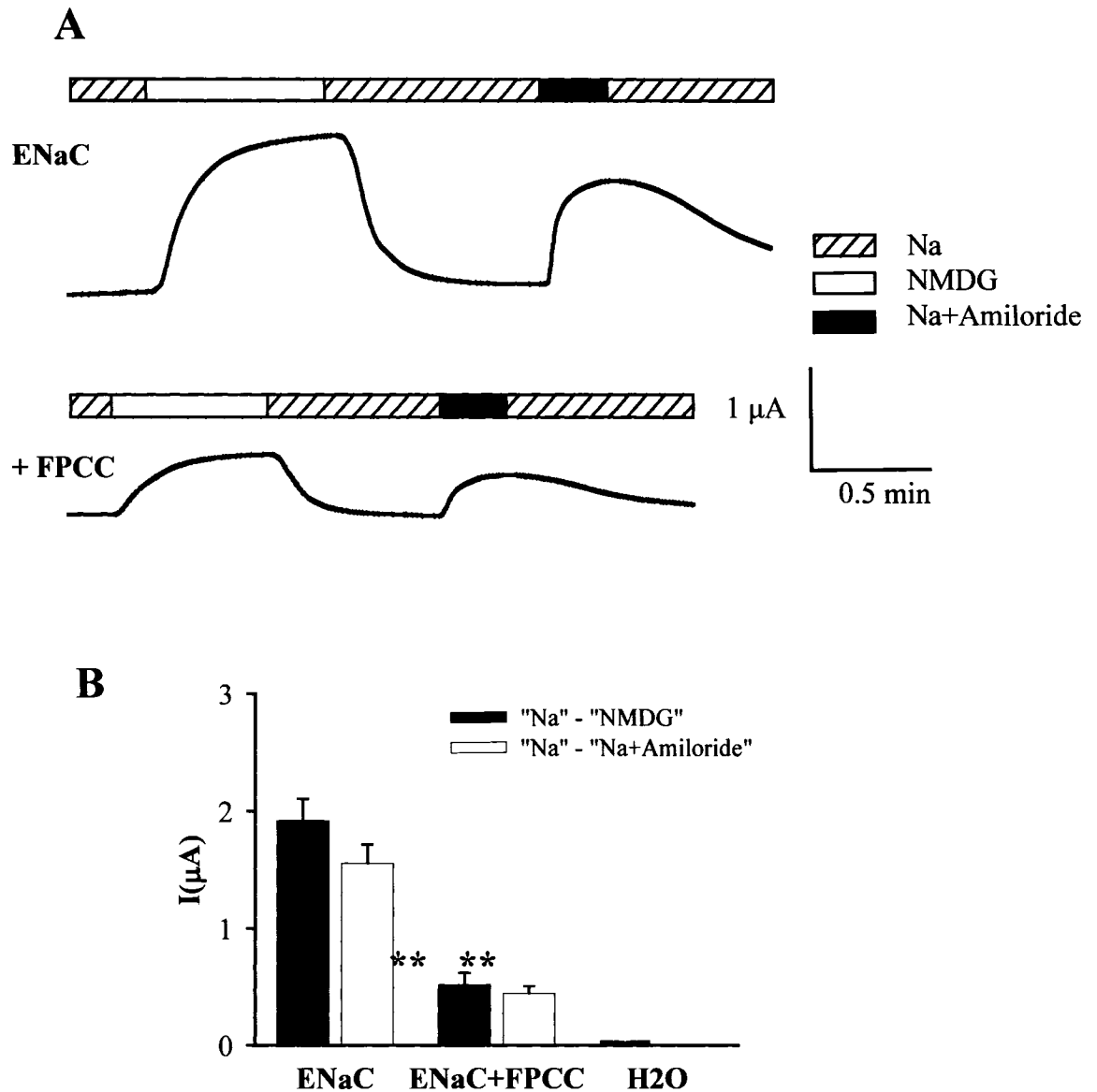


Fig. 3-7. Effects of FPCC on whole-cell transport mediated by $\alpha\beta\gamma$ -ENaC channel overexpressed in *Xenopus* oocytes. A, The ENaC-mediated whole-cell currents obtained with the two-microelectrode voltage-clamp. The currents were measured at -50 mV in the presence of the standard NaCl-containing solution (STD + 1 mM CaCl_2) \pm NMDG \pm amiloride (10 μ M). *Top*: the representative recording in an oocyte over-expressed with ENaC mRNA; *bottom*: the recording in another oocyte over-expressed with both ENaC+FPCC mRNA. B, The currents in the presence of NMDG and 10 μ M amiloride in oocytes overexpressed with ENaC (N=50) and ENaC+FPCC (N=35), respectively. Control levels were obtained using H_2O -injected oocytes. In the oocytes with ENaC+FPCC, the currents in NMDG (Na) and 10 μ M amiloride (Amiloride-sensitive) were decreased to 0.27 ± 0.03 , and 0.29 ± 0.02 of those in the oocytes with ENaC. ******* indicates very significant inhibition: $P < 0.01$.

A

Prey (PGADT7) Bait (PGBKT7)	FLNAC (2150-2647)	FLNBC (2105-2602)	FLNCC (2144-2725)	Vector (Control)
FPC (3882-4074)	++	++	+++	-
Vector (Control)	-	-	-	-

B

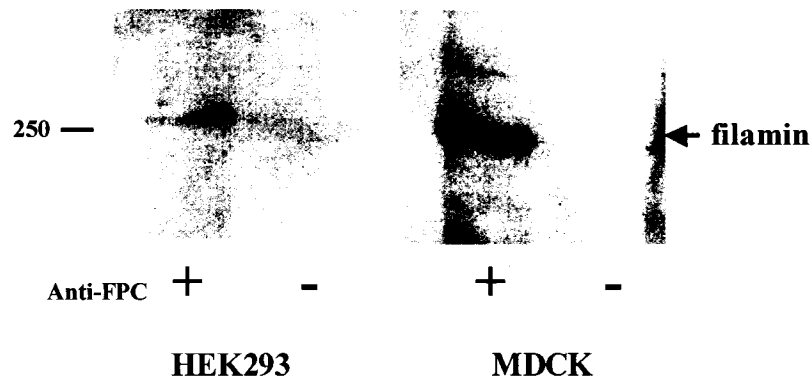


Fig. 3-8. Physical interactions between FPC and filamins. **A.** Interaction data revealed by β -GAL induction assay in the yeast two-hybrid system. The bait fragment of FPC proteins and prey fragments from filamins were co-transformed in Y187 strain and β -GAL activity were determined from the time that was taken for the colonies to turn blue in X-gal filter lift assays performed at 30°C. “+++”, “++”, “+” and “-” indicated for development of blue color within 1, 3 and 24 hr and no development of blue color within 24 hr, respectively. **B.** Association between endogenous FPC and FLNA in various renal lines by co-IP. Total proteins from HEK293 and MDCK cells, were precipitated with either anti-FPC antibody 3C10 or non-immune mouse IgG (-) and detected with FIL2.

3.6. REFERENCES

Awayda MS & Subramanyam M (1998). Regulation of the epithelial Na⁺ channel by membrane tension. *J Gen Physiol* **112**, 97-111.

Barbry P & Hofman P (1997). Molecular biology of Na⁺ absorption. *Am J Physiol* **273**, G571-G585.

Canessa CM, Horisberger JD, & Rossier BC (1993). Epithelial sodium channel related to proteins involved in neurodegeneration. *Nature* **361**, 467-470.

Cantiello HF (1997). Role of actin filament organization in cell volume and ion channel regulation. *J Exp Zool* **279**, 425-435.

Cantiello HF, Stow JL, Prat AG, & Ausiello DA (1991). Actin filaments regulate epithelial Na⁺ channel activity. *Am J Physiol* **261**, C882-C888.

Chasan B, Geisse NA, Pedatella K, Wooster DG, Teintze M, Carattino MD, Goldmann WH, & Cantiello HF (2002). Evidence for direct interaction between actin and the cystic fibrosis transmembrane conductance regulator. *Eur Biophys J* **30**, 617-624.

Feng Y & Walsh CA (2004). The many faces of filamin: a versatile molecular scaffold for cell motility and signalling. *Nat Cell Biol* **6**, 1034-1038.

Gormley K, Dong Y, & Sagnella GA (2003). Regulation of the epithelial sodium channel by accessory proteins. *Biochem J* **371**, 1-14.

Huber SM, Braun GS, & Horster MF (1999). Expression of the epithelial sodium channel (ENaC) during ontogenic differentiation of the renal cortical collecting duct epithelium. *Pflugers Arch* **437**, 491-497.

Ismailov II, Awayda MS, Berdiev BK, Bubien JK, Lucas JE, Fuller CM, & Benos DJ (1996). Triple-barrel organization of ENaC, a cloned epithelial Na⁺ channel. *J Biol Chem* **271**, 807-816.

Jovov B, Tousson A, Ji HL, Keeton D, Shlyonsky V, Ripoll PJ, Fuller CM, & Benos DJ (1999). Regulation of epithelial Na⁺ channels by actin in planar lipid bilayers and in the *Xenopus* oocyte expression system. *J Biol Chem* **274**, 37845-37854.

Kellenberger S & Schild L (2002). Epithelial sodium channel/degenerin family of ion channels: a variety of functions for a shared structure. *Physiol Rev* **82**, 735-767.

Kim J, Kim YH, Cha JH, Tisher CC, & Madsen KM (1999). Intercalated cell subtypes in connecting tubule and cortical collecting duct of rat and mouse. *J Am Soc Nephrol* **10**, 1-12.

Kizer N, Guo XL, & Hruska K (1997). Reconstitution of stretch-activated cation channels by expression of the alpha-subunit of the epithelial sodium channel cloned from osteoblasts. *Proc Natl Acad Sci U S A* **94**, 1013-1018.

Li Q, Dai XQ, Shen PY, Cantiello HF, Karpinski E, & Chen XZ (2004). A modified mammalian tandem affinity purification procedure to prepare functional polycystin-2 channel. *FEBS Lett* **576**, 231-236.

Li Q, Montalbetti N, Shen PY, Dai XQ, Cheeseman CI, Karpinski E, Wu G, Cantiello HF, & Chen XZ (2005). Alpha-actinin associates with polycystin-2 and regulates its channel activity. *Hum Mol Genet* **14**, 1587-1603.

Liu Y, Li Q, Tan M, Zhang Y-Y, Karpinski E, Zhou J, & Chen X-Z (2002). Modulation of the human polycystin-L channel by voltage and divalent cations. *FEBS Lett* **525**, 71-76.

Mano I & Driscoll M (1999). DEG/ENaC channels: a touchy superfamily that watches its salt. *Bioessays* **21**, 568-578.

Mazzochi C, Bubien JK, Smith PR, & Benos DJ (2006). The carboxyl terminus of the alpha-subunit of the amiloride-sensitive epithelial sodium channel binds to F-actin. *J Biol Chem* **281**, 6528-6538.

Nielsen S, Chou CL, Marples D, Christensen EI, Kishore BK, & Knepper MA (1995). Vasopressin increases water permeability of kidney collecting duct by inducing translocation of aquaporin-CD water channels to plasma membrane. *Proc Natl Acad Sci U S A* **92**, 1013-1017.

Noda Y, Horikawa S, Katayama Y, & Sasaki S (2004). Water channel aquaporin-2 directly binds to actin. *Biochem Biophys Res Commun* **322**, 740-745.

Onuchic LF, Furu L, Nagasawa Y, Hou X, Eggermann T, Ren Z, Bergmann C, Senderek J, Esquivel E, Zeltner R, Rudnik-Schoneborn S, Mrug M, Sweeney W, Avner ED, Zerres K, Guay-Woodford LM, Somlo S, & Germino GG (2002). PKHD1, the polycystic kidney and hepatic disease 1 gene, encodes a novel large protein containing multiple immunoglobulin-like plexin-transcription-factor domains and parallel beta-helix 1 repeats. *Am J Hum Genet* **70**, 1305-1317.

Pacha J, Frindt G, Antonian L, Silver RB, & Palmer LG (1993). Regulation of Na channels of the rat cortical collecting tubule by aldosterone. *J Gen Physiol* **102**, 25-42.

Rohatgi R, Greenberg A, Burrow CR, Wilson PD, & Satlin LM (2003). Na transport in autosomal recessive polycystic kidney disease (ARPKD) cyst lining epithelial cells. *J Am Soc Nephrol* **14**, 827-836.

Rossier BC, Pradervand S, Schild L, & Hummler E (2002). Epithelial sodium channel and the control of sodium balance: interaction between genetic and environmental factors. *Annu Rev Physiol* **64**:877-97., 877-897.

Satlin LM & Palmer LG (1996). Apical Na⁺ conductance in maturing rabbit principal cell. *Am J Physiol* **270**, F391-F397.

Satlin LM, Sheng S, Woda CB, & Kleyman TR (2001). Epithelial Na(+) channels are regulated by flow. *Am J Physiol Renal Physiol* **280**, F1010-F1018.

Schild L (2004). The epithelial sodium channel: from molecule to disease. *Rev Physiol Biochem Pharmacol* **151**:93-107. Epub@2004 May 14., 93-107.

Stossel TP, Condeelis J, Cooley L, Hartwig JH, Noegel A, Schleicher M, & Shapiro SS (2001). Filamins as integrators of cell mechanics and signalling. *Nat Rev Mol Cell Biol* **2**, 138-145.

Takafuta T, Saeki M, Fujimoto TT, Fujimura K, & Shapiro SS (2003). A new member of the LIM protein family binds to filamin B and localizes at stress fibers. *J Biol Chem* **278**, 12175-12181.

Theelin WR, Chen Y, Gentzsch M, Kreda SM, Sallee JL, Scarlett CO, Borchers CH, Jacobson K, Stutts MJ, & Milgram SL (2007). Direct interaction with filamins modulates the stability and plasma membrane expression of CFTR. *J Clin Invest* **117**, 364-374.

van der FA & Sonnenberg A (2001). Structural and functional aspects of filamins. *Biochim Biophys Acta* **1538**, 99-117.

Veizis IE & Cotton CU (2005). Abnormal EGF-dependent regulation of sodium absorption in ARPKD collecting duct cells. *Am J Physiol Renal Physiol* **288**, F474-F482.

Ward CJ, Hogan MC, Rossetti S, Walker D, Sneddon T, Wang X, Kubly V, Cunningham JM, Bacallao R, Ishibashi M, Milliner DS, Torres VE, & Harris PC (2002). The gene mutated in autosomal recessive polycystic kidney disease encodes a large, receptor-like protein. *Nat Genet* **30**, 259-269.

Wu Y, Dai XQ, Li Q, Chen CX, Mai W, Hussain Z, Long W, Montalbetti N, Li G, Glynn R, Wang S, Cantiello HF, Wu G, & Chen XZ (2006). Kinesin-2 mediates physical and functional interactions between polycystin-2 and fibrocystin. *Hum Mol Genet* **15**, 3280-3292.

Zerres K, Rudnik-Schoneborn S, Senderek J, Eggermann T, & Bergmann C (2003). Autosomal recessive polycystic kidney disease (ARPKD). *J Nephrol* **16**, 453-458.

Zuckerman JB, Chen X, Jacobs JD, Hu B, Kleyman TR, & Smith PR (1999). Association of the epithelial sodium channel with Apx and alpha-spectrin in A6 renal epithelial cells. *J Biol Chem* **274**, 23286-23295.

CHAPTER 4

PERMEATION AND INHIBITION OF POLYCYSTIN-L CHANNEL BY MONOVALENT ORGANIC CATIONS

This chapter was published in 2006:

Dai, X.-Q., Karpinski, E., and Chen, X.-Z. (2006) Permeation and inhibition of polycystin-L channel by monovalent organic cations. *Biochem. Biophys. Acta - Biomembrane* 1758, 197-205.

4.1. INTRODUCTION

Autosomal dominant polycystic kidney disease (ADPKD) is an inherited nephropathy, primarily characterized by the formation of fluid-filled cysts in the kidneys. It is one of the most frequent genetic disorders affecting approximately 0.1% of individuals and accounting for up to 10% of end-stage renal failure. ADPKD also exhibits extrarenal manifestations, such as hepatic and pancreatic cystogenesis, intracranial aneurysms and cardiac mitral valve prolapse, and is often associated with hypertension. *PKD1* and *PKD2* are the two known genes responsible for about 95% of ADPKD and have been mapped to chromosomes 16p13.3 and 4q21-23, respectively [26]. Polycystin-L (PCL), encoded by *PKDL*, is the third member of the polycystin family [16]. As members of the transient receptor potential (TRP) channels superfamily, polycystin-1 (PC1), -2 (PC2) and PCL have also been called TRPP1, TRPP2 and TRPP3 (TRP-polycystin), respectively [7]. PC1 is a large receptor-like integral membrane protein involved in cell-cell and cell-matrix interactions.

PCL and PC2 are highly homologous (70% similarity) but PCL seems not to be directly linked to ADPKD renal cyst formation. However, the mouse orthologue of PCL is deleted in *krd* (kidney and retinal defects) mice, resulting in defects in kidney and retina [10,16]. PCL may be one of the candidates linked to unmapped human genetic cystic disorders such as dominantly transmitted glomerulocystic kidney disease of post-infantile onset, isolated polycystic liver disease, and Hajdu-Cheney syndrome/serpentine fibula syndrome [16]. PCL is present in multiple tissues, including brain, retina, kidney, heart, testis, liver, pancreas and spleen. In adult kidney, PCL is predominantly localized in the apical region of the principal cells of inner medullary collecting ducts [3]. In embryonic kidney, it is found in the apical membrane of tubular epithelial cells. PCL shares similar membrane topology and modest sequence homology with TRP channels and the α -subunits of voltage-gated K, Na and Ca channels. For example, it comprises six transmembrane-spanning domains with both the carboxyl- and amino-termini being intracellular. It is still unknown how many subunits make up the pore of the PCL channel. PCL channel possesses an EF-hand calcium-binding motif in its C-terminus, suggesting a possible involvement of intracellular calcium in its function. It was reported that EF-hand serves to control (reduce) calcium-induced PCL channel activation [13].

Indeed, recent studies have demonstrated that PCL is a Ca-activated, Ca-permeable, non-selective cation channel [6,14]. PCL associates with troponin I which inhibits PCL channel activity [12].

Monovalent cations such as organic amines and tetra-alkylammonium (TAA) compounds have been employed to determine the pore diameters of ion channels. Methylamine (MA) is an endogenous compound that is increased during liver and renal failure, Alzheimer's disease, vascular dementia and diabetes. It alters some neurobehavioural functions, probably by acting as a potassium channel blocker [19]. Dimethylamine (DMA) was used to investigate the pore size of PC2 channel and ryanodine receptor [2] [24]. Triethylamine (TriEA), tetramethylammonium (TMA), tetraethylammonium (TEA), tetra-propylammonium (TPA) tetra-butylammonium (TBA) and tetra-pentylammonium (TPeA) are known to block ion permeation through K, Na and Cl channels, anthrax toxin channels, ryanodine and NMDA receptors [18,20,28]. They were also used to probe the structure of the internal and external vestibules of K channel pores [8,15,28] and the pore sizes of ryanodine receptor, K channel KcsA, NMDA receptor, PC2, and vanilloid receptor (TRPV6) [1,2,9,22,27]. Using TAA cations as permeant ions or inhibitors, the pore diameter of the PC2 channel was recently estimated to be at least 11 Å [2]. Previous reports revealed that ryanodine receptor has a minimum pore diameter of ~7 Å and that the NMDA channel pore size of ~11 Å. TRPV6, which belongs to the family of TRP channels, has a pore diameter of ~5.4 Å. These TAA compounds are also blockers of Na channels with affinities positively correlated to the length of alkyl side chains [18]. In the present study, we explored biophysical and pharmacological properties of the PCL channel through examining the permeation of and inhibition by monovalent organic amines and TAA cations.

4.2. MATERIAL AND METHODS

Oocyte preparation

Capped synthetic human *PCL* mRNA was synthesized by *in vitro* transcription from a linearized template inserted in the pTLN2 vector, using the mMACHINE1 Kit (Ambion, Austin, TX, USA). Stage V-VI oocytes were extracted from *Xenopus laevis* and defolliculated by collagenase type I (2.5 mg/ml) (Sigma-Aldrich Canada, Oakville, ON, Canada) in the Barth's solution (in mM, 88 NaCl, 1 KCl, 0.33 Ca(NO₃)₂, 0.41 CaCl₂, 0.82 MgSO₄, 2.4 NaHCO₃, 10 HEPES, and pH 7.5) at room temperature (21-23 °C) for 2 hr. Oocytes were injected with 50 nl of water containing 20 or 40 ng of each RNA 3-24 hr following defolliculation. An equal volume of RNAase-free water was injected into each control oocyte. Injected oocytes were incubated at 16-18°C in the Barth's solution supplemented with antibiotics for 3 ~ 4 days prior to experiments.

Two-electrode voltage clamp

Two-electrode voltage clamp was performed as described previously [14]. Briefly, the two electrodes (Capillary pipettes, Warner Instruments, Hamden, CT, USA) impaling *Xenopus* oocytes were filled with 3 M KCl to form a tip resistance of 0.3 - 2 MΩ. Oocyte whole-cell currents were recorded using a Geneclamp 500B amplifier and a Digidata1320A AD/DA converter (Axon Instruments, Union City, CA, USA). In experiments using a ramp protocol, currents and voltages were sampled at intervals of 200 μs and filtered at 2 kHz using an 8 pole Bessel filter. In experiments using a gap-free protocol, current/voltage signals were sampled at intervals of 200 ms. The modified Choline-Cl-containing solution contained (in mM): 100 Choline-Cl, 2 KCl, 0.2 MgCl₂, 10 HEPES, pH 7.5.

Single-channel patch clamp

Vitelline membranes of oocytes were removed manually following incubation of the oocytes at room temperature in a hypertonic solution containing (in mM): 220 NaCl, 50 sucrose, 1 EGTA, 1 MgCl₂, 10 HEPES, pH 7.5. Oocytes were then transferred to the Barth's solution and allowed to recover for 10 ~ 20 min before patch clamping.

Electrodes were filled with a pipette solution containing 123 mM K (in mM: 110 KCl, 13 KOH, 10 HEPES, and pH 7.4) to form a tip resistance of 3 - 6 M Ω . The Barth's solution was used in the bath. Single channel currents were recorded in cell-attached configuration using PC-ONE Patch Clamp amplifier (Dagan Corp., Minneapolis, MN), DigiData 1322A interface, and Clampex 9 software (Axon Instruments). Recording started after seal resistance reached at least 3 ~ 5 G Ω . Current/voltage signals were sampled every 200 μ s and filtered at 2 kHz. All chemicals were purchased from Sigma-Aldrich Canada.

Statistics and data analysis

Data obtained from the two-microelectrode voltage-clamp and patch-clamp experiments were analyzed using Clampfit 9. Single-channel conductance values were obtained from Gaussian fits to All-Point Histograms. The open probability times the number of channels in the patch (NP_o , designated 'open probability' hereafter) and channel mean open time (MOT) values were obtained from currents generated either by voltage pulses of 10 s per pulse or by gap-free recordings of 10 s long. For the MOT analysis, recordings with single openings were used and filtered at 500 Hz (Gaussian). Analyzed data were plotted using Sigmaplot 9 (Jandel Scientific Software, San Rafael, CA, USA) and expressed in the form of mean \pm SE (N), where SE represents the standard error of the mean and N indicates the number of oocytes (or oocyte patches) tested. Curve fitting and data filtering were performed using Clampfit 9 or Sigmaplot 9. Dose-response inhibition data were fitted with the Logistic equation: $I/I_{\max} = 1/\{1 + ([S]/IC_{50})^p\}$, where [S] represents the concentration of an inhibitor and p is the power (or Hill coefficient). Comparison between two sets of data was analyzed by t -test or two-way ANOVA, and a probability value (P) of less than 0.05 and 0.01 was considered significant and very significant, respectively.

4.3. RESULTS

To gain more insights into physical and pharmacological properties of PCL we utilized a series of organic amines and TAA cations with varying ionic diameters for their permeability through and inhibition of PCL channel expressed in *Xenopus* oocytes. PCL is a large conductance cation channel of 366 pS in the presence of 123 mM K [14]. Using the cell-attached mode of single-channel patch clamp we found that MA (3.8 Å), DMA (4.6 Å), TriEA (6 Å) and TMA (5.5 ~ 6.4 Å) were permeable through PCL channel with current amplitudes dependent on cation size (Fig. 4-1A and B). In fact, single-channel conductance inversely correlated with cation size (Fig. 4-1C). As expected, the outward single-channel current amplitudes at positive voltages ($+V_m$, 0 ~ +120 mV), presumably elicited by endogenous permeant cations inside oocytes, mainly K, were not significantly different, in the presence of extracellular 123 mM K, Cs, MA, DMA, TriEA or TMA (Fig. 4-1B).

Single channel conductance can depend on the mole fraction of two permeant ions in a peculiar way, such that the conductance is smaller than the one calculated based on mole fraction (anomalous mole-fraction behavior). To test whether PCL channel exhibits anomalous mole-fraction dependence, we measured the inward currents through PCL channel in the presence of K and TMA (61.5 mM each). We found that the resulting amplitudes were smaller than the arithmetic average of those obtained in the presence of 123 mM K and TMA alone (Fig. 4-1D). This result indicates that the two permeant cations exhibit interaction between them when passing through PCL channel.

We next tested the permeation of larger TAA cations through the PCL channel. In the presence of 123 mM TEA (6.1 ~ 8.2 Å) or TPA (9.8 Å) in the pipette, channel openings were observed at positive voltages ($\geq +20$ mV) but not at negative voltages (-180 ~ -20 mV) (Fig. 4-2A and B). This indicates that TEA and TPA were impermeable through PCL. There was no difference in the single-channel amplitudes of the PCL channel at positive voltages ($+V_m$), whether the pipette contained 123 mM K, TEA or TPA (Fig. 4-2B, N = 12). In contrast, in the presence of 123 mM TBA (11.6 Å) or TPpA (13.2 Å) in the pipette, at voltages between -180 and +180 mV, no channel openings were observed, indicating that these two cations are impermeable through PCL as well and

inhibit outward currents associated with effluxes of oocytes endogenous permeant cations through PCL.

We next examined inhibition of K currents by TEA, TPA, TBA and TPeA, using both single-channel patch clamp and whole-cell voltage clamp. Addition of TEA at 20 mM to the pipette containing 123 mM K reduced the NP_o and MOT values of inward and outward single-channel currents (Fig. 4-3A). In average, NP_o decreased from 0.35 ± 0.04 (N = 40) and 0.16 ± 0.02 (N = 35), in the absence of TEA, to 0.25 ± 0.03 (N = 15, $P < 0.05$) and 0.11 ± 0.02 (N = 12, $P < 0.05$), in the presence of pipette TEA (20 mM), at negative voltages ($-V_m$, -120 to -20 mV) and $+V_m$, respectively (Fig. 4-3D). Under the same condition, MOT decreased from 65 ± 4 (N = 40) and 19 ± 2 ms (N = 35) to 46 ± 5 (N = 15) and 15 ± 2 ms (N = 12) at $-V_m$ and $+V_m$, respectively. In contrast, TEA did not exhibit significant effect on the outward single-channel current amplitude. Inhibitory effect of TEA was also observed with whole-cell recordings (Fig. 4-3B and C). Inward currents at -50 mV in the presence of 100 mM Choline and 5 mM Ca decreased $44 \pm 7\%$ (N = 8) by 20 mM TEA, with an IC_{50} value of 23 ± 3 mM (N = 31).

TPA exhibited similar characteristics as TEA (Fig. 4-4A-C). TPA at 20 mM inhibited the single-channel activities of the PCL channel (Fig. 4-4A). In average, NP_o decreased to 0.14 ± 0.02 (N = 12, $P < 0.01$) and 0.08 ± 0.01 (N = 11, $P < 0.01$) at $-V_m$ and $+V_m$, respectively (Fig. 4-3D). MOT decreased to 41 ± 4 ms (N = 12) and 12 ± 1 ms (N = 11), respectively. Like TEA, TPA had no effect on the current amplitude. Inhibitory effect of TPA was also supported by whole-cell data (Fig. 4-4B and C). Inward currents at -50 mV in the presence of 100 mM Choline and 5 mM Ca decreased $68 \pm 7\%$ (N = 9) by 20 mM TPA (Fig. 4-4B), with an IC_{50} value of 13 ± 2 mM (N = 29).

In contrast to TEA and TPA, TBA exhibited inhibition of the PCL single-channel amplitude at the whole voltage range tested and had no effects on NP_o and MOT (Fig. 4-5A). The concentration dependence of the inhibition was represented by averaged current-voltage (I-V) curves obtained in the presence 0.1, 1, 10, 33 mM TBA in the pipette (Fig. 4-5B). For example, at -120 mV, the presence of 0.1, 1, 10 and 33 mM TBA in the pipette containing 123 mM K significantly reduced channel inward-current amplitude to $95 \pm 11\%$ ($P > 0.05$, N = 7), $75 \pm 9\%$ ($P < 0.05$, N = 10), $46 \pm 3\%$ ($P < 0.01$, N = 15) and $25 \pm 4\%$ ($P < 0.01$, N = 8). The IC_{50} values decreased with

hyperpolarization, from 16.2 mM at -40 mV to 6.8 mM at -120 mV, suggesting voltage-dependent inhibition by TBA (Fig. 4-5C). TBA inhibition was also demonstrated at the whole-cell level (Fig. 4-5D and E). Inward currents at -50 mV activated by 5 mM Ca were reduced to 18% by 10 mM TBA (Fig. 4-5D).

TPeA is the largest cation tested in the current study. TPeA did not permeate PCL (Fig. 4-2A) but acted as a high-affinity inhibitor. Using patch clamp, with 1 μ M TPeA in the pipette solution PCL channel activity was almost abolished at both $+V_m$ and $-V_m$. TPeA reduced NP_o and MOT, but not the single-channel conductance (Fig. 4-6A and 4-3D). The inhibition by TPeA was concentration-dependent, and TPeA at 10 μ M completely abolished PCL channel opening (Fig. 4-6B). The IC_{50} values for TPeA on NP_o were $1.2 \pm 0.1 \mu$ M at $+V_m$ and $0.60 \pm 0.02 \mu$ M at $-V_m$ (Fig. 4-6B, left). The IC_{50} values for TPeA on MOT were $0.54 \pm 0.16 \mu$ M at $+V_m$ and $0.72 \pm 0.17 \mu$ M at $-V_m$ (Fig. 4-6B, right). TPeA also exhibited potent inhibition of PCL whole-cell currents (Fig. 4-7A and B), with an IC_{50} value of $1.3 \pm 0.1 \mu$ M ($N = 15$) at -50 mV, much smaller than that for TBA (2.7 ± 0.2 mM, $N = 10$), TPA (13 ± 1.2 mM, $N = 11$) and TEA (23 ± 3 mM, $N = 13$) (Fig. 4-7C). Thus TPeA is the most potent inhibitor tested when compared with the three other inhibitors and the inhibition potency of these TAA compounds inversely correlated with their size (Fig. 4-7D).

4.4. DISCUSSION

In the present study we investigated the permeation and inhibition of the PCL channel by monovalent organic amines and TAA cations of various sizes, including MA, DMA, TriEA, TMA, TEA, TPA, TBA and TPeA, using the whole-cell two-microelectrode voltage clamp and single-channel patch clamp. The PCL single-channel conductance decreased as the size of cations increased (Fig. 4-1). Similar conclusion was previously drawn for ryanodine receptor [23]. TEA, TPA, TBA and TPeA are not permeable through PCL and inhibited whole-cell Ca-induced activated currents and basal single-channel activities of PCL. Inhibition potency correlates positively with cation size (Fig. 4-7D). TEA and TPA reduced NP_0 and MOT with low potency, while the inhibition by TPeA was at least three magnitudes more potent. These three inhibitors did not significantly affect single-channel amplitude, suggesting that they bind a site away from the PCL pore pathway. In contrast, TBA reduced single-channel current amplitudes of PCL but did not reduce NP_0 and MOT, suggesting binding to a site at the pore entry, which indicates that PCL may possess an extracellular vestibule of about 12 Å in size.

Monovalent inorganic and organic cations have been used as biophysical probes for delineating the pore and vestibule of ion channels. The largest tested cations permeable through PCL were TriEA and TMA and smallest tested cation impermeable through PCL was TEA. The sizes of TriEA, TMA and TEA are in the range of 6 ~ 7.2 Å [2,23], 5.5 ~ 6.4 Å [11,25] and 6.1 ~ 8.2 Å [2], respectively. Thus the PCL pore size can be estimated to be ~7 Å, which is comparable with TRPV6 (~5.4 Å), L-type voltage-gated Ca channel (6.2 Å)[5] and ryanodine receptor (~7 Å) [1,27].

Interestingly, although PCL and PC2 are highly homologous (with 70% similarity) and PC2 has smaller single-channel conductance than PCL, the pore size of PC2 was recently estimated to be at least 11 Å as it is permeable to TPeA [2]. This suggests that other differences in the pore geometry of these two homologous channels, eg, in selectivity filter and pore depth, may affect cation permeation.

TAA compounds are well-known inhibitors of K channels [17]. TEA and larger TAA compounds, such as TBA and TPeA, are known to block ion permeation through ryanodine receptor, neuronal chloride and anthrax toxin channels [1,4,21]. Using energy-minimized molecular models of TAA cations and independent molecular dynamics

analysis, it was found that the diameter of these molecules increased by ~ 2 Å per symmetrical addition of a methylene group: TMA has one carbon alkyl side chain with a size of 5.5 ~ 6.4 Å; TEA, 2 side chains, 6.1 ~ 8.2 Å; TPA, 3 side chains, 9.8 Å; TBA, 4 side chains, 11.6 Å; and TPeA, 5 side chains, 13.2 Å [17,24]. In fact, an increase in the molecular diameter of TAA cations due to addition of carbon alkyl side chains is accompanied by a proportional increase in their hydrophobicity. Whether/how the hydrophobicity of these TAA cations influences their potency of inhibition remains to be investigated.

In summary, we discovered novel physical and pharmacological properties of the PCL channel through examining the permeation of and inhibition by monovalent organic amines and TAA cations.

ACKNOWLEDGEMENTS

This work was supported by the Canadian Institutes of Health Research, the Canada Foundation for Innovation, and the Heard and Stroke Foundation of Canada (to X.-Z.C.). X.-Z.C. is an Alberta Heritage Foundation for Medical Research Scholar. X.-Q.D. is a recipient of an AHFMR Studentship.

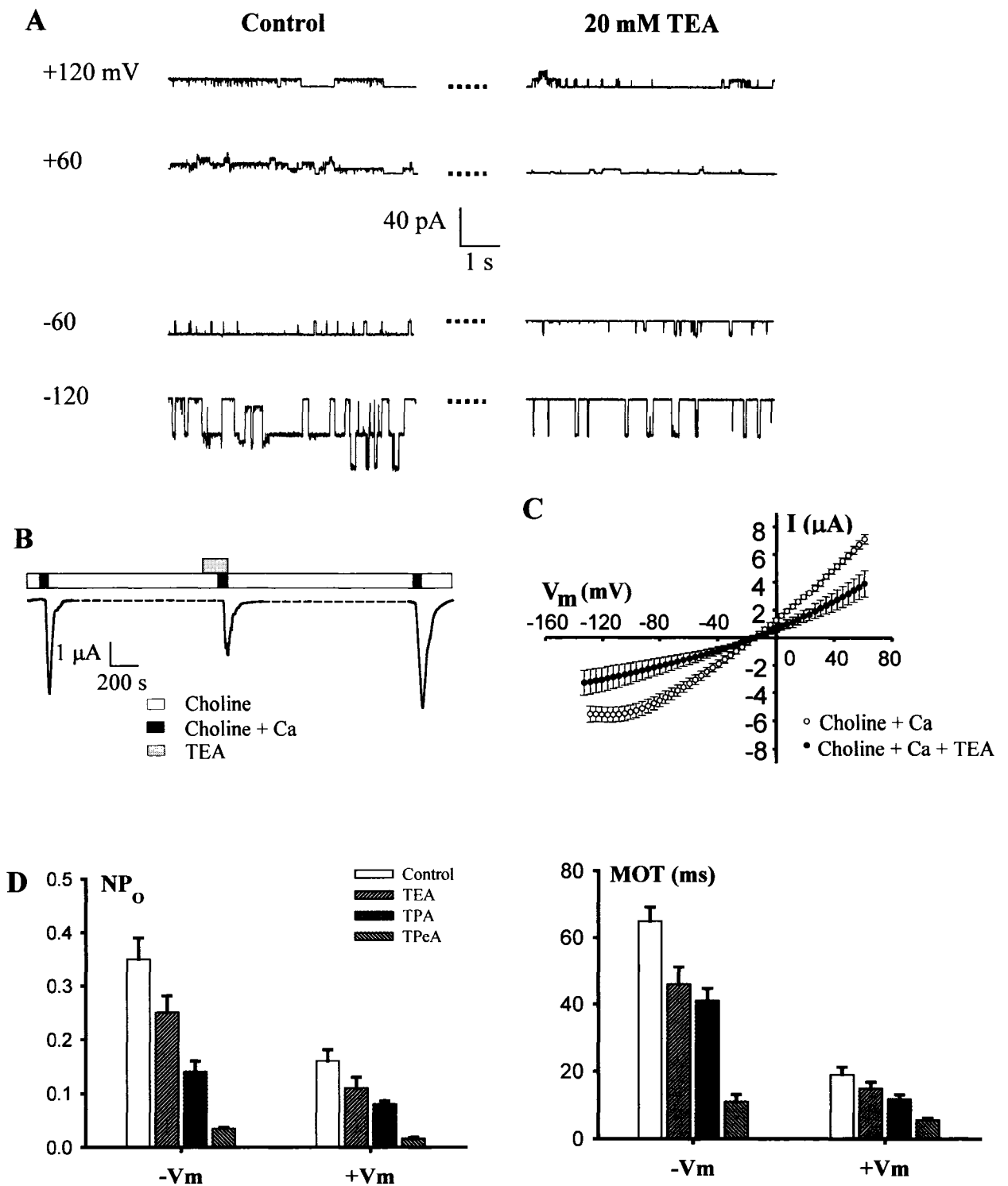


Fig. 4-3. Effects of TEA on PCL. **A.** Representative single-channel recordings obtained with or without TEA (20 mM). **B.** Representative whole-cell recording in a single oocyte voltage clamped at -50 mV. "Choline" indicates the solution containing (in mM): 100 Choline-Cl, 2 KCl, 0.2 MgCl₂, 10 HEPES, pH 7.5, and "Ca" 5 mM CaCl₂. The dashed lines represent 10-min periods during which the oocyte was not voltage clamped. **C.** Averaged whole-cell I-V curves before and after addition of 20 mM TEA (N = 10). **D.** Effects of 20 mM TEA (N = 10), 20 mM TPA (N = 11), and 1 μ M TPeA (N = 14) on NP_o and MOT at -V_m and +V_m.

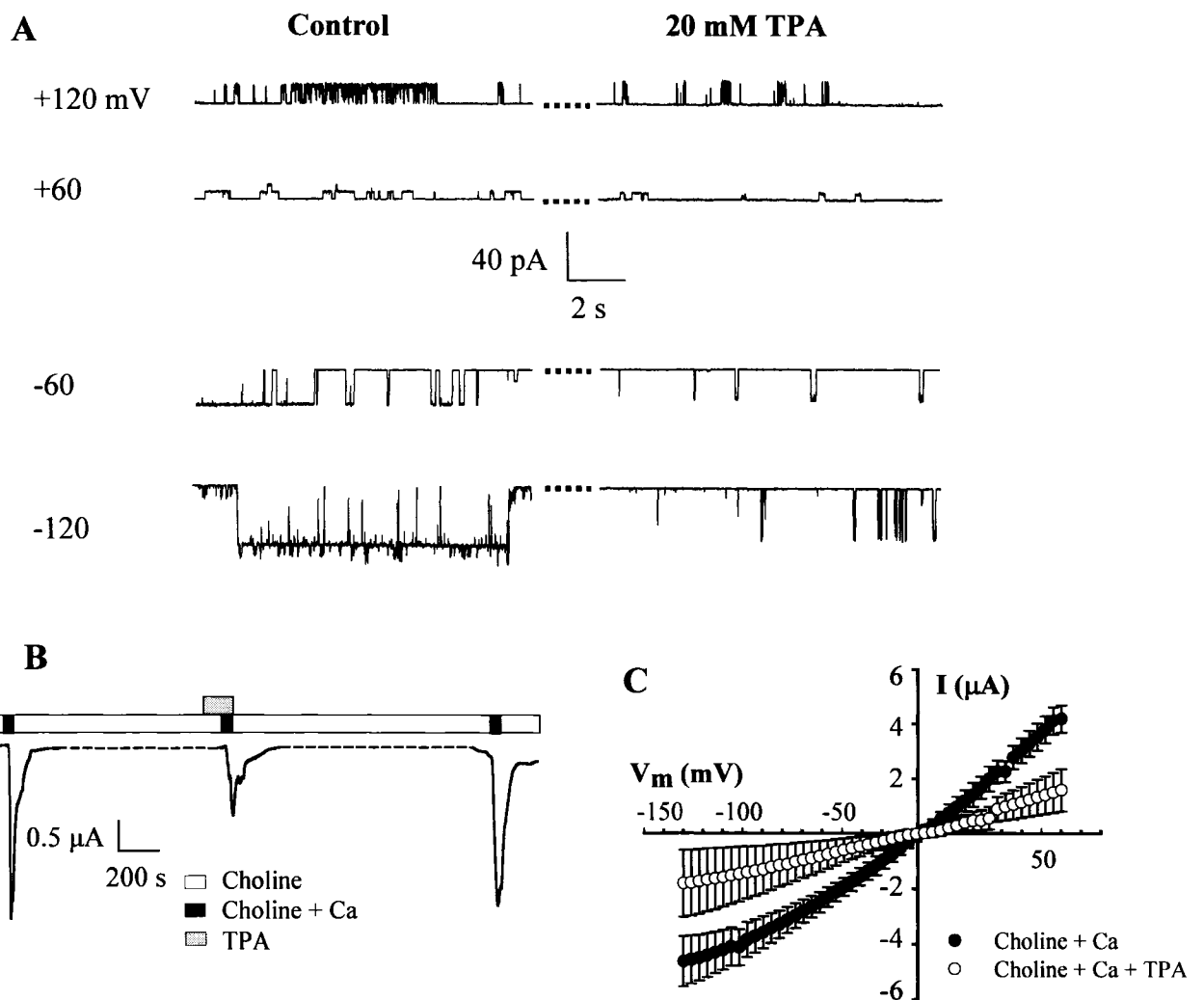


Fig. 4-4. Effects of TPA on PCL. **A.** Representative single-channel recordings obtained with or without TPA (20 mM). **B.** Representative whole-cell recording in a single oocyte voltage clamped at -50 mV. **C.** Averaged whole-cell I-V curves before and after addition of 20 mM TPA (N = 11).

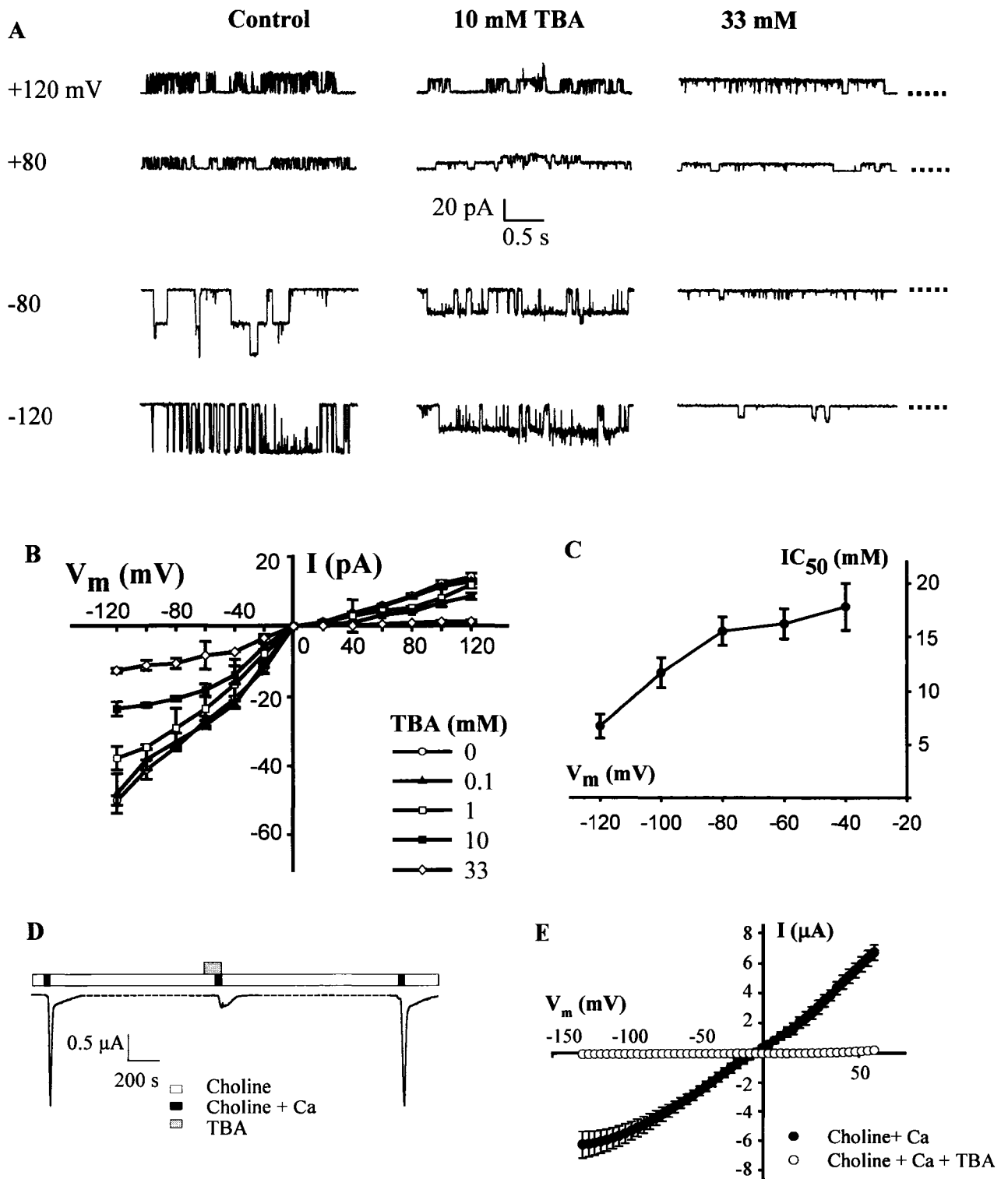


Fig. 4-5. Inhibition of PCL by TBA. **A.** Representative tracings obtained in the presence of 0 (Control), 10 or 33 mM TBA at various membrane potentials as indicated. **B.** Averaged I-V relationships (N = 25) obtained at various TBA concentrations. **C.** Voltage dependence of IC_{50} for TBA inhibition obtained from the data shown in panel B. **D.** Representative whole-cell recording in a single oocyte voltage clamped at -50 mV with or without 10 mM TBA. **E.** Averaged whole-cell I-V curves before and after addition of 10 mM TBA (N = 8).

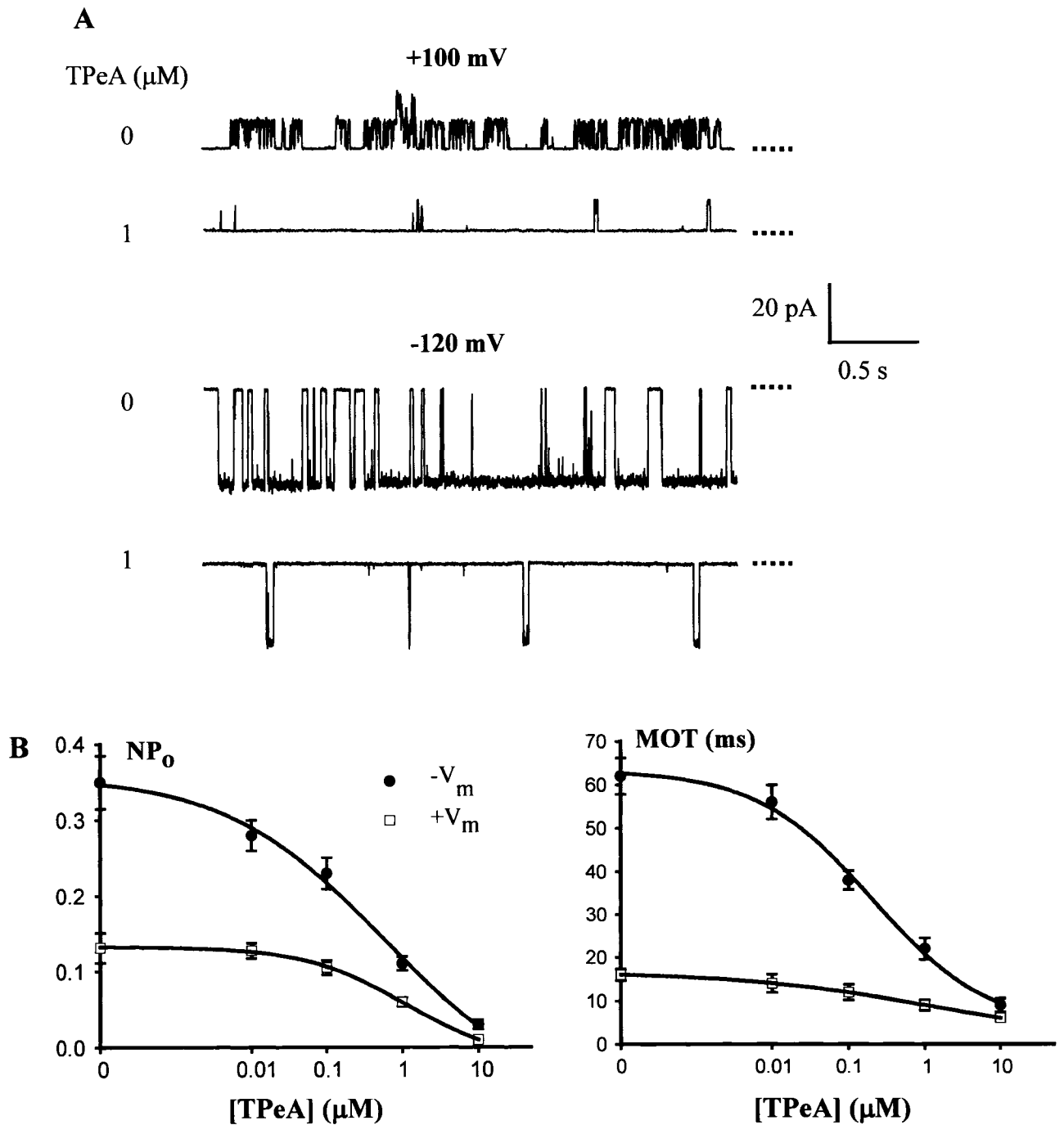


Fig. 4-6. Effects of TPeA on PCL single-channel currents. **A.** Representative recordings in the presence or absence of 1 μM TPeA in the pipette containing 123 mM K. **B.** Concentration-dependent effects of TPeA on NP_o (left panel) and MOT (right panel) at $+V_m$ or $-V_m$. Shown data were averaged from 20 measurements.

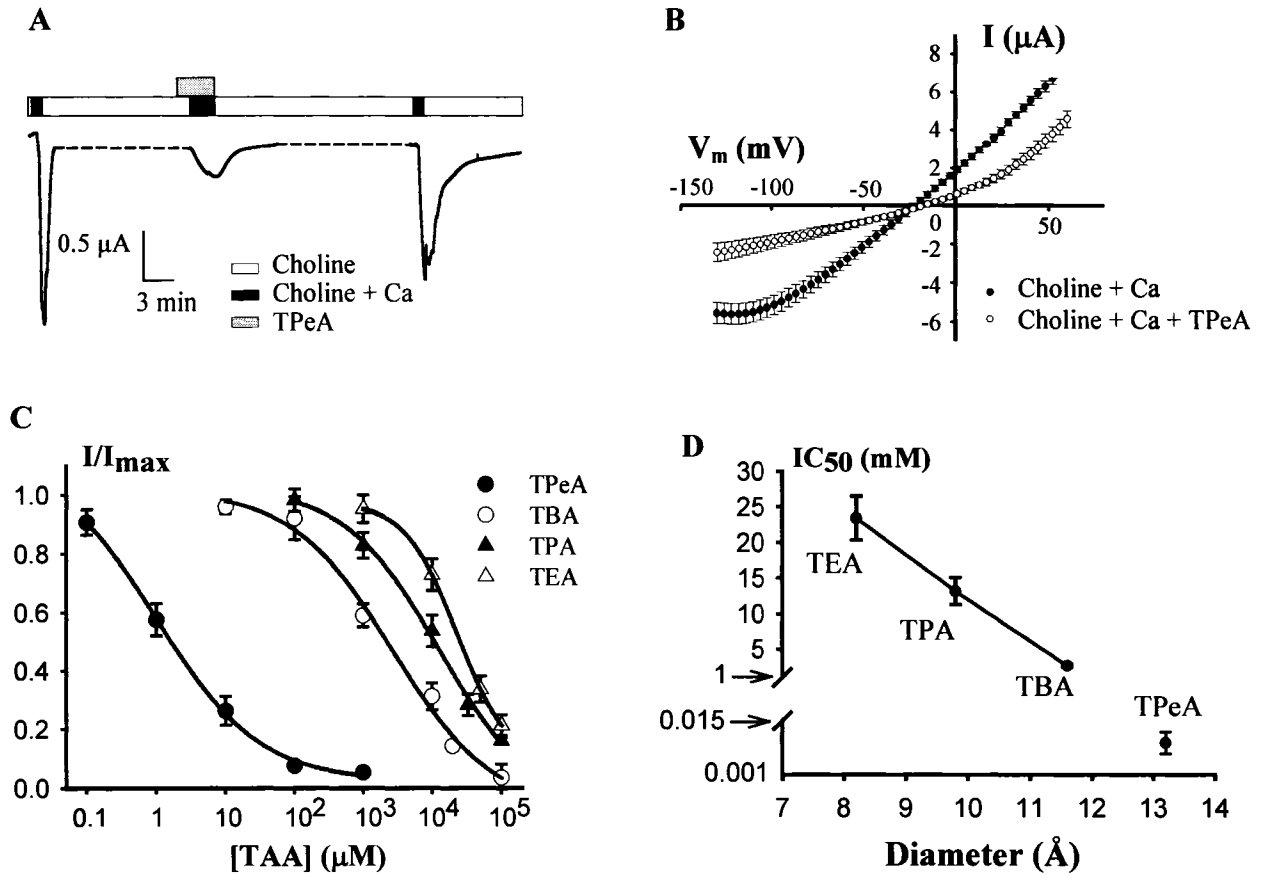


Fig. 4-7. Inhibition of PCL whole-cell currents by TPeA. **A.** Representative whole-cell current recording from an oocyte showing the inhibition of PCL channel activation by TPeA. Currents carried by Ca were measured at -50 mV. **B.** Averaged I-V relationships ($N = 13$) for PCL channels in the presence or absence of $1 \mu\text{M}$ TPeA. **C.** Concentration-dependent inhibition of PCL whole-cell current by the four TAA cations. Each point was averaged from 10 determinations. **D.** IC_{50} values for TAA cations inhibition as a function of their molecular sizes.

4.6. REFERENCES

- [1]G.I. Anyatonwu, E.D. Buck, B.E. Ehrlich, Methanethiosulfonate ethylammonium block of amine currents through the ryanodine receptor reveals single pore architecture, *J. Biol. Chem.* 278 (2003) 45528-45538.
- [2]G.I. Anyatonwu and B.E. Ehrlich, Organic cation permeation through the channel formed by polycystin-2, *J. Biol. Chem.* In press (2005).
- [3]N. Basora, H. Nomura, U.V. Berger, C. Stayner, L. Guo, X. Shen, J. Zhou, Tissue and cellular localization of a novel polycystic kidney disease-like gene product, polycystin-L, *J. Am. Soc. Nephrol.* 13 (2002) 293-301.
- [4]R.O. Blaustein and A. Finkelstein, Diffusion limitation in the block by symmetric tetraalkylammonium ions of anthrax toxin channels in planar phospholipid bilayer membranes, *J. Gen. Physiol* 96 (1990) 943-957.
- [5]M. Cataldi, E. Perez-Reyes, R.W. Tsien, Differences in apparent pore sizes of low and high voltage-activated Ca²⁺ channels, *J. Biol. Chem.* 277 (2002) 45969-45976.
- [6]X.Z. Chen, P.M. Vassilev, N. Basora, J.B. Peng, H. Nomura, Y. Segal, E.M. Brown, S.T. Reeders, M.A. Hediger, J. Zhou, Polycystin-L is a calcium-regulated cation channel permeable to calcium ions, *Nature* 401 (1999) 383-386.
- [7]D.E. Clapham, TRP channels as cellular sensors, *Nature* 426 (2003) 517-524.
- [8]D. del Camino, M. Holmgren, Y. Liu, G. Yellen, Blocker protection in the pore of a voltage-gated K⁺ channel and its structural implications, *Nature* 403 (2000) 321-325.
- [9]Y. Jiang, A. Lee, J. Chen, M. Cadene, B.T. Chait, R. MacKinnon, The open pore conformation of potassium channels, *Nature* 417 (2002) 523-526.
- [10]S.A. Keller, J.M. Jones, A. Boyle, L.L. Barrow, P.D. Killen, D.G. Green, N.V. Kapousta, P.F. Hitchcock, R.T. Swank, M.H. Meisler, Kidney and retinal defects (Krd), a transgene-induced mutation with a deletion of mouse chromosome 19 that includes the Pax2 locus, *Genomics* 23 (1994) 309-320.
- [11]H.H. Kerschbaum, J.A. Kozak, M.D. Cahalan, Polyvalent cations as permeant probes of MIC and TRPM7 pores, *Biophys. J.* 84 (2003) 2293-2305.

- [12]Q. Li, Y. Liu, P.Y. Shen, X.Q. Dai, S. Wang, L.B. Smillie, R. Sandford, X.Z. Chen, Troponin I binds polycystin-L and inhibits its calcium-induced channel activation, *Biochemistry* 42 (2003) 7618-7625.
- [13]Q. Li, Y. Liu, W. Zhao, X.Z. Chen, The calcium-binding EF-hand in polycystin-L is not a domain for channel activation and ensuing inactivation, *FEBS Lett.* 516 (2002) 270-278.
- [14]Y. Liu, Q. Li, M. Tan, Y.-Y. Zhang, E. Karpinski, J. Zhou, X.-Z. Chen, Modulation of the human polycystin-L channel by voltage and divalent cations, *FEBS Lett.* 525 (2002) 71-76.
- [15]A. Melishchuk and C.M. Armstrong, Mechanism underlying slow kinetics of the OFF gating current in Shaker potassium channel, *Biophys. J.* 80 (2001) 2167-2175.
- [16]H. Nomura, A.E. Turco, Y. Pei, L. Kalaydjieva, T. Schiavello, S. Weremowicz, W. Ji, C.C. Morton, M. Meisler, S.T. Reeders, J. Zhou, Identification of PKDL, a novel polycystic kidney disease 2-like gene whose murine homologue is deleted in mice with kidney and retinal defects, *J. Biol. Chem.* 273 (1998) 25967-25973.
- [17]M.E. O'Leary and R. Horn, Internal block of human heart sodium channels by symmetrical tetra-alkylammoniums, *J. Gen. Physiol* 104 (1994) 507-522.
- [18]M.E. O'Leary, R.G. Kallen, R. Horn, Evidence for a direct interaction between internal tetra-alkylammonium cations and the inactivation gate of cardiac sodium channels, *J. Gen. Physiol* 104 (1994) 523-539.
- [19]R. Pirisino, C. Ghelardini, A. Pacini, N. Galeotti, L. Raimondi, Methylamine, but not ammonia, is hypophagic in mouse by interaction with brain Kv1.6 channel subtype, *Br. J. Pharmacol.* 142 (2004) 381-389.
- [20]D.Y. Sanchez and A.L. Blatz, Block of neuronal chloride channels by tetraethylammonium ion derivatives, *J. Gen. Physiol* 106 (1995) 1031-1046.
- [21]D.Y. Sanchez and A.L. Blatz, Block of neuronal chloride channels by tetraethylammonium ion derivatives, *J. Gen. Physiol* 106 (1995) 1031-1046.
- [22]A.I. Sobolevsky, S.G. Koshelev, B.I. Khodorov, Probing of NMDA channels with fast blockers, *J. Neurosci.* 19 (1999) 10611-10626.
- [23]A. Tinker, A.R. Lindsay, A.J. Williams, Large tetraalkyl ammonium cations produce a reduced conductance state in the sheep cardiac sarcoplasmic reticulum Ca(2+)-release channel, *Biophys. J.* 61 (1992) 1122-1132.

- [24]A. Tinker and A.J. Williams, Probing the structure of the conduction pathway of the sheep cardiac sarcoplasmic reticulum calcium-release channel with permeant and impermeant organic cations, *J. Gen. Physiol* 102 (1993) 1107-1129.
- [25]R.W. Tsien, P. Hess, E.W. McCleskey, R.L. Rosenberg, Calcium channels: mechanisms of selectivity, permeation, and block, *Annu. Rev. Biophys. Biophys. Chem.* 16:265-90. (1987) 265-290.
- [26]M.A. van Dijk, P.C. Chang, D.J. Peters, M.H. Breuning, Intracranial aneurysms in polycystic kidney disease linked to chromosome 4, *J. Am. Soc. Nephrol.* 6 (1995) 1670-1673.
- [27]T. Voets, A. Janssens, G. Droogmans, B. Nilius, Outer pore architecture of a Ca²⁺-selective TRP channel, *J. Biol. Chem.* 279 (2004) 15223-15230.
- [28]G. Yellen, M.E. Jurman, T. Abramson, R. MacKinnon, Mutations affecting internal TEA blockade identify the probable pore-forming region of a K⁺ channel, *Science* 251 (1991) 939-942.

CHAPTER 5

INHIBITION OF TRPP3 BY AMILORIDE AND ANALOGS

This chapter was submitted to *Molecular Pharmacology*:

Xiao-Qing Dai, Alkarim Ramji, Yan Liu, Qiang Li, Edward Karpinski, and Xing-Zhen Chen*.

*Corresponding author: Xing-Zhen Chen

5.1. INTRODUCTION

TRPP3 (also called PKD2L1 or polycystin-L), initially cloned from human retina EST (Nomura *et al.*, 1998; Wu *et al.*, 1998), is a novel member of the transient receptor potential (TRP) superfamily of cation channels. TRPP3 has two homologs, TRPP2 (PKD2 or polycystin-2) and TRPP5 (PKD2L2 or polycystin-2L2), which share amino acid sequence similarity of ~70%. TRPP2 is part of a flow sensor and its mutations account for ~10% of autosomal dominant polycystic kidney disease (ADPKD), while the function and physiological roles of TRPP5 remain unknown. TRPP3 is localized to a subset of taste receptor cells in the tongue where it may play a crucial role in sour tasting (Huang *et al.*, 2006; Ishimaru *et al.*, 2006; LopezJimenez *et al.*, 2006), and to neurons surrounding the central canal of the spinal cord where it may account for the long-sought proton-dependent regulation of the frequency of action potential (Huang *et al.*, 2006). TRPP3 is present in neuronal or non-neuronal (eg epithelial) cells of other tissues, such as kidney, heart, retina, testis, liver, pancreas, and spleen (Basora *et al.*, 2002). In fact, TRPP3 is found in the ganglion cells of retina and collecting duct epithelial cells of kidney. We recently also revealed that TRPP3 is present in photoreceptor cells of mouse retina (unpublished data). However, the function of TRPP3 in retina has not been reported. It is thus interesting to determine whether there exists a common mechanism underlying its physiological roles in various tissues.

TRPP3 is a Ca-activated non-selective cation channel permeable to Ca, K, Na, Rb, NH₄, and Ba, inhibited by Mg, H, La and Gd (Chen *et al.*, 1999; Liu *et al.*, 2002). Based on its permeability to monovalent organic cations (methlyamine, dimethylamine and triethylamine and tetra-methylammonium) and inhibition by larger compounds tetra-ethylammonium, tetra-propylammonium, tetra-butylammonium and tetra-pentylammonium, a pore size of ~7 Å was estimated (Dai *et al.*, 2006). TRPP3 is not a voltage-gated channel but its channel properties show significant voltage-dependence (Chen *et al.*, 1999; Liu *et al.*, 2002). Interestingly, co-expression of TRPP3 with PKD1, a large receptor-like membrane protein mutated in 80-85% of ADPKD, in human embryonic kidney (HEK) 293 cells resulted in TRPP3 trafficking to the plasma membrane, where TRPP3 seemed to mediate Ca entry in the presence of a hypo-osmotic extracellular solution (Murakami *et al.*, 2005). Co-expression of mouse TRPP3 and

PKD1L3, an isoform of PKD1 with unknown function, but not the expression of TRPP3 or PKD1L3 alone, also target to the plasma membrane of HEK 293 cells and mediate pH-activated cation conductance (Ishimaru *et al.*, 2006). Whether the presence of PKD1L3, cell type and/or species difference account for the observed opposite pH dependence of TRPP3 function remain to be elucidated (Chen *et al.*, 1999; Ishimaru *et al.*, 2006). On the other hand, TRPP2 is a Ca-permeable non-selective cation channel involved in ER Ca homeostasis (Gonzalez-Perret *et al.*, 2001; Koulen *et al.*, 2002), and together with PKD1, forms a channel complex which acts as part of flow sensor in renal epithelial primary cilia (Nauli *et al.*, 2003). Thus, like other TRP members, TRPP2 and TRPP3 are likely to be part of cellular sensors (Clapham, 2003).

Amiloride (or *N*-amidino-3,5-diamino-6-chloropyrazinecarboxamide) and its analogs, such as 5-(*N*-ethyl-*N*-isopropyl) amiloride (EIPA), benzamil and phenamil (Fig. 1A), have been extensively used as probes for a wide variety of transport systems (Kleyman and Cragoe, Jr., 1988). Amiloride is a well known antagonist of ENaC, Na/Ca and Na/H exchangers, non-selective cation channels, and voltage-gated K and Ca channels (Doi and Marunaka, 1995; Hirsh, 2002; Kleyman and Cragoe, Jr., 1988; Kleyman and Cragoe, Jr., 1990; Murata *et al.*, 1995; Sariban-Sohraby and Benos, 1986; Stoner and Viggiano, 2000; Tytgat *et al.*, 1990). Interestingly, amiloride has been reported to inhibit all types of taste responses (sweet, bitter, umami, salty and sour) (Gilbertson *et al.*, 1993; Lilley *et al.*, 2004). In this study we examined the inhibitory effects of amiloride analogs on TRPP3, using *Xenopus* oocyte expression in combination with whole-cell and single-channel electrophysiology, as well as radiotracer uptake measurements.

5.2. MATERIALS AND METHODS

Oocyte preparation

Capped synthetic human TRPP3 mRNA was synthesized by *in vitro* transcription from a linearized template, using the mMMESSAGE mMACHINE1 Kit (Ambion, Austin, TX, USA). Stage V-VI oocytes were extracted from *Xenopus laevis* and defolliculated by collagenase type I (2.5 mg/ml) (Sigma-Aldrich Canada, Oakville, ON, Canada) in the Barth's solution (in mM, 88 NaCl, 1 KCl, 0.33 Ca(NO₃)₂, 0.41 CaCl₂, 0.82 MgSO₄, 2.4 NaHCO₃, 10 HEPES, and pH 7.5) at room temperature for about 2 hr. Each oocyte was injected with 50 nl of RNase-free water containing 25 ng of TRPP3 mRNA 5-20 hr following defolliculation. An equal volume of RNase-free water was injected into each control oocyte. Injected oocytes were incubated at 18°C in the Barth's solution supplemented with antibiotics, penicillin-streptomycin (Gibco, invitrogen Corporation, Grans island, NY) for 2-4 days prior to experiments.

⁴⁵Ca uptake measurement

Radiotracer uptake experiments were performed as previously described (Chen *et al.*, 1999). Briefly, the uptake solution was composed of the NaCl-containing solution (in mM: 100 NaCl, 2 KCl, 1 MgCl₂, 10 HEPES, pH 7.5) plus 1 mM non-radiolabelled CaCl₂ and 1:1000 radiolabelled ⁴⁵Ca with specific activity of 2 μCi/μl (Amersham Pharmacia Biotech, Montreal, QC, Canada). 10 oocytes were incubated in 0.5 ml of the uptake solution, for 30 min with gentle shaking from time to time. Uptake was terminated by washing oocytes in the ice-cold NaCl-containing solution. Amiloride, EIPA, benzamil and phenamil were purchased from Sigma-Aldrich Canada.

Two-microelectrode voltage clamp

Two-microelectrode voltage clamp was performed as described previously (Liu *et al.*, 2002; Li *et al.*, 2003). Briefly, the two electrodes (Capillary pipettes, Warner Instruments, Hamden, CT, USA) impaling *Xenopus* oocytes were filled with 3 M KCl to form a tip resistance of 0.3 ~ 3 MΩ. Oocyte voltages and whole-cell currents were recorded using an amplifier (Geneclamp 500B, Axon Instruments, Union City, CA, USA) and pClamp 9 software (Axon Instruments), and stored in a PC computer after AD/DA

conversion (Digidata1320A, Axon Instruments). Currents and voltages were sampled at intervals of 200 μ s and filtered at 2 kHz using an 8 pole Bessel filter. In experiments using a gap-free or ramp protocol, current/voltage signals were sampled at intervals of 0.2 or 200 ms, respectively. “Gap-free” protocol means continuous acquisition a holding potential. Using a ramp protocol, the membrane was depolarized via a positively orientated ramp from -130 mV to $+60$ mV at a rate of 1 mV/ms to determine the macroscopic current-voltage relationships. The standard NaCl-containing solution contained (in mM): 100 NaCl, 2 KCl, 0.2 MgCl₂, 10 HEPES, pH 7.5.

Patch clamp

The vitelline layer of oocytes was manually removed following incubation at room temperature in a hypertonic solution (Barth’s solution plus 200 mM sucrose). Oocytes were then transferred to a recording chamber with Barth’s solution and allowed to recover for 10 ~ 20 min before clamping. Electrodes were filled with a pipette solution containing 123 mM K (in mM: 110 KCl, 13 KOH, 10 HEPES, and pH 7.4) to form tip resistance of 3 ~ 8 M Ω . Single-channel currents were recorded in cell-attached configuration using PC-ONE Patch Clamp amplifier (Dagan Corp., Minneapolis, MN), DigiData 1322A interface, and pClamp 9 software. Recording started after seal resistance reached at least 3 G Ω . Current and voltage signals were sampled every 200 μ s and filtered at 2 kHz.

Statistics and data analysis

Data obtained from the two-microelectrode voltage clamp and patch clamp experiments were analyzed using Clampfit 9. Single-channel conductance values were obtained from Gaussian fits to density plots (all-point histograms). The open probability times the number of channels in the patch (NP_o , designated 'open probability' hereafter) and channel mean open time (MOT) values were obtained from currents generated either by voltage pulses of 10 s per pulse or by gap-free recordings of 10 s long. For the MOT analysis, recordings with single openings were used (without filtering). Analyzed data were plotted using Sigmaplot 9 (Jandel Scientific Software, San Rafael, CA, USA) and expressed in the form of mean \pm SE (N), where SE represents the standard error of the

mean and N indicates the number of oocytes (or oocyte patches) tested. Data filtering and curve fitting were performed using Clampfit 9 and Sigmaplot 9, respectively. The diameters of amiloride and its analogs were measured with *Spartan* (Version 4, Wavefunction Inc, Irvine, California). Concentration-dependent curves were fitted with the Logistic equation: $I/I_{\max} = 1/[1 + ([B]/IC_{50})^{n_H}]$, where [B] represents the concentration of amiloride or its analog and n_H represents the Hill coefficient. Comparison between two sets of data was analyzed by *t*-test or two-way ANOVA, and a probability value (P) of less than 0.05 and 0.01 was considered significant and very significant, respectively.

5.3. RESULTS

Inhibition of TRPP3-mediated ^{45}Ca uptake by amiloride and its analogs

We first utilized radiotracer uptake assays to assess the whole-cell Ca transport activities in *Xenopus* oocytes. Oocytes injected with TRPP3 mRNA exhibited increased Ca entry, compared to the control (H_2O -injected) oocytes. In the presence of 500 μM amiloride, 100 μM EIPA, 10 μM benzamil and 10 μM phenamil, ^{45}Ca uptake decreased from 79 ± 9 to 46 ± 4 (58% remaining), 27 ± 4 (34%), 29 ± 5 (37%), and 38 ± 4 (48%) pmol/oocyte/30 min ($N = 6$, $P = 0.008$), respectively (Fig. 1B). These compounds displayed little effects on the Ca transport of control oocytes, indicating that TRPP3-mediated Ca transport was significantly inhibited by amiloride and its analogs.

Inhibition of TRPP3-mediated whole-cell currents by amiloride analogs

We next employed the two-microelectrode voltage clamp technique to examine the inhibitory effects of amiloride and its analogs. In TRPP3-expressing oocytes, large inward currents were evoked by adding 5 mM Ca to the NaCl-containing solution at the holding potential of -50 mV. Currents were activated and reached a peak in 10 ~ 20 s after Ca was added and then inactivated. The Ca-activated TRPP3 inward current was reduced in the presence of extracellular amiloride at 100 μM ($40.3 \pm 8.6\%$ inhibition, $P = 0.0001$, $N = 18$) or 500 μM ($85.9 \pm 11.3\%$ inhibition, $P = 0.0005$, $N = 20$) (see eg Fig. 2A), but not at 10 μM ($P = 0.2$, $N = 13$), indicating a rather low-affinity inhibition. This inhibition by amiloride was reversible as the inward current recovered 8 ~ 10 min after washout (see representative tracing in Fig. 2A), which is also approximately the time required for evoking a second activation of the channel following the first activation (in the absence of amiloride) (Chen *et al.*, 1999). Using a ramp voltage protocol, we showed that amiloride also exhibited its inhibitory effect at other membrane potentials, notably at negative voltages, as shown by averaged current-voltage curves obtained in the presence and absence of amiloride (Fig. 2B), suggesting a voltage-dependent inhibition or a decrease in the rectification of the TRPP3 channel by amiloride.

Because amiloride is a low-affinity inhibitor of the TRPP3 channel, we wondered whether its analogs have similar effects on TRPP3. We tested the effects of phenamil, benzamil and EIPA, which are formed by replacing one of the two amino groups in

amiloride with more hydrophobic side chains (Fig. 1A). We found that phenamil, benzamil and EIPA rapidly and reversibly blocked Ca-activated TRPP3 channel activation at -50 mV as well as at other membrane potentials (Fig. 2C-F). When currents obtained at -50 mV in the presence of various concentrations of amiloride and its analogs were averaged and fitted with the Logistic equation (see Methods), we revealed the IC_{50} values of 143 ± 8 (N = 36), 0.14 ± 0.04 (N = 25), 1.1 ± 0.3 (N = 30) and 10.4 ± 2.2 μ M (N = 28) for amiloride, phenamil, benzamil and EIPA, respectively (Fig. 2G). Thus, the inhibition potency order is phenamil > benzamil > EIPA > amiloride, with the difference in affinity of roughly one order of magnitude between two consecutive inhibitors.

Our previous data showed that large TAA compounds, known as inhibitors of non-selective cation channels, inhibit TRPP3 (Dai *et al.*, 2006). To gain insights into whether these inhibitors bind to the same site as amiloride analogs we examined inhibition of phenamil in the presence of TPcA. We found that the IC_{50} value for phenamil is 3.50 ± 0.01 μ M in the presence of 0.5 μ M TPcA (the IC_{50} value for TPcA was 1.3 μ M), which is 24 fold higher than the value in the absence of TPcA (Fig. 2H). These data suggest that the two classes of inhibitor compete for the same binding site in TRPP3.

In the absence of Ca, the basal Na current was also reversibly inhibited by 100 - 500 μ M amiloride, 10 - 100 μ M EIPA, 1 - 10 μ M benzamil and 0.03 - 1 μ M phenamil, with similar affinity constants (Fig. 3) compared to the inhibition of Ca-activated currents (Fig. 2G). With 500 μ M amiloride, 100 μ M EIPA, 10 μ M benzamil or 1 μ M phenamil, the basal Na currents of the TRPP3 channel were significantly and reversibly inhibited (Fig. 3A-C). The basal Na currents in H₂O-injected oocytes were not significantly inhibited by 500 μ M amiloride or 1 μ M phenamil (data not shown). The IC_{50} values were 209, 19.5, 2.43 and 0.28 μ M for amiloride, EIPA, benzamil and phenamil, respectively (Fig. 3D).

Inhibition of single-channel activities of TRPP3 channel by amiloride analogs

To examine inhibitory effects of amiloride analogs on TRPP3 single-channel activities we used the cell-attached mode of patch clamp. In the presence of 123 mM K in the pipette, TRPP3 channel openings were observed in 245 out of 296 patches in oocytes

over-expressing TRPP3. With linear regression in negative ($-V_m$: $-20 \sim -120$ mV) and positive membrane potentials ($+V_m$: $+20 \sim +120$ mV), we calculated that TRPP3 had a larger inward single-channel conductance (399 ± 12 pS at $-V_m$, $N = 30$) than outward conductance (137 ± 10 pS at $+V_m$, $N = 26$), presumably due to inward rectification and the presence of asymmetrical concentrations of permeant ions on the two sides of the membrane (Liu *et al.*, 2002). No channel openings of similar main conductance were observed in H₂O-injected control oocytes ($N = 20$).

We performed cell-attached recordings in the presence or absence of pipette amiloride from patches of the same oocyte to minimize variations due to changes in the surface expression of different oocytes. At both positive and negative voltages, amiloride ($500 \mu\text{M}$) significantly decreased TRPP3 single-channel NP_o but not the amplitude (Fig. 4). A two-way ANOVA analysis revealed that $500 \mu\text{M}$ amiloride significantly inhibited NP_o ($P < 0.0001$) and that NP_o was voltage-dependent ($P < 0.0001$), with higher NP_o values at $-V_m$ (Fig. 4B). The MOT values were also altered by extracellular amiloride ($P = 0.002$) and were voltage-dependent ($P < 0.0001$), with higher MOT values at $-V_m$ (Fig. 4C). The voltage dependence of MOT was decreased by amiloride as well ($P = 0.01$). Of note, no effect on NP_o and MOT was observed when $10 \mu\text{M}$ amiloride was added to the pipette solution, indicative of low-affinity inhibition by amiloride. Similarly, we found that EIPA, benzamil and phenamil, exhibit inhibitory effects on NP_o and MOT, but not on the single-channel amplitude (Fig. 5-7). The inhibition by EIPA was concentration-dependent and the IC_{50} values for EIPA inhibition on NP_o were 13.7 ± 1.5 and $18.1 \pm 0.8 \mu\text{M}$ at -120 and $+120$ mV, respectively ($P < 0.01$, $N = 20$) (Fig. 5B). The IC_{50} values on MOT were 25 ± 4 and $28 \pm 5 \mu\text{M}$, respectively ($P < 0.01$, $N = 20$) (Fig. 5C). Those for benzamil on NP_o were 0.6 ± 0.01 and $1.1 \pm 0.3 \mu\text{M}$ at -120 and $+120$ mV ($P < 0.01$, $N = 11$), respectively, while those on MOT were 0.8 ± 0.03 and $1.2 \pm 0.3 \mu\text{M}$, respectively ($P < 0.01$, $N = 13$) (Fig. 6B-C). Phenamil exhibited similar inhibition characteristics than its analogs but with higher potency. The IC_{50} values for phenamil on NP_o were 0.24 ± 0.04 and $0.39 \pm 0.07 \mu\text{M}$ at -120 and $+120$ mV ($P < 0.05$, $N = 26$), respectively, while those on MOT were 0.45 ± 0.01 and $0.52 \pm 0.08 \mu\text{M}$, respectively ($P < 0.01$, $N = 19$) (Fig. 7 C-D). These amiloride analogs all inhibited TRPP3 channel activities more significantly at $-V_m$ than at $+V_m$ (Fig. 4-7). The inhibition effects on NP_o , MOT and mean current by $500 \mu\text{M}$

amiloride, 100 μ M EIPA, 1 μ M benzamil and 1 μ M phenamil at -120 mV and +120 mV were compared (Fig. 8A-C). Of note, we also examined the effects of intracellular amiloride analogs pre-injected 3 hr prior to experiments. No significant effect was observed (data not shown), suggesting that they do not exhibit similar inhibition from the intracellular side of the membrane.

5.4. DISCUSSION

As a well-known blocker of ENaC, Na/Ca and Na/H exchangers, non-selective cation channels and voltage-gated K and Ca channels, amiloride also inhibits the responses to all taste stimuli (Gilbertson *et al.*, 1993; Lilley *et al.*, 2004), currents induced by the expression of PKD1 C-terminal fragments in *Xenopus* oocytes (Vandorpe *et al.*, 2001), and those mediated by TRPP2 channels reconstituted in lipid bilayer or over-expressed in sympathetic neurons (Gonzalez-Perret *et al.*, 2001; Delmas *et al.*, 2004). Interestingly, recent reports showed that TRPP3 plays an important role in sour tasting and acid sensing (Huang *et al.*, 2006; Ishimaru *et al.*, 2006). TRPP3 is concentrated in the apical membrane (facing taste pores) of bipolar cells in taste buds, suggesting that it allows an initial cation influx triggered by low pH at the taste pore, which activates surrounding voltage-gated cation channels via local membrane depolarization and then leads to the firing of an action potential. In the whole length of the spinal cord, TRPP3 is present in neurons that project into the central canal, suggesting that it may also trigger an initial cation entry following a decrease in the canal pH (Huang *et al.*, 2006). However, it remains unclear as to why TRPP3 responds to two very different pH ranges in the tongue and spinal cord. It is possible that PKD1L3 plays a role in acid sensing.

In the present study we investigated the modulation of the TRPP3 channel function by amiloride and its analogs (phenamil, benzamil and EIPA), using whole-cell and single-channel electrophysiology and radiotracer uptake measurements. These compounds inhibited both the Ca-activated and basal, TRPP3-mediated cation transports in *Xenopus* oocytes. In radiotracer uptake experiments, oocytes are not voltage clamped (to negative membrane potentials, eg -50 mV), any significant Ca entry will immediately lead to membrane depolarization, which slows down further Ca entry. Thus, Ca entry should not be sufficient in these experiments to induce TRPP3 channel activation and should reflect the basal TRPP3 channel activity. In cell-attached experiments, because Ca was absent in the pipette solution, single-channel activities correspond also to the basal TRPP3 function. In fact, so far we have not been able to conclude as to whether Ca (5 mM) in the cell-attached pipette can induce activation of TRPP3 channels present in the patch. An important difference to the whole-cell voltage clamp may be that the Ca entry through the tiny membrane patch under the pipette does not cause sufficient increase in

the local intracellular Ca concentration in the proximity of the patch to activate these few TRPP3 channels, due to fast diffusion of Ca ions.

Amiloride analogs are 2-3 fold more effective, as judged by IC_{50} values, in blocking the Ca-activated current than the basal current. This might be due to the possibility that amiloride analogs are more potent inhibitors for the current carried by Ca ions which are about 5 times more permeant to TRPP3 than Na (Chen *et al.*, 1999). Another possibility is that the proportion of current already inhibited by 1 mM Mg in the solution differs between the basal and activation conditions. These inhibitors reduce the NP_o and MOT, but not the single-channel conductance, suggesting that they alter channel gating by binding to a site(s) on the channel protein outside the pore pathway, instead of competing with permeant ions such as Ca and Na. TRPP3 channel activity is inhibited by extracellular amiloride analogs in a voltage-dependent manner (Fig. 4-7). The observation of decreased voltage dependence of TRPP3 channel activities by these inhibitors may indicate that mobile charged amino acid residues important for channel gating may bind these inhibitors, resulting in a reduced mobility.

Interestingly, the hydrophobicity of the side chain, the molecular diameter, and the inhibition potency of these analogs follow the same order, phenamil>benzamil>EIPA>amiloride (Fig. 8D), which is different from one for ENaC (phenamil>benzamil>amiloride>EIPA) and Na/H exchanger (phenamil>EIPA>amiloride, benzamil) (Kleyman and Cragoe, Jr., 1988), suggesting that these membrane proteins have different binding kinetics or structures for the inhibitors. It is possible that the binding cassette in TRPP3 has a hydrophobic environment that promotes binding of ligands of higher hydrophobicity or that the size of the binding cassette is closer to that of phenamil than the other inhibitors. We previously estimated that TRPP3 channel possesses a pore diameter of ~ 7 Å and a binding cassette of at least 13 Å for organic cation inhibitors (Dai *et al.*, 2006). In that study we revealed that the largest inhibitor TPeA, with a size of ~ 13 Å, is most potent among the other organic cation inhibitors tested. We also found that these inhibitors, except TBA, reduced NP_o and MOT, but not the single-channel conductance. This raises the possibility that amiloride analogs and organic cation inhibitors may share the same binding site. This is supported by our

finding that the IC₅₀ value for phenamil was increased by 24 fold in the presence of 0.5 μM TPeA.

Renal Na reabsorption is crucial for Na and body fluid homeostasis. Amiloride-sensitive Na reabsorption constitutes a major ion transport pathway in the principal cells of cystic and non-cystic collecting tubules (Hirsh, 2002). It was reported that non-selective channels with unclear molecular identities may contribute to Na reabsorption in distal tubules and collecting ducts, and in cultured A6 kidney cells (Doi and Marunaka, 1995; Stoner and Viggiano, 2000). Interestingly, TRPP3 is present in the apical region of renal principal cells (Basora *et al.*, 2002) and part of Na reabsorption in collecting ducts was reported to be mediated by amiloride-sensitive non-selective cation channels (Vandorpe *et al.*, 1997), suggesting that TRPP3 may contribute to renal Na reabsorption. Of note, although TRPP3 channels over-expressed in *Xenopus* oocytes exhibit high unitary conductance and low sensitivity to amiloride inhibition, these parameters for *in vivo* TRPP3 channels in kidney and other organs might be substantially different because of possible presence of tissue-specific modulatory protein subunits. Thus understanding effects of amiloride on the TRPP3 channel may help to determine its physiological roles in kidney and other tissues.

The mouse orthologue of TRPP3 is deleted in *krd* (kidney and retinal defects) mice, resulting in defects in kidney and retina (Keller *et al.*, 1994; Nomura *et al.*, 1998). TRPP3 may be one of the candidates linked to unmapped human genetic cystic disorders such as dominantly transmitted glomerulocystic kidney disease of post-infantile onset, isolated polycystic liver disease, and Hajdu-Cheney syndrome/serpentine fibula syndrome (Nomura *et al.*, 1998). Although no evidence showed the TRPP3's direct involvement in ADPKD or ARPKD, a role for TRPP3 in cystogenesis is not excluded, as an interaction between TRPP3 and PKD1 exists (Murakami *et al.*, 2005). Co-expression of TRPP3 together with PKD1 resulted in the expression of TRPP3 channels on the cell surface, whereas TRPP3 expressed alone was retained with the ER (Murakami *et al.*, 2005). Monolayers formed by ARPKD principal cells of human fetal renal collecting ducts exhibit remarkably higher transepithelial Na reabsorption than control monolayers (Rohatgi *et al.*, 2003; Olteanu *et al.*, 2006). Interestingly, this increased Na movement is partially inhibited by amiloride with relatively low affinity. In contrast, the amiloride-

sensitive Na reabsorption is decreased in principal cells isolated from *bpk* ARPKD mice (Veizis *et al.*, 2003). Because the protein mutated in these ARPKD cells does not resemble an ion channel or transporter, we speculate that it may regulate the surface membrane expression and/or function of to-be-identified channels or transporters that are permeable to Na with low sensitivity to amiloride. The regulation could be through physical binding or indirectly through a cascade pathway that links a PKD protein to an ion channel or transporter. Interestingly, cyst growth can be interfered in animal and *in vitro* studies by a number of compounds, in particular, by the use of amiloride and its analogs (Ogborn, 1994).

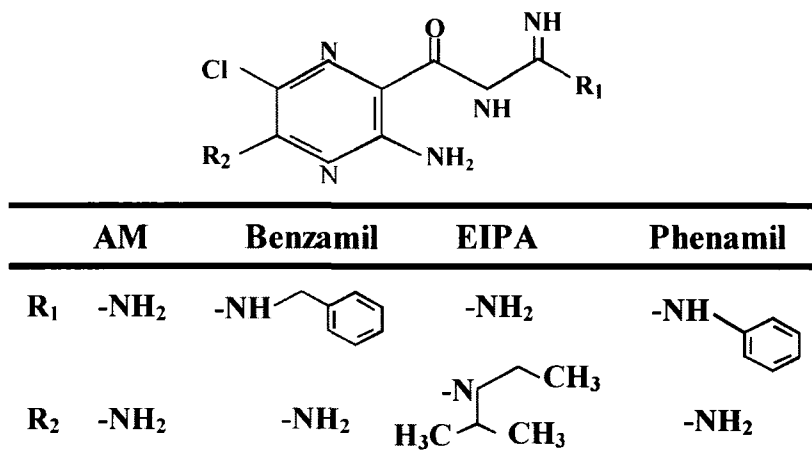
In summary, TRPP3 may account for amiloride-sensitive cation currents in some tissues and play critical physiological roles in both neuronal and non-neuronal cells, eg in brain, retina and kidney, by mediating amiloride-sensitive, pH-dependent cation fluxes.

ACKNOWLEDGEMENTS

We thank Dr. Mariusz Klobukowski for measurement of molecular diameters of amiloride and its analogs with Spartan. This work was supported by the Canadian Institutes of Health Research, the Alberta Heritage Foundation for Medical Research and the Kidney Foundation of Canada (to X.-Z.C.). X.-Z.C. is a an AHFMR Senior Scholar. X.-Q.D. is a recipient of the Alberta Heritage Foundation for Medical Research Studentship.

5.5. FIGURES

A



B

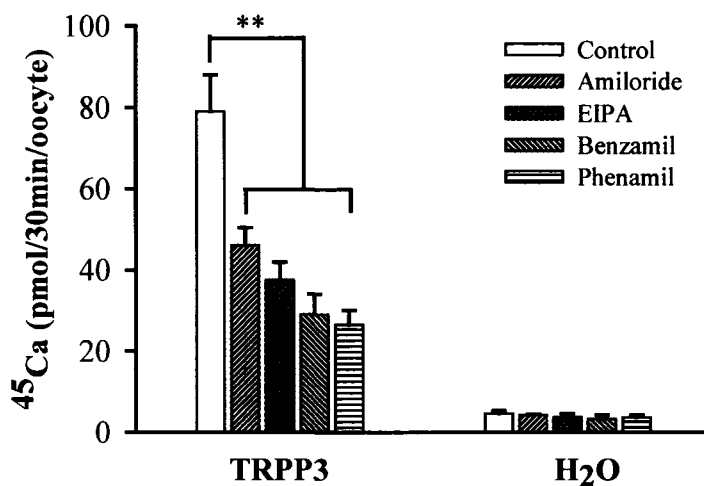
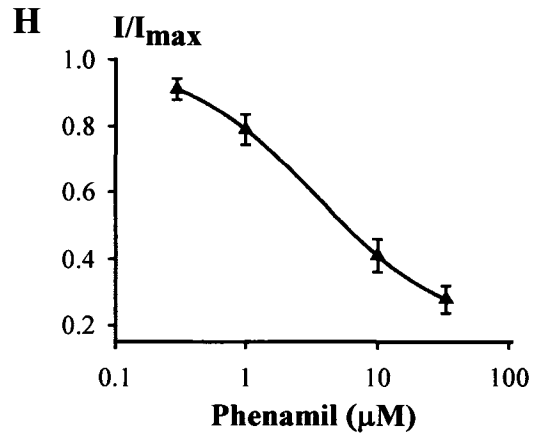
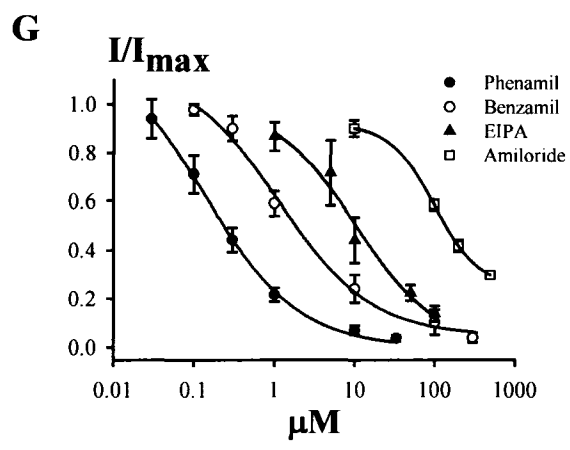
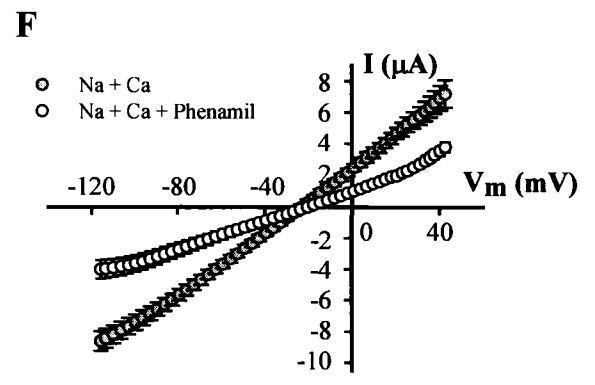
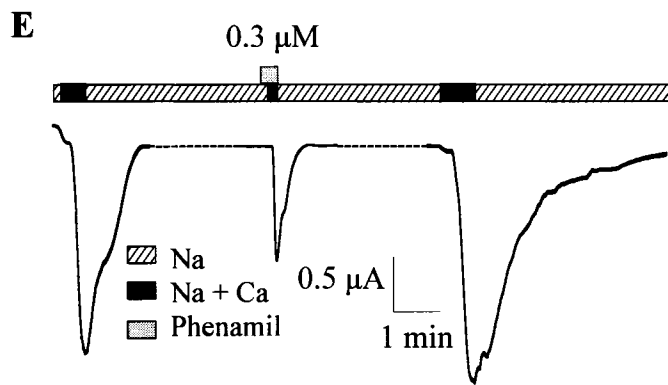
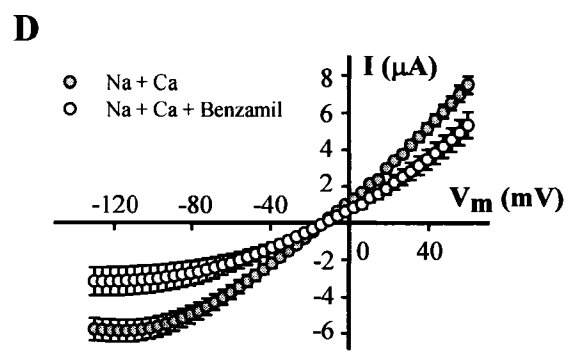
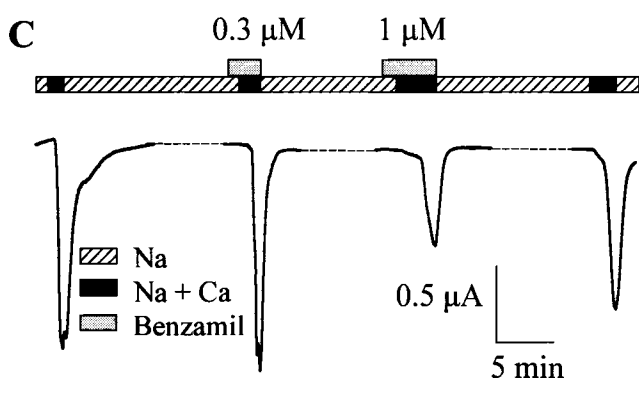
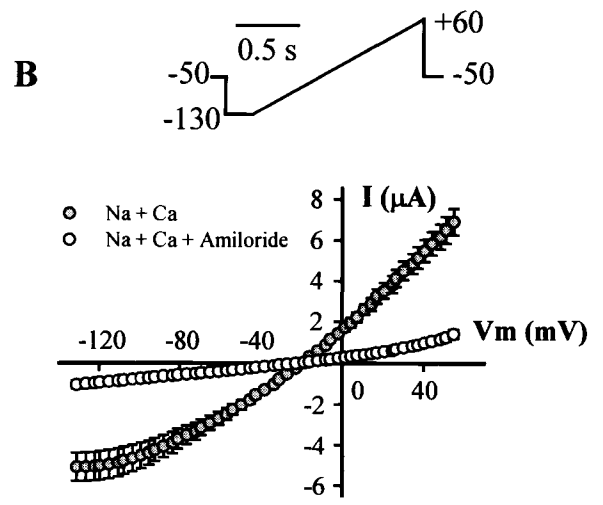
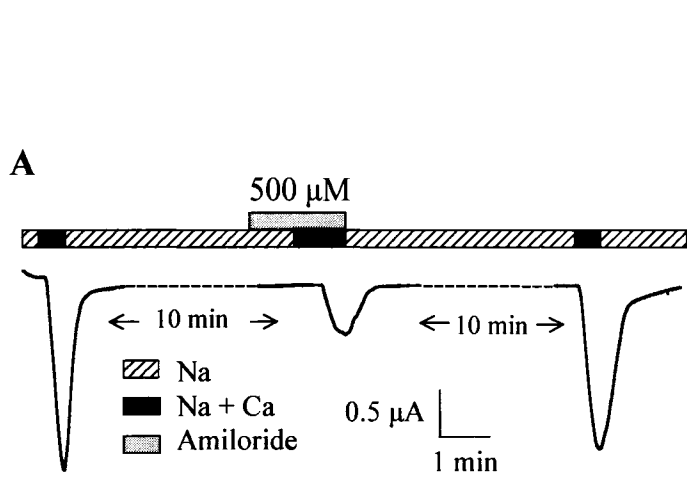


Fig. 5-1. Effects of amiloride analogs on the uptake mediated by TRPP3 expressed in *Xenopus* oocytes. A. Chemical structures of amiloride and its analogs. B. Uptake of radioactive ⁴⁵Ca mediated by TRPP3 channel using the standard NaCl-containing solution, plus 1 mM non-radiolabelled CaCl₂ and radiolabelled ⁴⁵Ca, in the presence and absence of 500 μM amiloride, 10 μM phenamil, 10 μM benzamil or 100 μM EIPA, respectively. Shown data are averages from six independent measurements. Control uptake level was obtained using H₂O-injected oocytes. '**' indicates very significant inhibition: P < 0.01.

Fig. 5-2. Effects of amiloride analogs on the Ca-activated whole-cell currents mediated by TRPP3 channel. **A.** The TRPP3-mediated whole-cell currents obtained using the two-microelectrode voltage clamp. Currents carried by Na and Ca were measured at -50 mV in the presence of the standard NaCl-containing solution ('Na') \pm Ca (5 mM) \pm amiloride (500 μ M). The duration between consecutive applications of 5 mM Ca was 10 min, for the TRPP3 channels to recover (same in **C** and **E**). 'Na + Ca' = the NaCl-containing solution + 5 mM CaCl₂. 'Amiloride' = 500 μ M amiloride. **B.** Averaged current-voltage relationships (I-V curves) in the presence or absence of 500 μ M amiloride (N = 16), obtained using a voltage ramp protocol (top). **C.** Effects of benzamil on the TRPP3-mediated whole-cell currents under voltage clamp (-50 mV). **D.** Averaged I-V curves in the presence or absence of 1 μ M benzamil (N = 15). **E.** Effects of 0.3 μ M phenamil on the whole-cell currents at -50 mV. **F.** Averaged I-V curves in the presence or absence of 0.3 μ M phenamil (N = 13). **G.** Averaged concentration-dependent curves for amiloride, EIPA, benzamil and phenamil (N = 36, 32, 30 and 28, respectively). Curves are fits with the Logistic equation (see Methods). **H.** In the presence of 0.5 μ M TPcA, concentration-dependent curve for phenamil (N = 32).



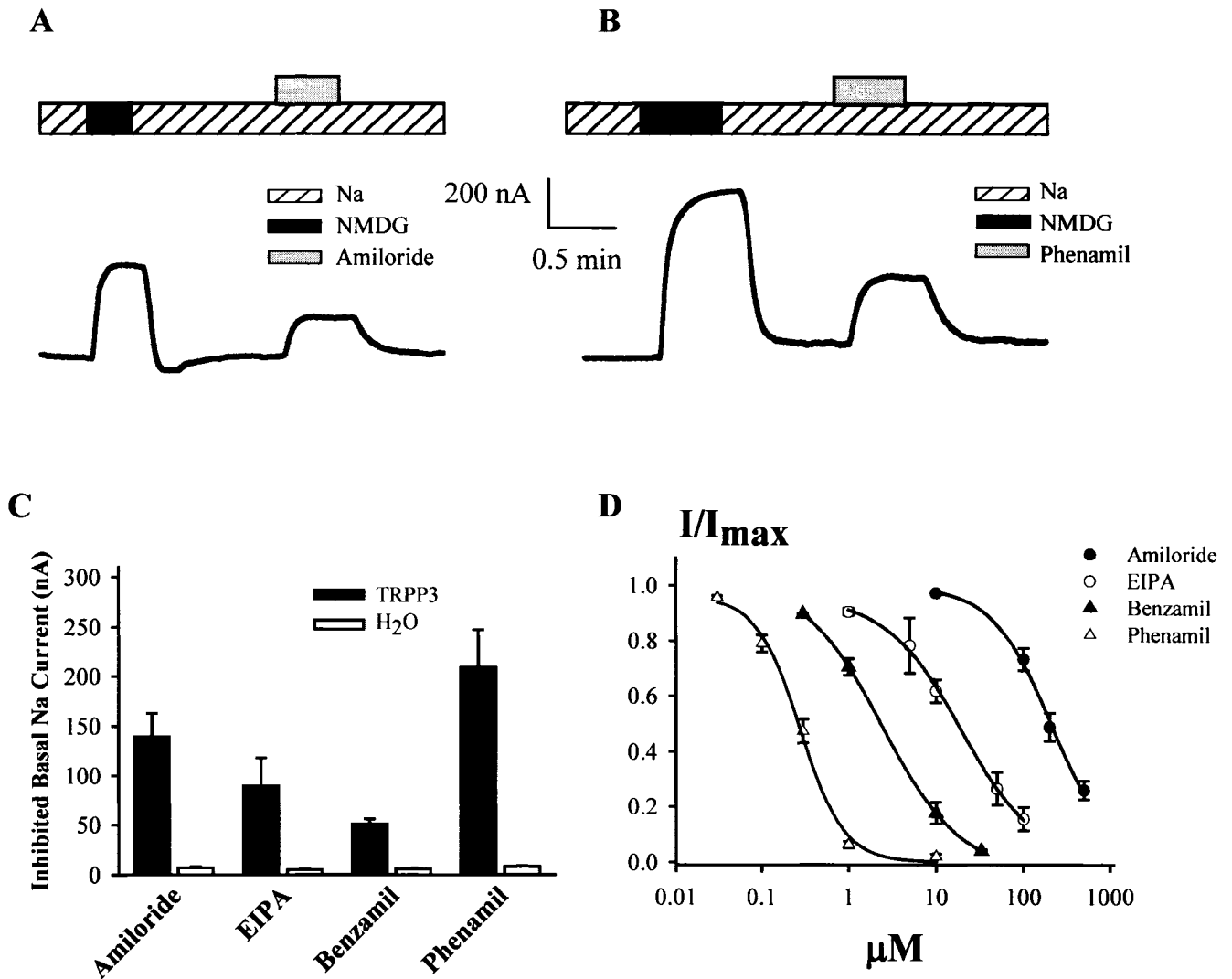
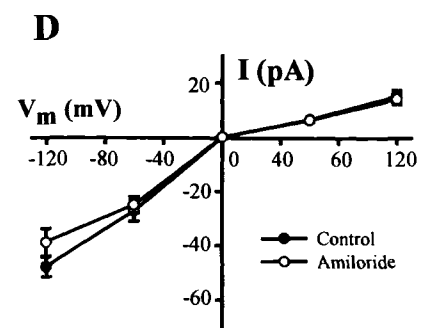
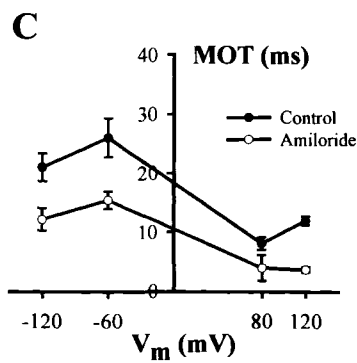
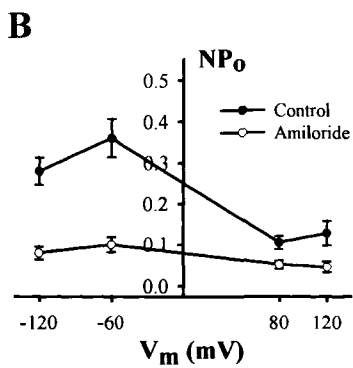
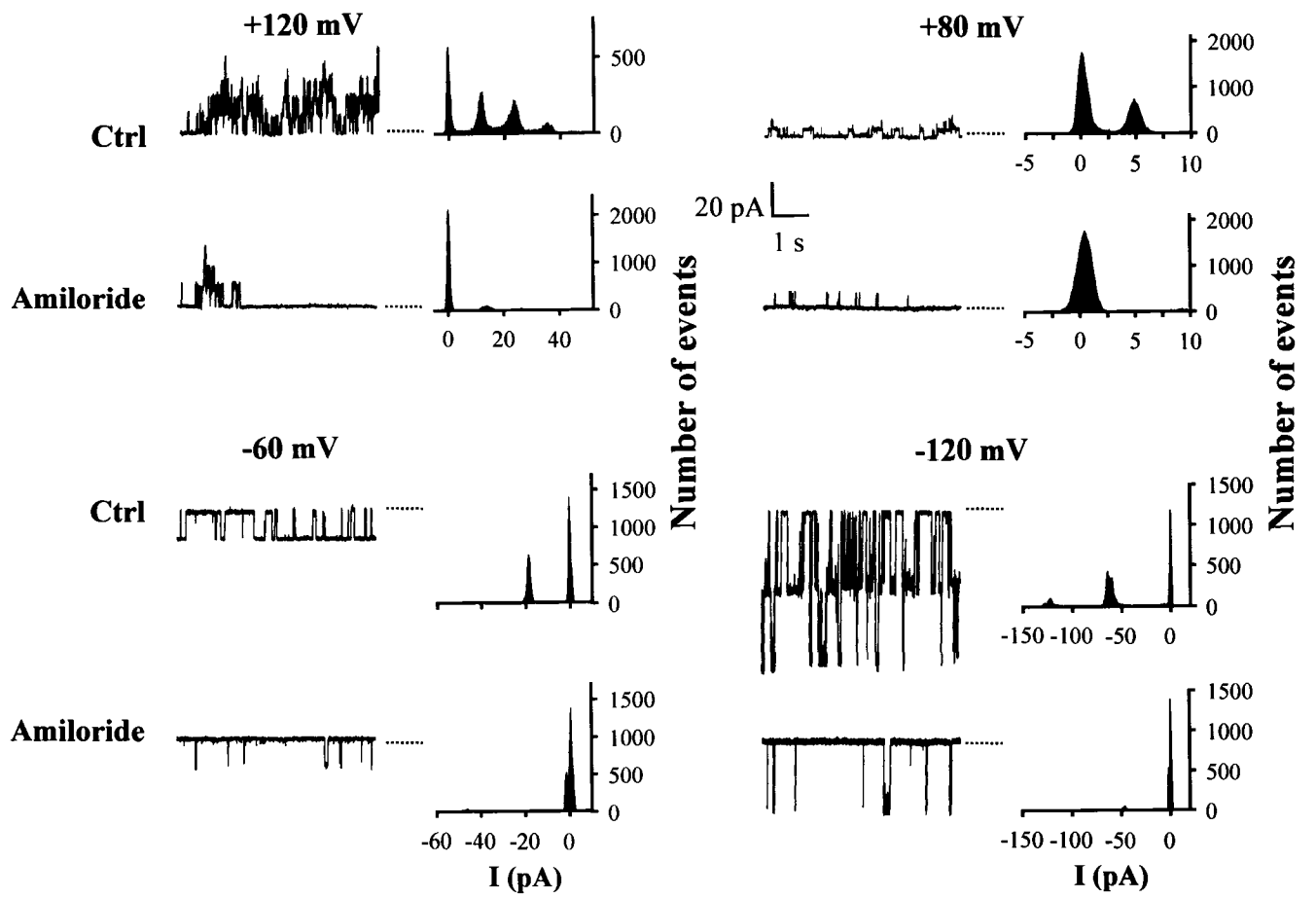


Fig. 5-3. Effects of amiloride analogs on the TRPP3-mediated basal Na currents. **A** and **B**. Representative current recording at -50 mV in an oocyte expressing TRPP3 in the presence or absence of amiloride ($500 \mu\text{M}$) (**A**) or phenamil ($1 \mu\text{M}$) (**B**). The inward current was largely abolished by replacing external Na with N-methyl-D-glucamine (NMDG), which is a large mono-cation and impermeant to TRPP3. The difference in the absence and presence of NMDG indicated the net Na currents mediated by TRPP3. **C**. Basal Na currents at -50 mV inhibited by $500 \mu\text{M}$ amiloride, $100 \mu\text{M}$ EIPA, $10 \mu\text{M}$ benzamil or $1 \mu\text{M}$ phenamil, in oocytes expressing TRPP3 or H_2O -injected oocytes. **D**. Averaged concentration dependence of normalized basal Na currents at -50 mV for various amiloride analogs. The IC_{50} values were estimated to be 155 ± 0.01 ($N = 23$), 12.2 ± 0.01 ($N = 18$), 2.43 ± 0.01 ($N = 22$) and $0.28 \pm 0.04 \mu\text{M}$ ($N = 22$) for amiloride, EIPA, benzamil and phenamil, respectively.

Fig. 5-4. Effects of amiloride on TRPP3 single-channel properties. The cell-attached mode of the patch clamp technique was used in these experiments. **A.** Representative recordings (left) and the corresponding density plots (right) at indicated voltages in the presence pipette 123 mM K (Control) \pm 500 μ M amiloride. The closed levels are indicated by horizontal dashed lines. Shown traces were Gaussian filtered at 200 Hz, using Clampfit 9. The tracings in the presence or absence of amiloride were from the same oocytes. **B.** Averaged ($N = 8$) NP_o values at various $V_m \pm$ amiloride (500 μ M). A two-way ANOVA analysis produced $P < 0.0001$ for amiloride and V_m , and $P = 0.008$ for the amiloride \times V_m interaction. **C.** Effects of amiloride on MOT. $P = 0.002$ for amiloride, $P < 0.0001$ for V_m , and $P = 0.01$ for the amiloride \times V_m interaction. **D.** Averaged single-channel amplitudes obtained in the presence or absence of amiloride (500 μ M) ($N = 15$, $P > 0.05$).



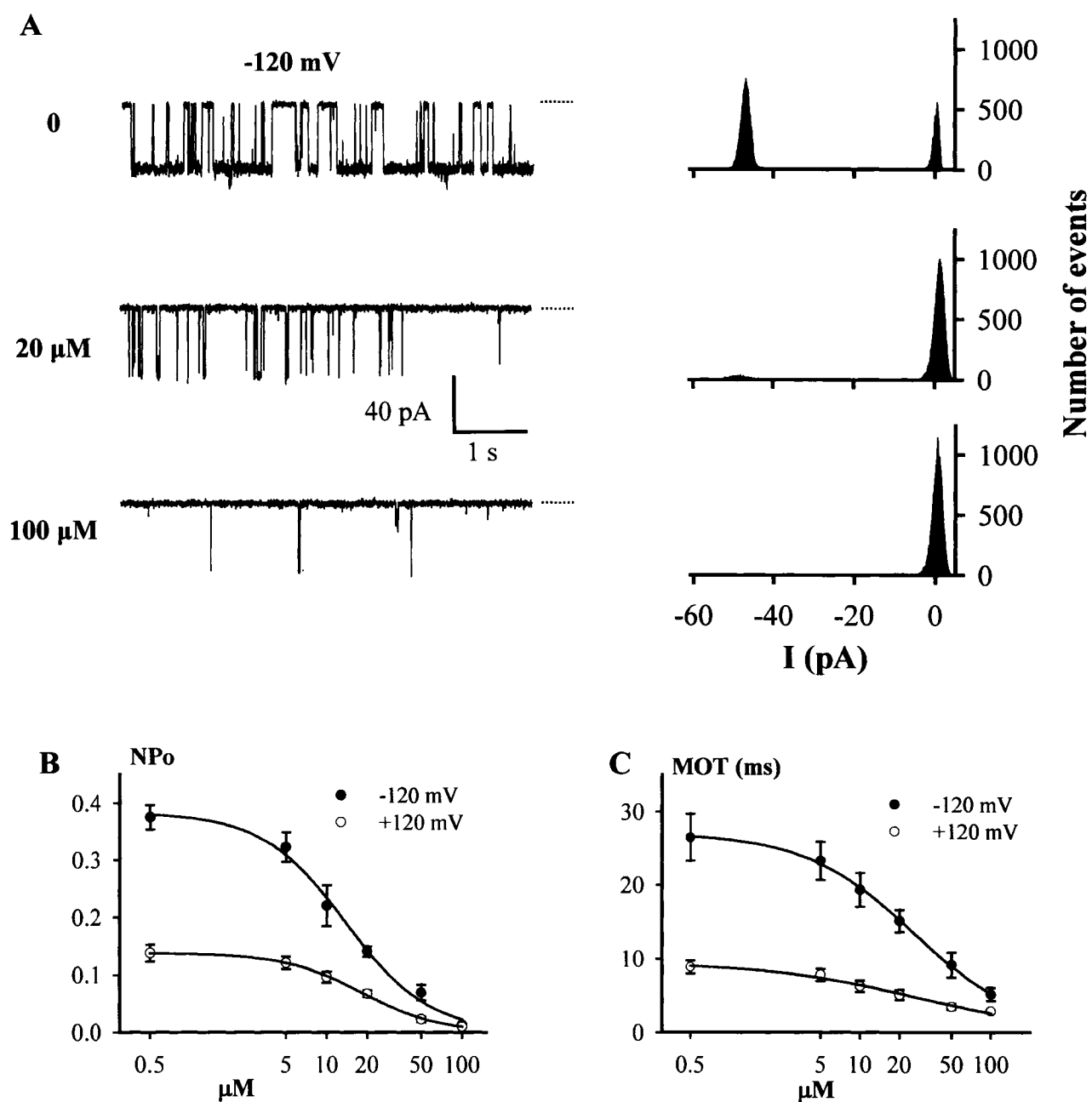


Fig. 5-5. Effects of EIPA. **A.** Representative recordings (left) at -120 mV in the presence of 123 mM K (control) in the pipette, plus 0, 0.5, 5, 10, 20, 50 or 100 μM EIPA, and the corresponding density plots (right). The tracings at different EIPA concentrations were from the same oocytes. **B.** Concentration-dependent curves for the inhibition of NP₀ by EIPA at -120 mV and +120 mV, respectively. Data were averaged from 20 determinations. The curves are fits by the Logistic equation. **C.** Concentration-dependent curves for the inhibition of MOT by EIPA (N = 20).

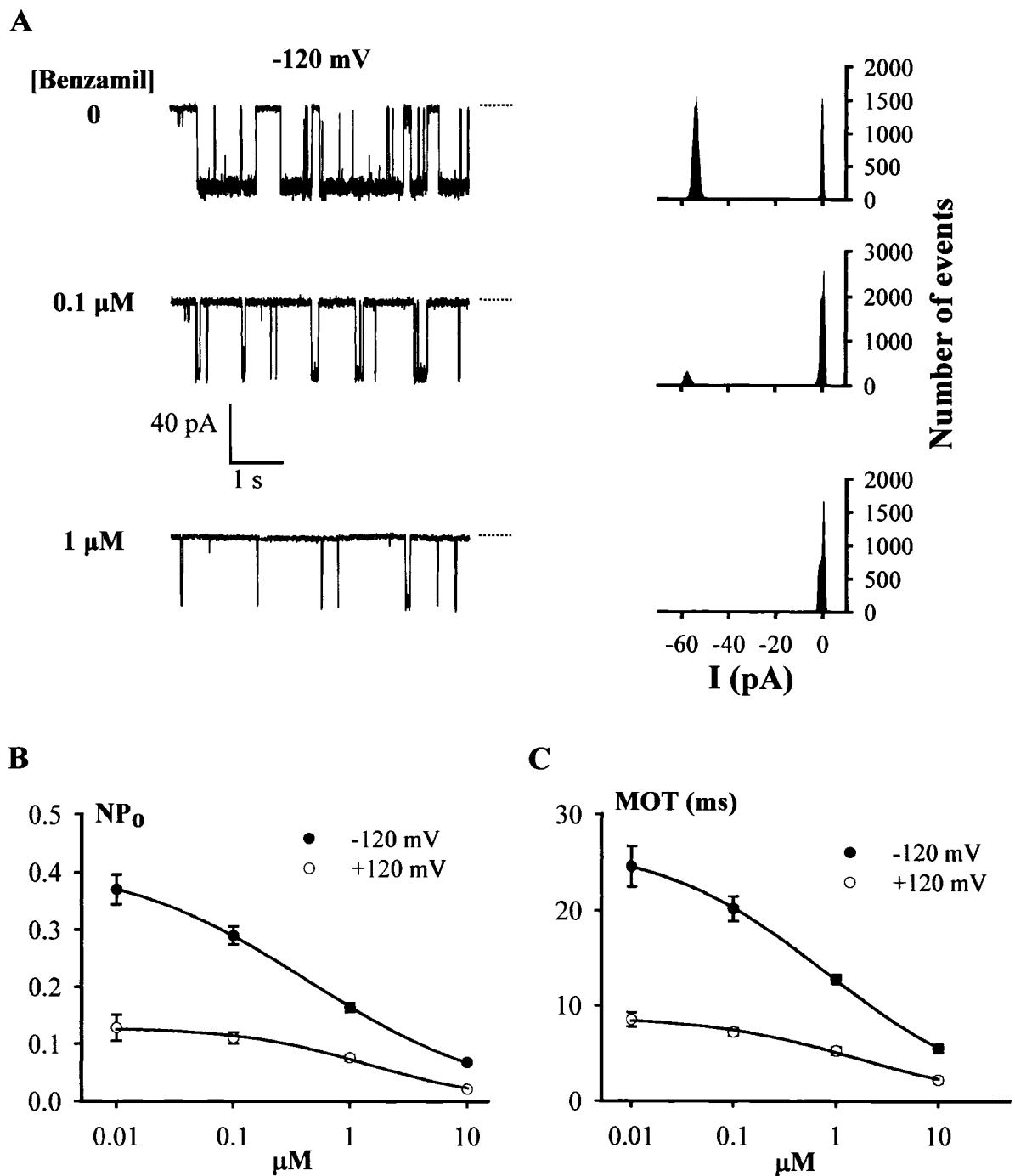


Fig. 5-6. Effects of benzamil. **A.** Representative recordings (left) at -120 mV in the presence of benzamil at various concentrations and the corresponding density plots (right), from the same oocytes. **B** and **C.** Concentration-dependent curves for the inhibition of NP₀ (N= 24) and MOT (N= 20) by benzamil at -120 and +120 mV, respectively. Each point was averaged from 13 determinations.

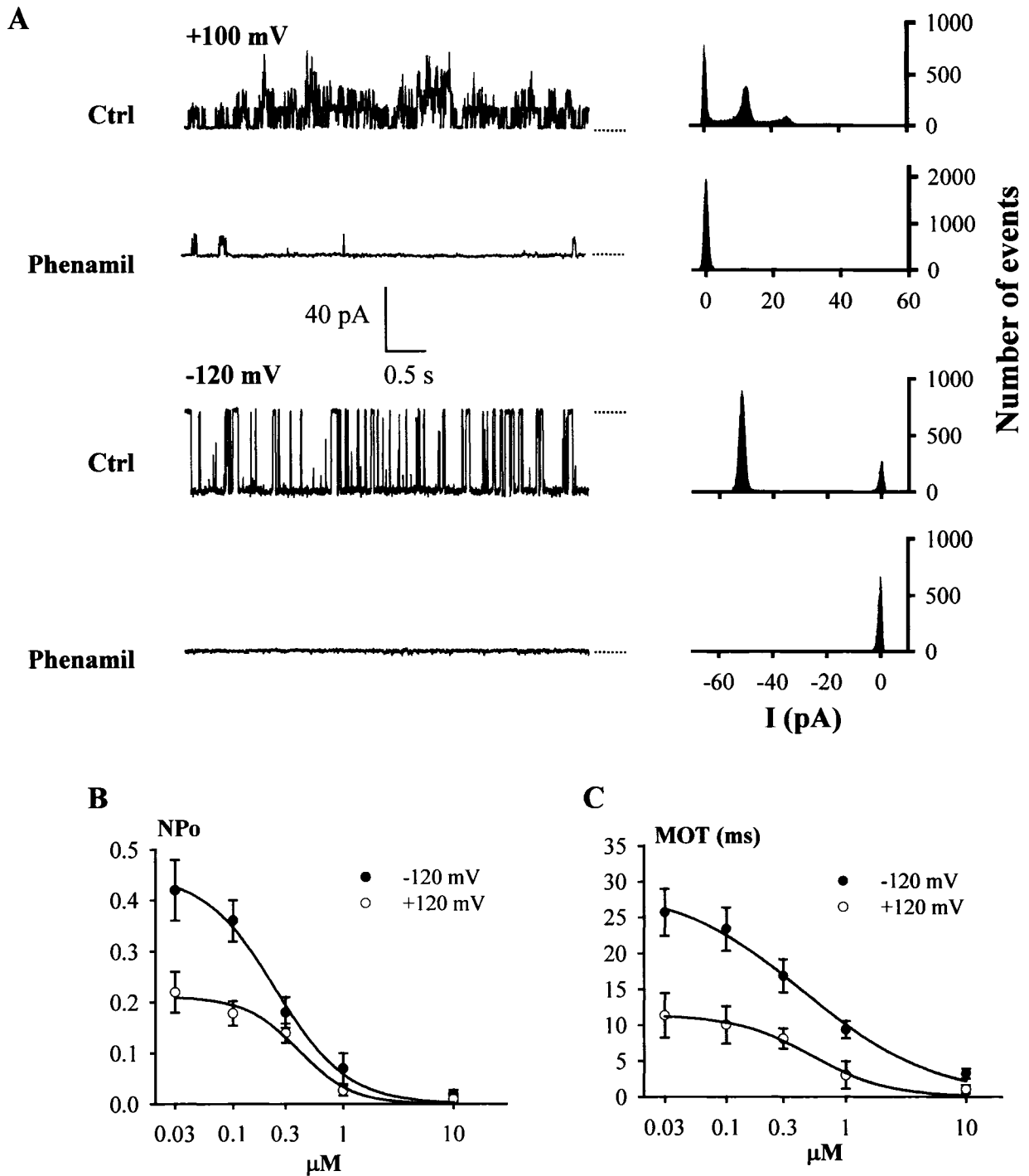


Fig. 5-7. Effects of phenamil. A. Representative recordings (left) at + 100 and -120 mV in the presence of phenamil at various concentrations and the corresponding density plots (right), from the same oocytes. B and C. Concentration-dependent curves for the inhibition of NP₀ (N = 26) and MOT (N = 19) by phenamil at -120 and +120 mV, respectively.

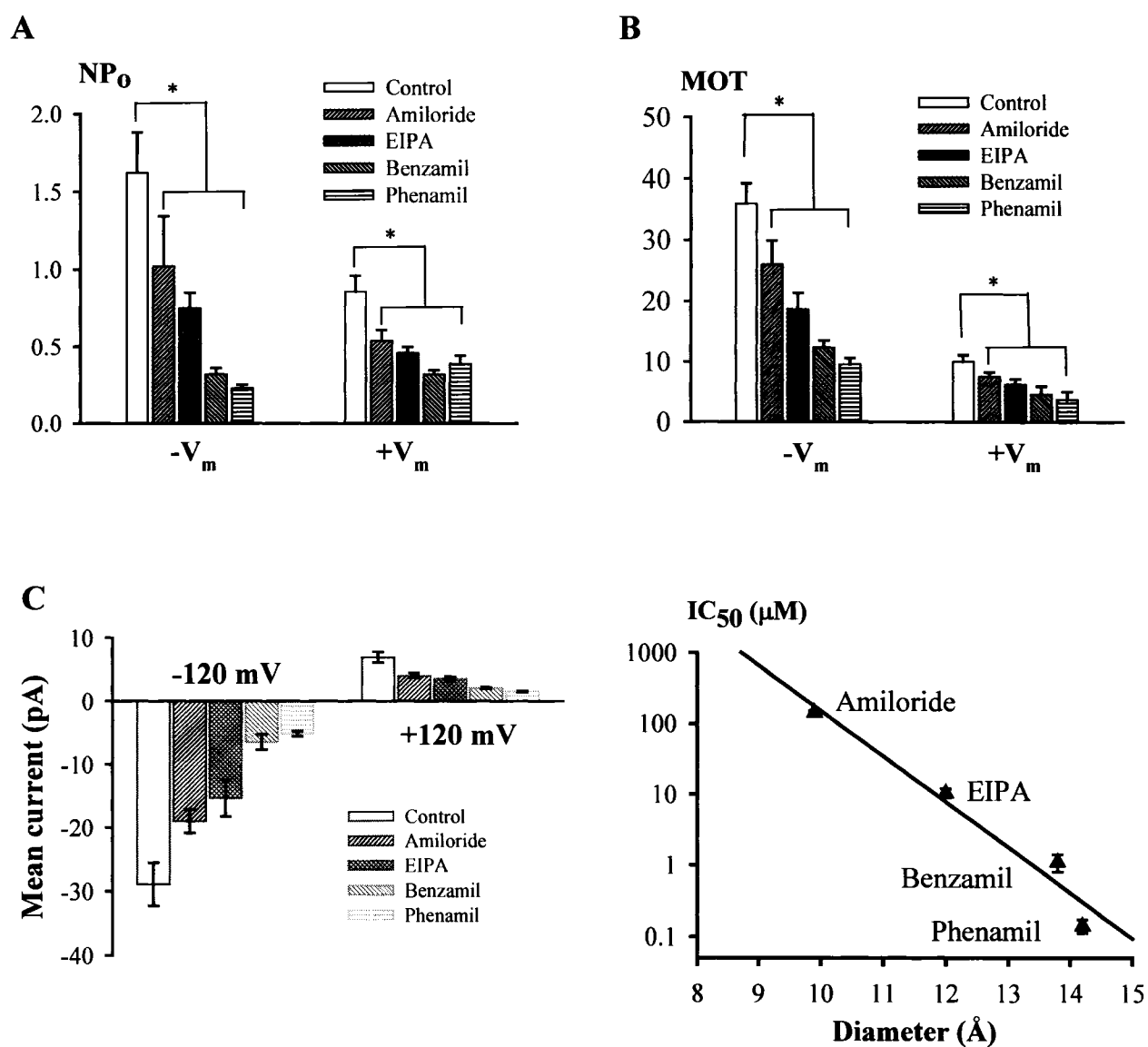


Fig. 5-8. Effects of amiloride analogs on TRPP3 single-channel parameters. 500 μM amiloride, 100 μM EIPA, 1 μM benzamil and 1 μM phenamil were used in the cell-attached experiments. **A** and **B**. Inhibition of NP_o and MOT at -V_m (N = 15-26) and +V_m (N = 11-20). **C**. Inhibition of mean currents at -120 mV (N = 15-26) and +120 mV (N = 11-20). **D**. IC₅₀ values for amiloride and its analogs as a function of their molecular sizes. Oocytes whole-cell currents activated by 5 mM Ca were used to determine the IC₅₀ values (in μM). IC₅₀ values for amiloride and its analogs correlate to their molecular diameters. The diameters of amiloride, EIPA, benzamil and phenamil are 9.9, 12, 13.8 and 14.2 Å (unfolded model), respectively. Shown are data averaged from 36, 25, 30 and 28 measurements for amiloride, EIPA, benzamil and phenamil, respectively.

5.6. REFERENCES

Basora N, Nomura H, Berger UV, Stayner C, Guo L, Shen X, & Zhou J (2002). Tissue and cellular localization of a novel polycystic kidney disease-like gene product, polycystin-L. *J Am Soc Nephrol* **13**, 293-301.

Chen XZ, Vassilev PM, Basora N, Peng JB, Nomura H, Segal Y, Brown EM, Reiders ST, Hediger MA, & Zhou J (1999). Polycystin-L is a calcium-regulated cation channel permeable to calcium ions. *Nature* **401**, 383-386.

Clapham DE (2003). TRP channels as cellular sensors. *Nature* **426**, 517-524.

Dai XQ, Karpinski E, & Chen XZ (2006). Permeation and inhibition of polycystin-L channel by monovalent organic cations. *Biochim Biophys Acta* **1758**, 197-205.

Delmas P, Nauli SM, Li X, Coste B, Osorio N, Crest M, Brown DA, & Zhou J (2004). Gating of the polycystin ion channel signaling complex in neurons and kidney cells. *FASEB J* **18**, 740-742.

Doi Y & Marunaka Y (1995). Amiloride-sensitive and HCO₃⁻-dependent ion transport activated by aldosterone and vasotocin in A6 cells. *Am J Physiol* **268**, C762-C770.

Gilbertson TA, Roper SD, & Kinnamon SC (1993). Proton currents through amiloride-sensitive Na⁺ channels in isolated hamster taste cells: enhancement by vasopressin and cAMP. *Neuron* **10**, 931-942.

Gonzalez-Perret S, Kim K, Ibarra C, Damiano AE, Zotta E, Batelli M, Harris PC, Reisin IL, Arnaout MA, & Cantiello HF (2001). Polycystin-2, the protein mutated in autosomal dominant polycystic kidney disease (ADPKD), is a Ca²⁺-permeable nonselective cation channel. *Proc Natl Acad Sci U S A* **98**, 1182-1187.

Hirsh AJ (2002). Altering airway surface liquid volume: inhalation therapy with amiloride and hyperosmotic agents. *Adv Drug Deliv Rev* **54**, 1445-1462.

Huang AL, Chen X, Hoon MA, Chandrashekar J, Guo W, Trankner D, Ryba NJ, & Zuker CS (2006). The cells and logic for mammalian sour taste detection. *Nature* **442**, 934-938.

Ishimaru Y, Inada H, Kubota M, Zhuang H, Tominaga M, & Matsunami H (2006). Transient receptor potential family members PKD1L3 and PKD2L1 form a candidate sour taste receptor. *Proc Natl Acad Sci U S A* **103**, 12569-12574.

Keller SA, Jones JM, Boyle A, Barrow LL, Killen PD, Green DG, Kapousta NV, Hitchcock PF, Swank RT, & Meisler MH (1994). Kidney and retinal defects (Krd), a transgene-induced mutation with a deletion of mouse chromosome 19 that includes the Pax2 locus. *Genomics* **23**, 309-320.

Kleyman TR & Cragoe EJ, Jr. (1988). Amiloride and its analogs as tools in the study of ion transport. *J Membr Biol* **105**, 1-21.

Kleyman TR & Cragoe EJ, Jr. (1990). Cation transport probes: the amiloride series. *Methods Enzymol* **191:739-55.**, 739-755.

Koulen P, Cai Y, Geng L, Maeda Y, Nishimura S, Witzgall R, Ehrlich BE, & Somlo S (2002). Polycystin-2 is an intracellular calcium release channel. *Nat Cell Biol* **4**, 191-197.

Li Q, Liu Y, Shen PY, Dai XQ, Wang S, Smillie LB, Sandford R, & Chen XZ (2003). Troponin I binds polycystin-L and inhibits its calcium-induced channel activation. *Biochemistry* **42**, 7618-7625.

Lilley S, LeTissier P, & Robbins J (2004). The discovery and characterization of a proton-gated sodium current in rat retinal ganglion cells. *J Neurosci* **24**, 1013-1022.

Liu Y, Li Q, Tan M, Zhang Y-Y, Karpinski E, Zhou J, & Chen X-Z (2002). Modulation of the human polycystin-L channel by voltage and divalent cations. *FEBS Lett* **525**, 71-76.

LopezJimenez ND, Cavenagh MM, Sainz E, Cruz-Ithier MA, Battey JF, & Sullivan SL (2006). Two members of the TRPP family of ion channels, Pkd113 and Pkd211, are co-expressed in a subset of taste receptor cells. *J Neurochem* **98**, 68-77.

Murakami M, Ohba T, Xu F, Shida S, Satoh E, Ono K, Miyoshi I, Watanabe H, Ito H, & Iijima T (2005). Genomic organization and functional analysis of murine PKD2L1. *J Biol Chem* **280**, 5626-5635.

Murata Y, Harada K, Nakajima F, Maruo J, & Morita T (1995). Non-selective effects of amiloride and its analogues on ion transport systems and their cytotoxicities in cardiac myocytes. *Jpn J Pharmacol* **68**, 279-285.

Nauli SM, Alenghat FJ, Luo Y, Williams E, Vassilev P, Li X, Elia AE, Lu W, Brown EM, Quinn SJ, Ingber DE, & Zhou J (2003). Polycystins 1 and 2 mediate mechanosensation in the primary cilium of kidney cells. *Nat Genet*.

Nomura H, Turco AE, Pei Y, Kalaydjieva L, Schiavello T, Weremowicz S, Ji W, Morton CC, Meisler M, Reeders ST, & Zhou J (1998). Identification of PKDL, a novel polycystic kidney disease 2-like gene whose murine homologue is deleted in mice with kidney and retinal defects. *J Biol Chem* **273**, 25967-25973.

Ogborn MR (1994). Polycystic kidney disease--a truly pediatric problem. *Pediatr Nephrol* **8**, 762-767.

Olteanu D, Yoder BK, Liu W, Croyle MJ, Welty EA, Rosborough K, Wyss JM, Bell PD, Guay-Woodford LM, Bevenssee MO, Satlin LM, & Schwiebert EM (2006). Heightened epithelial Na⁺ channel-mediated Na⁺ absorption in a murine polycystic kidney disease model epithelium lacking apical monocilia. *Am J Physiol Cell Physiol* **290**, C952-C963.

Rohatgi R, Greenberg A, Burrow CR, Wilson PD, & Satlin LM (2003). Na transport in autosomal recessive polycystic kidney disease (ARPKD) cyst lining epithelial cells. *J Am Soc Nephrol* **14**, 827-836.

Sariban-Sohraby S & Benos DJ (1986). The amiloride-sensitive sodium channel. *Am J Physiol* **250**, C175-C190.

Stoner LC & Viggiano SC (2000). Apical nonspecific cation channels in everted collecting tubules of potassium-adapted ambystoma. *J Membr Biol* **177**, 109-116.

Tytgat J, Vereecke J, & Carmeliet E (1990). Mechanism of cardiac T-type Ca channel blockade by amiloride. *J Pharmacol Exp Ther* **254**, 546-551.

Vandorpe DH, Chernova MN, Jiang L, Sellin LK, Wilhelm S, Stuart-Tilley AK, Walz G, & Alper SL (2001). The cytoplasmic C-terminal fragment of polycystin-1 regulates a Ca²⁺-permeable cation channel. *J Biol Chem* **276**, 4093-4101.

Vandorpe DH, Ciampolillo F, Green RB, & Stanton BA (1997). Cyclic nucleotide-gated cation channels mediate sodium absorption by IMCD (mIMCD-K2) cells. *Am J Physiol* **272**, C901-C910.

Veizis EI, Carlin CR, & Cotton CU (2003). Decreased amiloride-sensitive Na⁺ absorption in collecting duct principal cells isolated from bpk ARPKD mice. *Am J Physiol Renal Physiol* ..

Wu G, Hayashi T, Park JH, Dixit M, Reynolds DM, Li L, Maeda Y, Cai Y, Coca-Prados M, & Somlo S (1998). Identification of PKD2L, a human PKD2-related gene: tissue-specific expression and mapping to chromosome 10q25. *Genomics* **54**, 564-568.

CHAPTER 6

DIRECT BINDING OF α -ACTININ ENHANCES TRPP3 CHANNEL ACTIVITY

This chapter was submitted *J. Neuroscience*:

Qiang Li, Xiao-Qing Dai, Patrick Y. Shen, Yuliang Wu, Wentong Long, Carl X. Chen,
Zahir Hussain, Shaohua Wang and Xing-Zhen Chen#.

Corresponding author: Xing-Zhen Chen

6.1. INTRODUCTION

TRPP3 (also called polycystin-L or PKD2L1) is a membrane protein composed of 805 amino acids (in human) and exhibits similar membrane topology with the α -subunit of voltage-gated cation channels. It is classified as a member of the transient receptor potential (TRP) superfamily of cation channels. TRP members are sensory channels, responding to a number of environmental factors, including temperature, force, osmolarity, tastant, odorant and other stimuli (Clapham, 2003). TRPP3 is expressed in multiple tissues, including retina, brain, heart, testis, kidney, liver, pancreas and spleen (Nomura et al., 1998; Wu et al., 1998; Basora et al., 2002). TRPP3 has two homologues (Clapham, 2003), TRPP2 and TRPP5, of which TRPP2 is mutated in ~10% of autosomal dominant polycystic kidney disease (ADPKD), a common inherited disorder characterized by the progressive development of fluid-filled cysts in kidney and also associated with a number of extrarenal manifestations, including hepatic and pancreatic cysts, cardiac valvular abnormalities, hypertension, and cerebral and aortic aneurysms (Sutters and Germino, 2003). Orthologs in other species have recently been identified, including mouse, sea urchin, *C. elegans*, *Drosophila* and yeast, and are involved in diverse cellular functions, such as left-right axis determination, mechanotransduction, fertilization, mating, and cell wall synthesis. Mouse TRPP3 is located in a 7-centimorgan deleted in *Krd* mice which display kidney and retina defects and thus may be associated with the defects (Nomura et al., 1998). More recently, TRPP3 was shown to localize to a subset of taste receptor cells in the tongue where it may play a crucial role in sour tasting and acid sensing (Huang et al., 2006; LopezJimenez et al., 2006; Ishimaru et al., 2006), and to neurons surrounding the central canal of spinal cord where it may account for the long-sought mechanism of a proton-dependent regulation of action potential (Huang et al., 2006).

When expressed in *Xenopus* oocytes, human TRPP3 forms a Ca-activated non-selective cation channel permeable to Ca, K, Na, Rb, NH₄ and Ba, and inhibitable by Mg, proton, La and Gd (Chen et al., 1999; Liu et al., 2002). Its channel properties, including the channel open probability and mean open time, are modulated by membrane potential (Liu et al., 2002). Based on its permeability to monovalent organic cations (methlyamine, dimethylamine and triethylamine and tetra-methylammonium) and impermeability

to/inhibition by larger compounds tetra-ethylammonium/-propylammonium/-butylammonium/-pentylammonium, a pore size of ~ 7 Å was estimated (Dai et al., 2006). Further studies showed that the Ca-binding EF-hand domain and other parts of the carboxyl tail of TRPP3 are not determinants of channel activation (Li et al., 2002). Instead, the EF-hand serves as a controller/regulator of the TRPP3 channel activation induced by Ca, presumably to prevent the channel from over-activation. We discovered that troponin I, an important element of the actin filament complex in muscle cells and a novel angiogenesis inhibitor, binds to a TRPP3 C-terminal domain and inhibits its Ca-induced channel activation (Li et al., 2003b). Although over-expressed TRPP3 targets to the plasma membrane of *Xenopus* oocytes it mostly localizes in intracellular membranes in several mammalian cell lines ((Murakami et al., 2005); Fig. 6-1 and 6-2 of the present study). Interestingly, co-expression of TRPP3 with PKD1 in which mutations account for $\sim 80\%$ of ADPKD cases, in human embryonic kidney (HEK) 293 cells resulted in TRPP3 trafficking to the plasma membrane, where TRPP3 seemed to mediate Ca entry in the presence of a hypo-osmotic extracellular solution (Murakami et al., 2005). Mouse TRPP3 and PKD1L3 together, but not TRPP3 or PKD1L3 alone, also traffics to the plasma membrane of HEK 293 cells and mediate pH-activated cation conductance (Ishimaru et al., 2006). Whether the presence of PKD1L3, cell type and/or species difference account for the observed opposite pH dependence of TRPP3 function remain to be elucidated (Chen et al., 1999; Ishimaru et al., 2006).

In the present study, we employed planar lipid bilayer electrophysiology to examine effects of α -actinin on the channel properties of human TRPP3 purified from mammalian Madin-Darby canine kidney (MDCK) II stable cell line. We also investigated the physical association between the two proteins in various cell lines and tissues, such as HEK 293 and MDCK cells, brain and kidney, using *in vitro* and *in vivo* approaches.

6.2. MATERIALS AND METHODS

Generation of a TRPP3 antibody

The DNA fragment encoding the cytoplasmic C-terminus of human TRPP3 (TRPP3C, amino acid (aa) 562-805) was cloned into pGEX-5X-3 to produce a glutathione-S-transferase (GST) tagged TRPP3C fusion protein, which was used to generate an anti-TRPP3 antibody (called PR71). Polyclonal anti-TRPP3 serum was raised in New Zealand white rabbits according to a standard protocol. The serum was purified using the Montage antibody purification kit (Millipore, Billerica, MA).

Plasmids, reagents and tissues

The plasmid pGTAPC2-TRPP3 (as schematically shown in Fig. 6-2A) was used for mammalian cell expression and subsequent tandem affinity purification. Mouse monoclonal antibodies BM75.2 and EA53 (Sigma-Aldrich Canada, Oakville, ON) were used to recognize the non-muscle and muscle types of α -actinin. An anti-GST antibody was purchased from Santa Cruz Biotechnology (Santa Cruz, CA). Secondary antibodies, goat anti-mouse and anti-rabbit IgG conjugated with horseradish peroxidase were from Chemicon International (Temecula, CA), for dot and Western blotting.

Cell culture and transfection

MDCK and HEK 293 cells were cultured in Dulbecco's modified Eagle's medium (DMEM) supplemented with L-glutamine, penicillin-streptomycin, and 10% fetal bovine serum. Transfection of *PKDL* was performed on MDCK cells cultured to 90% confluency using Lipofectamine 2000 (Invitrogen, Toronto, ON) according to the manufacturer's protocol. For generation of stable cell lines, 600 $\mu\text{g}/\mu\text{l}$ G418 (Invitrogen) was added to DMEM to select viable clones one (recovery) day following transfection. The selection process was maintained for six weeks with daily medium change. Well-propagated colonies with strong fluorescent signals were selected under an Olympus IX81 immunofluorescence microscope.

Protein preparation and lipid bilayer electrophysiology

Commercial chicken gizzard α -actinin (Sigma-Aldrich Canada) was used as a modulator of TRPP3 channel. TRPP3 protein was prepared by a modified tandem affinity purification protocol (see Results) and reconstituted in a planar lipid bilayer system, as previously described (Li et al., 2004), to assess the channel activity. Briefly, bilayer membrane was formed with a mixture of 1-palmitoyl-2-oleoyl phosphatidyl-choline and phosphatidyl-ethanolamine (Avanti Polar Lipids, Birmingham, AL) at a 3:7 ratio in a Delrin cup inserted in an acrylic chamber (Harvard Apparatus, Montreal, QC). The *cis* (intracellular) compartment contained 150 mM KCl, 15 μ M Ca (by 1 mM EGTA and 1.01 mM CaCl₂), pH 7.4 (adjusted by Tris-base). The *trans* (extracellular) chamber either used the identical (symmetrical) solution as in *cis* or contained 15 mM KCl (asymmetrical). GTAP-purified TRPP3 protein (~0.5 μ g in 10 μ l) was added to the *cis* chamber in proximity of the membrane or was used to directly 'paint' the membrane. When studying its effect on TRPP3 channel, α -actinin (~8 μ g in 10 μ l) was added to the proximity of the membrane from the *cis* chamber, which was clamped to a range of voltages using a Gapfree protocol generated by Clampex 8 (Axon Instruments, Union City, CA), while the *trans* chamber was held at ground (0 mV). Currents and voltages were recorded at 200 μ s per sample and Bessel filtered at 1K or 3K Hz with the amplifier PC-ONE (Dagan Corporation, Minneapolis, MN), the AD/DA converter Digidata 1320A and the software Clampex 9 (Axon Instruments).

When performing paired experiments, current was recorded for 15-25 min at various voltages in the presence of TRPP3 alone prior to the addition of α -actinin. After an α -actinin addition, current was recorded in a similar way for a period of time (20-30 min) that is about 5 min longer than that before adding α -actinin, by taking into account our estimate that it takes roughly 5 min for α -actinin to reach and interact with TRPP3 proteins inserted in the membrane. We also performed experiments by adding 10 μ l water, in place of α -actinin, as controls. When performing unpaired experiments, TRPP3 or TRPP3 + α -actinin was introduced from the beginning and current was recorded for 30 min or longer.

Data analysis

Data obtained from the lipid bilayer experiments were analyzed using Clampfit 9. The all-point histogram was used to calculate single-channel amplitudes at various voltages. The open probability times the number of channels in the bilayer membrane (NPo, designated 'open probability'), and the mean TRPP3 single-channel current were obtained from currents generated by tracings of 60 s and 30 s long, respectively, at various voltages. Analyzed data were plotted using Sigmaplot 9 (Jandel Scientific Software, San Rafael, CA) and expressed in the form of mean \pm SEM (N), where SEM is the standard error of the mean and N the number of independent measurements. Two sets of data were compared by paired or unpaired *t*-test, and a probability value (*p*) of less than 0.05 and 0.01 was considered significant and very significant, respectively.

6.3. RESULTS

Characterization of a TRPP3 antibody

To further characterize TRPP3 proteins we generated a polyclonal anti-TRPP3 antibody (called PR71) raised from rabbit using the entire cytoplasmic C-terminus of human TRPP3 protein. We assessed the specificity of PR71 using TRPP3 expressed in oocytes and MDCK cells. PR71 detected a strong and single band with the expected size, using the total lysate of *Xenopus* oocytes expressing TRPP3 (Fig. 6-1A). This band was completely abolished when the blocking peptide GST-TRPP3C was pre-incubated with PR71 prior to Western blotting (Fig. 6-1B), indicating the specificity of the antibody. We also validated antibody PR71 by immunofluorescence using MDCK cells transiently expressing EGFP-tagged TRPP3. Staining with PR71 basically coincided with the EGFP signal (Fig. 6-1C) and the PR71-stained signal was abolished when GST-TRPP3C was pre-incubated with PR71 (Fig. 6-1D). These data thus demonstrated that PR71 is a TRPP3-specific antibody.

Purification of TRPP3 from MDCK cells

The tandem affinity purification approach has been developed for functional proteomic studies in various host cells. We recently modified this approach to purify human TRPP2 channel proteins expressed in MDCK cells and successfully observed TRPP2 channel function by planar lipid bilayer electrophysiology (Li et al., 2004). We also attempted to purify human TRPP3 channel proteins using the same protocol. However, we failed to collect sufficient amounts of TRPP3 proteins for Western blotting and lipid bilayer reconstitution, largely due to difficulty in establishing good stable cell lines over-expressing TRPP3. In fact, under the same condition, the population of TRPP3-expressing cells was 5-8 fold smaller than that of TRPP2 and overall expression levels of TRPP3 were also much lower than those of TRPP2. To facilitate the selection of positive cells we then further modified our pTAPC2 vector by inserting a fluorescent tag, an EGFP reporter gene, upstream of the TAP tags, which resulted in a new vector (called pGTAPC2) containing three consecutive tags (Fig. 6-2A). The first two tags, the EGFP and IgG binding domains, were cleaved during the purification process. We successfully

generated good stable cell lines with high expression levels of human TRPP3 by visual selection under an immunofluorescence microscope (Fig. 6-2B).

Upon purification as described (Li et al., 2004) using these newly established cell lines, a 150 kDa band in the total protein lysate and a 100 kDa band in the final elute were detected, as expected, by Western blotting probed with the anti-TRPP3 PR71 antibody (Fig. 6-2C). Thus, compared to the previous vector, using pGTAPC2 allowed purifying larger amounts of TRPP3 proteins from MDCK stable cell lines.

Characterization of TRPP3 channel reconstituted in lipid bilayer

To determine whether purified TRPP3 protein preserves its cation channel activity, we reconstituted it into planar lipid bilayer and performed single-channel current measurements under voltage clamp conditions, as described previously (Li et al., 2004; González-Perrett et al., 2001; Li et al., 2004). Experiments were conducted under asymmetrical (150 and 15 mM KCl in the *cis* and *trans* chambers, respectively) and symmetrical solution conditions (150 mM KCl in both *cis* and *trans*). Channel openings were observed at various voltages under asymmetrical or symmetrical solution conditions (Fig. 6-3A), demonstrating that purified TRPP3 proteins by this protocol possess the essential characteristics normally present under physiological conditions. TRPP3 channels also opened at multiple conductance states, a characteristic of TRPP3 observed when expressed in *Xenopus* oocytes ((Chen et al., 1999) and unpublished data). Under the asymmetrical solution condition the outward single-channel conductance for the main state was 142 ± 2 pS ($N = 7$, V_m from -40 to +160 mV). Under the symmetrical condition, TRPP3 opened at a main, intermediate or small state, with the corresponding conductance values of 67.2 ± 6.1 pS ($N = 11$), 39.9 ± 3.9 pS ($N = 12$) and 13.5 ± 2.2 pS ($N = 14$) (-160 to +160 mV), respectively (Fig. 6-3B). The conductance observed in the lipid bilayer system was smaller than the values obtained using the *Xenopus* oocyte expression system (Chen et al., 1999; Liu et al., 2002), possibly due to the absence of endogenous partner proteins, signaling molecules and/or intracellular chemicals in oocytes that modulate TRPP3 channel function. It could also be due in part to a difference in the lipid composition between the planar lipid bilayer and oocyte membrane.

Functional modulation of TRPP3 channel by α -actinin

α -actinins are important actin-binding and -bundling proteins that are abundantly present in both muscle and non-muscle cells (Dixson et al., 2003), and have been shown to regulate various types of ion channels, including Ca channels, K channels, NMDA receptors, and TRPP2 channel (Sadeghi et al., 2002; Maruoka et al., 2000; Krupp et al., 1999; Li et al., 2005). We thus examined whether α -actinin (from chicken gizzard) modulates the channel function of TRPP3 reconstituted in lipid bilayer. We observed multiple conductance states in the presence of α -actinin as well (Fig. 6-4). We found that the addition of α -actinin to the *cis* chamber elicited a substantial increase in single-channel activity (Fig. 6-4, paired experiments). In the presence of α -actinin, the main, intermediate and small states were still present, with the conductance values of 74.6 ± 3.5 , 28.6 ± 3.3 and 17.0 ± 5.3 pS ($N = 8$, -160 to +160 mV), respectively (Fig. 6-5A). α -actinin did not significantly affect the main and small conductance values, but decreased the intermediate conductance value. It remains unclear whether there is a physiological meaning for this decrease in the intermediate conductance, given the fact that the classification of channel openings into the three states was not a clear-cut. Thus, overall the single-channel conductance values were rather not affected by α -actinin. In paired experiments ($N = 8$), the presence of α -actinin increased the average channel open probability (NPo) value for the main state by 5 fold at negative voltages ($p = 10^{-7}$, -160 to -40 mV), and by 2 fold at positive voltages ($p = 0.0003$, +40 to +160 mV) (Fig. 6-5B). When analyzing the data from pooled unpaired experiments we also found substantially augmented NPo values in the presence of α -actinin (data not shown). In addition to NPo, we also employed the mean current to assess overall TRPP3 channel activity comprising the three conductance states. Based on the data obtained from paired and unpaired experiments together, α -actinin substantially increased the TRPP3 activity at all voltages (Fig. 6-5C), averaging an overall increase of about 2 fold. Taken together, our lipid bilayer reconstitution experiments revealed that TRPP3 channel activity is substantially stimulated by α -actinin.

***in vivo* interaction between TRPP3 and α -actinin**

To determine whether TRPP3 is associated with α -actinin *in vivo*, we performed co-immunoprecipitation (co-IP) experiments (Li et al., 2003a) using native MDCK and HEK293 cells, and human kidney and heart tissues. Using anti-TRPP3 PR71, anti- α -actinin BM75.2 (mainly recognizing the non-muscle type α -actinin) or anti- α -actinin EA53 (mainly recognizing the muscle type α -actinin) for precipitation, we detected precipitated proteins via Western blotting. Non-muscle α -actinin protein was detected in the PR71-derived immunoprecipitates of MDCK cells, HEK 293 cells and human kidney tissue, but not in non-immune IgG-derived immunoprecipitates (Fig. 6-6A). Reciprocally, TRPP3 was observed in the BM75.2-derived immunoprecipitates. These data demonstrated that TRPP3 and non-muscle α -actinin are in the same complex *in vivo*. Under the same conditions TRPP3 and muscle α -actinin were shown to be in the same complex in human heart tissues (Fig. 6-6B). Thus, TRPP3 is in complex with both non-muscle and muscle type of α -actinin in native cells and tissues.

Interestingly, TRPP3 was found to be abundantly present in adult mouse brain (Fig. 6-7A). The areas with high abundance of TRPP3 include pons, thalamus, olfactory bulb, hippocampus and spinal cord (Fig. 6-7B), in agreement with a recent report on the TRPP3's localization to spinal cord where TRPP3 presumably controls the rhythm of action potential in a pH-dependent manner (Huang et al., 2006). Of note, the protein size of TRPP3 is slightly smaller than those in other cell lines and tissues (Figs. 6-6 and 6-7), possibly due to tissue-specific splicing or post-translational modifications. Further, our co-IP experiments revealed that TRPP3 and α -actinin-2 are in the same complex in mouse brain (Fig. 6-7C).

The yeast two-hybrid system (Li et al., 2003a; Li et al., 2005) was used to assess whether TRPP3 directly associates with α -actinins. We found that the TRPP3 N-terminus (TRPP3N, aa 1-97) and C-terminus (TRPP3C, aa 562-805) associated with the C-terminal halves of α -actinin-1 and -2 (Fig. 6-8A). Furthermore, we also found that the SR domain IV of α -actinin-2 is sufficient to mediate the association with TRPP3N while a longer segment of α -actinin-2 is required for the association with TRPP3C (Fig. 6-8B).

***in vitro* binding between TRPP3 and α -actinin**

In vitro biochemical methods were applied to further characterize the interaction between TRPP3 and α -actinin. We first employed a GST fusion protein affinity binding method (Li et al., 2003a). For this purpose, polypeptides TRPP3N and TRPP3C were fused in frame with a GST epitope and expressed in bacterial strain BL21 in the presence of 1 mM IPTG. Cell extracts containing respective fusion protein were incubated with the commercial chicken gizzard α -actinin. Using anti- α -actinin antibody BM75.2, we showed that GST-TRPP3N and GST-TRPP3C, but not controls (GST alone and buffer without fusion protein lysates), co-precipitated with α -actinin (Fig. 6-9A).

We also performed dot blot overlay experiments (Li et al., 2005) to examine the TRPP3- α -actinin interaction. Purified GST-TRPP3N and GST-TRPP3C polypeptides were spotted onto a nitrocellulose membrane, followed by incubation with MDCK cell lysates in the presence of Ca (5 mM) or in its absence (1 mM EGTA). The membrane was then washed extensively and probed with BM75.2. α -actinin was detected in spots incubated with cell lysate, but not with bovine serum albumin (BSA) or binding buffer alone (Fig. 6-9B), indicative of specific binding between α -actinin and the cytoplasmic termini of TRPP3. Similar TRPP3- α -actinin binding signal intensities were displayed on membranes with or without Ca, indicating that these associations are rather Ca-independent.

6.4. DISCUSSION

TRPP3 is present in different types of neuron cells. It was first reported to be present in the ganglion cells of retina (Basora et al., 2002). We recently also revealed that TRPP3 is present in photoreceptor cells of mouse retina (unpublished data). However, the function of TRPP3 in retina has not been reported. In the tongue, it is localized to all four taste areas while its partner protein PKD1L3 is present in circumvallate and foliate, but not fungiform or palate (Huang et al., 2006). In fact, TRPP3 is concentrated in the apical membrane (facing taste pores) of bipolar cells in taste buds (Huang et al., 2006; Ishimaru et al., 2006), suggesting that it allows an initial cation influx triggered by low pH at the taste pore, which activates local voltage-gated cation channels via membrane depolarization and then leads to the firing of an action potential. In the whole length of the spinal cord, TRPP3 is present in neurons that project into the central canal, suggesting that it may also trigger an initial cation entry following a decrease in the canal pH (Huang et al., 2006). However, it remains unclear as to why TRPP3 responds to two very different pH ranges in the tongue and spinal cord. In particular, it is unknown whether PKD1L3 plays a role in acid sensing.

Lipid bilayer system is particularly useful for characterizing the function of purified channel proteins endogenously localized to intracellular membranes. The conventional TAP approach has allowed purification of a large number of cytoplasmic protein complexes from many organisms. In contrast, the application of the method to purifying mammalian membrane protein complexes has just been emerging. We recently improved the mammalian TAP procedure for TRPP2 channel proteins. To further ease the selection of stable cell lines we added an EGFP tag to the vector pTAPC2 and generated the new vector pGTAPC2 to express the *TRPP3* gene. This modification did not affect subsequent purification process and indeed facilitated the establishment of MDCK stable cell lines with high expression of TRPP3. This construct may also be applicable to purifying other difficult-to-express membrane proteins from mammalian cells.

Up to now the channel function of TRPP3 has primarily been studied using the *Xenopus* oocyte expression system (Chen et al., 1999; Li et al., 2002; Liu et al., 2002; Li et al., 2003b), except for the only report showing that co-expression of TRPP3 and TRPP1 in HEK 293 cells produced a transient increase in the intracellular Ca concentration by

hypo-osmotic stimulation, using calcium imaging (Murakami et al., 2005). Over-expressed TRPP3 in MDCK cells mainly localized to intracellular compartments although we did observe a small portion of TRPP3 expressed in the plasma membrane (Fig. 6-2B). Thus it is meaningful to characterize TRPP3 channel function in lipid bilayer in combination with our novel TAP procedure. Our studies showed that TRPP3 in artificial lipid bilayer exhibited certain properties of TRPP3 displayed in *Xenopus* oocytes, eg, cation selectivity and presence of multiple conductance states. In contrast, the main single-channel conductance of TRPP3 (~70 pS) with or without α -actinin is much smaller than in oocytes (~370 pS in the presence of 123 mM K) (Li et al., 2002; Liu et al., 2002). The larger conductance may plausibly be due to the presence of yet-to-be-identified intracellular interacting partners or chemical modulators endogenously present in oocytes.

Our present study also demonstrated that TRPP3 physically and functionally interacts with both muscle and non-muscle α -actinins. In non-muscle cells, two isoforms, α -actinin-1 and -4, bundle actin filaments and mediate membrane attachment at adherens junctions in a Ca-dependent manner (Honda et al., 1998). α -actinin-2 is expressed in muscle-type tissues and represents one of the major structural components of sarcomeric Z-lines of striated muscle and analogous dense bodies of smooth muscle (Mills et al., 2001). In contrast, α -actinin-3 is limited to a subset of fast-twitch skeletal fibers. Both α -actinin-2 and -3 anchor actin filaments in a constitutive manner. Recently, α -actinins were shown to be more widely distributed. For example, α -actinin-2 is abundantly present in brain where it binds the NR1 and NR2B subunits of the N-methyl-D-aspartate (NMDA) receptor, an important mediator of neuronal plasticity required for most forms of long-term potentiation in learning and memory (Wyszynski et al., 1997; Rycroft and Gibb, 2004). In the presence of Ca, calmodulin competes with α -actinin-2 for binding to NR1, presumably leading to NMDA receptor rundown and redistribution (Wyszynski et al., 1997). Furthermore, α -actinins also regulate the activity of other channels. For examples, α -actinin-2 directly interacts with voltage-gated K channel Kv1.5 and modulates its channel gating and current density (Maruoka et al., 2000); muscle type α -actinins regulate L-type Ca channel function (Sadeghi et al., 2002).

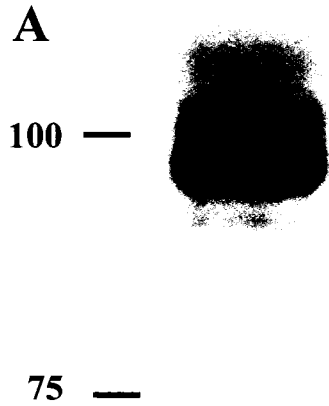
In summary, α -actinin anchors TRPP3 to the actin cytoskeleton not only for structural purposes but also functionally modulate its channel function. In future studies it is important to identify amino acid residues or small domain(s) in TRPP3 and α -actinin that mediate the physical binding, and to determine whether/how factors such as phosphorylation and intracellular calcium are implicated in the TRPP3-cytoskeleton interaction. Given that acid sensing is important in body fluids in many tissues, such as brain, retina, heart and kidney, it would of great interest to determine whether/how TRPP3 and the TRPP3- α -actinin interaction are important for acid sensing in these tissues.

ACKNOWLEDGEMENTS

This work was supported by the Canadian Institutes of Health Research, the Kidney Foundation of Canada (X.Z.C.), and the Heart and Stroke Foundation of Canada (X.Z.C. and S.W.). Q.L. is a recipient of the Polycystic Kidney Disease Foundation Fellowship. X.Q.D. is a recipient of the AHFMR studentship. X.Z.C. is a Senior Scholar of the Alberta Heritage Foundation for Medical Research.

Fig. 6-1. Characterization of the TRPP3 antibody PR71. **A.** Total protein extracts from *Xenopus* oocytes expressing human TRPP3 and control, H₂O-injected oocytes were resolved in 8% SDS-PAGE, transferred to nitrocellulose membrane, and immunoblotted with PR71. **B.** The same samples were immunoblotted with PR71 after pre-incubation with the blocking peptide GST-TRPP3C. **C and D.** MDCK cells expressing EGFP-tagged TRPP3 were stained with PR71 (red) or visualized for EGFP (green, no staining), in the absence (**C**) or presence of the blocking peptide.

6.5. FIGURES



B

TRPP3 Ctrl
PR71

TRPP3 Ctrl
PR71 + GST-TRPP3C

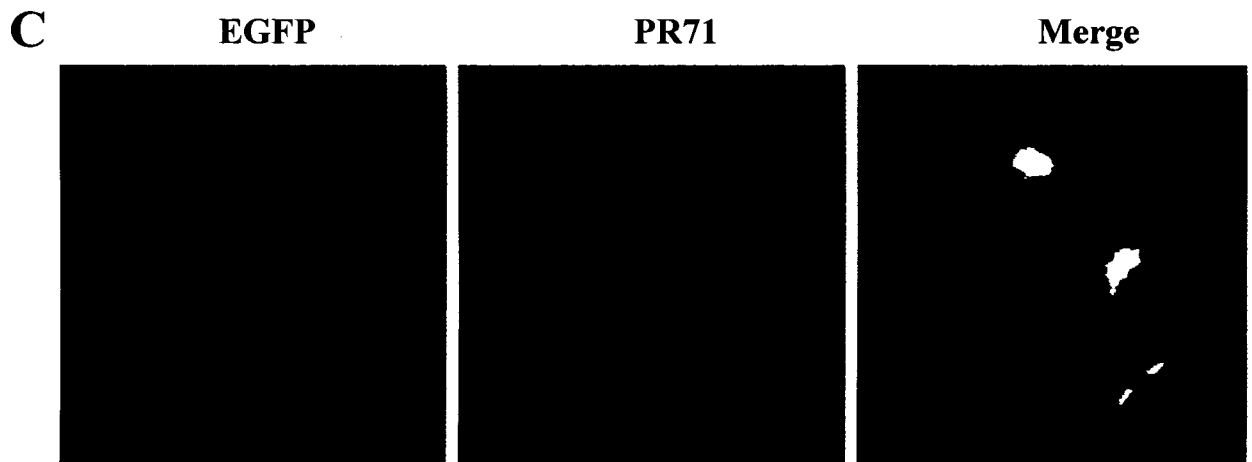


Fig. 6-2. Tandem affinity purification procedure for human TRPP3 channel protein in MDCK cells. A. Schematic representation of the plasmid pGTAPC2-TRPP3. The vector pGTAPC2 is derived from pTAPC2 by inserting an EGFP reporter gene upstream of the two consecutive IgG binding motifs. Three epitope tags and TEV cleavage site are indicated. B. Subcellular distribution of GTAP-purified TRPP3 stably expressed in MDCK cells. TRPP3 is distributed throughout the cell, predominantly surrounding the nucleus (right panel). A small portion of TRPP3 is present in the plasma membrane. Blue DAPI staining represents cell nuclei. C. A portion of total protein lysate (lane 1), protein A bead-purified and TEV-cleaved intermediate elute (lane 2), and final calmodulin bead-purified elute (lane 3) from MDCK cell lines transfected with pGTAPC2-TRPP3 were separated using 8% SDS-PAGE and probed with PR71.

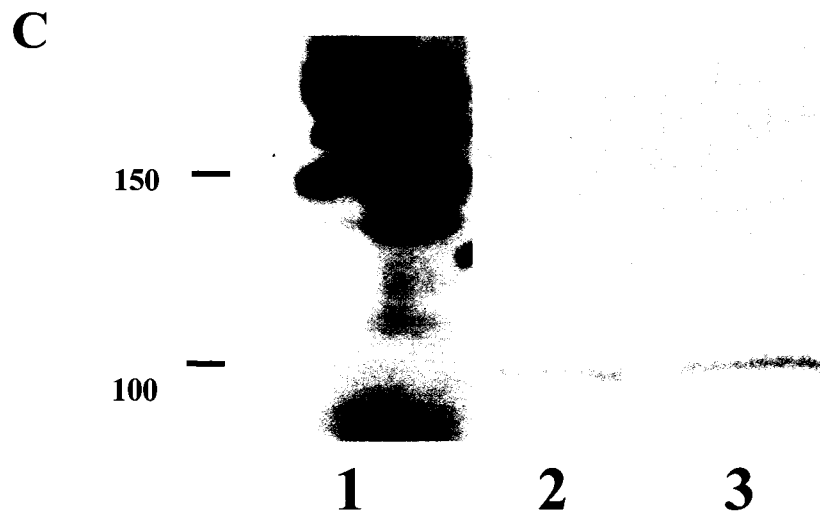
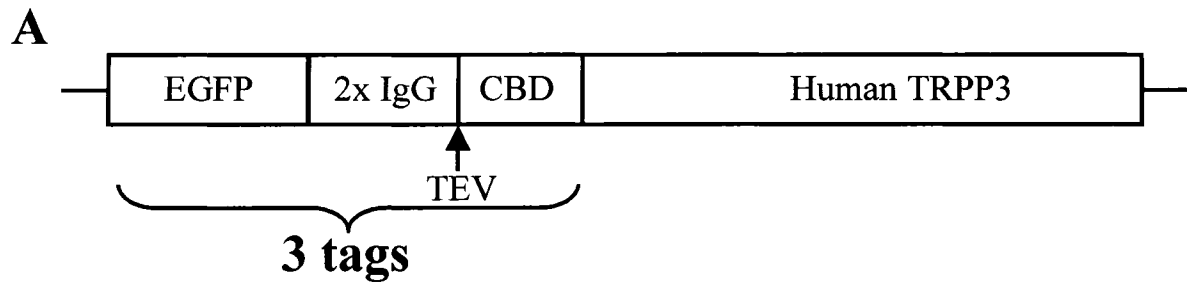


Fig. 6-3. Channel activity of TRPP3 reconstituted in planar lipid bilayer. A. Representative tracings of GTAP-purified TRPP3 channels recorded at various voltages and under the asymmetrical and symmetrical solution conditions, as indicated. Tracings were (Gaussian) filtered at 200 Hz in Clampfit 9. Horizontal lines indicate the close state. **B.** Current-voltage relationships of TRPP3 under the symmetrical solution condition, corresponding to the main, intermediate and small conductance states. Shown data are averaged from 11, 12 and 14 independent measurements, respectively.

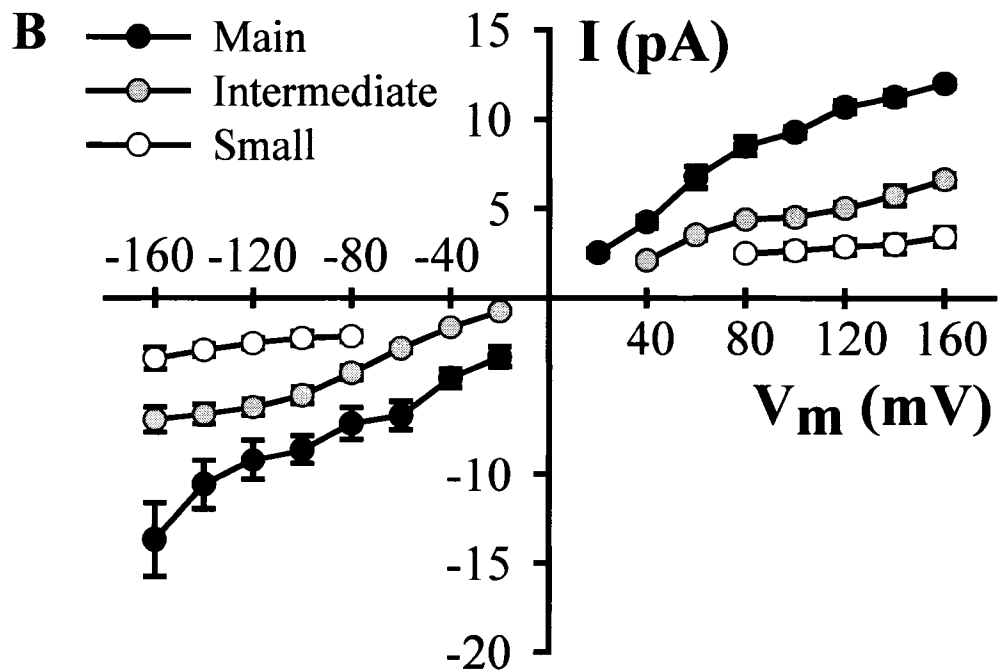
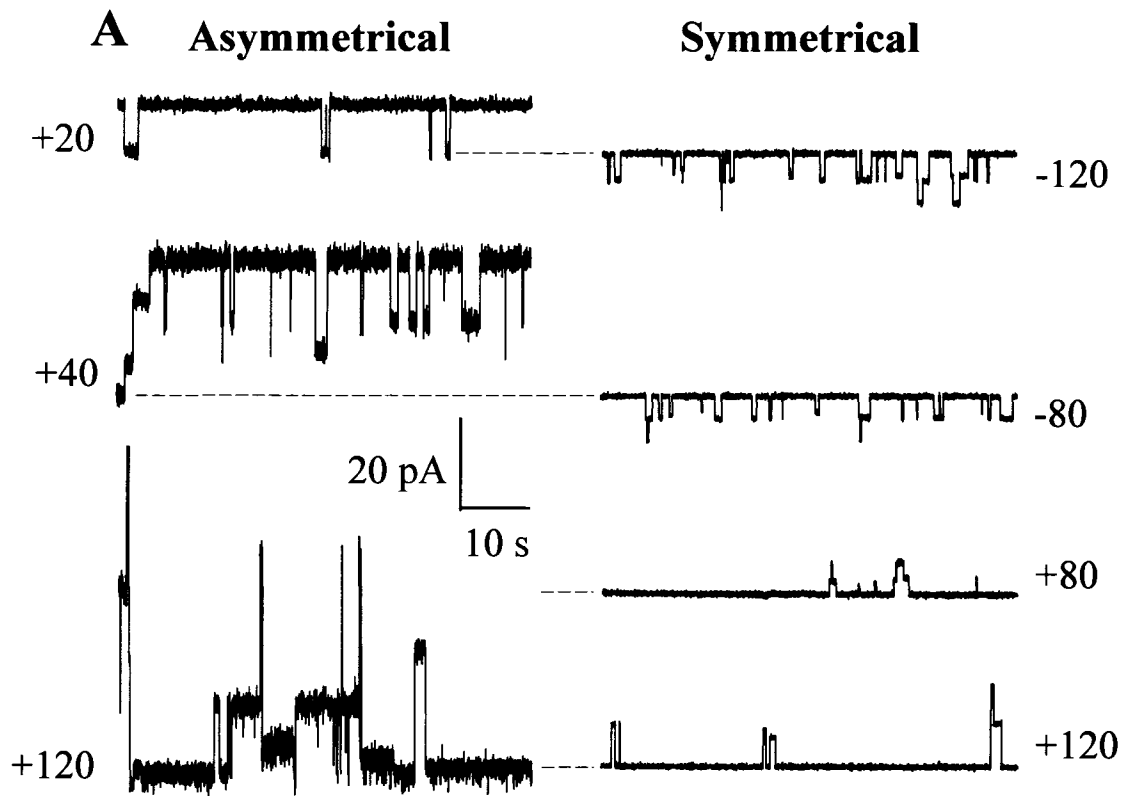


Fig. 6-4. Effect of α -actinin on TRPP3 channel activities. Experiments were performed under the symmetrical solution condition. Shown tracings are the most active 60 s out of 20-30 min recordings in paired experiments in the absence (left panels) and presence (right panels) of α -actinin, at indicated voltages. Signals were filtered at 200 Hz. Horizontal lines indicate the close state.

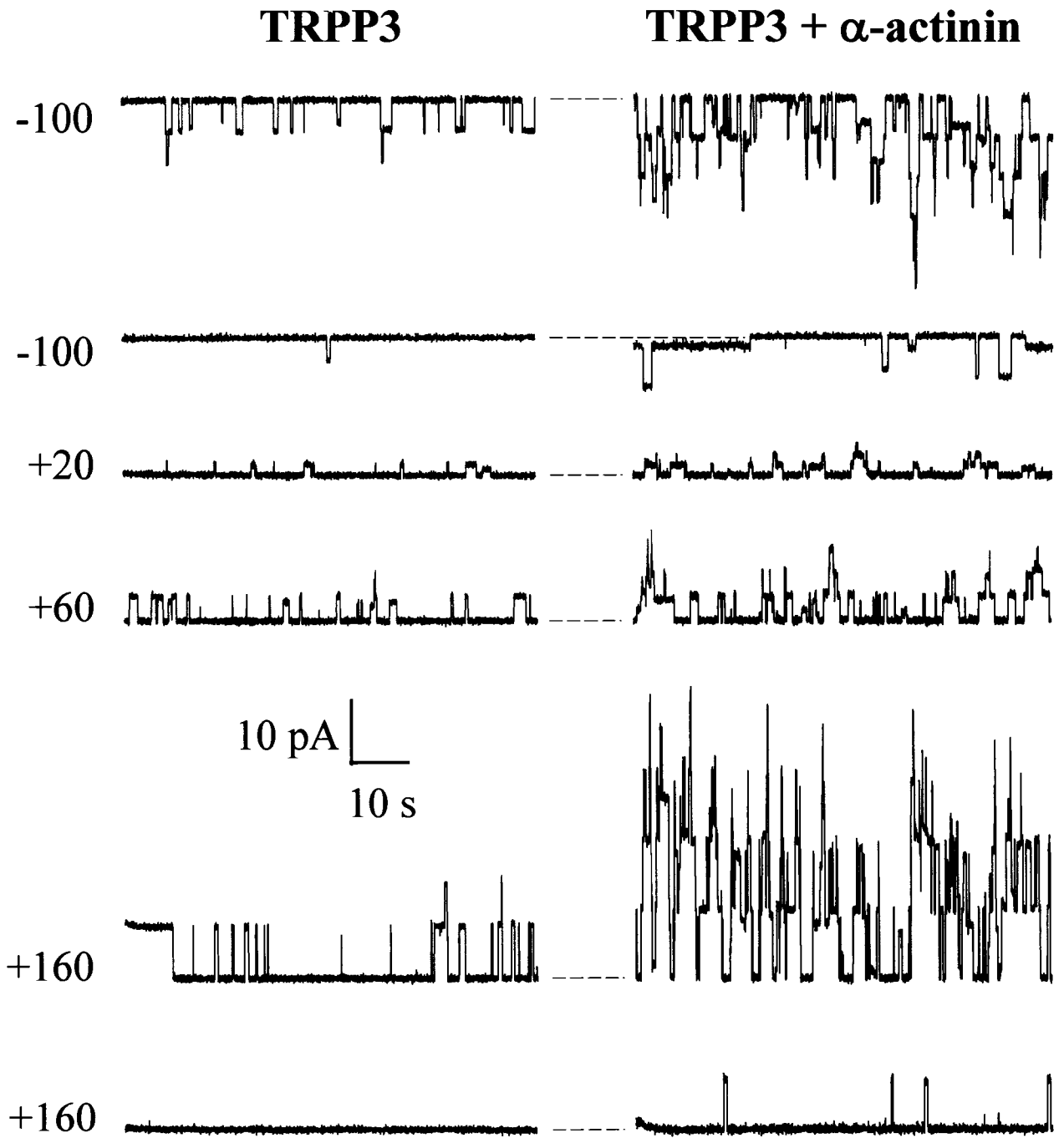


Fig. 6-5. Effect of α -actinin on the single-channel conductance, open probability and mean current of TRPP3. Experiments were performed under the symmetrical solution condition. A. Averaged current-voltage curves of TRPP3 in the presence of α -actinin, representing the main, intermediate and small conductance states ($N = 8$). B. Effects of α -actinin on NPo at positive ($+V_m$, +40 to +160 mV) and negative voltages ($-V_m$, -160 to -40 mV). Shown data are averaged NPo values in the absence or presence of α -actinin, from 8 paired experiments. C. The mean currents of TRPP3 at various voltages obtained in the absence or presence of α -actinin. Shown data were averaged from mean current values obtained from 10 and 8 independent measurements in the absence and presence of α -actinin, respectively.

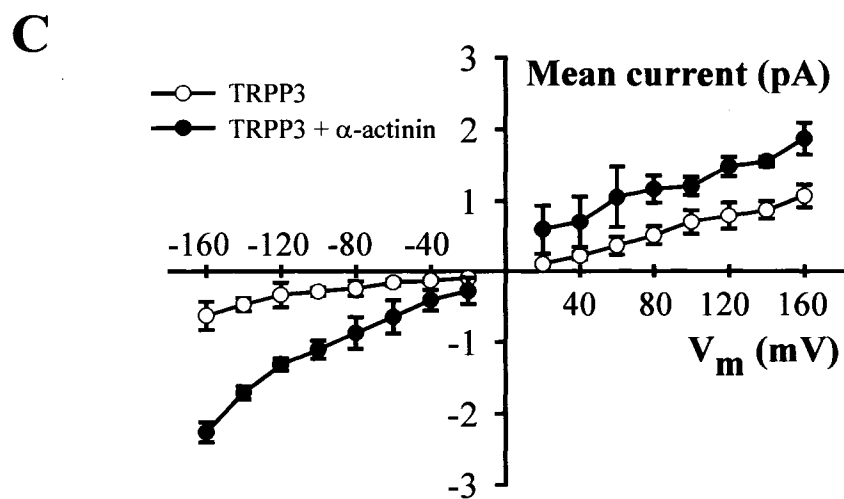
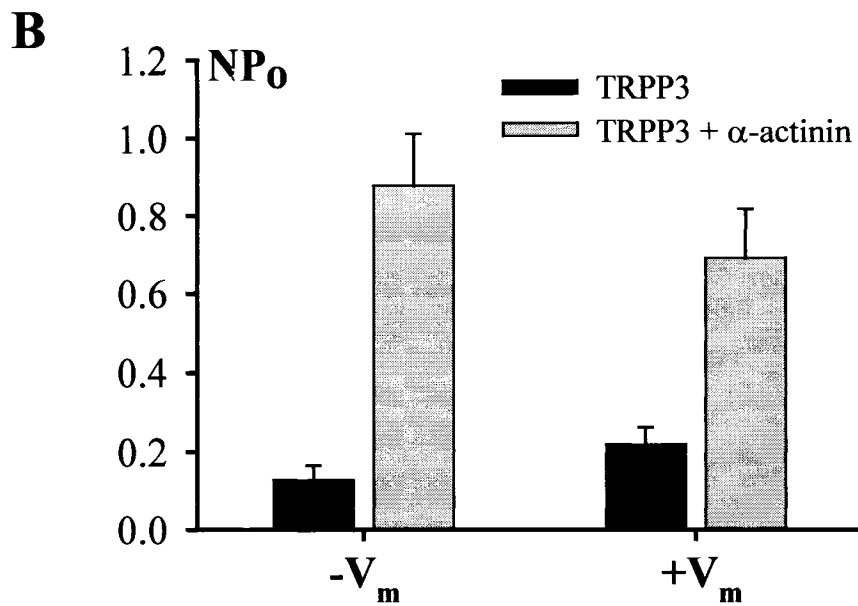
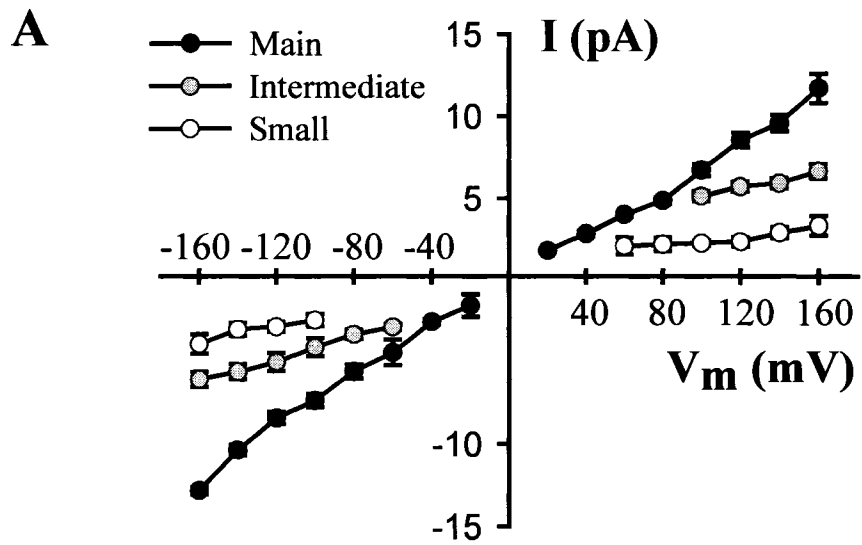


Fig. 6-6. Interaction between endogenous TRPP3 and α -actinins in MDCK and HEK 293 cells, and mouse brain, human kidney and heart tissues by co-IP. A. Upper panels, total proteins from MDCK cells, HEK 293 cells or human kidney tissues were precipitated with either PR71 or non-immune rabbit IgG (RIgG) and detected with non-muscle α -actinin (NMACTN) antibody BM75.2. Lower panels: reciprocal co-IP. Total proteins from the same samples were precipitated with either BM75.2 or non-immune mouse IgG (mIgG) and detected by PR71. **B.** Total proteins from human heart tissues were reciprocally precipitated and detected with muscle α -actinin (MACTN) antibody EA53 and TRPP3 antibody PR71. The molecular mass (in kDa) is indicated.

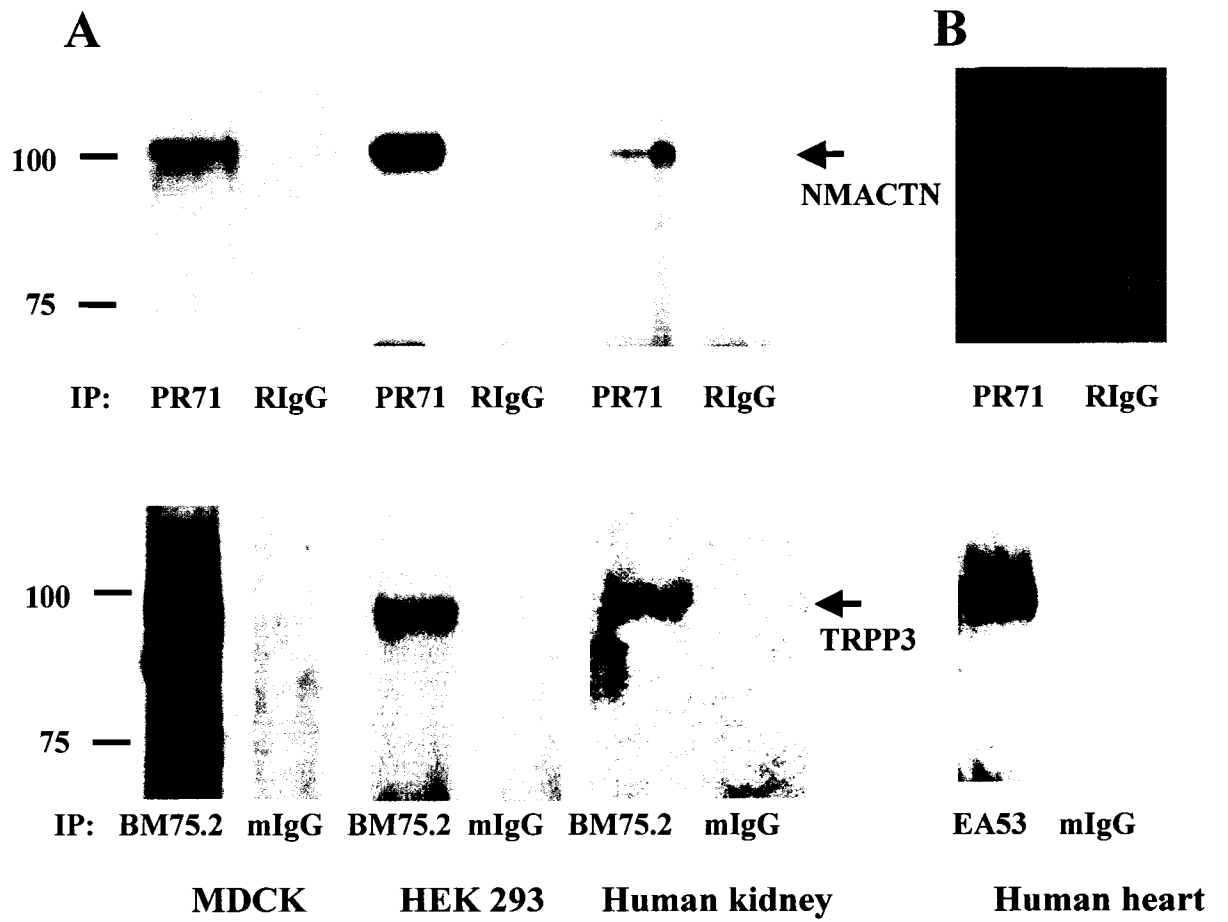


Fig. 6-7. Interaction between endogenous TRPP3 and α -actinin-2 in mouse brain. **A.** Total protein lysate (50 μ g) from adult mouse brain were loaded on SDS-PAGE and immunoblotted with PR71. **B.** Total protein lysates (30 μ g each) of 12 major and distinct areas of adult mouse brain was immunoblotted with PR71. 1. frontal cortex, 2. posterior cortex, 3. cerebellum, 4. hippocampus, 5. olfactory bulb, 6. striatum, 7. thalamus, 8. midbrain, 9. entorhinal cortex, 10. pons, 11. medulla, 12. spinal cord. **C.** Total proteins from mouse brain tissues were precipitated with either anti-TRPP3 PR71, anti- α -actinin-2 EA53, and detected by EA53/PR71.

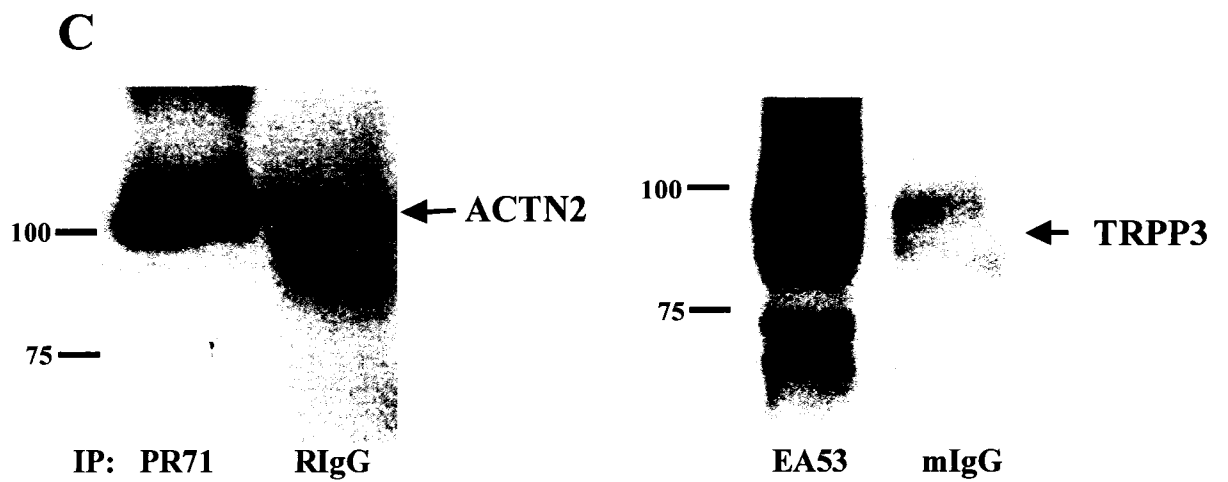
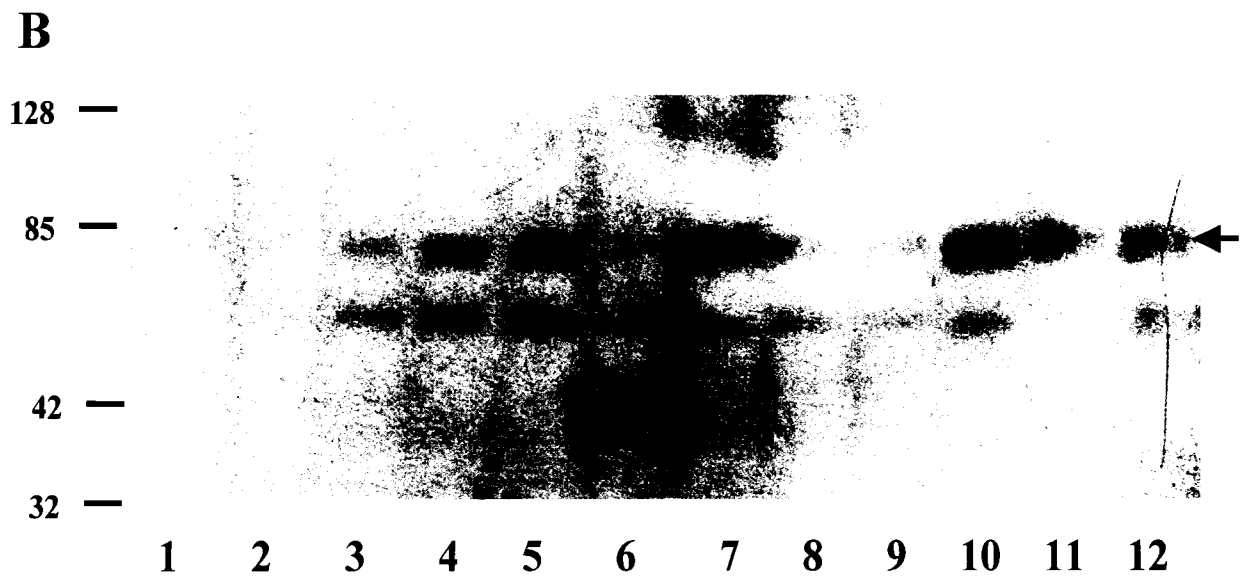
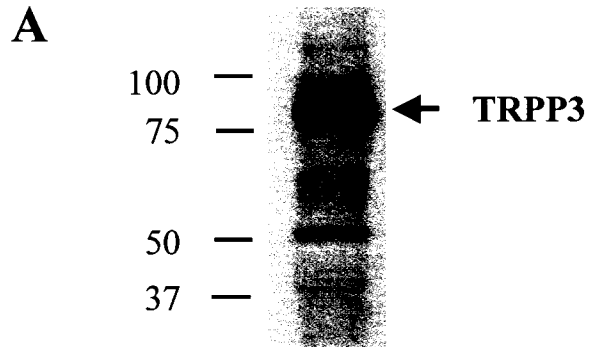


Fig. 6-8. Schematic representation of interaction between various TRPP3 and α -actinin fragments by yeast two-hybrid system. A. Human TRPP3 segments are marked with starting and ending amino-acid residue numbers. The N-terminus (N), transmembrane domains and loops between them (TMs) and C-terminus (C) are indicated. Their association with human α -actinin-1 (ACTN1) and α -actinin-2 (ACTN2) are indicated by “+++”, “++”, “+” and “-” for development of blue color within 1 hr, 3 hr, 24 hr and no development of blue color within 24 hr, respectively. **B.** ACTN2 segments and their association with GST-TRPP3N and GST-TRPP3C.

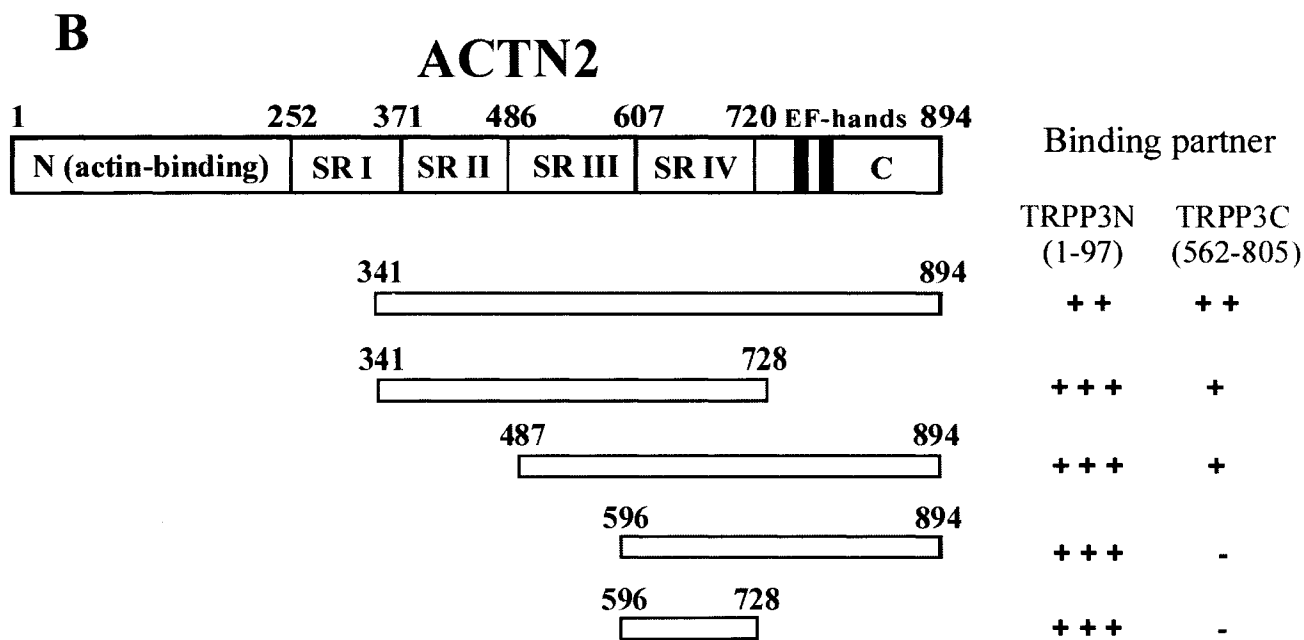
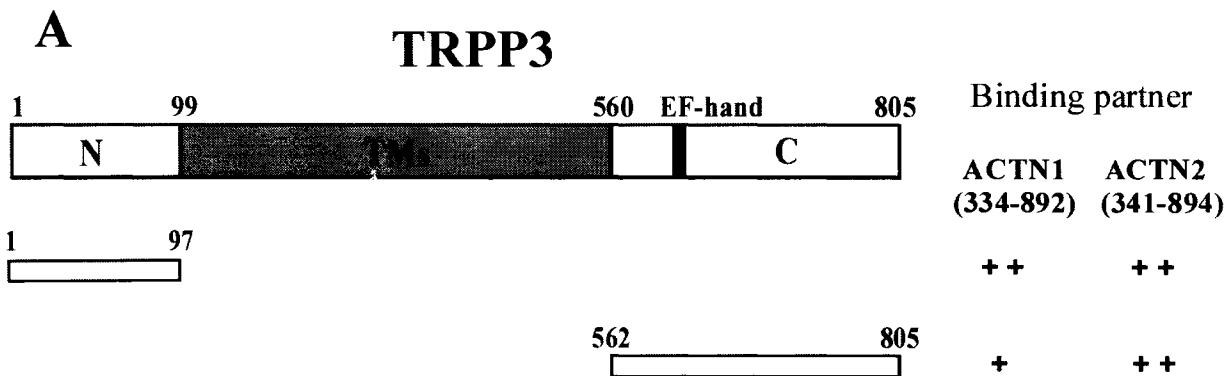
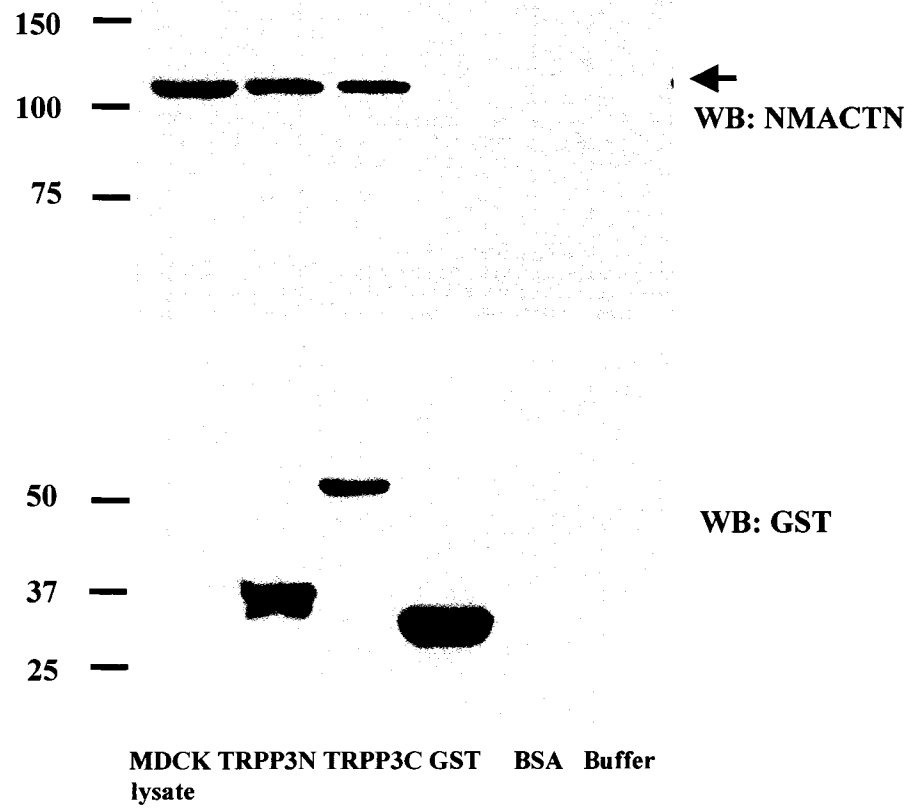
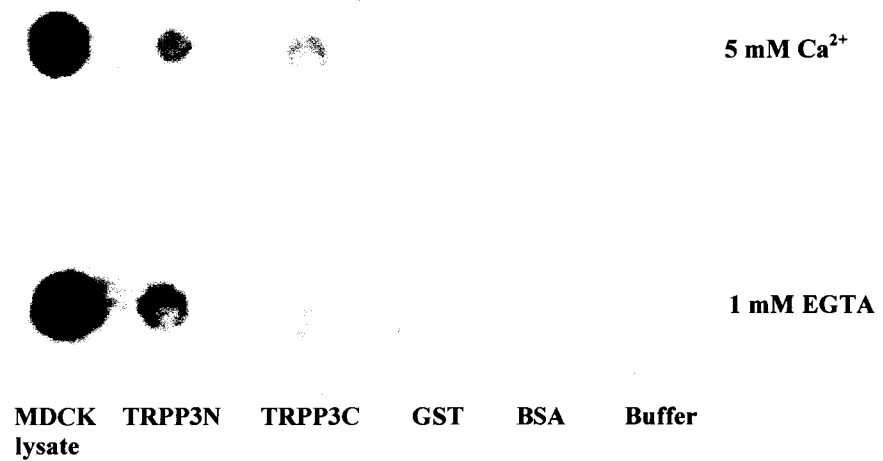


Fig. 6-9. *In vitro* interaction between TRPP3 fragments and α -actinin by GST pull-down and dot blot overlay. **A.** *E. coli* protein extracts expressing GST-TRPP3N, GST-TRPP3C or GST, or the binding buffer alone, were incubated with 2 μ g α -actinin purified from chicken gizzard. Glutathione-agarose beads were used to precipitate the GST-containing epitope and their binding proteins. The resultant protein samples were immunoblotted with non-muscle α -actinin antibody BM75.2 (top) or GST antibody (bottom). Total MDCK cell lysate was used as a positive control for detection of α -actinin by BM75.2. **B.** Purified GST-TRPP3N, GST-TRPP3C or GST, total MDCK cell lysate (positive control), BSA or the buffer alone (negative controls), were spotted on nitrocellulose membranes and incubated with the total protein lysates of MDCK cells in a blocking buffer containing 5 mM Ca or 1 mM EGTA. The membranes were immunoblotted by BM75.2 following washes.

A



B



6.6. REFERENCES

- Basora N, Nomura H, Berger UV, Stayner C, Guo L, Shen X, Zhou J (2002) Tissue and cellular localization of a novel polycystic kidney disease-like gene product, polycystin-L. *J Am Soc Nephrol* 13:293-301.
- Chen XZ, Vassilev PM, Basora N, Peng JB, Nomura H, Segal Y, Brown EM, Reeders ST, Hediger MA, Zhou J (1999) Polycystin-L is a calcium-regulated cation channel permeable to calcium ions. *Nature* 401:383-386.
- Clapham DE (2003) TRP channels as cellular sensors. *Nature* 426:517-524.
- Dai XQ, Karpinski E, Chen XZ (2006) Permeation and inhibition of polycystin-L channel by monovalent organic cations. *Biochim Biophys Acta* 1758:197-205.
- Dixson JD, Forstner MJ, Garcia DM (2003) The alpha-actinin gene family: A revised classification. *J Mol Evol* 56:1-10.
- González-Perrett S, Kim K, Ibarra C, Damiano AE, Zotta E, Batelli M, Harris PC, Reisin IL, Arnaout MA, Cantiello HF (2001) Polycystin-2, the protein mutated in autosomal dominant polycystic kidney disease (ADPKD), is a Ca²⁺-permeable nonselective cation channel. *Proc Natl Acad Sci U S A* 98:1182-1187.
- Honda K, Yamada T, Endo R, Ino Y, Gotoh M, Tsuda H, Yamada Y, Chiba H, Hirohashi S (1998) Actinin-4, a novel actin-bundling protein associated with cell motility and cancer invasion. *J Cell Biol* 140:1383-1393.
- Huang AL, Chen X, Hoon MA, Chandrashekar J, Guo W, Trankner D, Ryba NJ, Zuker CS (2006) The cells and logic for mammalian sour taste detection. *Nature* 442:934-938.
- Ishimaru Y, Inada H, Kubota M, Zhuang H, Tominaga M, Matsunami H (2006) Transient receptor potential family members PKD1L3 and PKD2L1 form a candidate sour taste receptor. *Proc Natl Acad Sci U S A* 103:12569-12574.
- Krupp JJ, Vissel B, Thomas CG, Heinemann SF, Westbrook GL (1999) Interactions of calmodulin and alpha-actinin with the NR1 subunit modulate Ca²⁺-dependent inactivation of NMDA receptors. *J Neurosci* 19:1165-1178.
- Li Q, Dai XQ, Shen PY, Cantiello HF, Karpinski E, Chen XZ (2004) A modified mammalian tandem affinity purification procedure to prepare functional polycystin-2 channel. *FEBS Lett* 576:231-236.
- Li Q, Dai Y, Guo L, Liu Y, Hao C, Wu G, Basora N, Michalak M, Chen XZ (2003a) Polycystin-2 associates with tropomyosin-1, an actin microfilament component. *J Mol Biol* 325:949-962.

- Li Q, Liu Y, Shen PY, Dai XQ, Wang S, Smillie LB, Sandford R, Chen XZ (2003b) Troponin I binds polycystin-L and inhibits its calcium-induced channel activation. *Biochemistry* 42:7618-7625.
- Li Q, Liu Y, Zhao W, Chen XZ (2002) The calcium binding EF-hand in polycystin-L is not a domain for channel activation and ensuing inactivation. *FEBS Lett* 516:270-278.
- Li Q, Montalbetti N, Shen PY, Dai XQ, Cheeseman CI, Karpinski E, Wu G, Cantiello HF, Chen XZ (2005) Alpha-actinin associates with polycystin-2 and regulates its channel activity. *Hum Mol Genet* 14:1587-1603.
- Liu Y, Li Q, Tan M, Zhang Y-Y, Karpinski E, Zhou J, Chen XZ (2002) Modulation of the human polycystin-L channel by voltage and divalent cations. *FEBS Lett* 525:71-76.
- LopezJimenez ND, Cavenagh MM, Sainz E, Cruz-Ithier MA, Battey JF, Sullivan SL (2006) Two members of the TRPP family of ion channels, Pkd113 and Pkd211, are co-expressed in a subset of taste receptor cells. *J Neurochem* 98:68-77.
- Maruoka ND, Steele DF, Au BP, Dan P, Zhang X, Moore ED, Fedida D (2000) alpha-actinin-2 couples to cardiac Kv1.5 channels, regulating current density and channel localization in HEK cells. *FEBS Lett* 473:188-194.
- Mills M, Yang N, Weinberger R, Vander Woude DL, Beggs AH, Eastal S, North K (2001) Differential expression of the actin-binding proteins, alpha-actinin-2 and -3, in different species: implications for the evolution of functional redundancy. *Hum Mol Genet* 10:1335-1346.
- Murakami M, Ohba T, Xu F, Shida S, Satoh E, Ono K, Miyoshi I, Watanabe H, Ito H, Iijima T (2005) Genomic organization and functional analysis of murine PKD2L1. *J Biol Chem* 280:5626-5635.
- Nilius B, Owsianik G, Voets T, Peters JA (2007) Transient receptor potential cation channels in disease. *Physiol Rev* 87:165-217.
- Nomura H, Turco AE, Pei Y, Kalaydjieva L, Schiavello T, Weremowicz S, Ji W, Morton CC, Meisler M, Reeders ST, Zhou J (1998) Identification of PKDL, a novel polycystic kidney disease 2-like gene whose murine homologue is deleted in mice with kidney and retinal defects. *J Biol Chem* 273:25967-25973.
- Ramsey IS, Delling M, Clapham DE (2006) An introduction to TRP channels. *Annu Rev Physiol* 68:619-647.
- Rycroft BK, Gibb AJ (2004) Regulation of single NMDA receptor channel activity by alpha-actinin and calmodulin in rat hippocampal granule cells. *J Physiol* 557:795-808.
- Sadeghi A, Doyle AD, Johnson BD (2002) Regulation of the cardiac L-type Ca²⁺ channel by the actin-binding proteins alpha-actinin and dystrophin. *Am J Physiol* 282:C1502-C1511.

Sutters M, Germino GG (2003) Autosomal dominant polycystic kidney disease: molecular genetics and pathophysiology. *J Lab Clin Med* 141:91-101.

Wu G, Hayashi T, Park JH, Dixit M, Reynolds DM, Li L, Maeda Y, Cai Y, Coca-Prados M, Somlo S (1998) Identification of PKD2L, a human PKD2-related gene: tissue-specific expression and mapping to chromosome 10q25. *Genomics* 54:564-568.

Wyszynski M, Lin J, Rao A, Nigh E, Beggs AH, Craig AM, Sheng M (1997) Competitive binding of alpha-actinin and calmodulin to the NMDA receptor. *Nature* 385:439-442.

CHAPTER 7

GENERAL DISCUSSION

This thesis describes my research during the past four years and nine months on proteins directly or broadly related to genetic PKDs, including PKD2, fibrocystin (FPC), ENaC and TRPP3. PKD2 is directly related to human ADPKD while FPC is the only known gene mutated in human ARPKD. ENaC is indirectly involved in PKD because its expression and amiloride-sensitive currents are altered in ARPKD cystic cells; it is in the same protein complex as FPC; and its expression and function are regulated by its binding partners filamin and FPC. TRPP3 is also related to PKD in that it has significant similarity in protein sequence and channel properties to PKD2 (also called TRPP2), and that it co-localizes or interacts with PKD1 and PKD1L3. While the first reported physiological role of TRPP3 is acid sensing, one of the roles of PKD2 is flow sensing. Thus, understanding the similarity and difference in the channel function and regulation between PKD2 and TRPP3 is important to determine the molecular mechanisms underlying their sensory functions. The discussions described in the next sections will be based on my published papers, submitted manuscripts and a manuscript in preparation for submission.

7.1. Cross talk between ADPKD and ARPKD

ADPKD and ARPKD exhibit similarities in cystic phenotypes. Common features of ADPKD and ARPKD include the renal collecting duct as the predominant site of cystogenesis, abnormal epithelial solute transport, increased cell proliferation and de-differentiation, mis-targeted Na/K ATPase to the apical membrane. There are also other common features, including thickening and disorganization of the basement membrane, increased cAMP levels, and altered localization of polycystins and FPC in renal primary cilia. Whether there exist common pathogenic pathways or molecular links between PKD1/PKD2 and FPC remained obscure. Moreover, mutations in a diverse number of PKD proteins, including kinesin-2, polaris, cystin and inversin, which have no sequence similarity with either polycystins or fibrocystin, also result in renal cyst development (Lin *et al.*, 2003; Otto *et al.*, 2003; Pazour *et al.*, 2000; Avner *et al.*, 1987). This raises the possibility that common molecular mechanisms of cystogenesis exist, namely, the possibility that these PKD proteins are present in the same complexes. Using different approaches, we demonstrated that FPC and PKD2 are indeed in the same protein complex

though they don't seem to associate with each other directly. However, the protein(s) mediating the PKD2-FPC complexing remained to be identified.

KIF3B, a subunit of microtubule-associated motor protein kinesin-2, mediates the interaction between FPC and PKD2 by physically binding to them, and forming a triplex, presumably in the form of PKD2-KIF3B-FPC. Of note, although our data did not support a direct interaction between the intracellular C-termini of PKD2 and FPC, the possibility of a direct interaction cannot be excluded, as physical interactions between other domains such as their extracellular domains may occur. Our results are consistent with a recent report showing that FPC and PKD2 are in the same protein complex in kidney epithelia (Wang *et al.*, 2007). We also discovered that KIF3B mediates the stimulation of PKD2 channel activity by FPC. Therefore, KIF3B represents the first molecular linker between ADPKD and ARPKD proteins, suggesting that the protein complex PKD2-KIF3B-FPC is part of a common molecular pathway generally implicated in renal cystic diseases.

Given the existence of triplex PKD2-KIF3B-FPC, it is important to determine where the three proteins colocalize as this would provide hints on their possible physiological roles. In ciliated IMCD3 cells, PKD2 partially colocalized with KIF3B and FPC in primary cilia. Together with a recent report that PKD2 and PKD1 in renal primary cilia constitute part of a shear stress sensor responsive to tubular flow (Nauli *et al.*, 2003), our data suggest the possibility that the flow sensor is composed of a larger complex, containing not only PKD1 and PKD2, but also KIF3B, FPC and possibly other proteins. Under this scenario, several proteins would regulate PKD2, a Ca-permeable channel in the primary cilium, including PKD1, FPC and others. This concept is supported by a recent report that loss of primary cilia results in deregulated and abated apical Ca entry in ARPKD collecting duct cells (Siroky *et al.*, 2006). Single-channel activity of PKD2 on the membrane of isolated primary cilia was recently detected (Raychowdhury *et al.*, 2005).

In sub-confluent IMCD3 cells, PKD2 and FPC localized to perinuclear regions, presumably the ER and Golgi membranes, while KIF3B preferentially localized to the nucleus (unpublished data) and centrosome. These three proteins showed partial colocalization on perinuclear regions, which suggests that the triplex may serve to regulate intracellular Ca concentration. It was recently reported that the C-terminus of

FPC (FPCC) interacts with a Ca modulating cyclophilin ligand (CAML), a protein involved in Ca signaling, supporting the possibility that FPC participates in the regulation of intracellular Ca (Nagano *et al.*, 2005). It would be interesting to examine the cross talk between CAML and the PKD2-KIF3B-FPC triplex, and evaluate its impact on intracellular Ca regulation.

Although KIF3B, a motor subunit of kinesin-2, directly binds PKD2 it has no functional effect on PKD2 channel, indicating that it primarily serves as a linker protein. In contrast, KIF3A, the other motor subunit of kinesin-2 and homologous to KIF3B, stimulates PKD2 channel activity but does not directly bind FPC. Further, the stimulation of PKD2 channel by FPC via KIF3B, or by KIF3A via direct binding (Li *et al.*, 2006), does not require hydrolysis of ATP. All this together suggests that the role of KIF3B in PKD2-KIF3B-FPC is different from its traditional role as a motor subunit of kinesin-2. Of note, we recently found that KIF3A and KIF3B are abundantly present in the nucleus (unpublished data), which may be supporting evidence suggesting that the two proteins have 'non-traditional' physiological roles.

Among the previously reported binding partners of PKD2, FPC and KIF3B, such as PKD1, α -actinin, TRPC1, KIF3A and KAP3 etc, some partners, eg, PKD1, may also be in the same complex with PKD2-KIF3B-FPC. Thus PKD2-KIF3B-FPC may potentially be part of a large protein complex which itself is part of a common pathway for dominant and recessive PKDs. Thus one possible scenario would be that triggering of the complex, eg, a ligand binding to FPC or PKD1, induces conformational changes to partners in the complex, which leads to modulating PKD2 channel activity, which then affects downstream processes. On the other hand, this triplex might also be a sensory unit that is different from the PKD1-PKD2 complex in cilia.

7.2. Regulation of ENaC by filamin and fibrocystin

An interesting question is why ENaC itself is not cystogenic but is still linked to ARPKD. Up to now, the precise molecular mechanisms underlying the phenotypes for PKDs remain largely obscure. At the cellular level, they are associated with a complex set of defects, including abnormal solute reabsorption, altered ciliary protein targeting and cilia dysfunction, thickening and disorganization of the basement membrane,

increased cAMP levels, decreased differentiation and increased proliferation. Thus, it is likely that pathogenic mutations in a PKD protein result in multiple cellular abnormalities, which together eventually produces PKD phenotypes. Our data together with previous reports support the concept that the actin-binding protein filamin and the ENaC are in a novel pathway linked to solute transport (Fig. 7-1). ENaC mediates amiloride-sensitive Na reabsorption in epithelial cells, including those in kidney, lung, colon, brain and secretory glands, and plays critical physiological (eg, Na homeostasis, extracellular volume and blood pressure) and pathophysiological (Liddle's syndrome, pseudohypoaldosteronism, cystic fibrosis) roles. In fact, amiloride-sensitive Na reabsorption increases by 50% and ENaC expression by 100% in FPC-mutated renal cystic cells (Rohatgi *et al.*, 2003). Olteanu et al. studied the trans-epithelial ion transport properties of mutant cortical collecting duct principal cells derived from the *orpk* mouse (This mouse has a hypomorphic mutation in the *Tg737* gene that encodes the primary cilia-associated protein, polaris) (Olteanu *et al.*, 2006). They compared these to similar cells that had been genetically rescued by the expression of the normal *Tg737* gene, and found an unexpected and large increase in Na reabsorption in the *Tg737*-deficient cells. Raychowdhury and colleagues found that PKD2, TRPC1 and α -ENaC co-localize on primary cilia of LLC-PK1 renal epithelial cells (Raychowdhury *et al.*, 2005). This suggests a cross talk between PKD proteins and ENaC or an involvement of ENaC in cystogenesis. ENaC may be one of many branch pathways linking to a PKD protein(s) (Fig. 7-1). Mutations in one pathway are not sufficient for cyst formation, but may contribute to or modulate cyst formation. Thus describing the molecular pathway linking ENaC to PKD is important in the understanding of PKD pathogenesis. For this we studied the interaction of ENaC with and its regulation by filamin and FPC. Filamins are a family of high molecular mass cytoskeletal proteins that organize filamentous actin in networks and stress fibers. Filamins play important roles in actin organization and membrane stabilization. In the last decade, it has been found that several repeat domains of filamins bind to a wide variety of proteins, including transmembrane receptors and signaling molecules (van der & Sonnenberg, 2001).

In collaboration with Dr. Qiang Li, we examined molecular links between ENaC and human ARPKD. We demonstrated that ENaC and FPC are in the same protein

complex but seem do not bind directly with each other. siRNA of FPC in IMCD cells results in a significant increase in the expression of ENaC. Further, over-expression of FPCC in oocytes leads to decreased α -ENaC expression and function. These are in agreement with findings in human ARPKD cells and a murine model (Rohatgi *et al.*, 2003; Olteanu *et al.*, 2006), and with the occurrence of early-onset hypertension in the majority of patients with ARPKD. However, a opposite result from Veizis and Cotton's laboratory (Veizis *et al.*, 2003; Veizis & Cotton, 2005) showed that Na reabsorption was abnormally regulated by epidermal growth factor (EGF) in mouse CD cells derived from *bpk* mice. In their studies, cystic cells showed a pronounced decrease in ENaC-mediated reabsorption upon exposure to apical EGF, a result probably explained by the mislocalization of EGF receptor (EGFR) to the apical membrane of these mutant cells. Thus a reduction in the Na reabsorption was touted as a possible contributory factor to ARPKD pathophysiology. Olteanu and colleagues were very careful to exclude EGF from their culture media and, in doing so, were able to observe the ENaC-mediated hyperabsorption in their cystic cells (Olteanu *et al.*, 2006). They argued that encapsulated cysts are not a feature of ARPKD, and thus EGF levels are unlikely to be raised in tubular fluid bathing ARPKD cells, in contrast to the situation in ADPKD.

We found that actin-binding protein filamin associates with FPC and ENaC using yeast two-hybrid, *in vitro* binding and co-IP. This suggests that filamin mediates their complexing via the formation of triplex FPC-filamin-ENaC. To determine whether filamin functionally regulates ENaC we utilized *Xenopus* oocytes expression and found that the ENaC-binding domains of FLNA and FLNB, ie, their C-terminus FLNAC and FLNBC are sufficient to reduce ENaC channel function. Western blot experiments showed that the filamin fragments reduce the expression of α -ENaC and electrophysiology experiments showed that FLNAC substantially decreases ENaC single-channel activity. In oocytes, it was observed that FPCC reduces ENaC expression and consequently whole-cell currents. Taken together, the present study showed that filamin and FPC regulate both the expression and channel function of ENaC, presumably via triplex FPC-filamin-ENaC, which constitutes the first demonstration of a cross talk between ARPKD and ENaC.

Besides the physiological implications of ENaC in ARPKD, the results also support the important roles of cytoskeleton proteins in channel regulation. There is increasing evidence that the actin-based cytoskeleton, composed of the actin filament and associated proteins, directly interacts with a number of ion channels, transporters and receptors (Noda *et al.*, 2004; Chasan *et al.*, 2002). The actin-based cytoskeleton is assembled into a dynamic intracellular network which is essential in the regulation of a variety of cellular events, including the stability of cell shape and the onset of cell motility, the distribution of integral membrane proteins and the control of hormone action (Cantiello, 1997). The hypothesis that the actin cytoskeleton was directly involved in the regulation of ENaC was first supported by immuno-colocalization studies showing that Na channels always appeared on the cell surface in close proximity to actin filaments (Cantiello *et al.*, 1991). This observation raised the possibility that a potential Na channel-actin filament interaction might be an early feature of epithelial cell development.

In summary, our data support that FPC regulates ENaC expression and channel function in an FLNA-dependent manner, presumably via triplex FPC-filamin-ENaC. FLNA acts as a bridging protein in the formation of multimeric complex FPC-filamin-ENaC. Similar to the PKD2-KIF3B-FPC triplex, there is no direct binding between FPC and ENaC, and one of the cytoskeletal components, filamin, mediates the interaction, which provides a novel evidence for the importance of the cytoskeleton in PKD. If filamin is able to bind FPC and ENaC does not infer that a given filamin molecule can simultaneously bind two partner proteins; eg, ENaC and FPC may compete for binding to the same site (or two overlapped sites) in filamin. FPC is more like a receptor or modulator of ENaC, similar to its role in PKD2-KIF3B-FPC triplex. Thus our current data are in agreement with the reported data using ARPKD cystic cells (Rohatgi *et al.*, 2003), and all these indicate a cross talk between FPC and ENaC, which may account for abnormal renal trans-epithelial transport mediated in part by ENaC once the cross talk is altered by mutations in FPC. Our work has gained novel insights into molecular mechanisms of ARPKD, which is clearly an important issue for understanding the disease process as well as for the development of new treatments for ARPKD.

Future studies could use filamin deficiency/siRNA/over-expression and Far Western blotting to examine the complexing between FPC, filamin and ENaC in order to

directly demonstrate whether triplex FPC-filamin-ENaC does exist. If yes, FPC may directly regulate the filamin x ENaC interaction within the triplex; if not, ie, only complexes FPC-filamin and ENaC-filamin exist, then the regulation should be due to competitive association of FPC and ENaC with filamin, which results in less filamin available for binding ENaC in the presence of FPC. Lipid bilayer electrophysiology experiments would be used to determine whether FPC regulates ENaC channel function via binding to filamin.

7.3. TRPP3 channel function, pharmacology and modulation by the cytoskeleton

7.3.1. Permeation and inhibition of TRPP3 by monovalent by organic cations

TRPP3, an isoform of PKD2, was shown in 2006 to mediate the response to sour stimulants in taste buds located on the lateral margins of the tongue and in the regulation of pH-dependent action potentials in the spinal cord (Huang *et al.*, 2006; Ishimaru *et al.*, 2006). TRPP3 was the first polycystin member to have its biophysical function described in 1999. TRPP3 is a Ca-modulated, Ca-activated non-selective cation channel permeable to mono- and divalent cations (Chen *et al.*, 1999). Some further biophysical properties of TRPP3 were discovered, including its dependence on membrane potential and voltage-dependent inhibition by Mg (Liu *et al.*, 2002b), and the role of its intracellular C-terminus in channel activation (Li *et al.* 2002). To understand the biophysical and pharmacological properties of TRPP3, I examined a series of organic cations for permeation and inhibition, using single-channel patch clamp and the two-microelectrode voltage clamp techniques in conjunction with *Xenopus* oocyte expression. It was observed that TRPP3 is permeable to organic cations of sizes up to ~ 7 Å and that larger organic cations act as inhibitors of the channel (Dai *et al.*, 2006). Inhibition by tetra-butylammonium (TBA) decreased the single-channel current amplitude and exhibited no effect on open probability (NP_o) or mean open time (MOT), suggesting that it blocks the TRPP3 permeation pathway. In contrast, tetra-ethylammonium (TEA), tetra-propylammonium (TPA), and tetra-pentylammonium (TPeA) reduced NP_o and MOT values but had no effect on the amplitude, suggesting that they bind to a different site on TRPP3, which affects the channel gating. These data provided an estimate of the channel pore size of ~ 7 Å for TRPP3, and revealed that inhibition of TRPP3 by large TAA cations occurs by two

different mechanisms, through binding either to the pore pathway to reduce permeant flux or to another site to regulate the channel gating. Interestingly, although PKD2 has smaller single-channel conductance, its pore size of reconstituted PKD2 channel in lipid bilayer was estimated to be at least 11 Å as it is permeable to TPeA (Anyatonwu & Ehrlich, 2005), indicating that the pore dimension is not the major determinant of the channel conductance for these two homologous channels. However, experimental approaches/conditions, potential existence of specific binding partners in a native membrane, phospholipid environment, and other membrane biophysical characteristics may affect channel properties (Luo *et al.*, 2003).

7.3.2. Inhibition of TRPP3 by amiloride and its analogs

We also examined the functional modulation of TRPP3 channel by amiloride and its analogs, including phenamil, benzamil and EIPA, using the *Xenopus* oocyte expression system in conjunction with radiotracer measurements and electrophysiology. Amiloride and analogs are well-known blockers of ENaC, Na/H exchanger and other transporters. We found that amiloride and its analogs inhibited TRPP3 channel activities at substantially different affinities, in an order of inhibition potency of phenamil > benzamil > EIPA > amiloride. The inhibition potency positively correlated with the size of the inhibitors. Amiloride analogs decreased the NP_o and MOT of single channels, but exhibited no effect on the single-channel conductance, suggesting that they regulate the channel gating rather than blocking the pore permeation. The inhibition of TRPP3 in the presence of phenamil and TPeA indicates that amiloride and large organic cation inhibitor compete for the same site located outside the channel pore to gate the channel activity.

Amiloride-sensitive non-selective cation channels with high or low affinity to amiloride were found in various tissues, and involve in many physiological roles, eg, acid sensing and renal Na transport. In addition to its roles in acid sensing in the tongue and spinal cord (Huang *et al.*, 2006; Ishimaru *et al.*, 2006), our data suggest the possibility that TRPP3 is involved in defining renal Na reabsorption and the electrochemical gradient. Thus, TRPP3 may play critical physiological roles in both neuronal and non-neuronal cells by mediating amiloride-sensitive, pH-dependent cation fluxes. TRPP3 was

predominantly found in the apical region of the principal cells of IMCD, suggesting that part of the observed renal Na reabsorption may be mediated by TRPP3. Interestingly, Na reabsorption in IMCD cells was reported to be mediated by amiloride-sensitive nonselective cation channels (Vandorpe et al., 1997). Thus understanding effects of amiloride on the TRPP3 channel may help to determine its physiological roles in renal collecting ducts and other tissues.

7.3.3. Modulation of TRPP3 by α -actinin

In cooperation with Dr. Qiang Li, we demonstrated that TRPP3 binds both muscle and non-muscle α -actinins which function in mediating membrane attachment at adherent junctions (Honda et al., 1998), and representing one of the major structural components of muscles (Mills et al., 2001). α -actinins have been shown to regulate the activity of some ion channels (Wyszynski *et al.*, 1997; Rycroft & Gibb, 2004). Our study has shown that α -actinin significantly increased the channel activity of TRPP3 by stimulating its channel NP_o but not the current amplitude. Thus, α -actinin anchors TRPP3 to the actin cytoskeleton not only for structural purposes but also functionally modulates its channel function.

Up to now the channel function of TRPP3 has primarily been studied using the *Xenopus* oocyte expression system (Chen *et al.*, 1999), except for the only report showing that co-expression of TRPP3 and TRPP1 in HEK 293 cells produced a transient increase in the intracellular Ca concentration by hypo-osmotic stimulation (Murakami *et al.*, 2005). Over-expressed TRPP3 in MDCK cells mainly localized to intracellular compartments although we did observe a small fraction of TRPP3 expressed in the plasma membrane. Thus it is meaningful to characterize TRPP3 channel function in lipid bilayer in combination with our novel tandem affinity purification procedure. Our studies showed that TRPP3 in artificial lipid bilayer exhibited certain properties of TRPP3 displayed in *Xenopus* oocytes, eg, cation selectivity and presence of multiple conductance states. In contrast, the main single-channel conductance of TRPP3 (~70 pS) with or without α -actinin is much smaller than in oocytes (~370 pS in the presence of 123 mM K) (Li *et al.*, 2002; Liu *et al.*, 2002a). The larger conductance may plausibly be due to the

presence of yet-to-be-identified intracellular interacting partners or chemical modulators endogenously present in oocytes.

Given that acid sensing is important in body fluids in many tissues, such as brain, retina, heart and kidney, it would be important to determine whether/how TRPP3 and the TRPP3- α -actinin interaction is important for acid sensing in these tissues. In future studies it is important to identify amino acid residues or small domain(s) in TRPP3 and α -actinin that mediate the physical binding, and to determine whether/how factors such as phosphorylation and intracellular Ca are implicated in the TRPP3-cytoskeleton interaction.

7.3.4. Physiological roles of TRPP3 and complexing between a TRPP channel and a PKD1 homologue

PKD1 and PKD2 form a receptor-ion channel complex in which PKD1 acts as a 'receptor' that regulates PKD2 channel activity and mediates G-protein signaling. In this model, the PKD1-PKD2 complex co-localized to primary cilia of renal epithelial cells can be envisaged as a mechanosensor that transduces stimulus energy into a change in the membrane permeability (Praetorius & Spring, 2001; Praetorius & Spring, 2003). Therefore, the balance between the PKD2 and PKD1 expression, and their functional interaction, which may be disrupted in ADPKD, might have a crucial role in the normal PKD1-PKD2 signaling. In *C. elegans*, PKD2 and LOV-1, a PKD1-like protein most similar to PKD1L3, are also co-localized to sensory cilia and required for normal male mating behavior, suggesting a role in either chemosensation or mechanosensation (Barr *et al.*, 2001; Barr, 2005).

TRPP3 and PKD1 are colocalized and may also form a complex (Murakami *et al.*, 2005; Bui-Xuan *et al.*, 2006). Co-expression of PKD1 resulted in the trafficking of TRPP3 channels to the cell surface, whereas TRPP3 expressed alone was retained in the ER. However, the physiological roles of such a complex remain unclear. In contrast, the complexing between TRPP3 and PKD1L3, a receptor-like PKD1 homologue, was recently reported to exist and be implicated in acid sensing in neurons of the tongue and spinal cord (Huang *et al.*, 2006; Ishimaru *et al.*, 2006). However, while these studies indicate that low pH stimulates the TRPP3 activity, studies in oocytes showed an

opposite pH dependence of the TRPP3 channel activity (Chen *et al.*, 1999). The reasons for this controversy about the TRPP3 pH sensitivity remain unclear. It is possible that this is due to the effect of PKD1L3 and/or the difference in the expression system. We recently found that TRPP3 channel expressed in oocytes is not activated by low pH (2.5 ~ 4.5) extracellular media (with or without Ca) but is activated when switching from low to normal pH (7.5) media in the absence of Ca. This observation reveals novel properties of TRPP3 and is not apparently consistent with those obtained from tongue, spinal cord and HEK cells. It is possible that low pH incubation leads to intracellular acidification and/or altered intracellular $[Ca]_i$, which regulate TRPP3.

It is consistent with the hypothesis that polycystins may function as heteromeric channels. PKD1L3, but not all PKD1 homologues, contains a strong ion-channel motif, suggesting that it has the potential to function as an ion channel itself or primarily as accessory subunits modulating the channel properties of PKD2-like channels, eg, TRPP3. By analogy to the PKD1-PKD2 interaction, the finding that PKD1L3 and TRPP3 are co-localized and associate with each other raises the possibility that, at least within taste receptor cells, they function as a heteromultimer in which TRPP3 functions as an ion channel with its activity regulated by PKD1L3. Thus, it seems that the TRPP3-PKD1 complex in kidney and TRPP3-PKD1L3 complex in sensory neurons (such as that in the tongue) execute very distinct physiological functions. It is interesting to determine which PKD1 homologue(s) complexes with TRPP3 in other tissues, such as spinal cord, brain, retina and heart. We believe that studies of the function and regulation of the TRPP3-PKD1 homologue channel complexes in different tissues should gain new and important insights into the biological functions of other PKD1 homologues and TRPP members. On the other hand, although TRPP3's direct involvement in ADPKD or ARPKD is unlikely, a secondary role for TRPP3 in cystogenesis should not be excluded, based on the complex of TRPP3 with PKD1.

Mainly because the physiological role of TRPP3 has remained unclear, research on the protein has not been as dynamic as that on PKD2. TRPP3 was previously reported to be present in retina ganglion cells (Basora *et al.*, 2002). In collaboration with Dr. Yves Sauve (Department of Physiology Univ. of Alberta), Dr. Chen's laboratory recently found that TRPP3 is also present in specific locations of retina photoreceptor cells. These

results are helpful for elucidating the physiological role of TRPP3 in retina (neuron cells), eg, light sensing. Therefore, it is very important to provide more data about the roles of TRPP3 in general. My studies discovered new biophysical and pharmacological properties of TRPP3 and its modulation by interacting partner proteins, which are essential in leading to better understanding of the physiological role of TRPP3. Despite some exciting new evidence, we are still in the early stage and many questions remain to be answered. Dr. Chen's laboratory has recently started to generate TRPP3 conditional knockout mice, in collaboration with a researcher at Vanderbilt University. Thus, it could be expected that we would further understand the regulation of TRPP3 by pH and discover the unknown physiological roles of TRPP3 in retina and brain.

7.4. Conclusion

Mutations in human PKD proteins (PKD2, FPC and PKD1) alter several signaling pathways, which results in multiple cellular (microscopic) abnormalities, which together eventually produces (macroscopic) phenotypes. Indeed PKD proteins are implicated in several cellular pathways in which numerous proteins are involved (Fig. 7-1). Thus, while mutations in a particular protein in a pathway, eg α -actinin in the pathway toward 'solute transport', may not be cystogenic, corrections to this altered pathway (due to mutations in a PKD protein) will reduce cellular alterations (eg, solute transport), which would alleviate cystogenesis. Therefore, it is important to elucidate all implicated signaling pathways. My past and current studies are related to part of these pathways. In particular, our data on the 'PKD protein-cytoskeleton-ENaC-solute transport' pathway constitutes the first molecular link between a PKD protein and ENaC. My studies on TRPP3 offer a new perspective into the importance of TRPP3 in health and disease. In the future, it will be of interest to carry out further studies on TRPP3 to establish the molecular mechanism of acid sensing, identify other roles of TRPP3 in neuronal and non-neuronal cells and determine whether/how binding partners of TRPP3 are important to executing its physiological functions. Thus, our data together represent important contribution to understanding molecular mechanisms of genetic PKD pathogenesis and cellular sensing by TRPP2 and TRPP3, respectively. This will provide knowledge for design of drugs that

7.5. REFERENCES

Anyatonwu GI & Ehrlich BE (2005). Organic cation permeation through the channel formed by polycystin-2. *J Biol Chem* **280**, 29488-29493.

Avner ED, Studnicki FE, Young MC, Sweeney WE, Jr., Piesco NP, Ellis D, & Fettermann GH (1987). Congenital murine polycystic kidney disease. I. The ontogeny of tubular cyst formation. *Pediatr Nephrol* **1**, 587-596.

Barr MM (2005). *Caenorhabditis elegans* as a model to study renal development and disease: sexy cilia. *J Am Soc Nephrol* **16**, 305-312.

Barr MM, DeModena J, Braun D, Nguyen CQ, Hall DH, & Sternberg PW (2001). The *Caenorhabditis elegans* autosomal dominant polycystic kidney disease gene homologs *lov-1* and *pkd-2* act in the same pathway. *Curr Biol* **11**, 1341-1346.

Basora N, Nomura H, Berger UV, Stayner C, Guo L, Shen X, & Zhou J (2002). Tissue and cellular localization of a novel polycystic kidney disease-like gene product, polycystin-L. *J Am Soc Nephrol* **13**, 293-301.

Bui-Xuan EF, Li Q, Chen XZ, Boucher CA, Sandford R, Zhou J, & Basora N (2006). More than colocalizing with polycystin-1, polycystin-L is in the centrosome. *Am J Physiol Renal Physiol* **291**, F395-F406.

Cantiello HF (1997). Role of actin filament organization in cell volume and ion channel regulation. *J Exp Zool* **279**, 425-435.

Cantiello HF, Stow JL, Prat AG, & Ausiello DA (1991). Actin filaments regulate epithelial Na⁺ channel activity. *Am J Physiol* **261**, C882-C888.

Chasan B, Geisse NA, Pedatella K, Wooster DG, Teintze M, Carattino MD, Goldmann WH, & Cantiello HF (2002). Evidence for direct interaction between actin and the cystic fibrosis transmembrane conductance regulator. *Eur Biophys J* **30**, 617-624.

Chen XZ, Vassilev PM, Basora N, Peng JB, Nomura H, Segal Y, Brown EM, Reeders ST, Hediger MA, & Zhou J (1999). Polycystin-L is a calcium-regulated cation channel permeable to calcium ions. *Nature* **401**, 383-386.

Dai XQ, Karpinski E, & Chen XZ (2006). Permeation and inhibition of polycystin-L channel by monovalent organic cations. *Biochim Biophys Acta* **1758**, 197-205.

Honda K, Yamada T, Endo R, Ino Y, Gotoh M, Tsuda H, Yamada Y, Chiba H, & Hirohashi S (1998). Actinin-4, a novel actin-bundling protein associated with cell motility and cancer invasion. *J Cell Biol* **140**, 1383-1393.

Huang AL, Chen X, Hoon MA, Chandrashekar J, Guo W, Trankner D, Ryba NJ, & Zuker CS (2006). The cells and logic for mammalian sour taste detection. *Nature* **442**, 934-938.

Ishimaru Y, Inada H, Kubota M, Zhuang H, Tominaga M, & Matsunami H (2006). Transient receptor potential family members PKD1L3 and PKD2L1 form a candidate sour taste receptor. *Proc Natl Acad Sci U S A* **103**, 12569-12574.

Li Q, Liu Y, Zhao W, & Chen X-Z (2002). The calcium binding EF-hand in polycystin-L is not a domain for channel activation and ensuing inactivation. *FEBS Lett* **516**, 270-278.

Li Q, Montalbetti N, Wu Y, Ramos A, Raychowdhury MK, Chen XZ, & Cantiello HF (2006). Polycystin-2 cation channel function is under the control of microtubular structures in primary cilia of renal epithelial cells. *J Biol Chem* **281**, 37566-37575.

Lin F, Hiesberger T, Cordes K, Sinclair AM, Goldstein LS, Somlo S, & Igarashi P (2003). Kidney-specific inactivation of the KIF3A subunit of kinesin-II inhibits renal ciliogenesis and produces polycystic kidney disease. *Proc Natl Acad Sci U S A* **100**, 5286-5291.

Liu Y, Li Q, Tan M, Zhang Y-Y, Karpinski E, Zhou J, & Chen X-Z (2002b). Modulation of the human polycystin-L channel by voltage and divalent cations. *FEBS Lett* **525**, 71-76.

Liu Y, Li Q, Tan M, Zhang Y-Y, Karpinski E, Zhou J, & Chen X-Z (2002a). Modulation of the human polycystin-L channel by voltage and divalent cations. *FEBS Lett* **525**, 71-76.

Luo Y, Vassilev PM, Li X, Kawanabe Y, & Zhou J (2003). Native polycystin 2 functions as a plasma membrane Ca²⁺-permeable cation channel in renal epithelia. *Mol Cell Biol* **23**, 2600-2607.

Mills M, Yang N, Weinberger R, Vander Woude DL, Beggs AH, Easteal S, & North K (2001). Differential expression of the actin-binding proteins, alpha-actinin-2 and -3, in different species: implications for the evolution of functional redundancy. *Hum Mol Genet* **10**, 1335-1346.

Murakami M, Ohba T, Xu F, Shida S, Satoh E, Ono K, Miyoshi I, Watanabe H, Ito H, & Iijima T (2005). Genomic organization and functional analysis of murine PKD2L1. *J Biol Chem* **280**, 5626-5635.

Nagano J, Kitamura K, Hujer KM, Ward CJ, Bram RJ, Hopfer U, Tomita K, Huang C, & Miller RT (2005). Fibrocystin interacts with CAML, a protein involved in Ca(2+) signaling. *Biochem Biophys Res Commun* **338**, 880-889.

Nauli SM, Alenghat FJ, Luo Y, Williams E, Vassilev P, Li X, Elia AE, Lu W, Brown EM, Quinn SJ, Ingber DE, & Zhou J (2003). Polycystins 1 and 2 mediate mechanosensation in the primary cilium of kidney cells. *Nat Genet* **33**, 129-137.

Noda Y, Horikawa S, Katayama Y, & Sasaki S (2004). Water channel aquaporin-2 directly binds to actin. *Biochem Biophys Res Commun* **322**, 740-745.

Olteanu D, Yoder BK, Liu W, Croyle MJ, Welty EA, Rosborough K, Wyss JM, Bell PD, Guay-Woodford LM, Bevenssee MO, Satlin LM, & Schwiebert EM (2006). Heightened epithelial Na⁺ channel-mediated Na⁺ absorption in a murine polycystic kidney disease model epithelium lacking apical monocilia. *Am J Physiol Cell Physiol* **290**, C952-C963.

Otto EA, Schermer B, Obara T, O'Toole JF, Hiller KS, Mueller AM, Ruf RG, Hoefele J, Beekmann F, Landau D, Foreman JW, Goodship JA, Strachan T, Kispert A, Wolf MT, Gagnadoux MF, Nivet H, Antignac C, Walz G, Drummond IA, Benzing T, & Hildebrandt F (2003). Mutations in INVS encoding inversin cause nephronophthisis type 2, linking renal cystic disease to the function of primary cilia and left-right axis determination. *Nat Genet* **34**, 413-420.

Pazour GJ, Dickert BL, Vucica Y, Seeley ES, Rosenbaum JL, Witman GB, & Cole DG (2000). Chlamydomonas IFT88 and its mouse homologue, polycystic kidney disease gene tg737, are required for assembly of cilia and flagella. *J Cell Biol* **151**, 709-718.

Praetorius HA & Spring KR (2001). Bending the MDCK cell primary cilium increases intracellular calcium. *J Membr Biol* **184**, 71-79.

Praetorius HA & Spring KR (2003). Removal of the MDCK cell primary cilium abolishes flow sensing. *J Membr Biol* **191**, 69-76.

Raychowdhury MK, McLaughlin M, Ramos AJ, Montalbetti N, Bouley R, Ausiello DA, & Cantiello HF (2005). Characterization of single channel currents from primary cilia of renal epithelial cells. *J Biol Chem* **280**, 34718-34722.

Rohatgi R, Greenberg A, Burrow CR, Wilson PD, & Satlin LM (2003). Na transport in autosomal recessive polycystic kidney disease (ARPKD) cyst lining epithelial cells. *J Am Soc Nephrol* **14**, 827-836.

Rycroft BK & Gibb AJ (2004). Regulation of single NMDA receptor channel activity by alpha-actinin and calmodulin in rat hippocampal granule cells. *J Physiol* **557**, 795-808.

Siroky BJ, Ferguson WB, Fuson AL, Xie Y, Fintha A, Komlosi P, Yoder BK, Schwiebert EM, Guay-Woodford LM, & Bell PD (2006). Loss of primary cilia results in deregulated and unabated apical calcium entry in ARPKD collecting duct cells. *Am J Physiol Renal Physiol* **290**, F1320-F1328.

van der FA & Sonnenberg A (2001). Structural and functional aspects of filamins. *Biochim Biophys Acta* **1538**, 99-117.

Vandorpe DH, Ciampolillo F, Green RB, & Stanton BA (1997). Cyclic nucleotide-gated cation channels mediate sodium absorption by IMCD (mIMCD-K2) cells. *Am J Physiol* **272**, C901-C910.

Veizis EI, Carlin CR, & Cotton CU (2003). Decreased amiloride-sensitive Na⁺ absorption in collecting duct principal cells isolated from bpk ARPKD mice. *Am J Physiol Renal Physiol* ..

Veizis IE & Cotton CU (2005). Abnormal EGF-dependent regulation of sodium absorption in ARPKD collecting duct cells. *Am J Physiol Renal Physiol* **288**, F474-F482.

Wang S, Zhang J, Nauli SM, Li X, Starremans PG, Luo Y, Roberts KA, & Zhou J (2007). Fibrocystin/polyductin, found in the same protein complex with polycystin-2, regulates calcium responses in kidney epithelia. *Mol Cell Biol* **27**, 3241-3252.

Wyszynski M, Lin J, Rao A, Nigh E, Beggs AH, Craig AM, & Sheng M (1997). Competitive binding of alpha-actinin and calmodulin to the NMDA receptor. *Nature* **385**, 439-442.